



UNIVERSITÄT
BAYREUTH



Department of Hydrology

HYDROLOGICAL DYNAMICS OF FORESTED CATCHMENTS AS INFLUENCED BY THE EAST ASIAN SUMMER MONSOON

Dissertation

submitted to the

Bayreuth Graduate School of Mathematical and Natural Sciences

of the

University of Bayreuth

to attain the degree of

Doctor of Natural Sciences (Dr. rer. nat.)

by

Jean-Lionel Payeur-Poirier

born on March 17th 1982, in Beauceville, Canada

Bayreuth, November 2016

This dissertation was prepared at the Department of Hydrology, University of Bayreuth, Bayreuth, Germany, between October 2012 and November 2016, under the supervision of Prof. Dr. Stefan Peiffer and Dr. Luisa Hopp.

This is a full reprint of the dissertation submitted to obtain the academic degree of Doctor of Natural Sciences (Dr. rer. nat.) and approved by the Bayreuth Graduate School of Mathematical and Natural Sciences (BayNAT) of the University of Bayreuth.

Date of submission: November 25th, 2016

Approval by Steering Committee: December 15th, 2016

Date of scientific colloquium: November 14th, 2017

Acting Director: Prof. Dr. Dirk Schüler

Doctoral Committee:

Prof. Dr. Stefan Peiffer	1 st reviewer
PD Dr. Christina Bogner	2 nd reviewer
Prof. Dr. Bernd Huwe	chairman
Prof. Dr. Egbert Matzner	

Prof. Dr. Thilo Streck	3 rd reviewer
------------------------	--------------------------

Summary

The East Asian summer monsoon (EASM) induces a pronounced seasonality in the hydrological regime and water quality of forested catchments of the Lake Soyang watershed. The generation of runoff in these catchments and the export of organic matter from these catchments are major determinants of the amount, timing and quality of the water input to Lake Soyang, as more than 90% of its watershed is covered by forests. In recent decades, increasing trends in the average and extremes of summer precipitation as well as in the frequency, intensity and duration of heavy rainfall events of the EASM have altered the hydroclimatic boundary conditions of these catchments. It is most likely that, as a consequence, changes in runoff generation and increases in the export of organic matter have occurred. As these trends are predicted to continue, the current water problematics of Lake Soyang related to the input of water during the EASM could likely be exacerbated. In this sense, the study of the influence of the EASM on runoff generation in forested catchments and on the export of organic matter from these catchments is an essential step in the development of solutions to these problematics.

Hydrological studies were conducted at two forested catchments of the Lake Soyang watershed, over the 2013 and the 2014 EASM. High-frequency water sampling in addition to hydrometric, hydrochemical, isotopic and meteorological measurements were conducted. The major hydrological fluxes and conditions were estimated, as well as the fluxes of solutes in runoff and the fluxes of dissolved and particulate organic matter. Runoff was separated into its major components by performing tracer-based hydrograph separations coupled with principal component analyses (PCA) and end-member mixing analyses (EMMA). The collected data and the results of initial analyses were jointly analysed for the study of hydrological dynamics as influenced by the EASM, and this for different forest cover types.

The 2013 and the 2014 EASM differed in precipitation by almost one order of magnitude and were representative of the future predicted hydroclimatic extremes. A threshold response of runoff generation to the sum of antecedent soil moisture and precipitation was observed. Below the threshold, runoff mainly consisted of groundwater and soil water from shallow layers of the near-stream area, and the latter likely contributed to runoff through soil matrix flow. Until the threshold was reached, evapotranspiration was the major water output. Above the threshold, rapid subsurface flow was likely enhanced at deeper soil layers of the hillslope area, as intermittent springs were activated and the contribution to runoff of soil water from this area increased and became continuous. This resulted in a shift towards higher runoff coefficients of rainfall events, in a decrease in stream water solute concentrations, in temporary increases in the extent of the stream, and in the likely recharge of the saturated zone by soil water. Lower fluxes of dissolved organic carbon (DOC) and higher fluxes of nitrate (NO_3^-) induced by major rainfall events were associated to a lower proportion of near-surface flow and a lower nitrogen (N) uptake in the coniferous forest cover type, in comparison to the deciduous type. The total fluxes of solutes, DOC and total dissolved nitrogen (TDN) were over one order of magnitude greater in 2013 than in 2014. These results suggest that the strength of the EASM and the forest cover type can strongly influence runoff generation and water quality in catchments of the Lake Soyang watershed, and clarify the couplings between the hydrological and biogeochemical functions of these catchments.

Zusammenfassung

In den bewaldeten Teileinzugsgebieten des Gesamteinzugsgebietes des Soyang-Sees bewirkt der ostasiatische Sommermonsun (OASM) eine ausgeprägte Saisonalität des hydrologischen Regimes und der Wasserqualität. Die Abflussbildung sowie der Austrag organischer Substanz aus den bewaldeten Einzugsgebieten, die über 90% des Soyang Einzugsgebiet ausmachen, bilden die zentralen Faktoren, die die zeitliche Verteilung der Quantität und Qualität des Seezuflusses bestimmen. Der in den letzten Jahrzehnten trendartige Anstieg von Durchschnitts- und Extremwerten sommerlicher Niederschlagsmengen sowie die Zunahme von Häufigkeit, Intensität und Dauer von Starkregenereignissen infolge des OASM hat die hydroklimatischen Rahmenbedingungen der Einzugsgebiete verändert. Es ist deshalb wahrscheinlich, dass auf lokaler Einzugsgebietsebene Veränderungen bei der Abflussbildung sowie ein zunehmender Austrag organischer Substanz stattgefunden haben. Ausgehend von Analysen, die die Fortführung dieser Trends bestätigen, ist davon auszugehen, dass die gegenwärtigen Wasserprobleme des Soyang sich infolge des durch den OASM verursachten Wasserzuflusses verstärken. Vor diesem Hintergrund liefert die Untersuchung des Einflusses des OASM auf die Abflussbildung sowie den Austrag organischer Verbindungen aus bewaldeten Einzugsgebieten einen wichtigen Beitrag zur Entwicklung von Problemlösungen.

Im Rahmen der vorliegenden Dissertation wurden über die Dauer des OASM in den Jahren 2013 und 2014 hydrologische Untersuchungen in jeweils zwei bewaldeten Teileinzugsgebieten des Soyang Sees durchgeführt. In den Arbeitsgebieten wurden zeitlich hochauflösend Wasserproben für hydrochemische und Isotopenuntersuchungen genommen. Zusätzlich wurden hydrometrische und meteorologische Messungen durchgeführt. Die hydrologischen Hauptabflusskomponenten und deren Bildungsbedingungen wurden auf Grundlage punktförmiger Messungen abgeschätzt. Die Quantität gelöster Stoffe, darunter gelöster sowie ungelöster organisch gebundener Kohlenstoff, wurde ebenfalls auf Grundlage punktförmiger Messungen abgeschätzt. Der Abfluss wurde durch die Anwendung einer Tracer-basierten Ganglinienseparation in Verbindung mit einer Hauptkomponenten- (PCA) und einer End-Member-Mixing-Analyse (EMMA) in seine Hauptkomponenten zerlegt. Für die weitergehenden Untersuchungen zur Charakterisierung der hydrologischen Dynamik des OASM in Abhängigkeit verschiedener Waldtypen wurden sowohl die erhobenen Daten als auch die Analyseergebnisse verwendet.

Die Niederschlagsmengen während des OASM in den Jahren 2013 und 2014 differierten um fast das Zehnfache. Somit wären sie repräsentativ für die prognostizierten hydroklimatischen Extremereignisse. Abfluss konnte erst nach Überschreitung eines Schwellenwerts, der sich aus vorhergehender Bodenfeuchte und Niederschlagsmenge zusammensetzt, beobachtet werden. Unterhalb des Schwellenwertes setzte sich der Abfluss hauptsächlich aus lateralen Komponenten des Grund- und des Bodenwassers in Stromnähe zusammen, wobei letzterer vor allem zum Abfluss in der Bodenmatrix beiträgt. Bis zum Erreichen des Schwellenwertes bildete Evapotranspiration die hauptsächlich Wasserausgangskomponente. Oberhalb des Schwellenwertes bildete sich vor allem in tieferen Bodenschichten der Hanglagen schneller unterirdischer Abfluss, was zur Reaktivierung intermittierender Quellen und zu einem kontinuierlichen Zwischenabfluss führte. Die beschriebenen hydrologischen Prozesse führten zu höheren Abflussbeiwerten der

Niederschlagsereignisse, zu abnehmenden Lösungskonzentrationen in den Vorflutern, zur zeitweiligen Flussausdehnung und wahrscheinlich zu Grundwasserneubildung. Starkregenereignisse waren durch niedrigere Mengen an gelöstem organisch gebundenen Kohlenstoff (DOC) und größeren Nitratmengen (NO_3^-) charakterisiert, die bei geringerem oberflächennahen Abflussanteil und niedrigerer Stickstoffaufnahme von Nadelwald im Vergleich zu Laubwald auftraten. Der Gesamtfluss an gelösten Stoffen, DOC sowie aller gelösten Stickstoffverbindungen sank um das zehnfache im Jahr 2014 im Vergleich zum Vorjahr. Die vorliegenden Ergebnisse legen nahe, dass die Intensität des OASM sowie die unterschiedlichen Waldtypen einen erheblichen Einfluss auf die Abflussbildung und die Wasserqualität in den Teileinzugsgebieten des Soyang Sees haben. Weiterhin trugen die Ergebnisse zu einem besseren Verständnis der hydrologischen und biogeochemischen Wechselwirkungen dieser Einzugsgebiete bei.

요약

동아시아지역의 여름철 장마는 소양호 유역의 수문 및 수질의 계절적 변화에 영향을 준다. 90% 이상이 산림으로 둘러 싸인 이 유역의 지표수의 발생과 유기물 유출은 소양호의 유입수, 유입 시기 및 수질의 주요 구성 요인이다. 최근 몇 십년간 여름철 장마 기간 동안 집중호우의 강도와 빈도가 증가하는 추세를 보이고 있는데 이는 소양호 유역의 물 기후 변화를 가져오고 있다. 이러한 추세는 지표수 발생과 유기물 유출의 변화를 가져온다. 이 추세가 지속적으로 유지 될 것이라고 예측해 보면 현재의 여름철 장마 기간 동안 소양호의 유입수와 관련한 수질 문제가 악화될 것으로 예상된다. 그러므로 이 연구는 산림 유역의 지표수 및 유기물 유출에 대한 장마의 영향을 알아보고, 그럼으로써 소양호 유역의 수질 문제의 해결 방안에 대한 기반을 마련할 근거가 될 수 있다.

이 연구는 2013년 - 2014년 여름철 장마 기간동안에 소양호 유역의 두 산림 소유역에서 물 샘플 조사와 추가적으로 유속, 수리화학, 동위원소 및 기상자료 측정이 이루어 졌다. 이에 따른 지표수의 용질, 용존 유기물, 미립자 유기물 등의주요 수문학적 흐름과 조건들이 추정되었다. 지표수는 주성분분석 (Principal component analysis, PCA) 과 끝성분혼합분석(End-member mixing analysis, EMMA) 을 이용한 수문곡선으로 분석하였다. 수집된 자료 및 초기 분석 결과는 산림 피복 종류에 따른 장마의 영향 등 수문 역학적 연구와 함께 분석하였다.

2013년 여름철 장마 기간 동안의 강수량과 2014년 같은 기간의 강수량은 큰 차이를 보이는데 물 기후에서 극한 미래 예측량을 대변할 만큼의 양적 차이를 보인다. 누적 선행 토양 수분 함량과 강수량에서는 지표수 발생의 임계치가 관측되었다. 임계치 아래로는 지표수는 주로 지하수와 하천 근처의 얇은 층의 토양 수분, 최종적으로 토양 매트리스를 통과하는 것으로 구성된다. 임계치까지 도달할 때 까지는 증발산량이 수분 유출의 주요 요인이다. 임계치 위로는 빠른 지중류 즉, 중간류의 흐름이 경사지의 깊은 토양층에서 집중적으로 발생한다. 즉, 지표수의 간헐적 분출이 활성화 되고 토양수분에서 나오는 지표수가 지속적으로 증가하게 된다. 강수에 대한 지표수 계수의 빠른 변환은 하천의 용질 농도의 감소, 하천의 일시적 확장, 토양수분에 의한 지하수층의 함량에 영향을 준다. 산림 종류에 따르면, 활엽수림에서 발생하는 주요 강수 발생에 의한 낮은 함량의 용존 유기물과 높은 함량의 질산염 (NO_3^-) 은 근 표면 흐름과 질소 흡수에 있어 침엽수림보다 높다. 총 용질량, 용존 유기물량과 총 용존 질소량은 2014년보다 2013년이 높다. 이 결과는 소양호 유역에서 여름철 장마에 대해 산림 종류에 따라 지표수 발생 및 수질 보존에 대해 수문학적 및 생지화학적 기능을 고려한 서로 다른 전략이 필요함을 제안한다.

Acknowledgements

The successful completion of my doctoral studies would not have been possible without the scientific, technical and moral support of the persons who accompanied me throughout this demanding, rewarding and life-changing journey.

First of all, I owe a deep gratitude to my supervisors, Prof. Dr. Stefan Peiffer and Dr. Luisa Hopp. The guidance you provided matched the highly trustful, respectful, and honest relationship we have had through the years, and helped me to improve my skills and autonomy as a scientist. I am also thankful to other members of the TERRECO-IRTG, Prof. Dr. Egbert Matzner, PD Dr. Trung Thanh Nguyen, Prof. Dr. Ji-Hyung Park and Prof. Dr. John Tenhunen.

My discovery of Germany and of South Korea, their landscapes, their languages, their people, their cultures and their cuisines would have been far less compelling and enjoyable without the presence, support and help from the friends and colleagues I met through my doctoral studies. I sincerely thank Sebastian Arnhold, Ik-Chang Choi, Youngsoon Choi, Hamada Elsayed Ali, Jaesung Eum, Jintae Hwang, Gwanyong Jeong, Eun-Young Jung, Bora Lee, Steve Lindner, Ganga Ram Maharjan, Bhone Nay Htoon, Thinh Duy Nguyen and Silvia Parra. I am grateful to all of you for sharing these joyful and unforgettable times. I especially thank Kwanghun Choi, Marco T. Lara Jiménez, Kiyong Kim, Cosmas Lambini and Mi-Hee Lee. Through the years, the moments, the laughter, the challenges, and a natural affinity with each other, we developed a friendship which I very much cherish and which will last, whatever the paths we continue upon. Your personalities enrich my life and broaden my horizons, and I feel privileged to be your friend!

I also thank the research associates and the technicians of the Department of Hydrology of Universität Bayreuth, Jutta Eckert, Dr. Sven Frei, Dr. Benjamin Gilfedder, Silke Hammer, Dr. Klaus-Holger Knorr, Martina Rohr, Dr. Moli Wan, Dr. Ruiwen Yan, Dr. Zhiguo Yu and Heidi Zier, for their contribution to the respectful, professional, collegial, convivial and cooperative atmosphere that prevailed throughout my doctoral studies. Besides, I thank most of you for helping me improve my skills in the German language.

Finally, I could never be grateful enough for the support of my wife, Sandra Seeger, sister, Jade Payeur-Poirier, mother, Renaude Payeur, father, Richard Poirier, as well as of my sister-in-law and her partner, Corinna Seeger and Hannes Pommer, mother-in-law, Eva Seeger, and father-in-law, Hansjörg Seeger, throughout this journey. Sandra, you were as supportive, patient and comprehensive as no one else could have been, and without you I wouldn't have become the man and the scientist I am today. *Merci de tout mon coeur.*

Table of contents

Summary.....	III
Zusammenfassung.....	IV
요약.....	VI
Acknowledgements.....	VII
List of figures.....	XI
List of tables.....	XIV
List of abbreviations.....	XVI
List of symbols.....	XVII

Chapter 1 – Synopsis

1.1. Background and motivation.....	1
1.1.1. Water problematics of the Lake Soyang watershed.....	1
1.1.2. Runoff generation and water quality of forested catchments of the East Asian summer monsoon region.....	5
1.1.3. The tracer-based hydrograph separation technique.....	8
1.2. Objectives and hypotheses.....	12
1.3. Study area and sites.....	13
1.4. Methods.....	15
1.5. Results and discussion.....	16
1.6. Conclusions.....	20
1.7. List of manuscripts and specification of contributions.....	22
References.....	25

Chapter 2 – A sudden shift in runoff generation processes at a forested catchment as induced by the East Asian summer monsoon

Abstract.....	34
2.1. Introduction.....	34
2.2. Materials and methods.....	36
2.2.1. Site description.....	36
2.2.2. Regional characteristics of the 2013 summer monsoon.....	41
2.2.3. Meteorological measurements.....	41
2.2.4. Hydrometric measurements.....	41
2.2.5. Water sampling.....	42
2.2.6. Chemical and isotopic analyses.....	43
2.2.7. Data analysis.....	44
2.2.7.1. Hydrograph separation.....	44
2.2.7.2. Individual rainfall events.....	47

2.2.7.3. Recession analysis and runoff coefficient.....	47
2.3. Results.....	47
2.3.1. Major hydrological fluxes and conditions.....	47
2.3.1.1. Precipitation and throughfall.....	47
2.3.1.2. Runoff.....	48
2.3.1.3. Soil moisture and water table.....	50
2.3.2. Water chemistry and isotopic abundance.....	52
2.3.3. Hydrograph separation.....	54
2.3.3.1. Selection of tracers.....	54
2.3.3.2. Mixing models and identification of end-members.....	56
2.3.3.3. Contributions of end-members to runoff.....	58
2.4. Discussion.....	62
2.4.1. Major hydrological fluxes and conditions.....	62
2.4.2. Validity of the mixing models.....	63
2.4.3. Runoff generation as influenced by the summer monsoon.....	65
2.4.3.1. Initial period.....	65
2.4.3.2. Major period.....	66
2.5. Conclusions.....	68
Acknowledgments.....	70
Appendix.....	70
References.....	71

Chapter 3 – Water fluxes and quality of a forested catchment over two hydrologically contrasting years of the East Asian summer monsoon

Abstract.....	79
3.1. Introduction.....	79
3.2. Materials and methods.....	81
3.2.1. Site description.....	81
3.2.2. Regional characteristics of the 2013 and the 2014 summer monsoon.....	83
3.2.3. Meteorological measurements.....	83
3.2.4. Hydrometric measurements.....	84
3.2.5. Water sampling, chemical analysis and isotopic analysis.....	85
3.2.6. Data analysis.....	86
3.2.6.1. Runoff and solute fluxes.....	86
3.2.6.2. Evapotranspiration.....	86
3.2.6.3. Hydrograph separation.....	87
3.3. Results.....	88
3.3.1. Water fluxes and hydrological conditions.....	88
3.3.1.1. Precipitation and throughfall.....	88
3.3.1.2. Runoff.....	89
3.3.1.3. Evapotranspiration.....	90
3.3.1.4. Soil moisture and water table.....	91
3.3.2. Water quality and solute fluxes.....	92
3.3.3. Runoff sources.....	95
3.4 Discussion.....	96
3.4.1. Water fluxes and runoff generation.....	96

3.4.2. Water quality.....	102
3.5. Conclusions.....	103
Acknowledgements.....	104
References.....	105

Chapter 4 – Variability in runoff fluxes of dissolved and particulate carbon and nitrogen from two watersheds of different tree species during intense storm events

Abstract.....	112
4.1. Introduction.....	112
4.2. Materials and methods.....	114
4.2.1. Study area and site.....	114
4.2.2. Experimental design.....	117
4.2.2.1. Water sampling.....	117
4.2.2.2. Soil sampling.....	118
4.2.3. Calculations.....	118
4.2.3.1. Fluxes of C and N in runoff.....	118
4.2.3.2. Statistics for origin of DOM and POM.....	119
4.2.4. Chemical analyses.....	119
4.3. Results.....	120
4.3.1. Soil and hydrological characteristics.....	120
4.3.2. Concentrations of carbon and nitrogen in runoff during storm events.....	123
4.3.3. Fluxes of carbon and nitrogen.....	124
4.3.4. Chemical properties of DOM and POM in runoff.....	126
4.4. Discussion.....	130
4.4.1. Different response of DOC to increased discharge at the mixed and the deciduous watershed.....	130
4.4.2. Organic and inorganic nitrogen in runoff.....	131
4.4.3. Particulate organic matter in runoff.....	132
4.5. Conclusions.....	132
Acknowledgements.....	133
References.....	134

Appendix

List of additional contributions.....	140
Protocol for the collection and storage of water samples.....	141
Guidelines for the installation of a V-notch weir.....	148
Guidelines for the construction of a passive rainfall/throughfall collector with a valve for the collection of samples.....	158
Metadata of measurements, sampling and analyses.....	160

Eidesstattliche Versicherungen und Erklärungen.....	165
---	-----

List of figures

Chapter 1

- Figure 1.1. Hypothesized hydrological and chemical processes of Lake Soyang over an annual cycle (from Peiffer et al., 2012). 4
- Figure 1.2. Major water fluxes and runoff generation processes in forested catchments (adapted from Brown, 1980). 6
- Figure 1.3. Maps of Asia, Korea, the Lake Soyang watershed and the first study site. 13
- Figure 1.4. Topography of the Lake Soyang watershed. The watershed boundary is delineated with a thin blue line. 13
- Figure 1.5. Pictures of the vegetation and topography at the first study site. 14
- Figure 1.6. Specific discharge (hourly mean), throughfall (hourly) and contributions of end-members to runoff (bihourly) as a function of time for selected major rainfall events of the 2013 summer monsoon. Blank areas correspond to missing values. 19

Chapter 2

- Figure 2.1. Location and detailed map of the study site. The equidistance of contour lines is 10 m and the precision is ± 10 m. 38
- Figure 2.2. (a) Specific discharge (hourly mean) and throughfall (hourly), (b) electrical conductivity (EC, hourly mean), Ca^{2+} and Mg^{2+} concentration and (c) relative abundance of deuterium ($\delta^2\text{H}$) of stream water as a function of time from June 1 to August 31, 2013. Ca^{2+} , Mg^{2+} , EC and $\delta^2\text{H}$ were the only tracers considered as conservative. The shaded areas correspond to the summer monsoon; the white lines separate the initial and the major period. Selected major rainfall events are labeled by order. 49
- Figure 2.3. Daily mean soil moisture (θ_v) and unsaturated hydraulic conductivity ($K(\theta_v)$) at three depths at the (a, d) hillslope, (b, e) toeslope and (c, f) riparian areas of the study site as a function of time from June 1 to August 31, 2013. The shaded areas correspond to the summer monsoon; the white lines separate the initial and the major period. 51
- Figure 2.4. Piper diagram of stream water solutes before, during and after the 2013 summer monsoon. Data are in units of percent meq l^{-1} 53
- Figure 2.5. Mixing subspaces of stream water tracer values for (a) the whole study period ($n=345$), (b) the initial period ($n=132$) with projected potential end-members and (c) the major period ($n=243$) with projected potential end-members. The percentage of variation explained by each principal component (Ux) follows the order of the component in parentheses. Soil water potential end-members are labeled by depth (cm). Error bars are interquartile ranges; some of the ranges extend beyond plot (c). The projections of the

identified end-members are linked by dotted lines. In plot (a), <i>U2</i> was not retained but plotted for ease of viewing.	57
Figure 2.6. Selected tracer values of stream water (Str), throughfall (Thr), groundwater (Grw) and soil water for (a, c, e) the initial and (b, d, f) the major period. Soil water is labeled by source area and depth (cm). Center lines are the median, boxes extend from the lower to the upper quartiles, and whiskers extend from the minimum to the maximum values; some whiskers extend beyond plots (b) and (f).....	59
Figure 2.7. Relative contributions of end-members to runoff (daily mean) and throughfall (daily) as a function of time for the initial and the major period The shaded areas correspond to the summer monsoon.....	61

Chapter 3

Figure 3.1. Location and detailed map of the Lake Soyang watershed, including Lake Soyang, the major rivers and the study site location. The relief is vertically exaggerated by a factor of 1.5. See Payeur-Poirier et al. (in preparation) for a detailed map of the study site.	82
Figure 3.2. Specific discharge (hourly mean) and throughfall (hourly) as a function of time for the period from June 1 to August 31 of 2013 and 2014. The shaded areas correspond to the summer monsoon.	90
Figure 3.3. Soil moisture (θ_v , daily mean) at 10-, 30- and 50-cm depth at the catchment scale as a function of time for the period from June 1 to August 24 of 2013 and 2014. The light grey areas correspond to the 2013 summer monsoon; the dark grey areas correspond to the 2014 summer monsoon.	91
Figure 3.4. Piper diagrams of stream water, soil water, spring water, throughfall and groundwater for the 2013 and the 2014 study period. Data are in units of % meq l ⁻¹	93
Figure 3.5. Stream water solute concentrations, electrical conductivity (EC) and relative abundance of deuterium ($\delta^2\text{H}$) as a function of time for the 2013 and the 2014 study period. The light grey areas correspond to the 2013 summer monsoon; the dark grey areas correspond to the 2014 summer monsoon. Ions and the compound are in units of mg l ⁻¹ , EC is in units of $\mu\text{S cm}^{-1}$ at 25 °C (daily mean), $\delta^2\text{H}$ is in units of ‰ in relation to VSMOW, DOC is in units of mg C l ⁻¹ , TDN is in units of mg N l ⁻¹	94
Figure 3.6. Orthogonal projections of stream water tracer values for the periods before, during and after the 2013 and the 2014 summer monsoon, in the mixing subspace of the 2013 values. The percentage of variation explained by each principal component (<i>U_x</i>) follows the order of the component in parentheses. <i>U2</i> was not retained but plotted for ease of viewing.	97
Figure 3.7. Total runoff for individual rainfall events of the 2013 and the 2014 summer monsoon as a function of (a) antecedent soil moisture index (ASMI), (b) precipitation and (c) the sum of ASMI and precipitation. The runoff coefficients of events (<i>r_c</i>) are identified per cluster. In plot (c), linear regressions were separately calculated for the events below and the events above the threshold value; the vertical dashed line corresponds to the threshold value.	99

Figure 3.8. Flow-duration curves of specific discharge (hourly mean) for the period from June 1 to August 16 of 2013 and 2014 (measurement period common to both years, which includes the summer monsoon). Vertical dashed lines correspond to the 1st, 5th, 50th, 95th and 99th percentiles..... 101

Figure 3.9. Stream water concentrations of NO₃-N and dissolved organic carbon (DOC) as a function of specific discharge for (a, c) the 2013 and (b, d) the 2014 summer monsoon. Black data points correspond to samples collected at low-flow conditions and grey data points correspond to samples collected during and following rainfall events. Two data points exceed the range of the abscissa of plots (a) and (c). 103

Chapter 4

Figure 4.1. Location and tree species composition of the two studied forested watersheds. Lake Soyang map was modified from Jung et al. (2015)..... 116

Figure 4.2. Soil profiles of ¹³C and ¹⁵N isotope abundance at the MC, MD, and DD plot. Error bars represent standard deviation (n=3). 121

Figure 4.3. Concentrations of a) dissolved organic carbon (DOC) and b) nitrogen (DON), d) particulate organic carbon (POC) and e) nitrogen (PON) and the ratios of c) DOC/DON and f) POC/PON in runoff with discharge during monsoon storm events. Dotted, solid and dashed lines correspond to the storm event of July 8th 2013, July 11th 2013 and July 14th 2013, respectively. 124

Figure 4.4. Fluxes of DOC, POC, DON, PON and NO₃-N in runoff with discharge during monsoon storm events..... 125

Figure 4.5. Specific ultraviolet absorbance (SUVA₂₈₀), humification index (HIX_{em}), protein-like fluorescence/humic-like fluorescence (PLF/HLF), protein-like fluorescence/fulvic-like fluorescence (PLF/FLF), ¹³C isotope abundance of dissolved organic carbon ($\delta^{13}\text{C}_{\text{DOC}}$) and ¹⁵N isotope abundance of total dissolved nitrogen ($\delta^{15}\text{N}_{\text{TDN}}$) in runoff with discharge during monsoon storm events. Only significant regressions are shown..... 127

Figure 4.6. Range of dissolved organic carbon and nitrogen ratio (DOC/DON ratio), specific ultraviolet absorbance (SUVA₂₈₀), humification index (HIX_{em}), and protein-like fluorescence/humic-like fluorescence (PLF/HLF) of throughfall, forest floor leachates, soil solution, and runoff during monsoon storm events. Box plots display minimum, lower quartile, median, upper quartile, maximum and outliers. Statistically significant differences between sample types (throughfall, forest floor leachates, soil solution, and runoff) are indicated by different letters in the box plots, significance level of $p < 0.05$. 128

Figure 4.7. Range of particulate organic carbon and nitrogen ratio (POC/PON ratio), $\delta^{13}\text{C}$ and $\delta^{15}\text{N}$ in Oi, Oe+Oa, upper soil (0-10 cm depth), deeper soil (40-50 cm depth at the MC and MD plot, 30-40 cm depth at the DD plot), and runoff. Box plots display minimum, lower quartile, median, upper quartile, maximum and outliers. Statistically significant differences between sample types (Oi, Oe+Oa, upper soil, deeper soil, and runoff) are indicated by different letters in the box plots, significance level of $p < 0.05$ 129

List of tables

Chapter 2

Table 2.1. Selected topographical, stand and soil characteristics of the study site.....	39
Table 2.2. Characteristics of selected major rainfall events of the 2013 summer monsoon. ...	50
Table 2.3. Patterns and relative root-mean-square errors (RRMSEs) of the residuals between the projected and the measured stream water tracer values plotted against the latter, in one- and two-dimensional subspaces for the initial and the major period.	54
Table 2.4. Medians of potential end-member selected tracer values for the initial and the major period. Values in parentheses are the respective percent differences between the projected and the measured values; values in bold have an absolute percent difference < 15%.....	55
Table 2.5. Relative root-mean-square errors (RRMSEs) of the residuals between the predicted and the measured stream water conservative tracer values for the initial and the major period.....	59
Table 2.6. Relative contributions of end-members to runoff for the initial and the major period. Values are followed by the respective standard deviations (SD).....	60
Table 2.7. Relative contributions of water sources to runoff before, during and after the 2013 summer monsoon (independently of soil depth). Values are followed by the respective standard deviations (SD).	69

Chapter 3

Table 3.1. Selected characteristics of the 2013 and the 2014 summer monsoon, and major hydrological fluxes and conditions at the study site.	89
Table 3.2. Total solute fluxes in runoff for the 2013 and the 2014 summer monsoon.	95
Table 3.3. Relative contributions of water sources to runoff for the periods before, during and after the 2013 and the 2014 summer monsoon. Values are followed by the respective standard deviations (SD).	96
Table 3.4. Percentile exceedance specific discharge (hourly mean) for the period from June 1 to August 16 of 2013 and 2014. Both periods include the summer monsoon.	101

Chapter 4

Table 4.1. Tree species composition and geomorphological characteristics of the studied forested watersheds.	117
---	-----

Table 4.2. Hydrological characteristics of sampled storm events and maximum concentration of dissolved organic carbon (DOC) and nitrogen (DON), particulate organic carbon (POC) and nitrogen (PON) in runoff. All dates are in 2013. 122

Table 4.3. Total precipitation, total runoff and integrated fluxes of dissolved organic carbon (DOC) and nitrogen (DON), nitrate (NO₃-N), particulate organic carbon (POC) and nitrogen (PON) in June and July 2013. 126

List of abbreviations

ANOVA	Analysis of variance
ASMI	Antecedent soil moisture index
AWS	Automated weather station
DD	Deciduous deciduous
DIW	Deionized water
DOC	Dissolved organic carbon
DOI	Digital object identifier
DOM	Dissolved organic matter
DON	Dissolved organic nitrogen
DOY	Day of year
EASM	East Asian summer monsoon
EC	Electrical conductivity
EMMA	End-member mixing analysis
FLF	Fulvic-like fluorescence
Grw	Groundwater
HLF	Humic-like fluorescence
IRTG	International research training group
MC	Mixed coniferous
MD	Mixed deciduous
MIT	Minimum inter-event time
ORCID	Open researcher and contributor ID
PCA	Principal component analysis
PLF	Protein-like fluorescence
POC	Particulate organic carbon
POM	Particulate organic matter
PON	Particulate organic nitrogen
RRMSE	Relative root-mean-square error
SD	Standard deviation
Str	Stream water
SWAT	Soil and water assessment tool
TDN	Total dissolved nitrogen
TERRECO	Complex terrain and ecological heterogeneity
Thr	Throughfall
UV	Ultraviolet
VSMOW	Vienna standard mean ocean water

List of symbols

α	Priestley-Taylor coefficient
C	Carbon
^{13}C	Carbon-13
Ca^{2+}	Calcium
CaCl_2	Calcium chloride
Cl^-	Chloride
δ	Relative abundance in relation to VSMOW
ET_d	Daily actual evapotranspiration
ET_p	Daily potential evapotranspiration
^2H	Deuterium
Hill ₄₀	Hillslope soil water at 40-cm depth
Hill ₆₅	Hillslope soil water at 65-cm depth
HIX _{em}	Humification index
H_2O	Water
K^+	Potassium
$K(\theta_v)$	Unsaturated hydraulic conductivity
K_{sat}	Saturated hydraulic conductivity
Mg^{2+}	Magnesium
N	Nitrogen
^{15}N	Nitrogen-15
Na^+	Sodium
NH_4^+	Ammonium
$\text{NH}_4\text{-N}$	Ammonium as nitrogen
NO_3^-	Nitrate
$\text{NO}_3\text{-N}$	Nitrate as nitrogen
O_2	Oxygen
^{17}O	Oxygen-17
^{18}O	Oxygen-18
Oa, Oe, Oi	Organic horizons of highly, moderately and slightly decomposed material
P	Phosphorus
q	Specific discharge
θ_v	Volumetric soil-water content
RC_x	Relative contribution of an end-member to runoff
Rip ₂₀	Riparian soil water at 20-cm depth
Rip ₃₀	Riparian soil water at 30-cm depth
Rip ₄₀	Riparian soil water at 40-cm depth
SiO_2	Silica
SO_4^{2-}	Sulphate
SUVA ₂₈₀	Specific ultraviolet absorbance at 280 nm
Toe ₄₀	Toeslope soil water at 40-cm depth
T_{st}	Tracer value of stream water
T_x	Value of a tracer
U	Principal component

Chapter 1

Synopsis

1.1. Background and motivation

1.1.1. Water problematics of the Lake Soyang watershed

In 2009, the Republic of Korea (hereinafter referred to as South Korea) implemented its National Strategy for Green Growth by adopting the first of its Five-Year Plans for Green Growth. The National Strategy for Green Growth is a stimulus package in response to the financial and economic crisis that erupted in late 2008, and is the most comprehensive environmental plan that South Korea has implemented since its establishment in 1948 (UNEP, 2010). The concept of green growth, as advanced by the South Korean government, consists of three elements (Committee on Green Growth, 2014):

- the virtuous cycle of the environment and the economy,
- improving the quality of life and the green revolution of daily life, and
- establishing a national standing corresponding with international expectations.

In the short-term, the strategy aims at stimulating job creation and revitalizing the economy. In the mid- and long-term, it aims at achieving the sustainable management of the nation's natural resources and mitigating climate change and its environmental impacts. In this sense, the strategy is also a response to the current and predicted environmental challenges faced by South Korea (UNEP, 2010). Due to the increasing urbanization and industrialization of the country, to the high population density, to the highly mountainous topography and to the highly seasonal precipitation regime, the South Korean environment and natural resources have been under pressure. For example, the United Nations defined South Korea as a water

hotspot in terms of flood frequency and projected that, in terms of water availability, the Seoul Capital Area will be under very severe water stress by 2050 ($< 500 \text{ m}^3$ of freshwater per person per year; WWAP, 2012). In recent decades, the pressure on the environment and natural resources has been exacerbated by changes in the South Korean climate, namely an above-world-average increase in surface temperature, a substantial increase in the frequency of heavy rainfall events, and a substantial increase in the intensity of these events, which are predicted to intensify until at least 2100 (Jung et al., 2002; Ministry of Environment, 2015; NIER, 2010). These changes could potentially have considerable, negative impacts on the nation's water resources in terms of water flow, balance and quality (Bae et al., 2008; Kim et al., 2011; Park et al., 2010). To prevent and mitigate these potential impacts, the South Korean government has implemented a series of measures (Ministry of Environment, 2015).

One of these measures is the Four Major Rivers Restoration Project, which was implemented through the first Five-Year Plan of the National Strategy for Green Growth. This project revolved around five core tasks (Ministry of Environment and Korea Environment Institute, 2009):

- securing water supply,
- flood control,
- water quality improvement and ecosystem restoration,
- development of spaces for cultural and leisure activities, and
- regional development around the four major rivers.

One of these four major rivers is the Han River, of which the basin is considered the heart of South Korea due to its population and the ecosystem services it provides to the population (WWAP, 2009). A major tributary of the Han River is the Soyang River, which flows within the Lake Soyang watershed and is the main tributary of Lake Soyang. The provision of water from the Lake Soyang watershed is a highly valued ecosystem service by a significant proportion of the South Korean population, as Lake Soyang is one of the main sources of freshwater for the Seoul National Capital Area. The watershed provides additional services, such as soil erosion prevention, plant production, flood regulation, carbon uptake, irrigation, fish habitat, recreation and weather regulation (Kang and Tenhunen, 2010). The Lake Soyang watershed is a good example of a socio-ecological system, where agricultural production and the provision of high-quality water to downstream regions are highly valued and desired, but sometimes opposed (Raskin et al., 1997). In recent decades, water problematics have emerged

from the aforementioned climate changes and changes in land use and land cover (Park et al., 2010). These problematics have been threatening the provision of ecosystem services by the Lake Soyang watershed. The Four Major Rivers Restoration Project targeted these problematics and furthered progress towards the sustainable management of water. Nevertheless, the achievement of this goal and the completion of the core tasks of this project require additional progress (Kang and Park, 2015; Lah et al., 2015). Although this doctoral project was not an official contribution to the Four Major Rivers Restoration Project, its results should provide accurate and relevant information for the sustainable management of water in the Lake Soyang watershed.

In recent decades, increasing trends of sediment load, nutrient load, and consequent turbidity and eutrophication of Lake Soyang have been observed (Cho et al., 1991; Kim and Jung, 2007; Kim et al., 1995; Kim et al., 2001). These trends are related to increasing rates of soil erosion and non-point source pollution within the watershed (Park et al., 2010). The development of agriculture in highland areas of the watershed has been a major factor in the increase in sediment load. In these areas, steep slopes prevail and a change in land cover from forest to agricultural field concurrent with the tilling of the land is usually followed by a substantial increase in the average rate of soil erosion (Yang et al., 2010). In addition, the high levels of fertilizer application practiced in the watershed and the production of animal manure result in the massive input of nutrients to the system, and ultimately to Lake Soyang and downstream regions (Kim et al., 2001). The transport of sediment and nutrients from agricultural areas to water bodies of the watershed is greatly enhanced by the occurrence of surface runoff during heavy rainfall events (Park et al., 2010). The precipitation intensity of typhoon- and East Asian summer monsoon (EASM)-related events can easily exceed the infiltration capacity of agricultural soils, resulting in the substantial production of surface runoff. In fact, most the inputs of sediment and nutrients to water bodies occur during and shortly following rainfall events of the EASM (Jo et al., 2010; Kim et al., 2000; Park et al., 2011). Figure 1.1 depicts the hypothesized processes of Lake Soyang and highlights the seasonality of these inputs.

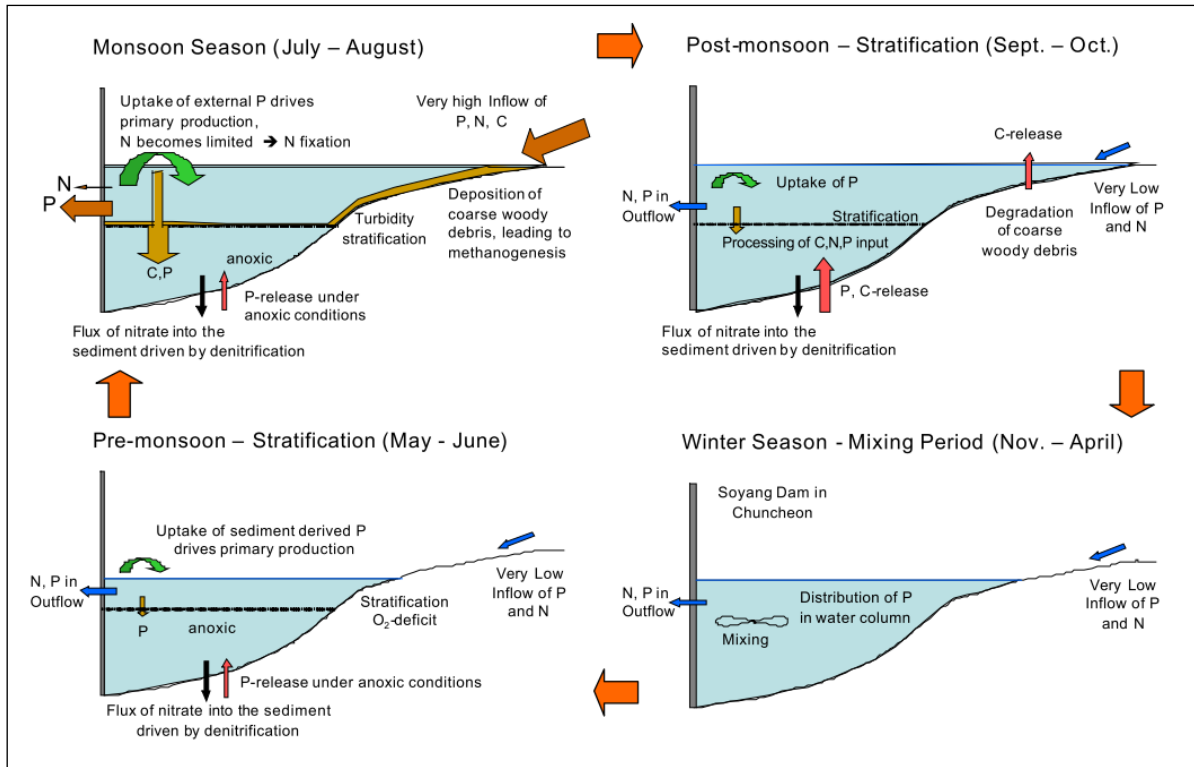


Figure 1.1. Hypothesized hydrological and chemical processes of Lake Soyang over an annual cycle (from Peiffer et al., 2012).

Although the bulk of the sediment and nutrient inputs to Lake Soyang originates from agricultural non-point sources, most of the water input to the lake originates from forested catchments, as more than 90% of the Lake Soyang watershed is covered by forests (KFS, 2010). In this sense, the water balance and quality of Lake Soyang are tightly linked to the hydrological processes occurring within these catchments. From a scientific point of view, an important question to be answered is: How are the hydrological and chemical processes within the Lake Soyang watershed coupled to the Lake Soyang internal chemical processes influencing water quality? This doctoral project aimed at providing a part of the answer by studying some of the hydrological processes occurring within typical forested catchments of the watershed. This project was realized with the conviction that understanding and assessing these processes are pre-requisites to providing suggestions and guidelines for the sustainable management of water in the Lake Soyang watershed.

1.1.2. Runoff generation and water quality of forested catchments of the East Asian summer monsoon region

The East Asian summer monsoon (EASM) region extends over vast expanses of forested catchments (FAO, 2015; Yihui and Chan, 2005). Across these catchments, analogous patterns of runoff generation and water quality arise from similarities in climate, soil, topography and vegetation.

Runoff generation in forested catchments of the EASM region has been studied for decades. The proposal of many perceptual and conceptual models of runoff generation and their relative agreement have helped to increase knowledge of the subject and guide subsequent research (Asano et al., 2002; Fujimoto et al., 2008; Katsuyama et al., 2009; Sidle et al., 2000; Sidle et al., 2001; Uchida et al., 2003; Uchida et al., 2006). The major processes inferred by these models vary in accordance with hydrological conditions and are summarized below. Figure 1.2 depicts the major water fluxes and runoff generation processes in forested catchments.

- Dry conditions:

- Dominance of groundwater flow
- Overland flow and subsurface flow from the riparian area
- Throughfall infiltrates soil and slightly replenishes soil moisture
- Channel interception

- Shift from Dry to Wet conditions:

- Substantial replenishment of soil moisture
- Mix of event water with pre-event soil water
- Formation of transient saturated zones
- Preferential flow organization, expansion and threshold response
- Connection of the hillslope area to the rest of the catchment through subsurface flow

- Wet conditions:

- Overland flow (infiltration-excess and saturation-excess)
- Importance of preferential flow from the hillslope area
- Hydrological connectivity of the entire catchment

- Wet conditions (continued)

- Transient saturated zones expand and discharge
- Channel expansion
- Recharge of the saturated zone

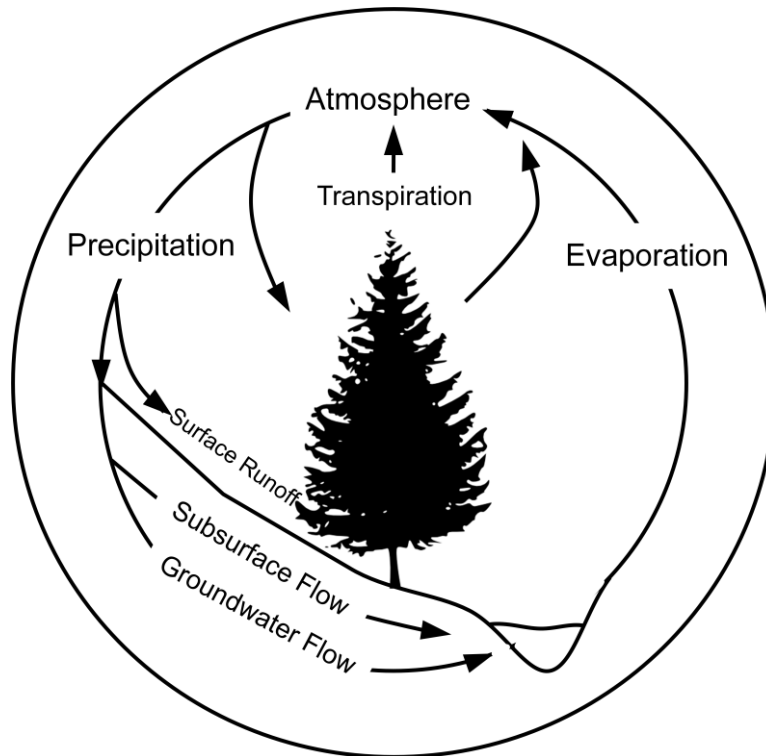


Figure 1.2. Major water fluxes and runoff generation processes in forested catchments (adapted from Brown, 1980).

Runoff generation processes can also vary with topography (Freer et al., 2002), landscape elements (McGlynn and McDonnell, 2003), vegetation (Jencso and McGlynn, 2011) and forest management practices (Dung et al., 2012; Sidle, 2006). What characterizes runoff generation in forested catchments of the EASM region is the combination of:

- the prompt mix of high amounts of event water with pre-event water,
- preferential flow through the macropores of steep soils,
- the transient connectivity of the hillslope area to the rest of the catchment,
- a pronounced seasonal partitioning in the contributions to runoff of subsurface flow and groundwater flow, and
- the low storage capacity of catchments.

Some of the concepts followed in this doctoral project were very well presented by Tsuboyama (2006), who conducted some experiments during the EASM and reported on transient saturated zones, the contribution from different landscape elements, and threshold responses. For storm events similar to those of the EASM, Gomi et al. (2010) reported on varying flow path dominance and the contribution at variable drainage scales. Choi et al. (2010) correlated storm event characteristics to event water contribution and reported large differences between events of the EASM. The findings of Kim et al. (2012), who coupled the ecohydrological and biogeochemical functions of a forested catchment, stress the importance of the linkages between these functions. In fact, temporal and spatial variability in runoff generation has been known to influence the water quality of forested catchments. For example, Tsujimura et al. (2001) reported that solute concentrations of runoff changed with the contribution of subsurface flow, being lowest at high contribution during rainfall events. However, the total outputs of nutrients are usually much higher for events than at low-flow conditions. Zhang et al. (2008) reported higher pollution loads at higher runoff volumes, for twenty-three forested catchments over a period extending beyond the EASM. Bartsch et al. (2013) established a link between the export of organic carbon and subsurface flow. Also, the findings of Asano et al. (2009) shed light on the coupling between the spatial and temporal patterns of water quality.

Numerous studies on the export of nutrients and organic matter from forested catchments of the EASM region have been conducted, mostly on the export of dissolved and particulate organic carbon (DOC and POC; Bartsch et al., 2013; Jeong et al., 2012; Jung et al., 2012; Jung et al., 2014; Kim et al., 2007; Kim et al., 2010; Lee et al., 2015; Shibata et al., 2001; Yang et al., 2015; Yoon et al., 2010). Organic carbon can strongly influence water quality through the regulation of biological processes (Kim et al., 2000), although the export of DOC and POC in runoff is usually a minor component of the carbon cycle of forest ecosystems (Kim et al., 2007; Lee et al., 2007). Kim et al. (2010) reported that 50% of the annual export of DOC and 80% of the annual export of POC from a small catchment occurred during the EASM, and corresponded to ~10% of the net ecosystem carbon exchange. The bulk of these exports usually occurs during rainfall events of the EASM, as concentrations in runoff have been reported to increase with discharge but also to display patterns of hysteresis (Bartsch et al., 2013; Jeong et al., 2012; Jung et al., 2014; Lee et al., 2015). The increase in concentration is usually much more pronounced for POC than for DOC, which is related to the process of surface erosion and subsequent transport of organic carbon to water bodies

(Jung et al., 2012). In this sense, as previously mentioned, runoff generation can influence the export of DOC and POC. One of the most reported findings on this subject is that subsurface flow in shallow soil layers increases the export of organic carbon in comparison with groundwater flow, as an important pool of organic carbon is usually present in these soil layers (Bartsch et al., 2013; Jeong et al., 2012; Kim et al., 2007; Yang et al., 2015).

The overall influence of the EASM was seldom reported and more focus should be directed towards the integrity of its influence on runoff generation and water quality of forested catchments. Such information could possibly well fit the needs of hydrological models aiming at partitioning the water budget of the Lake Soyang watershed. A good example of such a model is the Soil and Water Assessment Tool (SWAT) model, which has been widely used in South Korea (Shope et al. (2014) presented a solid assessment of the SWAT in a mountainous region of the Lake Soyang watershed). Although decades of research have strengthened the foundations and pushed the frontiers of forest hydrology in the EASM region, especially in Japan and South Korea, hydrological conditions are evolving and new challenges in water management lie ahead in time. This is particularly the case where water problematics have already emerged. In this sense, this doctoral project sought to analyse some of the major features of runoff generation and water quality of typical forested catchments of the Lake Soyang watershed. This was realized over periods extending beyond the duration of the EASM, and also for major rainfall events. To this end, the results of physical measurements, chemical analyses and isotopic analyses were jointly analysed. One of the major analytical techniques applied in this project is described in section 1.1.3.

1.1.3. The tracer-based hydrograph separation technique

Hydrograph separation can be defined as the process of separating streamflow into its different components, whether spatial or temporal. The development and application of the hydrograph separation technique has been motivated by an interest in deriving information on runoff generation processes from the hydrograph and from water quality. Some applications of this technique have made use of graphical and filtering methods to separate streamflow into its components of baseflow and direct runoff (Barnes, 1940; Chapman, 1999; Eckhardt, 2005; Hewlett and Hibbert, 1967; Linsley et al., 1975; Nathan and McMahon, 1990; Szilagyi and Parlange, 1998). However, as Beven (2001), Freeze (1972), Furey and Gupta (2001) and Hewlett and Hibbert (1967) mentioned, most of these methods lack a physical basis and are, to some extent, arbitrary. Furthermore, there has been a certain level of inconsistency in

terminology and in the definitions of baseflow and direct runoff, reducing the comparability of studies (Kulandaiswamy and Seetharaman, 1969). As opposed to most of the previously mentioned applications of this technique, tracer-based hydrograph separation can be considered to be both physically- and chemically-based; physically-based because it is based on the mass balance approach (Buttle, 1994; Pearce et al., 1986; Pinder and Jones, 1969; Sklash and Farvolden, 1979); chemically-based because it makes use of water quality data. Although inconsistency in terminology and definitions can still be an issue, the application of this technique has resulted in remarkable progress at deriving information on runoff generation processes, especially in combination with hydrometric data (Bonell, 1998; Hooper, 2001; Inamdar, 2011; Kirchner, 2003; Lischeid, 2008; Rice and Hornberger, 1998).

The tracer-based hydrograph separation technique makes use of tracers such as ions, chemical compounds, stable isotopes, temperature and other water quality parameters to solve mixing equations based on the mass balance approach. Following this approach, streamflow is considered as a mixture of different components and its tracer values are determined by the mixing proportions of the components and their original tracer values. The use of conservative tracers which linearly mix is intrinsic to this technique, and the following basic assumptions underlie this technique (Buttle, 1994; Inamdar, 2011; Lischeid, 2008):

- spatial invariance of flow component tracer values,
- temporal invariance of flow component tracer values,
- distinct flow component tracer values for at least one tracer, and
- unconsidered flow components either have similar tracer values or do not substantially contribute to streamflow.

There are additional assumptions if streamflow is to be separated into its pre-event and event components (Buttle, 1994; Sklash and Farvolden 1979):

- surface storage does not substantially contribute to streamflow, and
- soil water either does not substantially contribute to streamflow or has similar tracer values to those of groundwater.

Potential streamflow components can be classified in spatial and temporal components (Genereux and Hooper, 1998). Spatial components refer to geographical positions where water was located before it contributed to streamflow, such as the hillslope, toeslope, riparian, floodplain and wetland areas of a catchment. Spatial components can also be distinguished by

soil horizons. Since water can contribute to streamflow directly from its original geographical position, these components have often been considered to infer water flow paths, termed “*historical aspects*” by Sklash and Farvolden (1979). Temporal components refer to the timing of contributions of water to streamflow, and can only be distinguished for streamflow of which at least a part directly originates from precipitation or snowmelt events. The pre-event component is defined as liquid water that was present in the catchment before a precipitation or snowmelt event (soil water and/or groundwater), and the event component is defined as the direct contribution of an event to streamflow (precipitation, throughfall, snowmelt). Usually (but not restrictively), stable isotopes are used to separate streamflow into its temporal components and geochemical tracers are used to separate streamflow into its spatial components (Inamdar, 2011).

The tracer-based hydrograph separation technique has been greatly improved through the years, in part with the use of various tracers, the principal component analysis (PCA), the end-member mixing analysis (EMMA), diagnostic tools, and with the quantification of uncertainty and the identification of more explicit spatial components (Christophersen et al., 1990; Christophersen and Hooper, 1992; Genereux, 1998; Hooper, 2003; Hooper et al., 1990; Inamdar, 2011; Klaus and McDonnell, 2013). This technique has its strengths and weaknesses. It can provide information on integrated catchment responses, which is particularly useful for the calibration and validation of catchment-scale hydrological models. Depending on the flow components of interest, it can also provide information on the responses of different landscape elements, soil horizons, as well as saturated zones and unsaturated zones. Such information can help to identify catchment areas where runoff generation processes may differ from pre-conceptualized ideas and where further investigation could help to improve distributed hydrological models. Specific portions of the hydrograph and their associated processes can also be identified for further investigation. Combining the results of a tracer-based hydrograph separation with hydrometric data can enhance the study of water sources and flow paths and, ultimately, the development of mechanistic models of runoff generation. Hydrometric data can also be used to validate tracer-based results. As previously mentioned, this technique is underlain by several assumptions. A major weakness of this technique may be the considerable time and resources required to test the satisfaction of these assumptions. More often than not, the satisfaction is assumed and not tested, undermining the validity of the application of this technique (Buttle, 1998; Lischeid, 2008). In addition, depending on the flow components and scales of interest,

considerable time and resources may be required to sample flow components and analyse them for tracers. Even though the use of PCAs, EMMA and diagnostic tools has improved this technique, a certain level of subjectivity remains in the selection of tracers and identification of the most likely flow components. Finally, there is a growing consensus that the spatial components of streamflow may not necessarily infer water flow paths, but rather only correspond to the last geographic position of water before it contributed to streamflow (Inamdar, 2011).

The tracer-based hydrograph separation technique has been applied in forested catchments of the East Asian summer monsoon (EASM) region (Choi et al., 2007; Choi et al., 2010; Fujimoto et al., 2008; Fujimoto et al., 2011; Gomi et al., 2010; Katsuyama et al., 2001; Katsuyama et al., 2009; Kim et al., 2007; Kim et al., 2010; Kim and Yoo, 2007; Kubota and Tsuboyama, 2003; Lee et al., 2006; Yang et al., 2015). In the majority of cases, this technique was only applied to individual rainfall events. Due to the magnitude of the changes in hydrological conditions induced by the EASM, the satisfaction of several underlying assumptions has been difficult to prove for temporal scales greater than individual events. In these catchments, tracer values of flow components may greatly vary, as event water may easily infiltrate soils and mix with pre-event water. Hydrological connectivity between landscape elements and between soil layers may enhance the mix of flow components and render their differentiation complex. Moreover, the combined spatial heterogeneity and mostly accidented terrain of the EASM region constrain the ability to conduct spatially distributed, high-frequency sampling and, consequently, identify flow components and prove the satisfaction of the underlying assumptions.

This doctoral project aimed at applying the tracer-based hydrograph separation technique at a forested catchment for the entire duration of the EASM, while maximizing the satisfaction of its underlying assumptions. To begin with, the spatial arrangement of landscape elements within the catchment was analysed, and the temporal variability of the EASM as well. The experimental setup and sampling frequency were set accordingly. Then, some of the most recently developed methods in the application of this technique were rigorously applied. Finally, the analysis of the results was realized taking into account the limitations of this technique.

1.2. Objectives and hypotheses

The general objective of this doctoral project was to characterize and quantify the influence of the East Asian summer monsoon (EASM) on hydrological dynamics of forested headwater catchments of the Lake Soyang watershed. “Hydrological dynamics” were defined as the natural patterns of variation in runoff generation, hydrological fluxes and water quality. This characterization and quantification should further the understanding of the overall influence of the EASM in these patterns, and provide relevant and accurate information for the estimation and prediction of the water budget and its partitioning, as well as the water quality, of the Lake Soyang watershed. In order to attain the general objective, a set of specific objectives was derived and pursued, and specific hypotheses were tested.

The first specific objective was **to quantify the influence of the EASM on the water sources and flow paths of a forested headwater catchment, and characterize its overall influence on the associated runoff generation processes** (Chapter 2). The following hypothesis was stated:

- A shift in water sources and flow paths can be induced by the EASM.

The second specific objective was **to compare the influence of two hydrologically contrasting years of the EASM on water fluxes and quality of a forested headwater catchment** (Chapter 3). The following hypothesis was stated:

- The strength of the EASM influences water fluxes and quality of the catchment.

The third specific objective was **to assess the effects of forest cover type on the fluxes of organic matter in runoff induced by rainfall events of the EASM** (Chapter 4). The following hypotheses were stated:

- The fluxes of dissolved and particulate organic matter (DOM and POM) substantially differ between catchments of the mixed and the deciduous forest cover type.
- The quality and quantity of DOM and POM in throughfall, forest floor percolates, soil solution and runoff significantly differ between both catchments.

1.3. Study area and sites

The Lake Soyang watershed is located in the north-east of South Korea, and a small portion is located in the south-east of North Korea (Fig. 1.3). It has a total area of 2791 km². Elevation ranges from 80 to 1645 m and averages 637 m. The watershed is mostly mountainous (Fig. 1.4), and the average slope is fairly high at 15.9°. Most of the watershed is underlain by either orthogneiss belonging to the Gyeonggi gneiss complex or granitic gneiss belonging to the Gyeonggi massif (Lee and Cho, 2012). Soils are generally Cambisols of loam texture (NIAS, 2016). Average annual precipitation and temperature are 1321 mm and 10.5 °C, and the precipitation from June through August accounts on average for 60.5% of the annual precipitation (1981–2010; Chuncheon-si, Inje-gun and Hongcheon-gun averages; KMA, 2016). Forest accounts for 90.1% of land cover and is divided into 25.4% of coniferous stands, 51.8% of deciduous stands, and 22.8% of mixed stands (KFS, 2010). The watershed is scarcely inhabited with an approximate population of 74 000 and a density of ~26.5 inhabitants per km², a low figure compared to the national average of 503 inhabitants per km². Lake Soyang is the deepest reservoir of South Korea and has the greatest effective storage and total storage volume of all South Korean reservoirs (Hong et al., 1989).

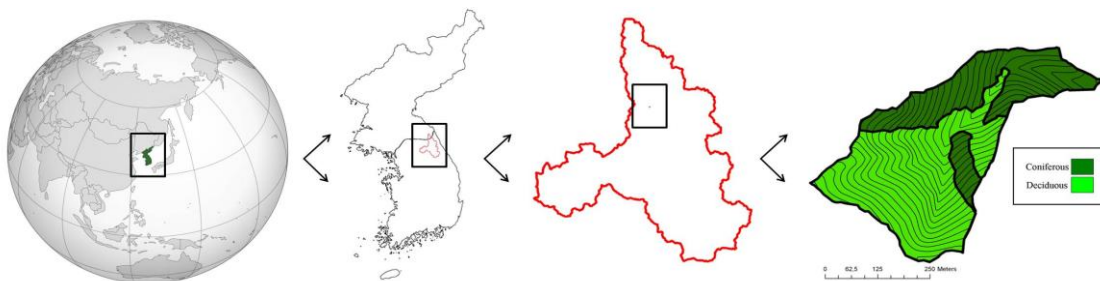


Figure 1.3. Maps of Asia, Korea, the Lake Soyang watershed and the first study site.

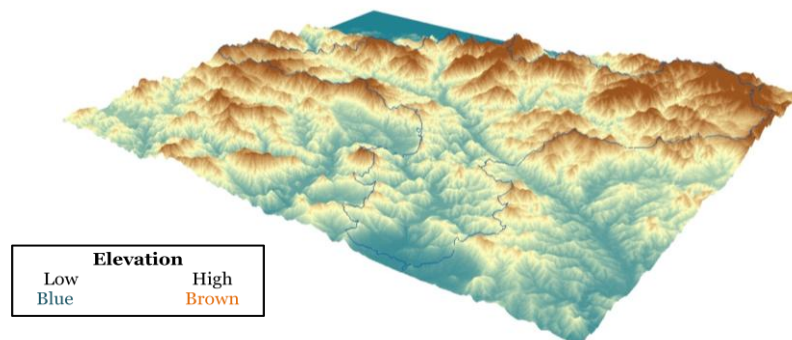


Figure 1.4. Topography of the Lake Soyang watershed. The watershed boundary is delineated with a thin blue line.

The first study site is located in the northern part of the Lake Soyang watershed (Fig. 1.3). In the first place, the author of this dissertation conducted an extensive search for sites that corresponded to the requirements of this doctoral project. Through the search for sites, the author of this dissertation developed a good sense of the natural environment of the region, and accordingly chose a site which is representative of the region in terms of catchment size, topography and vegetation. The site consists of a small (0.16 km^2) forested headwater catchment drained by a perennial stream of variable extent. Three well defined landscape elements compose the catchment: the hillslope area, the toeslope area, and the riparian area. The hillslope area dominates the catchment. The toeslope area was considered an important element of water flow, as stated by Lischeid (2008), and was defined as the lowest portion of the hillslope. The riparian area is narrow and stretches along the middle and upper sections of the streambed. The bedrock consists of orthogneiss. The soil is a Eutric Cambisol of loam texture, and is characterized as well to excessively drained. The catchment is covered at 61.3% by a purely deciduous stand and at 38.7% by a purely coniferous stand (see Fig. 1.5). This site was used for the studies presented in Chapter 2, Chapter 3 and Chapter 4 (in Chapter 4, the site is referred to as the “mixed watershed”).

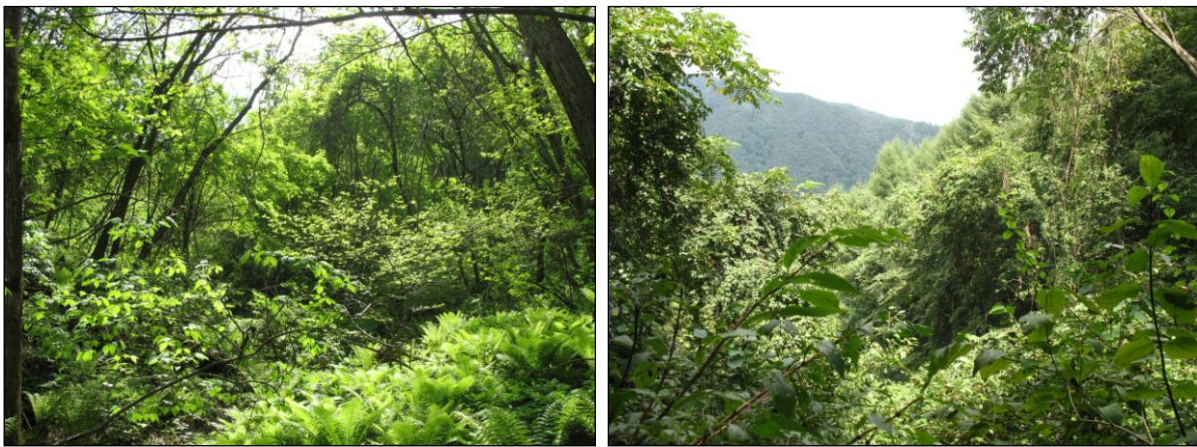


Figure 1.5. Pictures of the vegetation and topography at the first study site.

The second study site is located within the Haeon catchment, ~6 km north-west of the first study site. It also consists of a small (0.39 km^2) forested headwater catchment drained by a perennial stream. This site has been extensively used for various studies by the team of Prof. Dr. Bomchul Kim of the Department of Environmental Science of Kangwon National University. The site is composed of the same landscape elements as the first study site, and has an average slope of 24° . The soil is shallower than at the first site and characterized as

excessively drained. Bedrock outcrops cover a substantial proportion of the catchment area. The site is completely covered by deciduous stands. This site was used for the study presented in Chapter 4, and is referred to as the “deciduous watershed”.

1.4. Methods

The study period covered the months of June, July and August 2013, and the same months of 2014. At the first study site, a transect was established with three plots from the hillslope, to the toeslope, to the riparian area within the lower part of the catchment. At each plot, soil water was sampled at a minimum of four depths at least once per 2 days, piezometric head was measured at two depths at a 5-min frequency, and soil moisture (i.e. volumetric soil-water content) was measured at three depths (10, 30 and 50 cm) at a 5-min frequency. Piezometric head was also measured in the lower part of the riparian area. Two additional plots were established in the catchment; one in the coniferous and one in the deciduous part of the catchment. At these two plots, forest floor leachate and soil water (50-cm depth) were sampled at least once a week. Samples of soil organic horizons were collected at both plots, as well as samples of mineral soil. At the second study site, an identical plot to these two additional plots was established.

At both sites, stream discharge was measured at the outlet of the catchment at a 5-min frequency, as well as water temperature and electrical conductivity (EC). Stream water was sampled at least once per 2 days and, during and following major rainfall events, at least every 2 hours. An in situ measurement of pH was made at the collection of a subset of samples. At the first site, samples were also collected from two intermittent springs, following their activation. At both sites, precipitation and throughfall were measured following every rainfall event using passive collectors, from which samples were collected at the same frequency. Site characterization was realized by conducting soil depth measurements, soil infiltration capacity measurements and forest inventories. At the first site, temperature (°C), relative humidity (%) and throughfall (mm) were measured at a 5-min frequency using a weather station installed under the canopy. Data of temperature and precipitation measured by the automated weather stations number 594 and 518 of the Korea Meteorological Administration were acquired.

The concentrations of calcium (Ca^{2+}), magnesium (Mg^{2+}), potassium (K^+), sodium (Na^+), chloride (Cl^-), nitrate (NO_3^-), sulphate (SO_4^{2-}), silica (SiO_2), DOC and total dissolved nitrogen (TDN), as well as EC and the relative abundance of deuterium (^2H), were measured for a subset of water samples. For another subset of water samples, the concentrations of DOC, TDN, NO_3^- and ammonium (NH_4^+) were measured, and the concentration of dissolved organic nitrogen (DON) was calculated as the difference between total nitrogen and $\text{NO}_3^- + \text{NH}_4^+$. The particulate material of the samples was analysed for POC and particulate organic nitrogen (PON). For the same subset, the absorption spectra of DOM were measured at wavelengths from 200 to 600 nm, ultraviolet absorbance was measured at 280 nm, fluorescence intensity was measured, and specific ultraviolet absorbance (SUVA_{280}) as well as the humification index (HIXem) were calculated. The relative abundances of ^{13}C and ^{15}N of DOC and TDN were measured. The texture of soil samples was measured by sedimentation, and pH, total carbon and total nitrogen of the samples were measured.

The major hydrological fluxes and conditions were estimated at the catchment scale, including daily potential evapotranspiration which was estimated with the Priestley-Taylor equation (Priestley and Taylor, 1972). Most of these fluxes and conditions were estimated at the temporal scale of the East Asian summer monsoon (EASM) and of individual rainfall events. Tracer-based hydrograph separations were thoroughly performed, coupled with PCAs and EMMA, and the results were jointly analysed with hydrometric data. The fluxes of solutes in runoff, as well as those of POC and PON, were estimated. Correlations were derived between chemical properties of organic matter in runoff, solute concentrations of runoff, solute fluxes in runoff, and discharge. Correlations were also derived between runoff, antecedent soil moisture index and precipitation. The collected data and results of the analyses were compared between both years, between individual rainfall events, between both sites, between soil layers, and between possible sources of runoff.

1.5. Results and discussion

The East Asian summer monsoon (EASM) yielded 826 mm of precipitation in sixteen rainfall events and 94 mm in three events in 2013 and 2014, respectively. Only the three major events had return periods above one year (3.41, 2.17 and 1.25 years), and they occurred in 2013. The event of highest precipitation yielded 173 mm in 41 hours, at the deciduous

catchment. The highest throughfall intensity was measured at the mixed catchment at 113 mm h⁻¹ over a 5-min period. The proportion of throughfall to precipitation was similar between years of the EASM at the mixed catchment. These years of the EASM were, respectively, 206 and 32% of the average in precipitation since 1973, and were also both warmer than the average. South Korea experienced a severe drought during the 2014 summer. These years are comparable to the future predicted extremes in hydroclimatic conditions, and valuable for the partitioning of the water budget of the Lake Soyang watershed at the scales of events and seasons.

Soil moisture varied mainly at the rhythm of rainfall events and, during the 2013 EASM, a replenishment of soil moisture was topped and followed by a month-long period of relatively high values. Following the EASM, values gradually decreased at all areas. In 2014, a month-long period of relatively low values was followed by a drastic but gradual two-weeks-long decrease in values at all areas and depths. The values only reached those of 2013 following the EASM, except at 50-cm depth, where values in 2014 were the lowest measured. Soil moisture at this depth was much higher and much more responsive in 2013 than 2014. At the hillslope and riparian areas, unsaturated hydraulic conductivity at this depth varied over a wide range only in 2013. At approximately 50-cm depth, saturated hydraulic conductivity was higher than at the next upper layer, and was likely much higher due to the high fraction of coarse gravel and stones. From the combination of the steepness of the hillslope area, the percolation of newly added throughfall, and the proximity to bedrock, transient saturation and subsurface flow were likely induced. The observed threshold response of runoff to precipitation supported the existence of a rapid subsurface flow component. Else, groundwater flow was likely the major flow path of water. A slower component of soil matrix flow from the near-stream area was also likely present at shallower depths. A water table was measured only once for a few hours in the lower part of the riparian area, in 2013. However, a saturated area located in the streambed and its vicinity likely contributed to runoff, as groundwater was the main source of runoff during the EASM. The difference in the average daily mean contribution of groundwater between both years of the EASM is attributable to the much higher contribution of other sources in 2013.

The relative difference in runoff between both years of the EASM is much higher than the relative difference in precipitation. It can be seen in the difference in the runoff coefficients of both years, and involves that precipitation was converted to runoff through various generation processes and was also transferred through evapotranspiration. Saturated

flow and/or preferential flow probably occurred at the hillslope area, as springs emerged from the bottom of hillslopes during and following major rainfall events. In 2013, their first activation occurred around the time when a sudden shift from the dominance of groundwater flow towards higher contributions of subsurface flow from the hillslope and the riparian area likely occurred. A connection of the hillslope area with the rest of the catchment likely occurred and was sustained, and soil water also likely recharged the saturated area. Through forest litter, the forest cover type apparently had effects on the infiltration of throughfall in the soil and on the mobilization of DOM. The total fluxes of DOC and DON were higher at the deciduous (16 kg C ha^{-1} and 0.5 kg N ha^{-1}) than at the mixed catchment (6.7 kg C ha^{-1} and $0.26 \text{ kg N ha}^{-1}$), and the proportion of DOC in runoff originating from forest floor leachate was higher at the former. A higher proportion of near-surface flow in DOC-rich layers could be responsible for the higher total fluxes.

The fluxes of all solutes were over one order of magnitude greater in 2013 than in 2014, even though average solute concentrations were higher in 2014. The fluxes of DOC, DON and $\text{NO}_3\text{-N}$ in runoff were linearly correlated to discharge at both sites. In 2013, an initial flushing event was observed and followed by a dilution effect of stream water, as a shift in runoff generation processes likely occurred. At the deciduous catchment, an initial flush of POM was observed during the first major rainfall event. Results suggest that a threshold of 157 mm in the sum of antecedent soil moisture and precipitation of an event must be reached in order to induce a substantial contribution of hillslope soil water to runoff. This was supported by the clustering of the runoff coefficients of events above and below the threshold. The concentrations of DOC and DON also displayed a threshold response to discharge at high values. The higher average $\text{NO}_3\text{-N}$ concentration in 2014 could be due to a higher rate of production associated with a higher average stream water temperature. It is possible that a larger N uptake by deciduous trees than by coniferous trees reduced the available amount of N for leaching at the deciduous catchment.

The separated hydrographs of a series of individual rainfall events reveal the progression of the influence of the EASM on runoff generation (Figure 1.6). The threshold was reached shortly following the 5th event. Thereafter, the component of groundwater was less important, and the components of soil water were highly responsive to the input of throughfall. Throughout the series of events, the contribution of soil water at the riparian area was extending in time following the events. Even though the riparian area accounts for only 2.3% of the catchment area, its average relative contribution to runoff was substantial. The

accumulation of soil water at this area and its subsequent discharge to runoff might have occurred, as well as the recharge of the saturated zone by soil water of the riparian area. This is likely responsible for the high and continuous relative contribution from this area following the 2013 EASM.

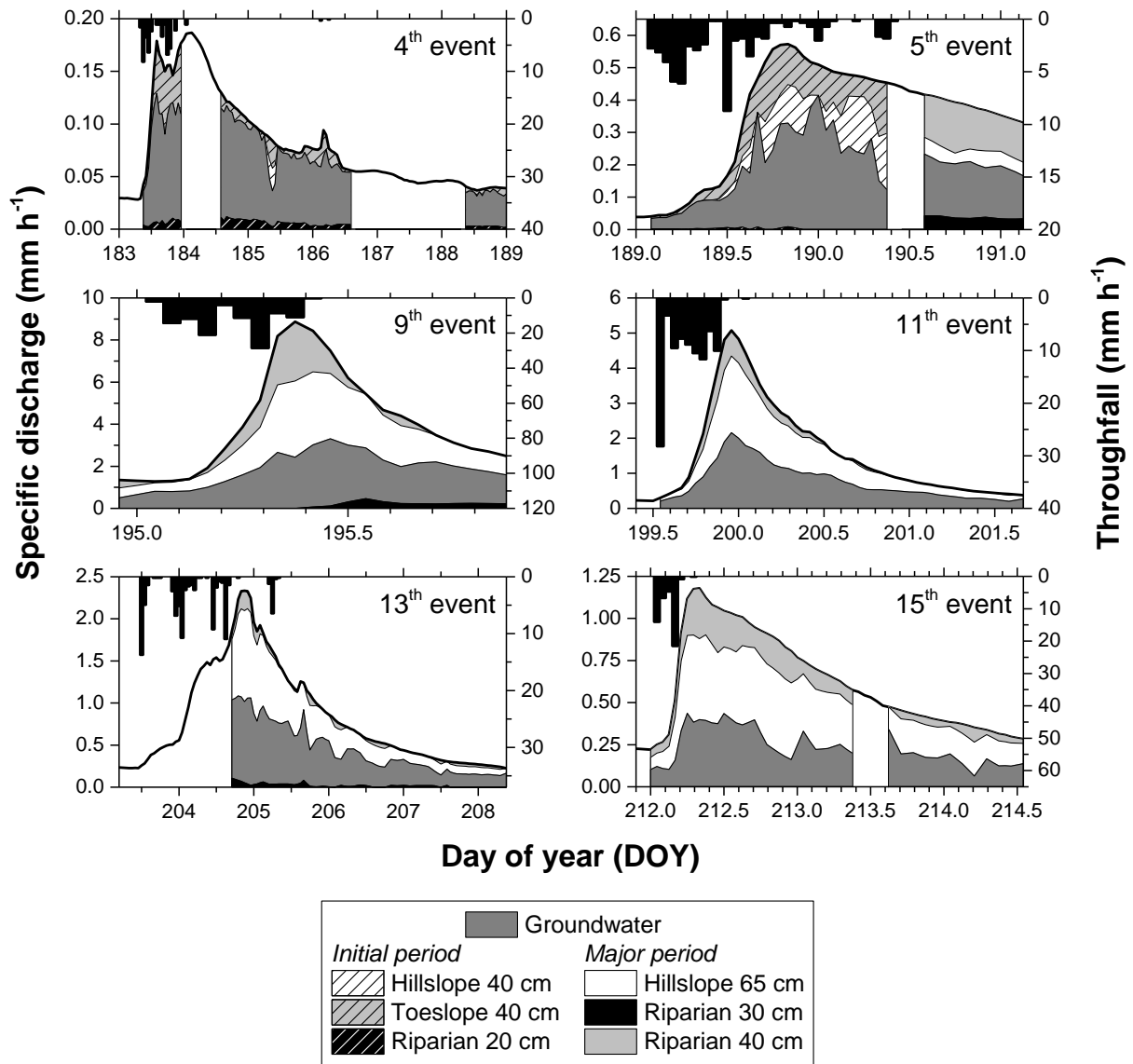


Figure 1.6. Specific discharge (hourly mean), throughfall (hourly) and contributions of end-members to runoff (bihourly) as a function of time for selected major rainfall events of the 2013 summer monsoon. Blank areas correspond to missing values.

1.6. Conclusions

It is concluded that the precipitation regime and the strength of the East Asian summer monsoon (EASM), as well as forest cover type, influenced the generation of runoff and water quality. The value this doctoral project adds to the fields of hydrology and biogeochemistry lies not only in the particularity of the region and climate component it concerns, but also in the realization of a thorough, spatiotemporal (two sites–two extreme years) analysis of high frequency data of ecosystem processes indicators. In space, this analysis was conducted at the scales of discrete soil depth, of the landscape element and of the catchment, and in time, it was conducted at the scales of individual rainfall event and of the EASM. This allowed for a detailed and comprehensive description of hydrological dynamics during the EASM, for their comparison between two hydrologically contrasting years of the EASM, and for their comparison between two forested cover types. The characterization of the overall influence of the EASM on the hydrological dynamics of forested catchments was based on the quantification of its influence on water fluxes, sources, flow paths and quality. The results suggest that the export of organic matter from forested catchments could possibly increase with the extremes in hydroclimatic conditions, and that drastic changes in runoff generation can occur during these extremes.

The results of this doctoral project have biogeochemical implications not only at the catchment-scale, but also for the Lake Soyang watershed. This was revealed by the particular hydrochemistry of Lake Soyang during both years of the study. The coupling of the ecohydrological and biogeochemical functions of forested catchments was highlighted. The results are also a contribution to the ongoing efforts to estimate the water budget and quality of the Lake Soyang watershed. Better estimations could help to improve water management and reach sustainable development. As stated by the United Nations (World Water Development Report 4 (2012)):

“Understanding the movement of water and the spatial and temporal variability of water availability are the most important aspects of water resources that need to be understood and incorporated in planning and management for resource sustainability”.

The project had some limitations in space and time. The experimental setup covered only parts of the catchments, and spatial variability within the catchments could not be assessed. Interyear variability in the EASM was only based two years of observation. Also, it

may be difficult to transmit the results to water managers of the Lake Soyang watershed, because of the language barrier.

It is recommend to pursue further studies in this field by enhancing the combination between hydrometric and hydrochemical data. The use of high- frequency, *in situ*, water-quality sensors can help in this direction. A valuable addition to the dataset would be the residence time of water, in order to estimate catchment storage. The results of carbon fluxes in runoff could be compared to those of atmospheric carbon fluxes, to have an overview of the carbon cycle in such catchments. The study of patterns of hysteresis can also provide further information on water sources and flow paths. Finally, it would be interesting to compare the effects of drought on the water cycle of Korean forests to those of other forests.

1.7. List of manuscripts and specification of contributions

First manuscript (Chapter 2)

Title	A sudden shift in runoff generation processes at a forested catchment as induced by the East Asian summer monsoon
Authors	Jean-Lionel Payeur-Poirier, Luisa Hopp, Stefan Peiffer
ORCID iDs	Payeur-Poirier:  http://orcid.org/0000-0001-8789-7110 Hopp: – Peiffer:  http://orcid.org/0000-0002-8326-0240
Status	In preparation
Contributions	Payeur-Poirier: concept and design of the study, field and laboratory work, data analysis, interpretation of results, writing of the manuscript Hopp: concept and design of the study, support of field work, interpretation of results, editing of the manuscript Peiffer: concept and design of the study, interpretation of results, editing of the manuscript

Samples were analysed at the Limnological Research Station, the Department of Hydrology and the Laboratory of Isotope Biogeochemistry of BayCEER at the University of Bayreuth, and at the Laboratory of the Institute of Landscape Ecology at the University of Münster. Payeur-Poirier is the corresponding author.

Second manuscript (Chapter 3)

Title	Water fluxes and quality of a forested catchment over two hydrologically contrasting years of the East Asian summer monsoon
Authors	Jean-Lionel Payeur-Poirier, Mi-Hee Lee, Luisa Hopp, Stefan Peiffer
ORCID iDs	Payeur-Poirier:  http://orcid.org/0000-0001-8789-7110
	Lee:  http://orcid.org/0000-0003-3330-0619
	Hopp: –
	Peiffer:  http://orcid.org/0000-0002-8326-0240
Status	In preparation
Contributions	Payeur-Poirier: concept and design of the study, field and laboratory work, data analysis, interpretation of results, writing of the manuscript Lee: support of field work, provision of data, editing of the manuscript Hopp: concept and design of the study, support of field work, interpretation of results, editing of the manuscript Peiffer: concept and design of the study, interpretation of results, editing of the manuscript

Samples were analysed at the Limnological Research Station, the Department of Hydrology, the Laboratory of Isotope Biogeochemistry and the Department of Soil Ecology of BayCEER at the University of Bayreuth, and at the Laboratory of the Institute of Landscape Ecology at the University of Münster. Payeur-Poirier is the corresponding author.

Third manuscript (Chapter 4)

Title Variability in runoff fluxes of dissolved and particulate carbon and nitrogen from two watersheds of different tree species during intense storm events

Authors Mi-Hee Lee, Jean-Lionel Payeur-Poirier, Ji-Hyung Park, Egbert Matzner

ORCID iDs Lee:  <http://orcid.org/0000-0003-3330-0619>

Payeur-Poirier:  <http://orcid.org/0000-0001-8789-7110>

Park:  <http://orcid.org/0000-0002-9083-2630>

Matzner: –

Status Published in *Biogeosciences*

Citation Lee, M.-H., Payeur-Poirier, J.-L., Park, J.-H., Matzner, E., 2016. Variability in runoff fluxes of dissolved and particulate carbon and nitrogen from two watersheds of different tree species during intense storm events. *Biogeosciences* 13, 5421-5432. DOI: [10.5194/bg-13-5421-2016](https://doi.org/10.5194/bg-13-5421-2016)

Contributions Lee: concept and design of the study, field and laboratory work, data analysis, interpretation of results, writing of the manuscript

Payeur-Poirier: support of field work, provision of data, editing of the manuscript

Park: concept and design of the study, data analysis, interpretation of results, editing of the manuscript

Matzner: concept and design of the study, data analysis, interpretation of results, editing of the manuscript

Samples were analysed at the Laboratory of Isotope Biogeochemistry, the Department of Soil Ecology and the Central Analytical Department of BayCEER at the University of Bayreuth. Matzner is the corresponding author.

References

- Asano, Y., Uchida, T., Ohte, N., 2002. Residence times and flow paths of water in steep unchannelled catchments, Tanakami, Japan. *J. Hydrol.* 261, 173–192. DOI: [10.1016/S0022-1694\(02\)00005-7](https://doi.org/10.1016/S0022-1694(02)00005-7)
- Asano, Y., Uchida, T., Mimasu, Y., Ohte, N., 2009. Spatial patterns of stream solute concentrations in a steep mountainous catchment with a homogeneous landscape. *Water Resour. Res.* 45, W10432. DOI: [10.1029/2008WR007466](https://doi.org/10.1029/2008WR007466)
- Bae, D.-H., Jung, I.W., Chang, H., 2008. Potential changes in Korean water resources estimated by high-resolution climate simulation. *Clim. Res.* 35, 213–226. DOI: [10.3354/cr00704](https://doi.org/10.3354/cr00704)
- Barnes, B.S., 1940. Discussion of analysis of runoff characteristics. *Trans. ASCE* 105, 106.
- Bartsch, S., Peiffer, S., Shope, C.L., Arnhold, S., Jeong, J.-J., Park, J.-H., Eum, J., Kim, B., Fleckenstein, J.H., 2013. Monsoonal-type climate or land-use management: Understanding their role in the mobilization of nitrate and DOC in a mountainous catchment. *J. Hydrol.* 507, 149–162. DOI: [10.1016/j.jhydrol.2013.10.012](https://doi.org/10.1016/j.jhydrol.2013.10.012)
- Beven, K.J., 2001. *Rainfall-Runoff Modelling – The Primer*. John Wiley & Sons Ltd., New York.
- Bonell, M., 1998. Selected challenges in runoff generation research in forests from the hillslope to headwater drainage basin scale. *J. Am. Water Resour. Assoc.* 34, 765–785. DOI: [10.1111/j.1752-1688.1998.tb01514.x](https://doi.org/10.1111/j.1752-1688.1998.tb01514.x)
- Brown, G.W., 1980. *Forestry and water quality*. O.S.U. Book Stores Inc., Corvallis.
- Buttle, J.M., 1994. Isotope hydrograph separations and rapid delivery of pre-event water from drainage basins. *Prog. Phys. Geogr.* 18, 16–41. DOI: [10.1177/030913339401800102](https://doi.org/10.1177/030913339401800102)
- Buttle, J.M., 1998. Fundamentals of small catchment hydrology, in: Kendall, C., McDonnell, J.J. (Eds.), *Isotope tracers in catchment hydrology*. Elsevier, pp. 1–49.
- Chapman, T., 1999. A comparison of algorithms for stream flow recession and baseflow separation. *Hydrol. Process.* 13, 710–714. DOI: [10.1002/\(SICI\)1099-1085\(19990415\)13:5<701::AID-HYP774>3.0.CO;2-2](https://doi.org/10.1002/(SICI)1099-1085(19990415)13:5<701::AID-HYP774>3.0.CO;2-2)
- Cho, K.-S., Kim, B.-C., Heo, W.-M., Kim, D.-S., 1991. Eutrophication of the major reservoirs in Korea. *Rep. Suwa Hydrobiol.* 7, 21–29.
- Choi, I.-H., Woo, N.C., Kim, S.-J., Moon, S.-K., Kim, J., 2007. Estimation of the groundwater recharge rate during a rainy season at a headwater catchment in Gwangneung, Korea. *Korean J. Agric. For. Meteorol.* 9, 75–87. DOI: [10.5532/KJAFM.2007.9.2.075](https://doi.org/10.5532/KJAFM.2007.9.2.075)
- Choi, H.T., Kim, K., Lee, C.H., 2010. The effect of antecedent moisture conditions on the contributions of runoff components to stormflow in the coniferous forest catchment. *J. Korean For. Soc.* 99, 755–761.

- Christophersen, N., Neal, C., Hooper, R.P., Vogt, R.D., Andersen, S., 1990. Modelling streamwater chemistry as a mixture of soilwater end-members—a step towards second-generation acidification models. *J. Hydrol.* 116, 307–320. DOI: [10.1016/0022-1694\(90\)90130-P](https://doi.org/10.1016/0022-1694(90)90130-P)
- Christophersen, N., Hooper, R.P., 1992. Multivariate analysis of stream water chemical data: the use of principal components analysis for the end-member mixing problem. *Water Resour. Res.* 28, 99–107. DOI: [10.1029/91WR02518](https://doi.org/10.1029/91WR02518)
- Committee on Green Growth, 2014. Green Growth Korea—Now & the Future. Available from <http://www.greengrowth.go.kr/> (accessed 06.06.2016)
- Dung, B.X., Gomi, T., Miyata, S., Sidle, R.C., Kosugi, K., Onda, Y., 2012. Runoff responses to forest thinning at plot and catchment scales in a headwater catchment draining Japanese cypress forest. *J. Hydrol.* 444, 51–62. DOI: [10.1016/j.jhydrol.2012.03.040](https://doi.org/10.1016/j.jhydrol.2012.03.040)
- Eckhardt, K., 2005. How to construct recursive digital filters for baseflow separation. *Hydrol. Process.* 19, 507–515. DOI: [10.1002/hyp.5675](https://doi.org/10.1002/hyp.5675)
- FAO (Food and Agriculture Organization of the United Nations), 2015. Global Forest Resources Assessment 2015—Country Report. FAO, Rome.
- Freer, J., McDonnell, J.J., Beven, K., Peters, N.E., Burns, D., Hooper, R., Aulenbach, B., Kendall, C., 2002. The role of bedrock topography on subsurface storm flow. *Water Resour. Res.* 38, 1269. DOI: [10.1029/2001WR000872](https://doi.org/10.1029/2001WR000872)
- Freeze, R.A., 1972. Role of subsurface flow in generating surface runoff: 1. Base flow contributions to channel flow. *Water Resour. Res.* 8, 609–623. DOI: [10.1029/WR008i003p00609](https://doi.org/10.1029/WR008i003p00609)
- Fujimoto, M., Ohte, N., Tani, M., 2008. Effects of hillslope topography on hydrological responses in a weathered granite mountain, Japan: comparison of the runoff response between the valley-head and the side slope. *Hydrol. Process.* 22, 2581–2594. DOI: [10.1002/hyp.6857](https://doi.org/10.1002/hyp.6857)
- Fujimoto, M., Ohte, N., Tani, M., 2011. Effects of hillslope topography on runoff response in a small catchment in the Fudoji Experimental Watershed, central Japan. *Hydrol. Process.* 25, 1874–1886. DOI: [10.1002/hyp.7943](https://doi.org/10.1002/hyp.7943)
- Furey, P.R., Gupta, V.K., 2001. A physically based filter for separating base flow from streamflow time series. *Water Resour. Res.* 37, 2709–2722. DOI: [10.1029/2001WR000243](https://doi.org/10.1029/2001WR000243)
- Genereux, D., 1998. Quantifying uncertainty in tracer-based hydrograph separations. *Water Resour. Res.* 34, 915–919. DOI: [10.1029/98WR00010](https://doi.org/10.1029/98WR00010)
- Genereux, D.P., Hooper, R.P., 1998. Oxygen and hydrogen isotopes in rainfall-runoff studies, in: Kendall, C., McDonnell, J.J. (Eds.), *Isotope tracers in catchment hydrology*. Elsevier, pp. 319–346.
- Gomi, T., Asano, Y., Uchida, T., Onda, Y., Sidle, R.C., Miyata, S., Kosugi, K., Mizugaki, S., Fukuyama, T., Fukushima, T., 2010. Evaluation of storm runoff pathways in steep nested catchments draining a Japanese cypress forest in central Japan: a geochemical approach. *Hydrol. Process.* 24, 550–566. DOI: [10.1002/hyp.7550](https://doi.org/10.1002/hyp.7550)

- Haga, H., Matsumoto, Y., Matsutani, J., Fujita, M., Nishida, K., Sakamoto, Y., 2005. Flow paths, rainfall properties, and antecedent soil moisture controlling lags to peak discharge in a granitic unchanneled catchment. *Water Resour. Res.* 41, W12410. DOI: [10.1029/2005WR004236](https://doi.org/10.1029/2005WR004236)
- Hewlett, J.D., Hibbert, A.R., 1967. Factors affecting the response of small watersheds to precipitation in humid areas. *For. Hydrol.* 1, 275–290.
- Hong, G. H., Kim, S. H., Kim, K. T., 1989. Watershed geochemistry of Lake Soyang, Korea. *Kor. J. Limnol* 22, 245–260.
- Hooper, R.P., Christophersen, N., Peters, N.E., 1990. Modelling streamwater chemistry as a mixture of soilwater end-members—An application to the Panola Mountain catchment, Georgia, USA. *J. Hydrol.* 116, 321–343. DOI: [10.1016/0022-1694\(90\)90131-G](https://doi.org/10.1016/0022-1694(90)90131-G)
- Hooper, R.P., 2001. Applying the scientific method to small catchment studies: a review of the Panola Mountain experience. *Hydrol. Process.* 15, 2039–2050. DOI: [10.1002/hyp.255](https://doi.org/10.1002/hyp.255)
- Hooper, R.P., 2003. Diagnostic tools for mixing models of stream water chemistry. *Water Resour. Res.* 39, 1055. DOI: [10.1029/2002WR001528](https://doi.org/10.1029/2002WR001528)
- Inamdar, S., 2011. The use of geochemical mixing models to derive runoff sources and hydrologic flow paths, in: Levia, D.F., Carlyle-Moses, D., Tanaka, T. (Eds.), *Forest hydrology and biogeochemistry. Synthesis of past research and future directions.* Springer, pp. 163–183.
- Jencso, K.G., McGlynn, B.L., 2011. Hierarchical controls on runoff generation: Topographically driven hydrologic connectivity, geology, and vegetation. *Water Resour. Res.* 47, W11527. DOI: [10.1029/2011WR010666](https://doi.org/10.1029/2011WR010666)
- Jeong, K.-Y., Lee, D.-R., Moon, J.-W., 2003. Analysis of seasonal water quality and quantity characteristics for Seolmacheon experimental watershed. *Proc. Joint Conf. Korea Water Environ. Assoc.*, 185–188. (in Korean)
- Jeong, J.-J., Bartsch, S., Fleckenstein, J.H., Matzner, E., Tenhunen, J.D., Lee, S.D., Park, S.K., Park, J.-H., 2012. Differential storm responses of dissolved and particulate organic carbon in a mountainous headwater stream, investigated by high-frequency, in situ optical measurements. *J. Geophys. Res.* 117, G03013. DOI: [10.1029/2012JG001999](https://doi.org/10.1029/2012JG001999)
- Jo, K.-W., Lee, H.-J., Park, J.-H., Owen, J.S., 2010. Effects of monsoon rainfalls on surface water quality in a mountainous watershed under mixed land use. *Korean J. Agric. For. Meteorol.* 12, 197–206. DOI: [10.5532/KJAFM.2010.12.3.197](https://doi.org/10.5532/KJAFM.2010.12.3.197)
- Jung, H.-S., Choi, Y., Oh, J.-H., Lim, G.-H., 2002. Recent trends in temperature and precipitation over South Korea. *Int. J. Climatol.* 22, 1327–1337. DOI: [10.1002/joc.797](https://doi.org/10.1002/joc.797)
- Jung, B.J., Lee, H.J., Jeong, J.J., Owen, J., Kim, B., Meusburger, K., Alewell, C., Gebauer, G., Shope, C., Park, J.H., 2012. Storm pulses and varying sources of hydrologic carbon export from a mountainous watershed. *J. Hydrol.* 440–441, 90–101. DOI: [10.1016/j.jhydrol.2012.03.030](https://doi.org/10.1016/j.jhydrol.2012.03.030)
- Jung, B.-J., Lee, J.-K., Kim, H., Park, J.-H., 2014. Export, biodegradation, and disinfection byproduct formation of dissolved and particulate organic carbon in a forested headwater

- stream during extreme rainfall events. *Biogeosci.* 11, 6119–6129. DOI: [10.5194/bg-11-6119-2014](https://doi.org/10.5194/bg-11-6119-2014)
- Kang, S.-K., Tenhunen, J., 2010. Complex terrain and ecological heterogeneity (TERRECO): Evaluating ecosystem services in production versus water quantity/quality in mountainous landscapes. *Korean J. Agric. For. Meteorol.* 12, 307–316. DOI: [10.5532/KJAFM.2010.12.4.307](https://doi.org/10.5532/KJAFM.2010.12.4.307) (in Korean)
- Kang, M.G., Park, S.W., 2015. An adaptive watershed management assessment based on watershed investigation data. *Environ. Manage.* 55, 1006–1021. DOI: [10.1007/s00267-014-0442-4](https://doi.org/10.1007/s00267-014-0442-4)
- Katsuyama, M., Ohte, N., Kobashi, S., 2001. A three-component end-member analysis of streamwater hydrochemistry in a small Japanese forested headwater catchment. *Hydrol. Processes* 15, 249–260. DOI: [10.1002/hyp.155](https://doi.org/10.1002/hyp.155)
- Katsuyama, M., Kabeya, N., Ohte, N., 2009. Elucidation of the relationship between geographic and time sources of stream water using a tracer approach in a headwater catchment. *Water Resour. Res.* 45, W06414. DOI: [10.1029/2008WR007458](https://doi.org/10.1029/2008WR007458)
- KFS (Korea Forest Service), 2010. Statistical Yearbook of Forestry. Korea Forest Service, Seoul. (in Korean)
- Kim, B.-C., Heo, W.-M., Hwang, G.-S., Kim, D.-S., Choi, K.-S., 1995. The distribution of phosphorus fractions in Lake Soyang. *Korean J. Limnol.* 28, 151–157. (in Korean)
- Kim, B., Choi, K., Kim, C., Lee, U.-H., Kim, Y.-H., 2000. Effects of the summer monsoon on the distribution and loading of organic carbon in a deep reservoir, Lake Soyang, Korea. *Water Res.* 34, 3495–3504. DOI: [10.1016/S0043-1354\(00\)00104-4](https://doi.org/10.1016/S0043-1354(00)00104-4)
- Kim, B., Park, J.-H., Hwang, G., Jun, M.-S., Choi, K., 2001. Eutrophication of reservoirs in South Korea. *Limnol.* 2, 223–229. DOI: [10.1007/s10201-001-8040-6](https://doi.org/10.1007/s10201-001-8040-6)
- Kim, B., Jung, S., 2007. Turbid storm runoffs in Lake Soyang and their environmental effect. *J. Korean Soc. Environ. Eng.* 29, 1185–1190. (in Korean)
- Kim, K., Yoo, J.-Y., 2007. Hydrograph Separation using Geochemical tracers by Three-Component Mixing Model for the Coniferous Forested Catchment in Gwangneung Gyeonggi-do, Republic of Korea. *J. Korean For. Soc.* 96, 561–566.
- Kim, S.-J., Lee, D., Kim, J., Kim, S., 2007. Hydro-biogeochemical approaches to understanding of water and carbon cycling in the Gwangneung forest catchment. *Korean J. Agric. For. Meteorol.* 9, 109–120. DOI: [10.5532/KJAFM.2007.9.2.109](https://doi.org/10.5532/KJAFM.2007.9.2.109)
- Kim, S., Kim, J., Kim, K., 2010. Organic carbon efflux from a deciduous forest catchment in Korea. *Biogeosci.* 7, 1323–1334. DOI: [10.5194/bg-7-1323-2010](https://doi.org/10.5194/bg-7-1323-2010)
- Kim, B.-S., Kim, B.-K., Kwon, H.-H., 2011. Assessment of the impact of climate change on the flow regime of the Han River basin using indicators of hydrologic alteration. *Hydrol. Process.* 25, 691–704. DOI: [10.1002/hyp.7856](https://doi.org/10.1002/hyp.7856)
- Kim, S.-J., Choi, H.T., Kim, K., Lee, C., 2012. Ecohydrology and biogeochemistry in a temperate forest catchment, in: Blanco, J.A. and Lo, Y.-H. (Eds.), *Forest ecosystems—more than just trees*. InTech, pp. 181–208.

- Kirchner, J.W., 2003. A double paradox in catchment hydrology and geochemistry. *Hydrol. Process.* 17, 871–874. DOI: [10.1002/hyp.5108](https://doi.org/10.1002/hyp.5108)
- KMA (Korea Meteorological Administration), 2016. Available from <http://web.kma.go.kr/> (accessed 12.06.2016)
- Klaus, J., McDonnell, J.J., 2013. Hydrograph separation using stable isotopes: review and evaluation. *J. Hydrol.* 505, 47–64. DOI: [10.1016/j.jhydrol.2013.09.006](https://doi.org/10.1016/j.jhydrol.2013.09.006)
- Kubota, T., Tsuboyama, Y., 2003. Intra-and inter-storm oxygen-18 and deuterium variations of rain, throughfall, and stemflow, and two-component hydrograph separation in a small forested catchment in Japan. *J. For. Res.* 8, 179–190. DOI: [10.1007/s10310-002-0024-9](https://doi.org/10.1007/s10310-002-0024-9)
- Kulandaiswamy, V.C., Seetharaman, S., 1969. A note on Barnes' method of hydrograph separation. *J. Hydrol.* 9, 222–229.
- Lah, T.J., Park, Y., Cho, Y.J., 2015. The Four Major Rivers Restoration Project of South Korea—An assessment of its process, program, and political dimensions. *J. Environ. Dev.* 24, 375–394. DOI: [10.1177/1070496515598611](https://doi.org/10.1177/1070496515598611)
- Lee, K.-S., Park, Y., Kim, Y., Jeong, J.-H., Park, S.-K., Shin, H.-S., Bong, Y.-S., 2006. A preliminary hydrograph separation study in a small forested watershed using natural tracers. *J. Geol. Soc. Korea* 42, 427–437. (in Korean)
- Lee, D., Kim, J., Kim, S., Moon, S., Lee, J., Lim, J., Son, Y., Kang, S., Kim, S., Kim, K., others, 2007. Lessons from cross-scale studies of water and carbon cycles in the Gwangneung forest catchment in a complex landscape of monsoon Korea. *Korean J. Agric. For. Meteorol.* 9, 149–160. DOI: [10.5532/KJAFM.2007.9.2.149](https://doi.org/10.5532/KJAFM.2007.9.2.149)
- Lee, S.R., Cho, K., 2012. Precambrian crustal evolution of the Korean peninsula. *J. Petrol. Soc. Korea* 21, 89–112. DOI: [10.7854/JPSK.2012.21.2.089](https://doi.org/10.7854/JPSK.2012.21.2.089) (in Korean)
- Lee, H.-J., Chun, K.-W., Shope, C.L., Park, J.-H., 2015. Multiple time-scale monitoring to address dynamic seasonality and storm pulses of stream water quality in mountainous watersheds. *Water* 7, 6117–6138. DOI: [10.3390/w7116117](https://doi.org/10.3390/w7116117)
- Linsley, R.K., Kohler, M.A., Paulhus, J.L.H., 1975. *Hydrology for engineers*. McGraw-Hill, New York.
- Lischeid, G., 2008. Combining hydrometric and hydrochemical data sets for investigating runoff generation processes: tautologies, inconsistencies and possible explanations. *Geogr. Compass* 2, 255–280. DOI: [10.1111/j.1749-8198.2007.00082.x](https://doi.org/10.1111/j.1749-8198.2007.00082.x)
- McGlynn, B.L., McDonnell, J.J., 2003. Quantifying the relative contributions of riparian and hillslope zones to catchment runoff. *Water Resour. Res.* 39, 1310. DOI: [10.1029/2003WR002091](https://doi.org/10.1029/2003WR002091)
- Ministry of Environment and Korea Environment Institute, 2009. Four Major River Restoration Project of Republic of Korea. *Korea Env. Policy Bull.* 3.
- Ministry of Environment, 2015. *ECOREA—Environmental review 2015*, Korea. Ministry of Environment, Sejong-si.

- Nathan, R.J., McMahon, T.A., 1990. Evaluation of automated techniques for base flow and recession analyses. *Water Resour. Res.* 26, 1465–1473. DOI: [10.1029/WR026i007p01465](https://doi.org/10.1029/WR026i007p01465)
- NIAS (National Institute of Agricultural Sciences), 2016. Available from <http://soil.rda.go.kr/soil/index.jsp> (accessed 12.06.2016)
- NIER (National Institute of Environmental Research), 2010. Korean climate change assessment report 2010. National Institute of Environmental Research, Seoul.
- Park, J.-H., Duan, L., Kim, B., Mitchell, M.J., Shibata, H., 2010. Potential effects of climate change and variability on watershed biogeochemical processes and water quality in Northeast Asia. *Environ. Int.* 36, 212–225. DOI: [10.1016/j.envint.2009.10.008](https://doi.org/10.1016/j.envint.2009.10.008)
- Park, S.-J., Baek, K.-W., Kang, Y.-B., Choi, H.-K., 2011. Estimation of delivery pollution load by the runoff characteristics of Soyang Lake basin. *J. Korean Soc. Hazard Mitig.* 11, 317–324. DOI: [10.9798/KOSHAM.2011.11.6.317](https://doi.org/10.9798/KOSHAM.2011.11.6.317) (in Korean)
- Pearce, A.J., Stewart, M.K., Sklash, M.G., 1986. Storm runoff generation in humid headwater catchments: 1. Where does the water come from? *Water Resour. Res.* 22, 1263–1272. DOI: [10.1029/WR022i008p01263](https://doi.org/10.1029/WR022i008p01263)
- Peiffer, S., Gebauer, G., Matzner, E., Park, J.-H., Kim, K., Lee, M.-H., Parra, S., Payeur-Poirier, J.-L., Strohmeier S., 2012. The transport and fate of nutrient elements in the Soyang Lake and watershed. Review of the phase II International Research Training Group–Complex Terrain and Ecological Heterogeneity (TERRECO). Oral and poster presentations. TERRECO, Bayreuth.
- Pinder, G.F., Jones, J.F., 1969. Determination of the ground-water component of peak discharge from the chemistry of total runoff. *Water Resour. Res.* 5, 438–445. DOI: [10.1029/WR005i002p00438](https://doi.org/10.1029/WR005i002p00438)
- Priestley, C.H.B., Taylor, R.J., 1972. On the assessment of surface heat flux and evaporation using large-scale parameters. *Mon. Weather Rev.* 100, 81–92. DOI: [10.1175/1520-0493\(1972\)100<0081:OTAOSH>2.3.CO;2](https://doi.org/10.1175/1520-0493(1972)100<0081:OTAOSH>2.3.CO;2)
- Raskin, P., Gleick, P., Kirshen, P., Pontius, G., Strzepek, K., 1997. Water futures: Assessment of long-range patterns and problems. Comprehensive assessment of the freshwater resources of the world. Stockholm Env. Inst., Stockholm.
- Rice, K.C., Hornberger, G.M., 1998. Comparison of hydrochemical tracers to estimate source contributions to peak flow in a small, forested, headwater catchment. *Water Resour. Res.* 34, 1755–1766. DOI: [10.1029/98WR00917](https://doi.org/10.1029/98WR00917)
- Schoeneberger, P.J., Wysocki, D.A., Benham, E.C. (Eds.), 2011. Field book for describing and sampling soils, version 3.0. Natural Resources Conservation Service, National Soil Survey Center, Lincoln.
- Seo, K.-H., Son, J.-H., Lee, J.-Y., 2011. A new look at Changma. *Atmos.* 21, 109–121. (in Korean)
- Shibata, H., Mitsuhashi, H., Miyake, Y., Nakano, S., 2001. Dissolved and particulate carbon dynamics in a cool-temperate forested basin in northern Japan. *Hydrol. Process.* 15, 1817–1828. DOI: [10.1002/hyp.241](https://doi.org/10.1002/hyp.241)

- Shope, C.L., Bartsch, S., Kim, K., Kim, B., Tenhunen, J., Peiffer, S., Park, J.-H., Ok, Y.S., Fleckenstein, J., Koellner, T., 2013. A weighted, multi-method approach for accurate basin-wide streamflow estimation in an ungauged watershed. *J. Hydrol.* 494, 72–82. DOI: [10.1016/j.jhydrol.2013.04.035](https://doi.org/10.1016/j.jhydrol.2013.04.035)
- Shope, C.L., Maharjan, G.R., Tenhunen, J., Seo, B., Kim, K., Riley, J., Arnhold, S., Koellner, T., Ok, Y.S., Peiffer, S., Kim, B., Park, J.-H., Huwe, B., 2014. Using the SWAT model to improve process descriptions and define hydrologic partitioning in South Korea. *Hydrol. Earth Syst. Sci.* 18, 539–557. DOI: [10.5194/hess-18-539-2014](https://doi.org/10.5194/hess-18-539-2014)
- Sidele, R.C., Tsuboyama, Y., Noguchi, S., Hosoda, I., Fujieda, M., Shimizu, T., 2000. Stormflow generation in steep forested headwaters: a linked hydrogeomorphic paradigm. *Hydrol. Process.* 14, 369–385. DOI: [10.1002/\(SICI\)1099-1085\(20000228\)14:3<369::AID-HYP943>3.0.CO;2-P](https://doi.org/10.1002/(SICI)1099-1085(20000228)14:3<369::AID-HYP943>3.0.CO;2-P)
- Sidele, R.C., Noguchi, S., Tsuboyama, Y., Laursen, K., 2001. A conceptual model of preferential flow systems in forested hillslopes: Evidence of self-organization. *Hydrol. Process.* 15, 1675–1692. DOI: [10.1002/hyp.233](https://doi.org/10.1002/hyp.233)
- Sidele, R.C., 2006. Stormflow generation in forest headwater catchments: a hydrogeomorphic approach, *For. Snow Landsc. Res* 80, 115–128.
- Sklash, M.G., Farvolden, R.N., 1979. The role of groundwater in storm runoff. *J. Hydrol.* 43, 45–65. DOI: [10.1016/0022-1694\(79\)90164-1](https://doi.org/10.1016/0022-1694(79)90164-1)
- Szilagyi, J., Parlange, M.B., 1998. Baseflow separation based on analytical solutions of the Boussinesq equation. *J. Hydrol.* 204, 251–260. DOI: [10.1016/S0022-1694\(97\)00132-7](https://doi.org/10.1016/S0022-1694(97)00132-7)
- Tsuboyama, Y., 2006. An experimental study on temporal and spatial variability of flow pathways in a small forested catchment. *Bull. FFPRI* 5, 135–174.
- Tsujimura, M., Onda, Y., Ito, J., 2001. Stream water chemistry in a steep headwater basin with high relief. *Hydrol. Process.* 15, 1847–1858. DOI: [10.1002/hyp.243](https://doi.org/10.1002/hyp.243)
- Uchida, T., Asano, Y., Ohte, N., Mizuyama, T., 2003. Analysis of flowpath dynamics in a steep unchannelled hollow in the Tanakami Mountains of Japan. *Hydrol. Processes* 17, 417–430. DOI: [10.1002/hyp.1133](https://doi.org/10.1002/hyp.1133)
- Uchida, T., McDonnell, J.J., Asano, Y., 2006. Functional intercomparison of hillslopes and small catchments by examining water source, flowpath and mean residence time. *J. Hydrol.* 327, 627–642. DOI: [10.1016/j.jhydrol.2006.02.037](https://doi.org/10.1016/j.jhydrol.2006.02.037)
- UNEP (United Nations Environment Programme), 2010. Overview of the Republic of Korea's National Strategy for Green Growth. UNEP, Nairobi.
- WWAP (World Water Assessment Programme), 2009. The United Nations World Water Development Report 3: Water in a Changing World. Case Study Volume: Facing The Challenges. UNESCO, Paris.
- WWAP (World Water Assessment Programme), 2012. The United Nations World Water Development Report 4: Managing Water under Uncertainty and Risk. UNESCO, Paris.

- Yang, J.-E., Ryu, J.-H., Kim, S.-J., Chung, D.-Y., 2010. Management strategies to conserve soil and water qualities in the sloping uplands in Korea. *Korean J. Agric. Sci.* 37, 435–449.
- Yang, L., Chang, S.-W., Shin, H.-S., Hur, J., 2015. Tracking the evolution of stream DOM source during storm events using end member mixing analysis based on DOM quality. *J. Hydrol.* 523, 333–341. DOI: [10.1016/j.jhydrol.2015.01.074](https://doi.org/10.1016/j.jhydrol.2015.01.074)
- Yihui, D., Chan, J.C., 2005. The East Asian summer monsoon: an overview. *Meteorol. Atmos. Phys.* 89, 117–142. DOI: [10.1007/s00703-005-0125-z](https://doi.org/10.1007/s00703-005-0125-z)
- Yoon, S.W., Chung, S.W., Oh, D.G., Lee, J.W., 2010. Monitoring of non-point source pollutants load from a mixed forest land use. *J. Environ. Sci.* 22, 801–805. DOI: [10.1016/S1001-0742\(09\)60180-7](https://doi.org/10.1016/S1001-0742(09)60180-7)
- Zhang, Z., Fukushima, T., Onda, Y., Mizugaki, S., Gomi, T., Kosugi, K., Hiramatsu, S., Kitahara, H., Kuraji, K., Terajima, T., Matsushige, K., Tao, F., 2008. Characterisation of diffuse pollutions from forested watersheds in Japan during storm events—its association with rainfall and watershed features. *Sci. Total Environ.* 390, 215–226. DOI: [10.1016/j.scitotenv.2007.09.045](https://doi.org/10.1016/j.scitotenv.2007.09.045)

Chapter 2

A sudden shift in runoff generation processes
at a forested catchment as induced by the East
Asian summer monsoon

Jean-Lionel Payeur-Poirier, Luisa Hopp, Stefan Peiffer

Department of Hydrology, Bayreuth Center of Ecology and Environmental Research
(BayCEER), University of Bayreuth, Bayreuth, Germany

Correspondence: jean.lionel.payeur.poirier@gmail.com (J.-L. Payeur-Poirier)

Status: in preparation

Abstract

Forested catchments of the East Asian summer monsoon region usually receive ~60% of their annual precipitation within three months. A thorough study of the influence of the East Asian summer monsoon (EASM) on runoff generation was conducted at a forested headwater catchment of South Korea. Hydrometric, hydrochemical, isotopic, and meteorological measurements were made before, during and after the 2013 EASM. Tracer-based hydrograph separations were performed, coupled with principal component analyses (PCA) and end-member mixing analyses (EMMA). The results were jointly analyzed with hydrometric data to study the dynamics of water sources and flow paths and of associated runoff generation processes. During the EASM, discharge increased by more than two orders of magnitude (0.02 to 8.88 mm hr^{-1}) and runoff likely consisted of a mixture of groundwater ($60.1 \pm 8.3\%$) and soil water from the hillslope area ($20.7 \pm 6.2\%$), the riparian area ($10.7 \pm 8.9\%$) and the toeslope area ($8.5 \pm 3.9\%$). As the EASM progressed, a sudden shift from the dominance of groundwater flow towards higher contributions of subsurface flow from the hillslope and the riparian area, which also shifted to deeper soil layers, likely occurred. This shift appeared to result from the sufficient input of throughfall to replenish soil moisture, for water to percolate to deeper soil layers, for the occurrence of transient saturation, for subsurface flow to be enhanced, and for the recharge of the saturated zone. Concurrent with the shift were an increase in the average runoff coefficient of individual rainfall events (23.6 ± 12.9 to $72.7 \pm 28.9\%$) and a decrease in stream water solute concentrations. These results illustrate a drastic hydrological response to the EASM. They also quantify the dynamics of water sources and flow paths as influenced by the EASM, and should be useful for better incorporating the overall influence of the EASM on runoff generation into regional scale hydrological models.

Keywords: hydrological fluxes and conditions, water sources and flow paths, tracer-based hydrograph separation, headwaters, South Korea.

2.1. Introduction

The East Asian summer monsoon (EASM) induces a pronounced seasonality in the hydrological regime of forested headwater catchments. The precipitation regime of the EASM

is characterized by heavy rainfall events associated with convective storms (Chung et al., 2004; Ho et al., 2003), which have the potential to generate extreme hydrological catchment responses. The prevalent properties of these catchments, namely steep slopes of short lengths, shallow and permeable soils, and low ratios of riparian to hillslope area (Gomi et al., 2002; Shin, 2002; Sidle et al., 1998) add to this potential. Hydrological responses induced by the EASM have been observed and include increases in discharge of one or several orders of magnitude (Haga et al., 2005; Jeong et al., 2003; Shope et al., 2013), increases in the export of sediment and nutrients (Jung et al., 2012; Lee et al., 2015; Ohte et al., 2010), variations in runoff generation processes (Gomi et al., 2010; Kim and Yoo, 2007) and decreases in the residence time of water (Kim et al., 2007; Kim et al., 2009). These responses and their magnitudes are largely controlled by the dynamics of water sources and flow paths.

The tracer-based hydrograph separation technique has been applied to study the water sources and flow paths of forested headwater catchments of the EASM region (Choi et al., 2010; Fujimoto et al., 2011; Gomi et al., 2010; Katsuyama et al., 2001; Katsuyama et al., 2009; Kim and Yoo, 2007). This technique is based on the assumption that runoff is a mixture of distinct components and is used to estimate the relative proportions of these components in runoff (Pinder and Jones, 1969; Sklash et al., 1976; Sklash and Farvolden, 1979). The joint analysis of tracer-based and hydrometric data can enhance the study of water sources and flow paths, and has been strongly advocated by researchers (Bonell, 1998; Hooper, 2001; Lischeid, 2008; Rice and Hornberger, 1998). Some of the major findings derived from the joint analysis of such data from the EASM region include (1) the substantial but temporally varying contribution of groundwater to runoff, (2) the occurrence of overland flow, as infiltration-excess or saturation-excess, and its contribution to direct runoff, (3) the occurrence and threshold response of preferential flow, and (4) the influence of antecedent hydrological conditions, such as soil moisture, on the contributions of components to runoff. These and additional findings contributed to the development of conceptual models of runoff generation at the hillslope and catchment scales (Asano et al., 2002; Fujimoto et al., 2008; Katsuyama et al., 2009; Sidle et al., 2000; Sidle et al., 2001; Uchida et al., 2003; Uchida et al., 2006).

The vast majority of studies conducted at forested headwater catchments of the EASM region focused on a limited number of monsoon- and/or typhoon-related events. Although single events can have substantial effects on runoff generation, the overall influence of the EASM was seldom reported. We believe that the study of the influence of the EASM should encompass the complete range of hydrological conditions, from those preceding the onset of

the EASM, to those during the EASM, to those following the end of the EASM. We also argue that the application of the tracer-based hydrograph separation technique to extreme hydrological responses requires high-frequency sampling of stream water and of many potential components of runoff. These considerations are essential for a well-founded characterization of runoff generation throughout the EASM (Gomi et al., 2010; Inamdar et al., 2013; Tsuboyama, 2006).

In the current article, we report on the hydrometric, hydrochemical, isotopic and meteorological measurements made before, during and after the 2013 East Asian summer monsoon (EASM) at a forested headwater catchment of South Korea. High-frequency measurements and sampling conducted over a wide range of hydrological conditions provided a dataset required for an in-depth analysis of runoff generation. We also attempt to characterize the temporal variability of subsurface flow in terms of contributing areas and depths. Furthermore, we discuss our findings in the light of existing perceptual and conceptual models of runoff generation in forested catchments of the EASM region. We state the hypothesis that a shift in water sources and flow paths can be induced by the EASM. Our objectives were (1) to quantify the major hydrological fluxes and conditions, (2) to identify the most likely components of runoff and estimate their proportions in runoff, and (3) to characterize the overall influence of the EASM on runoff generation. In this study, the EASM was defined as occurring between the spring rain period (April to mid-May) and the post-EASM period (mid-August to early September) in South Korea (Ha et al., 2012; Seo et al., 2011). The EASM is hereinafter referred to as the summer monsoon.

2.2. Materials and methods

2.2.1. Site description

This study was conducted at a site located in the north-east of South Korea, within the Lake Soyang watershed (Fig. 2.1). This mountainous region belongs to the temperate continental forest ecological zone (FAO, 2012) and the snow, fully humid, warm summer climate of the Köppen-Geiger classification (Kottek et al., 2006). Annual precipitation and temperature are on average 1211 mm and 10.1 °C (1981–2010; KMA, 2013) and the growing season extends from May to mid-October (Jeong et al., 2013). The summer monsoon is an

inherent component of the climate of this region, as described by Park et al. (2010). The precipitation from June through August accounts on average for 59.4% of the annual precipitation (KMA, 2013).

The site consists of a small forested headwater catchment drained by a stream. The catchment has an area of 0.16 km² (Table 2.1). Elevation ranges from 368 to 682 m and averages 529 m. With an average slope of 23.9° and a relief ratio of 0.43, the catchment is steep and comprises mostly straight-convex and -concave slopes. The hillslope area covers 97.7% of the catchment and extends to the streambed along its lower section, while a narrow riparian area stretches along the middle and upper sections of the streambed over ~300 m (Fig. 2.1). The toeslope area was defined as the foot of the hillslope area. The riparian area extends beyond the observed maximum extent of the stream and was delineated in the field by combining observations of geomorphology, soil and vegetation. Over the study period, streamflow occurred only over a limited section of the streambed. During low-flow and receding conditions, the stream surfaced 65 m upstream from the catchment outflow. During and shortly following major rainfall events, the stream expanded up to 226 m upstream from the catchment outflow. At the location where the stream reached its maximum extent, water emerged over a short length at all times. The upslope accumulated area of this location accounts for 82% of the catchment area. Upstream and downstream from this location, the slope of the streambed sharply increases. Two intermittent springs flowing directly to the stream were observed downstream from this location during and following most rainfall events (Fig. 2.1).

The bedrock consists of low-permeability quartzofeldspathic orthogneiss belonging to the Gyeonggi gneiss complex (Lee and Cho, 2012). The soil is a Eutric Cambisol (following IUSS Working Group WRB, 2014) of loam texture overlain by a 1 to 8-cm thick organic horizon (Lee, 2016). It is characterized as well to excessively drained (following Schoeneberger et al., 2011). Soil depth ranges from 0 to 233 cm, has an average of 55 cm at the hillslope area and 66 cm at the riparian area (excluding bedrock outcrops), and is maximal at the toeslope area (Table 2.1). Bedrock outcrops were estimated to cover ~5% of the catchment area. Down to 50-cm depth, the mineral soil has a low bulk density and a high fraction of coarse gravel and stones (Table 2.1; Lee, 2016). At the hillslope area, the soil is underlain by a very hard and compact layer of hardpan-like features which was assumed to have low permeability. From the measurements of soil texture and bulk density at several depths at the hillslope area (Lee, 2016), van Genuchten water retention parameters and values

of saturated hydraulic conductivity (K_{sat} , mm h^{-1}) were derived. Unsaturated soil hydraulic conductivity functions were then determined following van Genuchten (1980). Soil infiltration capacity (mm h^{-1}) was also measured at eighteen random locations within the site (Table 2.1).

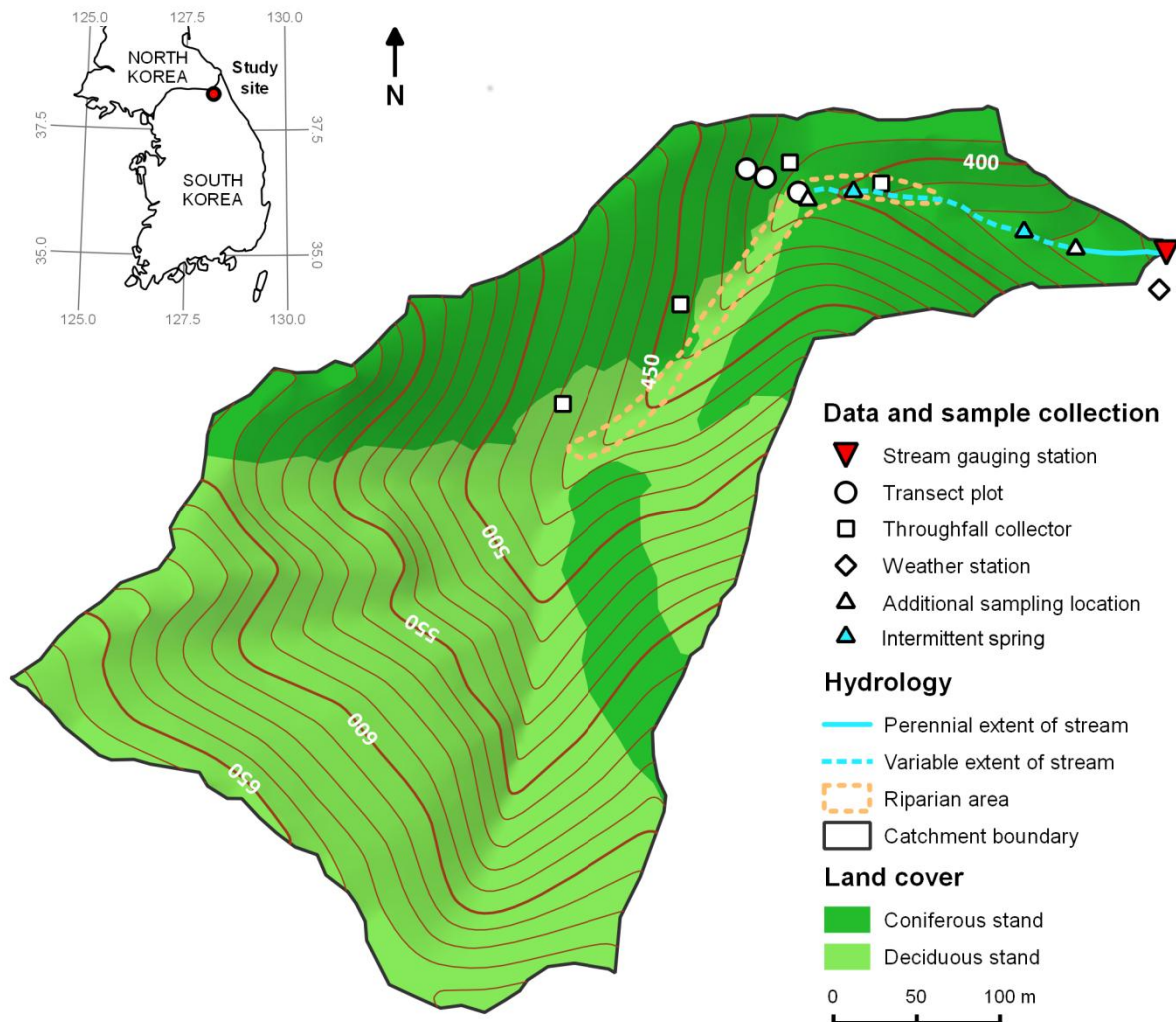


Figure 2.1. Location and detailed map of the study site. The equidistance of contour lines is 10 m and the precision is ± 10 m.

The catchment is covered at 61.3% by a purely deciduous stand, roughly corresponding to the upper part of the catchment, and at 38.7% by a purely coniferous stand, roughly corresponding to the lower part of the catchment (Fig. 2.1). The deciduous stand originated from natural regeneration following harvest and is dominated by *Juglans*

mandshurica Maxim., *Tilia amurensis* Kom. and *Acer pictum* subsp. *mono* (Maxim.) H. Ohashi. Kim et al. (2015) defined this type of forest cover as mixed mesophytic. The coniferous stand originated from plantation following harvest and is almost exclusively composed of *Larix kaempferi* (Lamb.) Carr., with a few scattered *Pinus densiflora* Siebold & Zucc. The coniferous stand was 38-years old in 2013, which corresponds with the reforestation programs implemented from 1973 onwards in South Korea (Bae et al., 2012). The age of the deciduous stand was estimated to be similar. Following harvest and plantation, the site was only slightly managed and it developed a pristine character. Further site characteristics are presented in Table 2.1.

Table 2.1. Selected topographical, stand and soil characteristics of the study site.

<i>Topographical characteristics</i>	
Geographic coordinates (decimal degrees of centre point)	E 128.1816°, N 38.2051°
Catchment area (m ²)	155380
Elevation range (m a.s.l.)	368 to 682
Elevation mean (m a.s.l.)	529
Hillslope area (% of catchment area)	97.7
Riparian area (% of catchment area) ^a	2.3
Slope range (°)	0.1 to 42.4
Slope mean (°)	23.9
Slope length maximum (m)	370
Slope aspect mean (°)	141
Drainage density range (m m ⁻²) ^b	0.42 to 1.45
Relief ratio	0.43
Form factor ^c	0.29
<i>Stand characteristics</i> ^d	
Age (year, in 2013)	38
Cover (% of catchment area)	
Coniferous	38.7
Deciduous	61.3
Density (tree ha ⁻¹)	
Coniferous	864
Deciduous	823
DBH mean (diameter at breast height, cm)	
Coniferous	22
Deciduous	19

Tree height mean (m)	
Coniferous	23
Deciduous	17
<i>Soil characteristics</i>	
Depth range (cm)	0 to 233
Depth mean (cm) ^e	
Hillslope area	55
Riparian area	66
Organic horizon thickness range (cm) ^f	1 to 8
Textural class ^f	Loam
Bulk density mean (g cm ⁻³) ^f	1.05
Coarse gravel and stones fraction mean (volumetric %) ^f	21.8
Infiltration capacity mean (mm h ⁻¹)	
Hillslope area	276
Riparian and toeslope area	535
Saturated hydraulic conductivity (mm h ⁻¹) ^g	
0-10 cm	86.8
10-20 cm	46.9
20-30 cm	24.2
30-40 cm	16.6
40-50 cm	37.5
Bedrock outcrop (% of catchment area) ^h	~5

a.s.l.: above sea level.

^a Including the streambed section within the area.

^b From the minimum to the maximum stream extent.

^c Ratio of the catchment area to the square of the catchment length.

^d Trees > 9.1 cm diameter at breast height.

^e Excluding bedrock outcrops.

^f Lee (2016).

^g Depth from the top of the mineral soil. Derived from values of soil texture and bulk density provided by Lee (2016).

^h Estimated from observation.

2.2.2. Regional characteristics of the 2013 summer monsoon

The 2013 summer monsoon was much longer, wetter and warmer than on average. In this region, the duration of the summer monsoon is on average 32 days, from late June to late July (Seo et al., 2011), and the average precipitation is 396 mm (GRMA, 2013). In 2013, the summer monsoon lasted 49 days, from June 17 to August 4, and was the longest summer monsoon that had occurred in this region since 1973 (earliest available records). The precipitation was 817 mm, which is 206% of the average value since that year. The temperature from June through August averaged 25.0 °C, which had made this period the warmest since 1973 (1.9 °C above the average). The temporal distribution of precipitation was uneven, as the summer monsoon accounted for 84.9% of the precipitation from June through August, while accounting on average for 49.7% (GRMA, 2013). In terms of annual precipitation, the year 2013 was slightly higher than the long-term average and 56.7% was attributed to the summer monsoon (KMA, 2013).

2.2.3. Meteorological measurements

Throughfall (mm) was measured at a 5-min frequency from June 1 to August 31, 2013, using a weather station installed under the canopy at a 3-m height (WS-GP1, Delta-T Devices Ltd., Cambridge, UK). It was also measured with four passive collectors randomly distributed within the site (Fig. 2.1), and catchment-scale throughfall was estimated as the average of all measurements. Precipitation (mm) was measured with a passive collector installed in an open area located 850 m south-east of the site. Depths were measured following every rainfall event over the same period.

2.2.4. Hydrometric measurements

A V-notch weir was installed at the outflow of the catchment, where water stage (cm) was measured at a 5-min frequency from June 1 to August 31, 2013, using a pressure transducer (Levellogger Gold M10, Solinst Canada Ltd., Georgetown, Canada) that was barometrically compensated with a barometric pressure transducer (Barologger Gold M1.5, Solinst Canada Ltd.) installed at the same location. A stage-discharge rating equation was applied following WMO (2010) and specific discharge (mm h^{-1}) was calculated. Discharge was also measured on two occasions by the timed volumetric method and the results agreed with those of the rating equation. Electrical conductivity (EC, $\mu\text{S cm}^{-1}$ at 25 °C) was

measured at the same location and frequency from June 1 to August 16, 2013, using a handheld meter with datalogger (Cond 340i, WTW GmbH, Weilheim, Germany). Water temperature was measured at the locations where the intermittent springs flowed directly to the stream, in order to detect their activation (HOBO Pendant UA-002-08, Onset Computer Corp., Bourne, USA).

Three plots were established to form a 50-m long transect from the hillslope, to the toeslope, to the riparian area within the lower part of the catchment (Fig. 2.1). The transect location was determined by its correspondence with the dominant topographical characteristics of the catchment and the distribution of landscape elements within the catchment. The slope of the transect gradually decreases from 40° at the hillslope plot to 16° at the riparian plot, with a sharp transition from 28° to 21° at the toeslope plot. At each plot, two piezometers were installed in which total head (cm) was measured at a 5-min frequency from June 1 to August 31, 2013, using pressure transducers (Levelogger Junior Model 3001, Solinst Canada Ltd.). The piezometers were installed at until-tool-refusal-depth and were screened on the lower two thirds of their depth. The piezometers reached depths of 56 and 43 cm at the hillslope plot, 233 and 133 cm at the toeslope plot, and 90 and 60 cm at the riparian plot. The pressure transducers were barometrically compensated with a barometric pressure transducer (Barologger Gold M1.5, Solinst Canada Ltd.) installed at the toeslope plot. Two piezometers were also installed in the lower part of the riparian area, where an intermittent spring flowed directly to the stream (Fig. 2.1; depths of 70 and 44 cm). Volumetric soil-water content (θ_v , m³ m⁻³; hereinafter referred to as soil moisture) was measured at each plot at depths of 10, 30 and 50 cm at the same frequency and over the same period, using multisensors (5TE, Decagon Devices Inc., Pullman, USA). The sensors were calibrated at 0% in air and 100% in water.

2.2.5. Water sampling

Samples were collected from stream water, groundwater, spring water, soil water and throughfall from June 3 to August 16, 2013, i.e. before, during and after the summer monsoon. For stream water, samples were collected at least once per 2 days over the whole period and, during and following major rainfall events, at least every 2 hours. Samples were collected in the V-notch weir either by grab or automatic sampling (6712 Portable Sampler, Teledyne Isco Inc., Lincoln, USA). Samples were also collected at the two upstream locations where the stream surfaced and where water emerged, and this at least once per 2 days over the

whole period (Fig. 2.1, as additional sampling locations). At the location where water emerged, the samples collected during the period of lowest flow (Fig. 2.2, between day of year (DOY) 159 and 172) were considered as groundwater. Along the streambed, water was also sampled from the two observed intermittent springs (Fig. 2.1). Sample collection of spring water followed the activation of springs.

For soil water, four suction lysimeters were installed at each plot in a vertical position at depths of 10, 20, 30 and 40 cm. The lysimeters were sampled at least once per 2 days over the whole period and almost every day during the most intensive period of the summer monsoon in terms of rainfall events. At the hillslope and toeslope plots, additional lysimeters were installed at depths of 65 and 88 cm, respectively, which at the hillslope plot corresponded to the until-tool-refusal-depth. Within a plot, the suction lysimeters were installed at 1-m intervals along a line perpendicular to the slope orientation. In terms of chemistry and isotopic abundance, each sample was considered as the average for the interval between sample collection times. Before installation, the porous cups of the lysimeters were flushed several times with dilute acid and then with deionized water, as prescribed by Weihermüller et al. (2007). After installation and before the start of the sampling period, the first three water samples collected from each lysimeter were discarded.

For throughfall, grab samples were collected from the passive collectors directly following every rainfall event, over the whole period. In terms of chemistry and isotopic abundance, each sample was considered as the average for an event and a volumetric-weighted average for a particular event was calculated to obtain a catchment-scale value. The collectors were rinsed with deionized water between events.

At the time of collection, each sample was split into two parts: one for chemical analysis, kept in a 15 ml polypropylene test tube, and one for isotopic analysis, kept in a gas-tight 1.5 ml glass bottle. The bottles and tubes were sealed with plastic paraffin film and the samples were stored in a dark environment at a temperature of ~4 °C until analyses.

2.2.6. Chemical and isotopic analyses

The water samples were analyzed for the concentrations (mg l^{-1}) of calcium (Ca^{2+}), magnesium (Mg^{2+}), potassium (K^+), sodium (Na^+), chloride (Cl^-), nitrate (NO_3^-), sulphate (SO_4^{2-}) and silica (SiO_2), for electrical conductivity (EC) and for the relative abundance of deuterium ($\delta^2\text{H}$, ‰ in relation to VSMOW). The concentrations of Ca^{2+} , Mg^{2+} , K^+ , Na^+ and

SiO₂ were measured by inductively coupled plasma optical emission spectrometry (Optima 3200 XL, PerkinElmer LAS GmbH, Rodgau, Germany). The concentrations of Cl⁻, NO₃⁻ and SO₄²⁻ were measured by ion chromatography (Metrohm IC Separation Center with Suppressor Module, Metrohm AG, Herisau, Switzerland). Prior to the measurements, the samples were filtered with 0.45 μm (for spectrometry) and 0.2 μm (for chromatography) nylon filters. EC was measured at the time of sample collection using a handheld meter (Cond 340i, WTW GmbH). A detailed description of δ²H measurements is found in the appendix. The spring water samples were not analyzed for δ²H.

2.2.7. Data analysis

2.2.7.1. Hydrograph separation

A tracer-based mass balance hydrograph separation was performed following the procedures detailed by Christophersen and Hooper (1992), Hooper (2003) and Sklash and Farvolden (1979). The number and nature of components required to explain most of the variation in the composition of stream water collected at the catchment outflow were determined by performing a principal component analysis (PCA) and an end-member mixing analysis (EMMA). As a factor analysis, the PCA allows to explain discrete levels of the variation in the chemistry and isotopic abundance of runoff, concurrent with a reduction in dimensionality of the dataset (Abdi and Williams, 2010; Christophersen and Hooper, 1992). The EMMA is a systematic approach applied to identify the most likely components (i.e. end-members) of runoff (Christophersen et al., 1990; Hooper et al., 1990; Hooper, 2003). The potential end-members were throughfall, groundwater, and soil water at several depths at the hillslope, toeslope, and riparian areas of the catchment (see Table 2.4). Soil water was separated into distinct end-members on the basis of landscape elements and layering of the soil in terms of saturated hydraulic conductivity (Table 2.1). Precipitation was not considered a potential end-member as opposed to throughfall, since the catchment is covered at ~100% by a forest canopy.

Prior to these analyses, the conservative nature and linear mixing of the measured natural tracers were assessed. Bivariate plots of all tracer pairs of stream water were generated and linear correlation was assessed. A residual analysis of tracer values was performed following Hooper (2003). A tracer was considered to be conservative and to linearly mix if it was linearly correlated with at least one other tracer ($r^2 > 0.5$, $p < 0.01$; following Barthold et

al., 2011), the residuals between the destandardized orthogonal projections of the values and the measured values plotted against the latter displayed a random pattern, and the relative root-mean-square error (RRMSE; Taylor, 1997) of the plot was relatively low ($\leq 15\%$). The degree of randomness of the pattern and the RRMSE of the residuals plotted against the measured values in one- and multi-dimensional subspaces were also assessed in relation to the dimensionality of the mixing subspace. Only conservative tracers which linearly mixed were used for further analyses.

A PCA was performed on the correlation matrix of the tracer values of stream water. The number of principal components (i.e. eigenvectors) to retain was selected by applying the rule of one, which states that only principal components with eigenvalues ≥ 1 should be retained (Preisendorfer et al., 1981). The dimensionality of the resulting mixing subspace (i.e. U -space) corresponded to the number of principal components retained. An EMMA was initiated by standardizing the median and quartiles of the tracer values of potential end-members to stream water values. The standardized values were then projected into the mixing subspace defined by the orthogonal projections of stream water values. For m principal components retained, the minimum number of end-members required to explain most of the variation in the composition of stream water is $m+1$ and, for n tracers used, the maximum number of end-members is $n+1$. A subset of end-members was selected on the basis of four criteria outlined by Ali et al. (2010). The subset should comprise end-members which have distinct tracer values for at least one tracer, which have a lower temporal variability in tracer values than stream water, and of which the orthogonal projections bound the projections of stream water values while being as close as possible. The differences between the projected and the measured values of the selected end-members should also be $< 15\%$, which indicates a good fit in the mixing subspace. By assessing the fulfillment of these criteria by different combinations of end-members and their ability to circumscribe the projections of stream water values, further subsets of end-members were selected and used in the mixing model. The subset for which the mixing model could best reproduce the measured values was finally identified, and consisted of the most likely end-members of runoff.

In order to estimate the relative contributions (i.e. proportions, %) of the most likely end-members to runoff, mixing equations based on the mass balance approach (Eqs. (1) – (3)) were solved by the use of matrix operations (Eqs. (4) – (6)). This approach was adapted from its initial use for a two-component hydrograph separation (Pinder and Jones, 1969; Sklash and Farvolden, 1979) to account for multi-component contributions to runoff (Christophersen et

al., 1990; Hooper et al., 1990). An assessment of the data regarding the assumptions underlying the hydrograph separation technique (Buttle, 1994; Inamdar, 2011) was realized and taken into account for the interpretation of the results (refer to section 2.4.2). In the case of two principal components retained, three tracers used and four end-members identified, the following equations were solved:

$$RC_1 + RC_2 + RC_3 + RC_4 = 1 \quad (1)$$

$$T_1 RC_1 + T_2 RC_2 + T_3 RC_3 + T_4 RC_4 = T_{st} \quad (2)$$

$$T_x RC_x = T_{st} \quad (3)$$

$$T_x = \begin{vmatrix} 1 & 1 & 1 & 1 \\ T_1^1 & T_2^1 & T_3^1 & T_4^1 \\ T_1^2 & T_2^2 & T_3^2 & T_4^2 \\ T_1^3 & T_2^3 & T_3^3 & T_4^3 \end{vmatrix} \quad (4)$$

$$RC_x = \begin{vmatrix} RC_1 \\ RC_2 \\ RC_3 \\ RC_4 \end{vmatrix} \quad (5)$$

$$T_{st} = \begin{vmatrix} 1 \\ T_{st}^1 \\ T_{st}^2 \\ T_{st}^3 \end{vmatrix} \quad (6)$$

where RC is the relative contribution of an end-member to runoff; T is the value of a tracer; subscripts denote end-members and superscripts denote tracers; and T_{st} is the tracer value of stream water. The ability of the mixing model to reproduce the measured stream water tracer values was then assessed by analyzing the residuals between the predicted and the measured values. The negative fractions of relative contributions associated with projections of stream water values exceeding the mixing subspace set by the identified end-members were forced to null, as outlined by Ali et al. (2010). Daily mean values of relative contribution were calculated.

2.2.7.2. Individual rainfall events

Individual rainfall events were identified following the criteria (1) that events induced an increase in discharge greater than the maximum diurnal variation in discharge at low-flow conditions, and (2) a minimum inter-event time (MIT) of 6 hours. It was observed that the peak in discharge induced by an event always occurred during the event or within 6 hours of its end. The MIT was set as a compromise between the duration of the variation in discharge and the intra-event variability in precipitation intensity.

2.2.7.3. Recession analysis and runoff coefficient

In order to calculate the total runoff of individual rainfall events shortly followed by subsequent events, a recession analysis of the hydrograph was performed following Tallaksen (1995). An initial analysis of the data revealed that recession rates greatly varied within a few hours and that more than half of the recession periods were shorter than 2 days. These facts and the will to examine runoff responses to individual events prompted our choice of hourly discharge values over daily values, and of the individual segments procedure. A total of seven segments with recession rates following the Dupuit-Boussinesq exponential equation were extracted (Eq. (2a) in Tallaksen, 1995). Constants were derived, which for the respective segments were almost equal for all events except for the third segment, for which two constants were derived (one from the two most important events in terms of precipitation and one from the rest of events). The runoff coefficient of each individual rainfall event was then calculated by dividing total runoff from the start of the event to when discharge on the receding limb was measured or calculated as equal to its initial value, by total precipitation of the event (following WMO, 2009).

2.3. Results

2.3.1. Major hydrological fluxes and conditions

2.3.1.1. Precipitation and throughfall

The summer monsoon precipitation measured in close proximity to the study site was 826 mm, which was similar to the regional value and accounted for 84.7% of the precipitation

from June through August. During the summer monsoon, sixteen individual rainfall events occurred and yielded 95.8% of the total precipitation for this period. The events were unevenly distributed over time, as nine events occurred over a period of only 16 days and accounted for 72.5% of the summer monsoon precipitation (Fig. 2.2, from DOY 189 to 204). The individual events varied in characteristics, as precipitation ranged from 8 to 127 mm, duration ranged from 1.75 to 33.9 h, and average precipitation intensity ranged from 1.8 to 10.4 mm h⁻¹. Throughfall for the summer monsoon was 788 mm, accounting for 95.4% of the precipitation. Average throughfall intensity for individual events ranged from 1.7 to 9.4 mm h⁻¹. Throughfall intensity reached a maximum of 113 mm h⁻¹ over a 5-min period. Further characteristics of six major rainfall events selected to cover the most intense period of the summer monsoon in terms of events are presented in Table 2.2 (see also Fig. 2.2).

2.3.1.2. Runoff

Catchment runoff for the summer monsoon totaled 617 mm and, from June through August, 684 mm. Over the former, hourly specific discharge ranged from 0.02 to 8.88 mm hr⁻¹ and averaged 0.50 ± 0.86 mm hr⁻¹ (Fig. 2.2). A diurnal variation in discharge was observed at low-flow conditions, of which the maximum value was 0.017 mm hr⁻¹. Before the summer monsoon, discharge followed a decreasing trend and did not reach a steady baseflow value (Fig. 2.2). From the onset of the summer monsoon onward, discharge was very responsive to rainfall events as its initial increase usually occurred between 5 and 30 min following the start of an event. Following the 4th event of the summer monsoon, discharge did not return to low-flow conditions for the rest of the study period. The recession analysis revealed that following the summer monsoon, discharge would have receded for ~18 days before reaching its value at the onset of the summer monsoon. The constants derived from the recession rate equations ranged from 0.02 to 0.15. The two intermittent springs were first activated on the 4th and 7th rainfall events (DOY 183 and 192), respectively, and following the end of an event flowed for periods ranging from hours to several days.

The runoff coefficient of individual rainfall events ranged from 9.4 to 124.7%, with a median of 67.3%. Throughout the summer monsoon, the coefficient followed an initial increasing trend, stabilized for the most intense period in terms of events, and remained high or higher thereafter. The runoff coefficients of six selected major rainfall events are presented in Table 2.2.

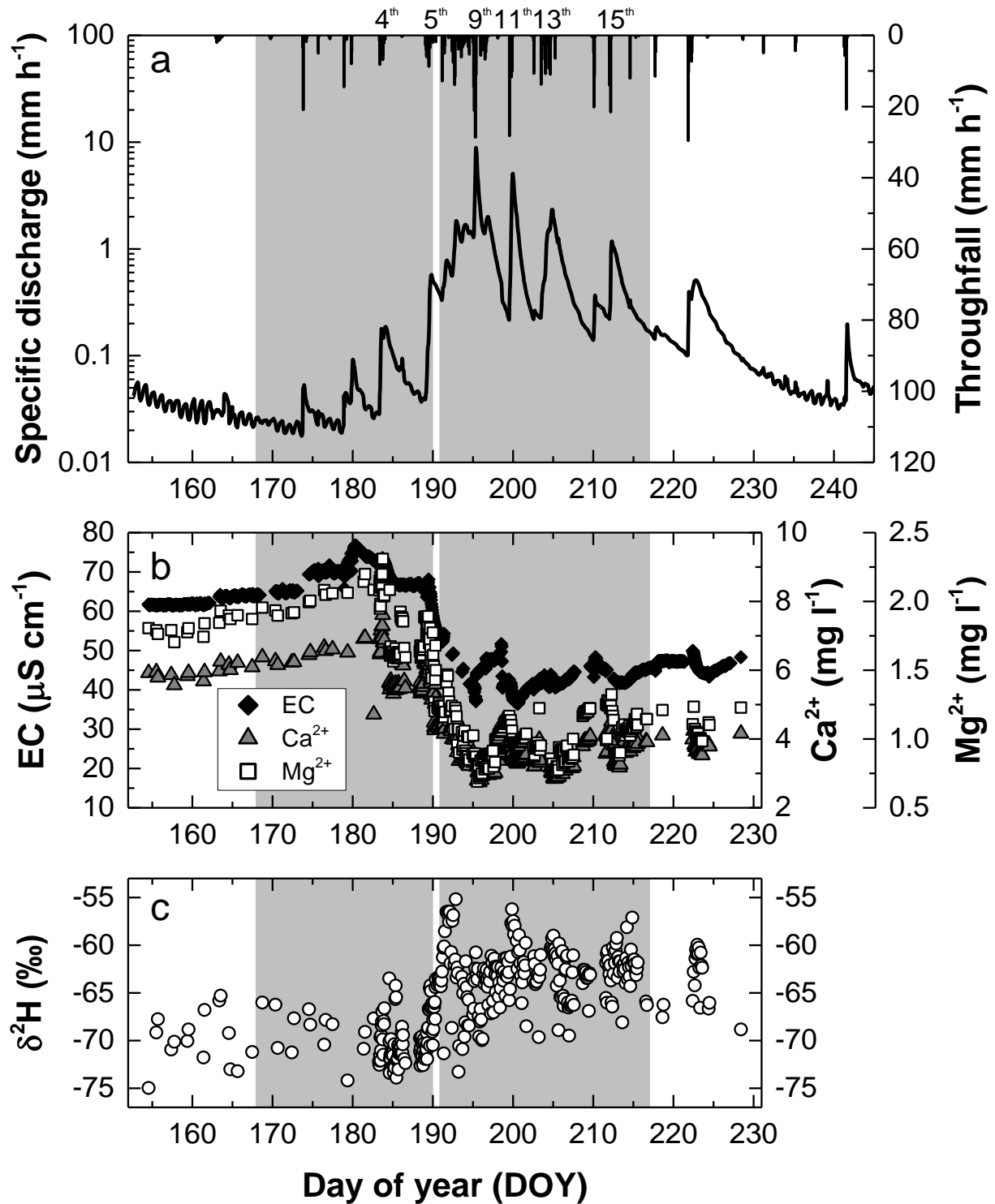


Figure 2.2. (a) Specific discharge (hourly mean) and throughfall (hourly), (b) electrical conductivity (EC, hourly mean), Ca²⁺ and Mg²⁺ concentration and (c) relative abundance of deuterium ($\delta^2\text{H}$) of stream water as a function of time from June 1 to August 31, 2013. Ca²⁺, Mg²⁺, EC and $\delta^2\text{H}$ were the only tracers considered as conservative. The shaded areas correspond to the summer monsoon; the white lines separate the initial and the major period. Selected major rainfall events are labeled by order.

Table 2.2. Characteristics of selected major rainfall events of the 2013 summer monsoon.

Event order	4 th	5 th	9 th	11 th	13 th	15 th
Start (day of year)	183.4	189.1	194.9	199.5	203.5	212.0
Duration (h)	17	32	12	13	31	6
Precipitation (mm)	41	64	127	106	81	48
Throughfall (mm)	45	60	115	97	90	48
Throughfall intensity mean (mm h ⁻¹) ^a	2.6	1.9	9.4	7.7	2.8	8.0
Throughfall intensity max (mm h ⁻¹) ^b	41.2	49.1	112.8	58.4	67.2	50.4
Runoff (mm) ^c	13	42	104	91	101	41
Runoff coefficient (%)	31.7	65.6	81.9	85.8	124.7	85.4

^a Excluding intra-event rainless periods.

^b Based on values measured at a 5-min frequency.

^c From the start of the event to when discharge on the receding limb was measured or calculated as equal to its initial value.

2.3.1.3. Soil moisture and water table

Soil moisture (θ_v) measured at a 5-min frequency ranged from 14.5 to 40.1%. Its temporal dynamics were mainly governed by the sequence of rainfall events. θ_v generally increased with depth, except at some periods and at the hillslope area (Fig. 2.3). Temporal variation patterns in θ_v differed between areas and depths, although differences in values were at some periods insignificant. At each depth, the largest range in daily θ_v over the study period was observed at the riparian area, followed by the hillslope and toeslope areas. During the summer monsoon, lag times in increase following the start of an event varied between 5 min and ~1 day and recession periods were usually in the order of a few days. θ_v reached its lowest values at around the onset of the summer monsoon. It then rapidly increased with the occurrence of rainfall events until the 5th event, and thereafter varied at a lesser extent with the occurrence of events until after the summer monsoon. θ_v then receded and, if not for a typhoon-related event that occurred at the end of the study period, it would have likely receded near or to the values at the onset of the summer monsoon within the study period (Fig. 2.3). The values of θ_v fell within the ranges reported for the same period of the year for analogous sites in South Korea (Jeong et al., 2012; Jung et al., 2010; Jung et al., 2012; Kwon et al., 2009). Unsaturated soil hydraulic conductivity ($K(\theta_v)$) displayed greater absolute ranges and differences between some depths than θ_v (Fig. 2.3). At the hillslope area, $K(\theta_v)$ at 50-cm

depth was much more responsive to events than at shallower depths, especially from the 5th rainfall event onward. At the riparian area, $K(\theta_v)$ at 30 and 50-cm depth was generally similar and generally much higher than at 10-cm depth, also especially from the 5th rainfall event onward.

Despite the relatively shallow soil, a water table was measured only once for a period of 12 hours in the piezometers installed in the lower part of the riparian area, starting 2 hours before the maximum throughfall intensity of the summer monsoon. It lasted 1 hour longer at the piezometer located closer to the intermittent spring flowing at this location and further away from the stream than at the other piezometer. The water table had a maximum depth of 38 cm and did not intersect the soil surface. A water table was not measured at any other time or any other piezometer over the study period. However, at the location where the stream reached its maximum extent, the emergence of water at all times indicated the presence of a saturated zone. Water depth at this location was a maximum of ~40 cm higher during and following rainfall events than at low-flow conditions, independently of the extent of the stream.

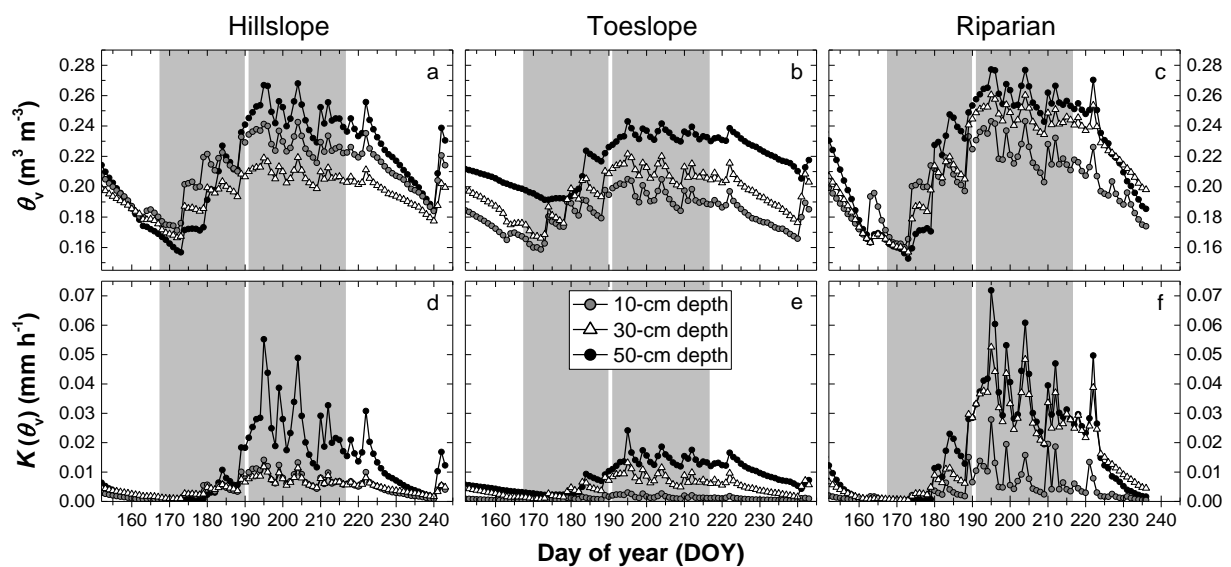


Figure 2.3. Daily mean soil moisture (θ_v) and unsaturated hydraulic conductivity ($K(\theta_v)$) at three depths at the (a, d) hillslope, (b, e) toeslope and (c, f) riparian areas of the study site as a function of time from June 1 to August 31, 2013. The shaded areas correspond to the summer monsoon; the white lines separate the initial and the major period.

2.3.2. Water chemistry and isotopic abundance

The proportions of solute milliequivalents of stream water were very stable for the measured cations, while greater variation was observed for the measured anions (Fig. 2.4). The ranges in these proportions for the periods preceding and following the summer monsoon were similar and fell within the greater ranges for the summer monsoon. A visual analysis of the time-series of stream water chemistry revealed a general pattern in the variation of Ca^{2+} , Mg^{2+} , EC (Fig. 2.2), K^+ , NO_3^- , and, at a lesser extent, Na^+ , SO_4^{2-} and SiO_2 . From the start of the study period, the values were first relatively stable or gradually increasing. In response to the 4th rainfall event, the values generally reached their maximum and subsequently decreased until the respective approximate value at the onset of the summer monsoon. From the 5th event and for the following 6 days, the values drastically decreased in response to heavy rainfall events and generally reached their minimum (occurrence of six events for a total precipitation of 389 mm). Thereafter and until the end of the study period, the values responded to rainfall events within limited ranges and followed a generally increasing trend (Fig. 2.2 for Ca^{2+} , Mg^{2+} and EC). In the cases of K^+ , Na^+ , NO_3^- , SO_4^{2-} and SiO_2 , the values eventually reached or slightly exceeded the respective approximate value at the start of the study period. For Ca^{2+} , Mg^{2+} and EC, the values remained below the respective initial value. No pattern was visible for Cl^- . The temporal variation of stream water $\delta^2\text{H}$ did not follow a pattern as clear as chemistry did. Before the 5th rainfall event, the values varied between -75.0 and -63.5‰, with a median of -70.4‰. From this event onward, the values varied between -73.3 and -55.2‰, with a median of -62.8‰ (Fig. 2.2).

A comparison of chemistry and $\delta^2\text{H}$ between samples collected at the catchment outflow and samples collected at the upstream location where water emerged revealed that, before the 1st rainfall event (DOY 173), values were considerably lower for the latter. These samples were considered as groundwater. Then, until the 5th event, values at the upstream location varied between groundwater values and values at the catchment outflow. After this event and for the rest of the study period, values at the upstream location were much lower (for chemistry) and slightly higher (for $\delta^2\text{H}$) than groundwater values, were slightly lower (for both) than at the catchment outflow and followed very similar trends to those at the catchment outflow. The chemistry of the upper spring compared very well with that at the upstream location, while the chemistry of the lower spring compared very well with that at the

catchment outflow. However, differences were small and the chemistry of both intermittent springs also compared well with each other.

Soil water chemistry generally followed a similar pattern to that of stream water (i.e. initially stable higher values, followed by a rapid decrease, and subsequently stable lower values), with some exceptions (data not shown). At 40-cm depth at the riparian area, values increased around the 5th rainfall event and quickly became stable. At shallower depths at the toeslope area, values either rapidly increased around the 5th event or remained stable. The values at 88-cm depth at the toeslope area only slightly varied throughout the study period. At the three areas, the values of soil water $\delta^2\text{H}$ were initially lowest at the deepest depths. The values at all depths were initially stable and, following the 5th rainfall event, $\delta^2\text{H}$ at shallower depths shifted to lower values, whereas $\delta^2\text{H}$ at the deepest depths increased and exceeded the values at all shallower depths with the exception of the 20-cm depth at the riparian area.

Throughout the study period, the values of throughfall chemistry were low and relatively stable, while $\delta^2\text{H}$ varied between -90.0 and -42.9‰. The median of rainfall events was -58.3‰ and the volumetric-weighted average was -61.2‰.

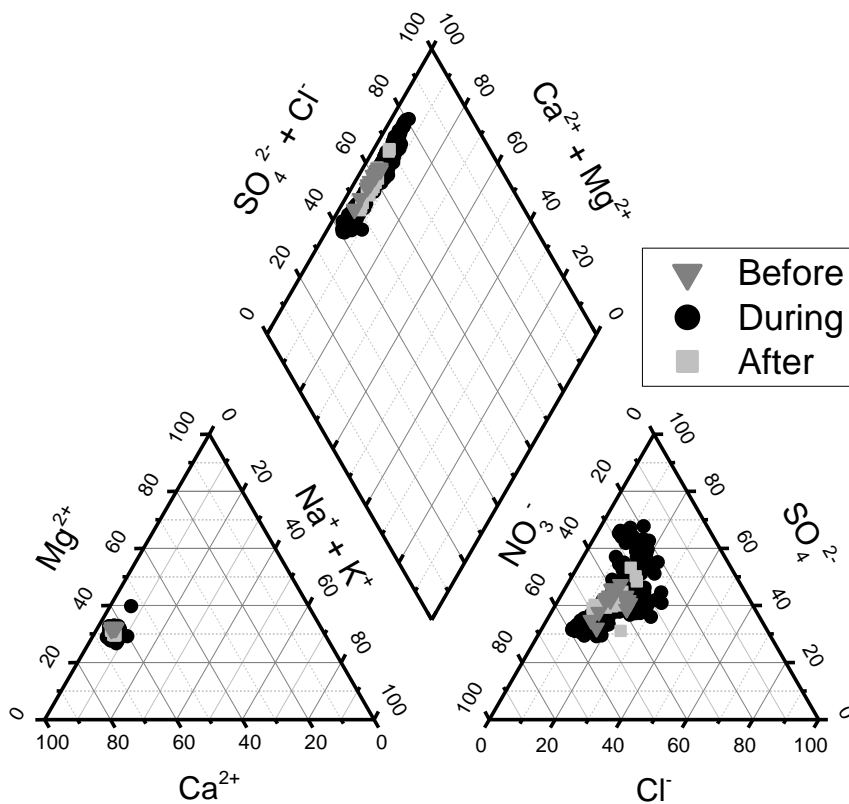


Figure 2.4. Piper diagram of stream water solutes before, during and after the 2013 summer monsoon. Data are in units of percent meq l^{-1} .

2.3.3. Hydrograph separation

2.3.3.1. Selection of tracers

The assessment of the conservative nature and linear mixing of tracers and their subsequent selection for further analyses were iteratively realized with the principal component analysis (PCA) and the end-member mixing analysis (EMMA). As further explained in section 2.3.3.2, the stream water dataset was divided into two parts corresponding to distinct periods, and mixing models were separately applied for each period. For both periods, only Ca^{2+} , Mg^{2+} , EC and $\delta^2\text{H}$ fulfilled the established criteria (Table 2.4). None of the other tracers were linearly correlated with another at the required level. As further explained in section 2.3.3.2, the use of only three of the four selected tracers was sufficient in both mixing models. Since Ca^{2+} and Mg^{2+} displayed the highest correlation level of all tracer pairs (data not shown) and since the residual analysis resulted in a higher RRMSE for Mg^{2+} than for Ca^{2+} for both periods (Table 2.3), only Ca^{2+} , EC and $\delta^2\text{H}$ were used in the models. Mg^{2+} was subsequently used with the other selected tracers to assess the ability of the models to reproduce the measured values.

Table 2.3. Patterns and relative root-mean-square errors (RRMSEs) of the residuals between the projected and the measured stream water tracer values plotted against the latter, in one- and two-dimensional subspaces for the initial and the major period.

	One-dimensional subspace		Two-dimensional subspace	
	Pattern	RRMSE (%)	Pattern	RRMSE (%)
<i>Initial period</i>				
Ca^{2+}	Random	5.04	Random	3.90
Mg^{2+}	Slightly structured	7.14	Random	4.35
EC	Slightly structured	27.91	Random	9.42
$\delta^2\text{H}$	Structured	28.39	Random	6.53
<i>Major period</i>				
Ca^{2+}	Random	4.46	Random	3.45
Mg^{2+}	Random	5.65	Random	4.11
EC	Structured	34.24	Random	13.79
$\delta^2\text{H}$	Structured	32.35	Random	12.58

Table 2.4. Medians of potential end-member selected tracer values for the initial and the major period. Values in parentheses are the respective percent differences between the projected and the measured values; values in bold have an absolute percent difference < 15%.

Source	Depth (cm)	<i>n</i> ^a	Ca ²⁺ (mg l ⁻¹)		EC (μS cm ⁻¹)		δ ² H (‰)	
			Initial period	Major period	Initial period	Major period	Initial period	Major period
Throughfall	–	8–13	0.68 (-86)	0.34 (40)	25.3 (21)	14.1 (62)	-62.3 (2)	-57.3 (-8)
Groundwater	–	12	4.82 (-12)	4.82 (-6)	53.1 (8)	53.1 (7)	-73.2 (-1)	-73.2 (-2)
Hillslope soil water	10	8–15	4.71 (19)	1.71 (1)	61.8 (-11)	24.8 (28)	-52.8 (3)	-63.0 (-6)
Hillslope soil water	20	20–16	3.44 (30)	1.69 (5)	54.4 (-15)	27.0 (14)	-50.2 (4)	-60.0 (-3)
Hillslope soil water	30	20–16	0.72 (75)	0.49 (140)	32.5 (-13)	17.7 (45)	-54.2 (2)	-60.2 (-8)
Hillslope soil water	40	5–15	1.62 (1)	0.90 (126)	49.9 (0)	21.3 (55)	-59.2 (0)	-66.0 (-10)
Hillslope soil water	65	13–18	0.79 (-35)	0.74 (-9)	25.8 (8)	22.9 (14)	-62.8 (-1)	-54.4 (-5)
Toeslope soil water	10	4–14	7.21 (1)	8.11 (-11)	64.9 (-1)	96.4 (-25)	-53.1 (0)	-61.9 (21)
Toeslope soil water	20	19–14	4.42 (-1)	3.96 (-9)	45.5 (1)	72.5 (-29)	-52.4 (0)	-58.8 (20)
Toeslope soil water	30	19–17	3.47 (-7)	3.63 (-23)	39.2 (5)	44.3 (-9)	-56.3 (-1)	-60.8 (4)
Toeslope soil water	40	14–17	9.85 (4)	3.74 (-13)	89.3 (-4)	39.9 (8)	-57.5 (1)	-65.0 (-2)
Toeslope soil water	88	9–18	1.01 (-63)	1.23 (-7)	23.8 (21)	17.6 (22)	-66.0 (-2)	-53.4 (-4)
Riparian soil water	10	7–16	8.15 (58)	14.03 (-16)	140.9 (-26)	82.9 (-3)	-53.8 (16)	-58.4 (4)
Riparian soil water	20	7–18	6.79 (13)	2.08 (5)	98.3 (-5)	73.8 (-41)	-55.7 (12)	-53.8 (29)
Riparian soil water	30	13–18	3.53 (61)	2.20 (13)	74.2 (-23)	80.4 (-14)	-53.9 (7)	-58.3 (13)
Riparian soil water	40	18–18	4.05 (10)	6.64 (-6)	53.4 (-6)	76.5 (-9)	-57.9 (1)	-56.2 (10)

^a Number of samples collected from day of year (DOY) 154 to 190.4 (initial period) and from DOY 190.5 to 228 (major period). Groundwater samples were collected between DOY 159 and 172 and used for both periods.

2.3.3.2. Mixing models and identification of end-members

The application of the mixing models and identification of the most likely end-members were iteratively realized with the selection of tracers. We initially performed PCAs and EMMAs using all four selected tracers, to find that only four end-members were required to explain most of the variation in the composition of stream water and, consequently, that the use of only three tracers was sufficient in the mixing models. As explained in section 2.3.3.1, Mg^{2+} was excluded from the models, and the results presented in the current section were obtained using only Ca^{2+} , EC and $\delta^2\text{H}$ as tracers.

A PCA was initially performed with the entire stream water dataset (Fig. 2.5a). The correlations between principal components and tracers were examined by plotting the loadings of the tracers in the mixing subspace (data not shown). A visual analysis of the plot revealed that all tracers had an influence of similar weight on the model, and that values of Ca^{2+} and EC were highly and negatively correlated with values of $\delta^2\text{H}$. The first principal component ($U1$) explained 87.4% of the variation in the dataset and was associated with a “ $\text{Ca}^{2+} - \text{EC}$ versus $\delta^2\text{H}$ ” axis; higher values of Ca^{2+} and EC with lower values of $\delta^2\text{H}$ corresponding to positive values of $U1$, and the opposite corresponding to negative values of $U1$. We observed that, within the mixing subspace, the orthogonal projections of stream water tracer values formed two distinct clusters, one on each side of the ordinate (Fig. 2.5a). These clusters corresponded to samples collected before (positive $U1$ values) and after (negative $U1$ values, except for one sample) DOY 190.4, i.e. shortly following the 5th rainfall event of the summer monsoon. The first period consisted of the period preceding the onset of the summer monsoon and the initial, less intensive period of the summer monsoon in terms of rainfall events, and was termed the “initial period”. The second period consisted of the most intensive period of the summer monsoon in terms of rainfall events and the period following the end of the summer monsoon, and was termed the “major period”. We interpreted this clustering as resulting from substantial differences in the contributions of end-members to runoff, or substantial differences in the tracer values of end-members, or both. A comparison of end-member tracer values between both periods revealed substantial differences for most end-members and tracers (Table 2.4 and Fig. 2.6). We accordingly decided to apply separate mixing models for each period.

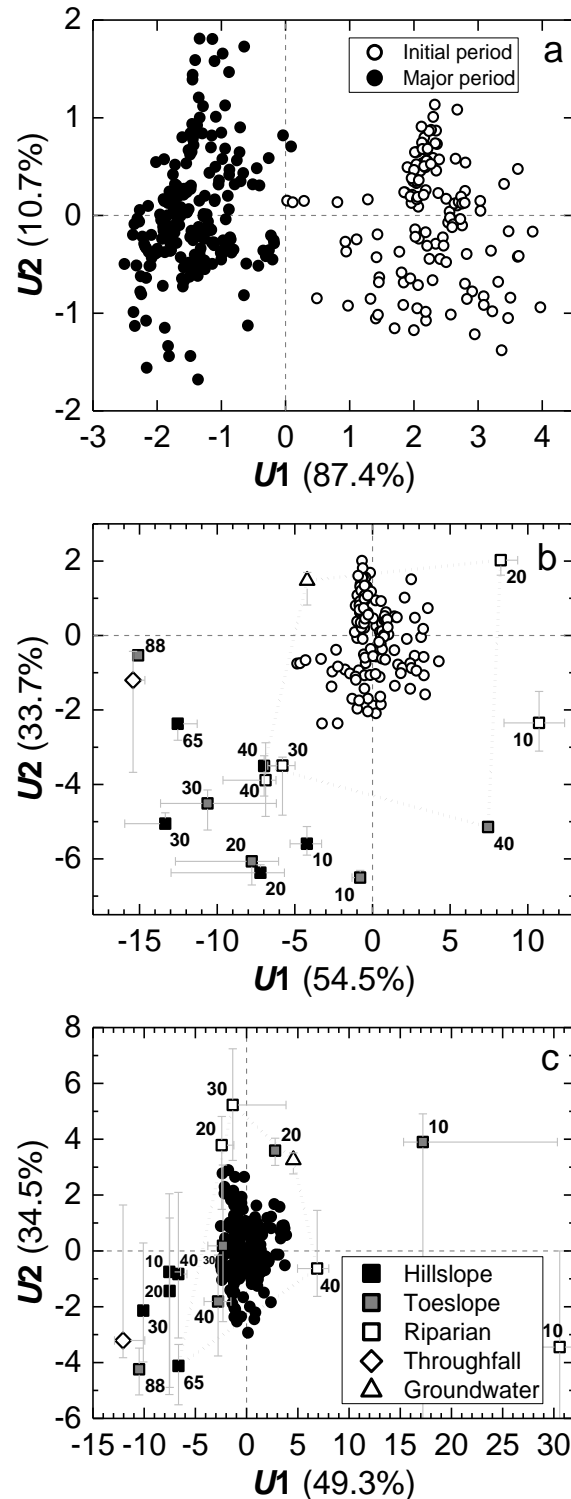


Figure 2.5. Mixing subspaces of stream water tracer values for (a) the whole study period ($n=345$), (b) the initial period ($n=132$) with projected potential end-members and (c) the major period ($n=243$) with projected potential end-members. The percentage of variation explained by each principal component (U_x) follows the order of the component in parentheses. Soil water potential end-members are labeled by depth (cm). Error bars are interquartile ranges; some of the ranges extend beyond plot (c). The projections of the identified end-members are linked by dotted lines. In plot (a), U_2 was not retained but plotted for ease of viewing.

For each model, the application of the rule of one resulted in a two-dimensional mixing subspace, which was confirmed by the analysis of the residuals (Table 2.3). The mixing models for the initial and the major period respectively explained 88.2 and 83.8% of the variation in the datasets. Median and quartile tracer values of end-members were calculated for each period and projected into the respective mixing subspaces (Fig. 2.5b and 2.5c). The same values for groundwater were used for both periods. Out of all the end-members, none fully fulfilled the established criteria for their selection, although groundwater almost did. Consequently, a modest level of flexibility was introduced in the selection process, especially for the criteria of distinct end-member tracer values and lower temporal variability than stream water values. Several combinations of three or four selected end-members were then analyzed for each mixing model. For the initial period, the combination of groundwater, hillslope and toeslope soil water at 40-cm depth (Hill₄₀ and Toe₄₀) and riparian soil water at 20-cm depth (Rip₂₀) provided the most accurate mixing model. For the major period, the combinations of groundwater, hillslope soil water at 65-cm depth (Hill₆₅), and riparian soil water at 30 and 40-cm depth (Rip₃₀ and Rip₄₀) provided the most accurate mixing model (Table 2.5 and Fig. 2.5). For both models, most of the other combinations of selected end-members circumscribed only portions of the projected stream water values. All of the other combinations provided models with RRMSEs of the residuals between the predicted and the measured values > 23%, for all selected tracers. Since a pure event water end-member (i.e. throughfall) was not identified as a one of the most likely end-members, runoff could only be separated into spatial components.

2.3.3.3. Contributions of end-members to runoff

Results of the hydrograph separation suggested that, for the initial period, runoff mainly consisted of groundwater (Table 2.6). Before the occurrence of the 5th rainfall event of the summer monsoon, its relative contribution to runoff varied between 63.1 and 86.6% (Fig. 2.7). It either increased or decreased in response to rainfall events, and between events generally slightly decreased. The 5th event initiated a drastic decrease in the relative contribution of groundwater. The second average relative contribution to runoff in importance was of Toe₄₀, which contribution was initially stable and, as the initial period progressed, became responsive to rainfall events. The average relative contributions of Rip₂₀ and Hill₄₀ were low (Table 2.6). The relative contribution of the latter was intermittent and varied between 0.0 and 24.1% (Fig. 2.7).

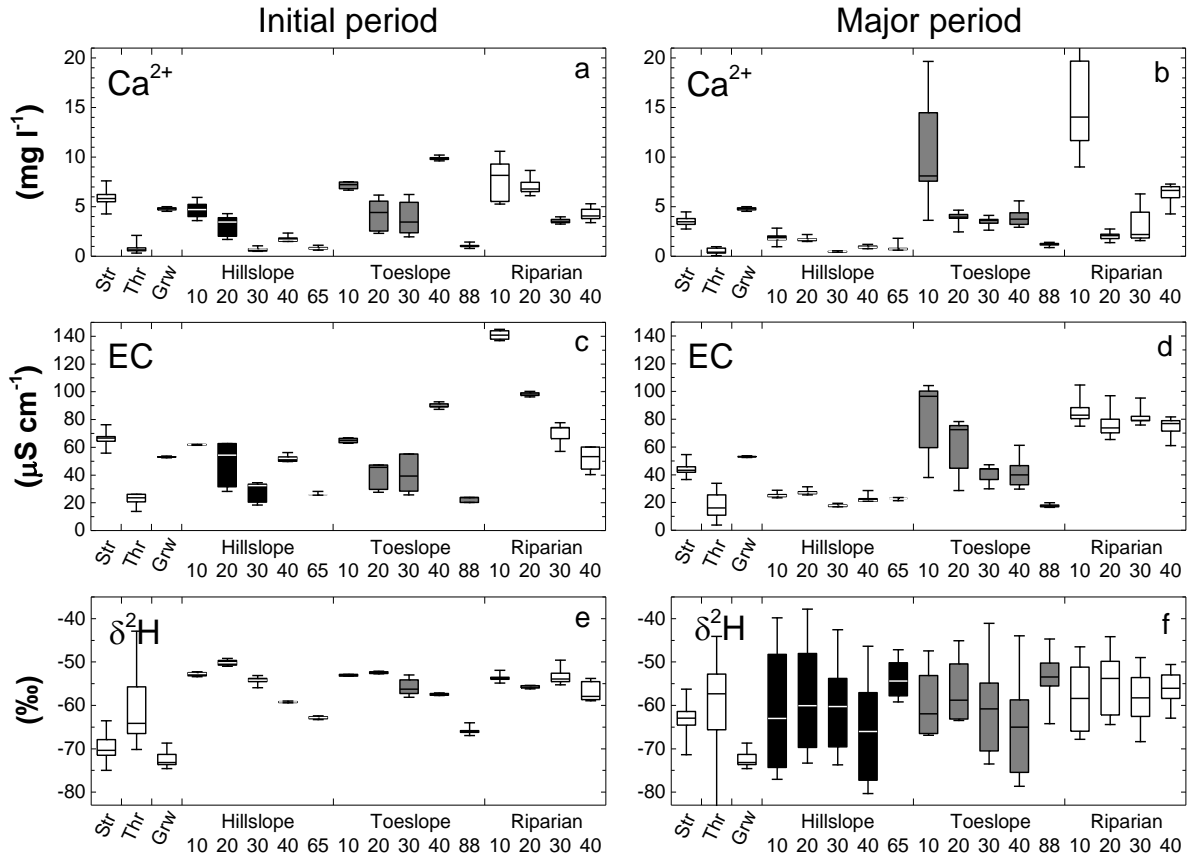


Figure 2.6. Selected tracer values of stream water (Str), throughfall (Thr), groundwater (Grw) and soil water for (a, c, e) the initial and (b, d, f) the major period. Soil water is labeled by source area and depth (cm). Center lines are the median, boxes extend from the lower to the upper quartiles, and whiskers extend from the minimum to the maximum values; some whiskers extend beyond plots (b) and (f).

Table 2.5. Relative root-mean-square errors (RRMSEs) of the residuals between the predicted and the measured stream water conservative tracer values for the initial and the major period.

	Initial period RRMSE (%)	Major period RRMSE (%)
Ca^{2+}	6.82	8.56
Mg^{2+}	7.42	10.12
EC	3.14	4.25
$\delta^2\text{H}$	2.08	3.73

During the major period, results suggested that the average relative contribution of groundwater to runoff was still considerable but not dominant (Table 2.6). The decrease in its relative contribution initiated by the 5th rainfall event persisted for the two subsequent events and was followed by a rapid increase (Fig. 2.7). Until shortly after the end of the summer monsoon, with the exception of the 15th and 16th events (DOY 212 and 214), its relative contribution varied between 37.0 to 62.0%. Thereafter, it was exceeded by the contributions of Hill₆₅ and Rip₄₀ (Fig. 2.7). From the initial to the major period, the contribution from the hillslope area likely shifted to a deeper layer. The relative contribution from Hill₆₅ was continuous and, on average, the second highest (Table 2.6 and Fig. 2.7). It generally increased in response to major events and, from the 8th event (DOY 193) onward, was likely always higher than 30%. A shift in the contribution from the riparian area towards deeper layers also likely occurred following the 5th event (Table 2.6). The relative contribution from Rip₃₀ was low and episodic, while that from Rip₄₀ was quasi-continuous and relatively high for a few events. A general increase in the relative contribution of Rip₄₀ was initiated by the 15th event, shortly after the contribution of Rip₃₀ to runoff ceased (Fig. 2.7).

Table 2.6. Relative contributions of end-members to runoff for the initial and the major period. Values are followed by the respective standard deviations (SD).

Source	Depth (cm)	Average daily mean contribution to runoff (%)	
		Initial period ^a	Major period ^b
Hillslope soil water	40	5.9 ± 7.5	–
Hillslope soil water	65	–	36.8 ± 11.1
Toeslope soil water	40	17.0 ± 7.0	–
Riparian soil water	20	4.2 ± 3.3	–
Riparian soil water	30	–	5.0 ± 3.0
Riparian soil water	40	–	16.9 ± 17.0
Groundwater ^c	–	72.9 ± 8.2	41.3 ± 18.7

^a From day of year (DOY) 154 to 190.4.

^b From DOY 190.5 to 228.

^c Groundwater that was initially present before the 1st rainfall event of the summer monsoon.

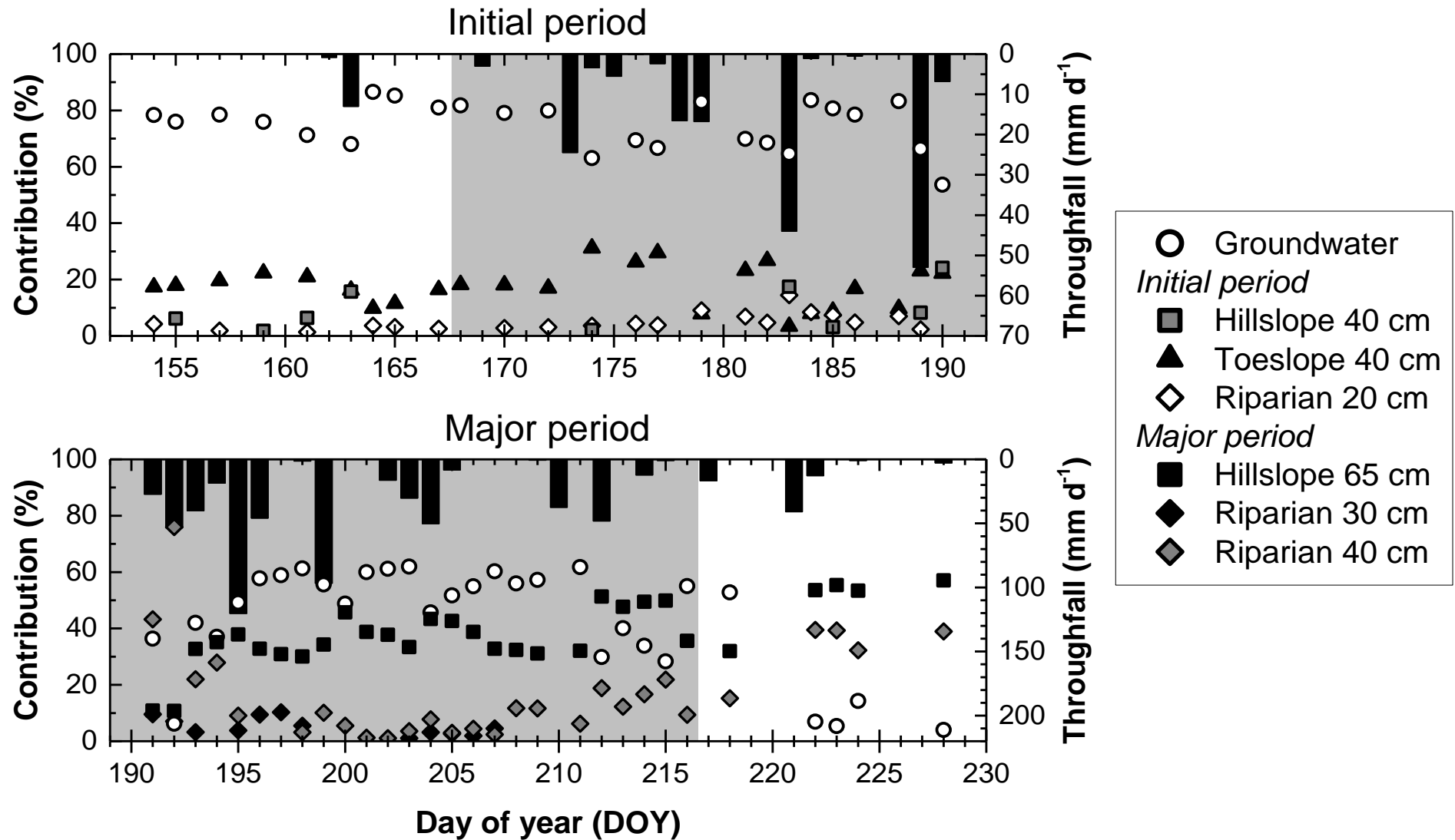


Figure 2.7. Relative contributions of end-members to runoff (daily mean) and throughfall (daily) as a function of time for the initial and the major period. The shaded areas correspond to the summer monsoon.

2.4. Discussion

2.4.1. Major hydrological fluxes and conditions

The influence of the summer monsoon on runoff did not become substantial until the occurrence of the 5th rainfall event, after which discharge remained above one order of magnitude greater than at low-flow conditions through most of the rest of the summer monsoon (Fig. 2.2). Not only did the frequency of events substantially increase from this event onward, but their influence on runoff as well, as the runoff coefficients of individual rainfall events averaged $23.6 \pm 12.9\%$ for the preceding events and $72.7 \pm 28.9\%$ from the 5th rainfall event onward. Neither average nor maximum throughfall intensity was found to significantly correlate with runoff coefficient (see Table 2.2 for selected major events). Rather, a likely explanation for the initially lower coefficients is the replenishment of soil moisture (θ_v) by most of the throughfall that occurred before the 5th event, as a gradual wet-up of the catchment was observed (Fig. 2.3). Given that throughfall was not identified as a most likely component of runoff, that the maximum throughfall intensity was well below the average soil infiltration capacities (Table 2.1), and that θ_v initially displayed a lagged response to rainfall events with increasing depth (Fig. 2.3), it is likely that throughfall promptly infiltrated the soil and gradually percolated through the soil profile, replenishing soil moisture.

From the 5th rainfall event onward, most of the events greatly exceeded the previous events in terms of throughfall. However, θ_v at 50-cm depth did not accordingly increase, and it decreased between events (Fig. 2.3). At the hillslope and riparian areas, θ_v at 50-cm depth even had shorter recession periods than at shallower depths. This implies that soil water at this depth either percolated to deeper layers or laterally flowed towards the streambed. Since a saturated zone was not present at the measured locations and depth, we believe that, from the 5th event onward, substantial amounts of soil water percolated to deeper layers. The responsiveness to rainfall events of unsaturated hydraulic conductivity ($K(\theta_v)$) at 50-cm depth at the hillslope and riparian areas is consistent with this inference (Fig. 2.3).

Although a water table was not measured at any time or location (except on one occasion and location), we do not exclude that localized, transient saturated zones may have formed in other parts of the catchment in response to rainfall events, as observed by Haga et al. (2005), Katsuyama et al. (2009), Sidle et al. (2000) and Uchida et al. (2002). The

formation of such saturated zones could have resulted from the percolation of soil water until the soil-bedrock interface which, at the study site, is on average between 55 and 66 cm below the soil surface (Table 2.1). Combined with the steepness of the hillslope area, the occurrence of transient saturation would have likely generated subsurface flow towards the streambed. The responsiveness of discharge to events (Fig. 2.2), the variable upstream extent of the stream, and the flow of intermittent springs are consistent with the occurrence of rapid, spatially variable, subsurface flow at the hillslope area. In fact, the first activation of springs corresponded to the approximate period when soil water is believed to have started substantially percolating to deeper layers. Also, the one occasion at which a water table was measured was related to the flow of an intermittent spring. Transient saturation might even have occurred beyond the duration of rainfall events, as the extension of the stream and the flow of intermittent springs lasted beyond the duration of events. These indications could explain the higher runoff coefficients of individual rainfall events from the 5th rainfall event onward, as the contribution of rapid subsurface flow to runoff could have substantially increased.

The wide range in the constants derived from the recession rate equations reflects the contribution from components of different flow velocities, as explained by Tallaksen (1995). Transient saturation could also have recharged the observed saturated zone at the location where the stream reached its maximum extent. The fluctuations in water depth of this zone in response to rainfall events indicated that it was at least temporarily recharged.

2.4.2. Validity of the mixing models

The reliability of the tracer-based hydrograph separation technique strongly depends on the satisfaction of the assumptions underlying this technique. Although the violation of some of these assumptions may introduce uncertainty in the results, the extensive and now standard application of this technique has proven useful in producing plausible perceptual models of runoff generation (Buttle, 1994; Inamdar, 2011). In the current study, a rigorous set of criteria derived from the literature was established in order to maximize the satisfaction of these assumptions. Recommendations on how to appropriately apply the technique in terms of data collection and analysis were followed, and diagnostic tools were used to test the conservative nature of tracers. The selection of tracers and identification of the most likely end-members were iteratively performed, as strongly suggested by Hooper (2001) to reduce the level of subjectivity of the process and consequently refine the use of mixing models. The

agreement between the application of the rule of one and the results of the residual analyses of stream water tracer values (Table 2.4) suggested that the selected tracers were conservative and linearly mixed (Hooper, 2003). The linear mixing of Ca^{2+} and Mg^{2+} was also supported by a visual analysis of the Piper diagram (Fig. 2.4). We rejected the possibility of a substantial evaporative enrichment of stream water $\delta^2\text{H}$, as $\delta^2\text{H}$ of the samples collected at the catchment outflow was not significantly higher than that of the samples collected at the location where the stream surfaced during low-flow and receding conditions (Fig. 2.1).

The assumption of temporal invariance of end-member tracer values was clearly violated for throughfall and soil water. The significance of this violation was greatly reduced by dividing the dataset into two parts for which the variation in values was much lower, and applying separate mixing models. We further reduced this significance by using medians instead of averages. For consistency, we chose to use median throughfall tracer values calculated for both periods instead of volumetric-weighted averages for individual rainfall events, as opposed to what McDonnell et al. (1990) prescribed. Since a direct and substantial contribution from this end-member was not expected, and since the absolute differences between medians and volumetric-weighted averages were $< 5\%$, we did not consider that this choice significantly influenced the results of the mixing models.

Due to the restricted extent of the experimental setup, it was not possible to test the assumption of spatial invariance of end-member tracer values. Regarding the assumption of distinct end-member tracer values, we considered that it was satisfied for most end-members and most tracers (Fig. 2.6). However, differences were not statistically assessed and, in some cases, were very small. Although soil water displayed substantial differences in tracer values between some end-members, the values of other soil water end-members were similar. A mixing amongst end-members could have occurred, which we were not able to discard. In this sense, the separation of soil water into some distinct end-members was undermined.

In each mixing subspace, the combination of the identified end-members circumscribed the quasi-totality of stream water projections (Fig. 2.5). The models were rather successful in reproducing the measured values of a conservative tracer which was not used to build the models (Mg^{2+} , RRMSEs of 7.42 and 10.12%, Table 2.5). Overall, these are good indications that the models were valid (Hooper, 2003; Inamdar, 2011). However, we fully acknowledge that the models entailed certain levels of subjectivity, model uncertainty and statistical uncertainty (Joerin et al., 2002). The temporal and spatial variance of end-member

tracer values certainly induced some uncertainty in the results. The reliability of these results was improved by their comparison with hydrometric data. The division of the dataset into the initial and the major period was set as a compromise between the satisfaction of the assumptions of the hydrograph separation technique and the reproduction of the hydrological dynamics of the study site.

2.4.3. Runoff generation as influenced by the summer monsoon

2.4.3.1. Initial period

Along with groundwater, Toe_{40} was a major source of runoff during the initial period, and its depth coincided with that of the soil water contribution from the hillslope area (Table 2.6). At this approximate depth, the value of K_{sat} is much lower than at shallower depths (Table 2.1; 30-40 cm), possibly indicating that percolation at this depth was reduced, and that soil matrix flow towards the streambed was enhanced. Accordingly, Toe_{40} could have contributed to runoff through the process of soil matrix flow. The steepness of the hillslope area could facilitate soil matrix flow towards the toeslope area where, due to the sharp break in slope, water would flow at a lower rate, accumulate, change in composition by chemical weathering and isotopic evaporative enrichment, and subsequently discharge to runoff. The differences in the Ca^{2+} , EC and δ^2H values between Toe_{40} and Toe_{88} and between $Hill_{40}$ and $Hill_{65}$ are consistent with the inference of an initial hydraulic barrier, and the differences in values between Toe_{40} and $Hill_{40}$ are consistent with the inference of a change in composition (Fig. 2.6). Moreover, θ_v at 50-cm depth at this area was initially higher than at shallower depths and higher than at the hillslope and riparian areas. It also displayed longer recession periods and was less responsive to rainfall events (Fig. 2.3). This might be attributed to a steady lateral input of water from the hillslope area. We also believe this was reflected in the relative contribution of Toe_{40} to runoff, which was continuous and varied in accordance with the contribution of other end-members, expressing its stability (Fig. 2.7). The direct contribution of Toe_{40} to runoff may explain the differences in chemistry observed between samples collected at the catchment outflow and samples collected at the upstream location where water emerged. Tsuboyama (2006) reported that soil matrix flow accounted for 87% of the yearly outflow from a soil profile in a forested catchment, which supports our inference that, at low-flow conditions, soil matrix flow can substantially contribute to runoff generation.

The stability of the relative contribution of Rip₂₀ to runoff led us to believe that Rip₂₀ might also have contributed to runoff through soil matrix flow. The contribution from a single shallow layer was initially startling. However, an analysis of the θ_v time-series of this area for the initial period indicated that water may not have substantially percolated to 30 and 50-cm depth following rainfall events (Fig. 2.3). In this steep and narrow riparian area, water percolating vertically and laterally might have reached the streambed before it reached deeper layers, relating to the assumption made by Sidle et al. (2000). This was supported by the fact that when θ_v reached its lowest values, for a period of 10 days soil water could only be sampled at 10 and 20-cm depth. In contrast to Sidle et al. (1998), we rejected the possibility of the occurrence of saturation-excess overland flow at the riparian area, since a water table intersecting the soil surface was never measured.

The velocity of soil matrix flow is usually low, which is not consistent with the responsiveness of the hydrograph to the rainfall events of the initial period (Fig. 2.2). A likely explanation would be that Hill₄₀ contributed to runoff through the process of saturated flow. While the average relative contribution of Hill₄₀ to runoff was low (Table 2.6), its relative contribution greatly increased in response to major rainfall events (Fig. 2.7). This reflects an initially intermittent connectivity of the hillslope area to the stream, and is consistent with the findings of Katsuyama et al. (2001) who reported an intermittent but increasing contribution to runoff of transient saturated zones at the hillslope area over a gradual wet-up of the catchment.

2.4.3.2. Major period

The likely formation of localized, transient saturated zones and the consequent enhancement of subsurface flow could have enhanced the connectivity of the hillslope area to the stream, and triggered the sudden shift in runoff generation processes. This shift is very similar to the development in runoff generation processes described by Tani (1997) over a transition from dry to wet conditions. However, we could not definitely determine if the rapid component of subsurface flow was saturated flow or preferential flow, or a mixture of both. The continuous nature of the soil water contribution to runoff as well as its prompt response to rainfall events strongly suggested that it occurred through a mixture of both. Preferential flow has been recognized as a major and very dynamic flow path of forested headwater catchments of the EASM region, and usually displays a threshold response (Sidle et al., 2001; Tsuboyama, 2006). It is possible that a network of macropores developed at the soil-bedrock

interface and that effective hydraulic conductivity was much higher than what was estimated, as Uchida et al. (2002) reported. Preferential flow through macropores could have contributed to rapid subsurface flow at the hillslope area. This may well have led to the formation of the two observed intermittent springs, of which the chemistry fell within the ranges in soil water chemistry. Through the major period, the activation of springs was more responsive to rainfall events and its duration following events was greater than during the initial period. The relative contribution of Hill₆₅ to runoff was responsive to rainfall events, but also sustained once intermittent springs had ceased to flow. In this sense, a certain portion of subsurface flow from the hillslope area would have bypassed the toeslope area and directly contributed to runoff through both saturated and preferential flow, as reported by Uchida et al. (2002) and Uchida et al. (2003). It also possible that soil water from the hillslope area directly contributed to runoff while simultaneously recharging the saturated zone and subsequently contributed to runoff through the flow of the mixture of soil water and groundwater that was initially present. This is consistent with the chemistry of the observed saturated zone, which ranged between that of groundwater and that of stream water. Haga et al. (2005), Katsuyama et al. (2009), Sidle et al. (2000) and Uchida et al. (2002) suggested that transient saturated zones contribute to the recharge of the saturated zone and, via preferential flow paths, directly to runoff. A separation of both water flow paths for the same end-member was not possible, which is similar to the problematic mentioned by Hugenschmidt et al. (2014).

For the first few days of the major period, the relative contribution of Rip₄₀ was high. This could be explained by the capacity of such a steep and narrow riparian area to rapidly transfer water to the stream. Even though the riparian area accounts for only 2.3% of the catchment area, its average relative contribution to runoff was substantial (Table 2.6). This either means that the riparian area exerted a strong regulation on the production of runoff, or that water believing to originate from the riparian area just “passed through” and originated from other sources. The accumulation of soil water at this area and its subsequent discharge to runoff might have occurred, as well as the recharge of the saturated zone by soil water of the riparian area. Following the end of the summer monsoon, soil moisture values at all areas decreased in the same pattern it did before the onset of the summer monsoon and almost reached the initial values (Fig. 2.3). Given the fact that contributions from Hill₆₅ and Rip₄₀ were at this period sustained, we believe that the observed saturated zone then consisted of a mixture of relatively new soil water from these end-members. As explained by Sidle et al.

(2000), the low storage capacity of steep, narrow riparian areas allows the input of soil water to greatly influence the level and quality of groundwater.

The presence of groundwater was inferred by the emergence of water at low-flow conditions at the location where the stream reached its maximum extent. The comparatively lower $\delta^2\text{H}$ of groundwater supported the assumption that it initially was a distinct source of water and not a mixture of other end-members (Table 2.4 and Fig. 2.6). The rate of groundwater flow very likely remained stable or only slightly increased through the transition from the initial to the major period, which could explain the drastic decrease in its relative contribution to runoff following the 5th rainfall event, as discharge greatly increased (Figs. 2.2 and 2.7). Following the subsequent increase and until before the 15th rainfall event (DOY 212), the relative contribution of groundwater varied within a narrow range even if discharge varied within a wide range, implying that the rate of groundwater flow was influenced by the input of throughfall in a similar way that discharge itself was. This is congruent with the findings of Koh et al. (2001), who reported event-related variations in isotopic composition which were similar between the saturated zone and stream water. Furthermore, between rainfall events, the relative contribution of groundwater to runoff gradually increased as discharge decreased, which is the opposite of what was observed during the initial period. We propose that, over this period, increased and sustained rates in the recharge of the saturated zone resulted in increased and sustained rates of groundwater flow. The occurrence of successive summer monsoon rainfall events likely resulted in the simultaneous and gradual recharge of the saturated zone and depletion of the groundwater that was initially present. This relates to the relatively high groundwater recharge rates of individual events reported by Choi et al. (2007). However, it disagrees with the findings of Lee et al. (2007) who reported that only half of the yearly groundwater recharge was attributed to summer monsoon events. We believe that this discrepancy is due to a difference in storage capacity between both study sites, as the study of Lee et al. (2007) was conducted at a site much greater in area.

2.5. Conclusions

This study has quantified the influence of the East Asian summer monsoon (EASM) on the water sources and flow paths of a forested catchment, and characterized its overall influence on runoff generation. The first few rainfall events of the EASM replenished soil

moisture and induced a gradual wet-up of the catchment. As the EASM further progressed, a sudden shift from the dominance of groundwater flow towards higher contributions of subsurface flow from the hillslope and riparian areas, which also shifted to deeper soil layers, likely occurred. This shift was associated with transient saturation at the hillslope area and the recharge of the saturated zone, which also likely resulted in the increase in runoff coefficients of rainfall events. Following the end of the EASM, the catchment returned to its initial state in terms of discharge and soil moisture, but not in terms of runoff components, as the relative contribution of soil water from the hillslope and riparian areas exceeded that of groundwater (Table 2.7).

The magnitude and complexity of hydrological responses to the EASM has been an impediment to the study of its overall influence on runoff generation. This study clarifies the generation of runoff in forested catchments as influenced by the EASM. Our findings agree with the findings reported in other studies and, more importantly, provides insight on variations in responsive water sources and flow paths. Our findings are also a significant contribution to the ongoing efforts to estimate the water balance and quality of the Lake Soyang watershed. The shift in runoff generation processes we infer has biogeochemical implications which should be considered in the water management of this watershed.

Table 2.7. Relative contributions of water sources to runoff before, during and after the 2013 summer monsoon (independently of soil depth). Values are followed by the respective standard deviations (SD).

Source	Average daily mean contribution to runoff (%)		
	Before the summer monsoon ^a	During the summer monsoon ^b	After the summer monsoon ^c
Groundwater ^d	78.2 ± 5.8	60.1 ± 8.3	16.7 ± 18.4
Hillslope soil water	3.3 ± 5.0	20.7 ± 6.2	50.3 ± 9.3
Toeslope soil water	16.6 ± 3.7	8.5 ± 3.9	0
Riparian soil water	1.9 ± 1.0	10.7 ± 8.9	33.0 ± 9.3

^a From day of year (DOY) 154 to 167, period of 14 days.

^b From DOY 168 to 216, period of 49 days.

^c From DOY 217 to 228, period of 12 days.

^d Groundwater that was initially present before the 1st rainfall event of the summer monsoon.

Acknowledgments

We are grateful for the help and advice from Jutta Eckert, Kwanghun Choi, Youngsoon Choi, Jae-Sung Eum, Gwanyong Jeong, Bomchul Kim, Kiyong Kim, Mi-Hee Lee, Thinh Duy Nguyen, Ji-Hyung Park and John Tenhunen through this study. This study was conducted within the framework of the International Research Training Group TERRECO (Kang and Tenhunen, 2010) which was funded by the German Research Foundation at the University of Bayreuth, Bayreuth, Germany, and the Korea Research Foundation at Kangwon National University, Chuncheon, South Korea. The isotopic analyses of soil water were conducted at the laboratory of the Institute of Landscape Ecology, University of Münster, Münster, Germany, supervised by Klaus-Holger Knorr.

Appendix

For stream water and throughfall, $\delta^2\text{H}$ was measured using a mass spectrometer (DELTA V Advantage, Thermo Fisher Scientific GmbH, Bremen, Germany) coupled to a high-temperature pyrolysis reactor (HTO, HEKAtech GmbH, Wegberg, Germany) and a continuous flow interface (ConFlo IV, Thermo Fisher Scientific GmbH). See Gehre and Strauch (2003) for a description of the set-up and method. The analyzer was calibrated with the Standard Light Antarctic Precipitation (Gonfiantini, 1978), Greenland Ice Sheet Precipitation (IAEA, 2007) and Standard Mean Ocean Water (Craig, 1961) standards and one blank sample for every five samples. Each sample was analyzed five times; the first three measurements were discarded and the last two averaged. Ratios were defined in relation to Vienna Standard Mean Ocean Water (VSMOW; Gonfiantini, 1978) and the analytical precision of the measurements was $\pm 0.84\text{‰}$. For soil water, $\delta^2\text{H}$ was measured by off-axis integrated cavity output spectroscopy (TIWA-45EP, Los Gatos Research Inc., Mountain View, USA) and the analyzer was calibrated with four certified standards provided by the manufacturer. Each sample was analyzed six times; the first two measurements were discarded and the last four averaged. Ratios were defined in relation to VSMOW and the analytical precision of the measurements was $\pm 0.23\text{‰}$. A set of twenty randomly selected samples were measured by both methods, and the average difference in absolute value between methods was $4.53 \pm 2.95 \text{‰}$. We concluded that the results of both methods were comparable, which was also supported by the literature (Brand et al., 2009; Jung et al., 2013; Schultz et al., 2011; West et al., 2010; Zhao et al., 2011).

References

- Abdi, H., Williams, L.J., 2010. Principal component analysis. *Wiley Interdiscip. Rev. Comput. Stat.* 2, 433–459. DOI: [10.1002/wics.101](https://doi.org/10.1002/wics.101)
- Ali, G.A., Roy, A.G., Turmel, M.-C., Courchesne, F., 2010. Source-to-stream connectivity assessment through end-member mixing analysis. *J. Hydrol.* 392, 119–135. DOI: [10.1016/j.jhydrol.2010.07.049](https://doi.org/10.1016/j.jhydrol.2010.07.049)
- Asano, Y., Uchida, T., Ohte, N., 2002. Residence times and flow paths of water in steep unchannelled catchments, Tanakami, Japan. *J. Hydrol.* 261, 173–192. DOI: [10.1016/S0022-1694\(02\)00005-7](https://doi.org/10.1016/S0022-1694(02)00005-7)
- Bae, J.S., Joo, R.W., Kim, Y.-S., 2012. Forest transition in South Korea: reality, path and drivers. *Land Use Policy* 29, 198–207. DOI: [10.1016/j.landusepol.2011.06.007](https://doi.org/10.1016/j.landusepol.2011.06.007)
- Barthold, F.K., Tyralla, C., Schneider, K., Vaché, K.B., Frede, H.-G., Breuer, L., 2011. How many tracers do we need for end member mixing analysis (EMMA)? A sensitivity analysis. *Water Resour. Res.* 47, W08519. DOI: [10.1029/2011WR010604](https://doi.org/10.1029/2011WR010604)
- Bonell, M., 1998. Selected challenges in runoff generation research in forests from the hillslope to headwater drainage basin scale. *J. Am. Water Resour. Assoc.* 34, 765–785. DOI: [10.1111/j.1752-1688.1998.tb01514.x](https://doi.org/10.1111/j.1752-1688.1998.tb01514.x)
- Brand, W.A., Geilmann, H., Crosson, E.R., Rella, C.W., 2009. Cavity ring-down spectroscopy versus high-temperature conversion isotope ratio mass spectrometry; a case study on $\delta^2\text{H}$ and $\delta^{18}\text{O}$ of pure water samples and alcohol/water mixtures. *Rapid Commun. Mass Spectrom.* 23, 1879–1884. DOI: [10.1002/rcm.4083](https://doi.org/10.1002/rcm.4083)
- Buttle, J.M., 1994. Isotope hydrograph separations and rapid delivery of pre-event water from drainage basins. *Prog. Phys. Geogr.* 18, 16–41. DOI: [10.1177/030913339401800102](https://doi.org/10.1177/030913339401800102)
- Choi, I.-H., Woo, N.C., Kim, S.-J., Moon, S.-K., Kim, J., 2007. Estimation of the groundwater recharge rate during a rainy season at a headwater catchment in Gwangneung, Korea. *Korean J. Agric. For. Meteorol.* 9, 75–87. DOI: [10.5532/KJAFM.2007.9.2.075](https://doi.org/10.5532/KJAFM.2007.9.2.075)
- Choi, H.T., Kim, K., Lee, C.H., 2010. The effect of antecedent moisture conditions on the contributions of runoff components to stormflow in the coniferous forest catchment. *Jour. Korean For. Soc.* 99, 755–761.
- Christophersen, N., Neal, C., Hooper, R.P., Vogt, R.D., Andersen, S., 1990. Modelling streamwater chemistry as a mixture of soilwater end-members—a step towards second-generation acidification models. *J. Hydrol.* 116, 307–320. DOI: [10.1016/0022-1694\(90\)90130-P](https://doi.org/10.1016/0022-1694(90)90130-P)
- Christophersen, N., Hooper, R.P., 1992. Multivariate analysis of stream water chemical data: the use of principal components analysis for the end-member mixing problem. *Water Resour. Res.* 28, 99–107. DOI: [10.1029/91WR02518](https://doi.org/10.1029/91WR02518)
- Chung, Y.-S., Yoon, M.-B., Kim, H.-S., 2004. On climate variations and changes observed in South Korea. *Clim. Change* 66, 151–161. DOI: [10.1023/B:CLIM.0000043141.54763.f8](https://doi.org/10.1023/B:CLIM.0000043141.54763.f8)

- Craig, H., 1961. Standard for reporting concentrations of deuterium and oxygen-18 in natural waters. *Science* 133, 1833–1834. DOI: [10.1126/science.133.3467.1833](https://doi.org/10.1126/science.133.3467.1833)
- FAO (Food and Agriculture Organization of the United Nations), 2012. Global ecological zones for FAO forest reporting: 2010 Update. Forest Resources Assessment Working Paper 179. FAO, Rome.
- Fujimoto, M., Ohte, N., Tani, M., 2008. Effects of hillslope topography on hydrological responses in a weathered granite mountain, Japan: comparison of the runoff response between the valley-head and the side slope. *Hydrol. Processes* 22, 2581–2594. DOI: [10.1002/hyp.6857](https://doi.org/10.1002/hyp.6857)
- Fujimoto, M., Ohte, N., Tani, M., 2011. Effects of hillslope topography on runoff response in a small catchment in the Fudoji Experimental Watershed, central Japan. *Hydrol. Processes* 25, 1874–1886. DOI: [10.1002/hyp.7943](https://doi.org/10.1002/hyp.7943)
- Gehre, M., Strauch, G., 2003. High-temperature elemental analysis and pyrolysis techniques for stable isotope analysis. *Rapid Commun. Mass Spectrom.* 17, 1497–1503. DOI: [10.1002/rcm.1076](https://doi.org/10.1002/rcm.1076)
- Gomi, T., Sidle, R.C., Richardson J.S., 2002. Understanding processes and downstream linkages of headwater systems. *BioSci.* 52, 905–916. DOI: [10.1641/0006-3568\(2002\)052\[0905:UPADLO\]2.0.CO;2](https://doi.org/10.1641/0006-3568(2002)052[0905:UPADLO]2.0.CO;2)
- Gomi, T., Asano, Y., Uchida, T., Onda, Y., Sidle, R. C., Miyata, S., Kosugi, K., Mizugaki, S., Fukuyama, T., Fukushima, T., 2010. Evaluation of storm runoff pathways in steep nested catchments draining a Japanese cypress forest in central Japan: a geochemical approach. *Hydrol. Processes* 24, 550–566. DOI: [10.1002/hyp.7550](https://doi.org/10.1002/hyp.7550)
- Gonfiantini, R., 1978. Standards for stable isotope measurements in natural compounds. *Nature* 271, 534–536. DOI: [10.1038/271534a0](https://doi.org/10.1038/271534a0)
- GRMA (Gangwon Regional Meteorological Administration), 2013. Gangwon province summer months (June-August) meteorological characteristics. KMA, Seoul. (in Korean)
- Ha, K.-J., Heo, K.-Y., Lee, S.-S., Yun, K.-S., Jhun, J.-G., 2012. Variability in the East Asian Monsoon: a review. *Meteorol. Appl.* 19, 200–215. DOI: [10.1002/met.1320](https://doi.org/10.1002/met.1320)
- Haga, H., Matsumoto, Y., Matsutani, J., Fujita, M., Nishida, K., Sakamoto, Y., 2005. Flow paths, rainfall properties, and antecedent soil moisture controlling lags to peak discharge in a granitic unchanneled catchment. *Water Resour. Res.* 41, W12410. DOI: [10.1029/2005WR004236](https://doi.org/10.1029/2005WR004236)
- Ho, C.-H., Lee, J.-Y., Ahn, M.-H., Lee, H.-S., 2003. A sudden change in summer rainfall characteristics in Korea during the late 1970s. *Int. J. Climatol.* 23, 117–128. DOI: [10.1002/joc.864](https://doi.org/10.1002/joc.864)
- Hooper, R.P., Christophersen, N., Peters, N.E., 1990. Modelling streamwater chemistry as a mixture of soilwater end-members—an application to the Panola Mountain catchment, Georgia, USA. *J. Hydrol.* 116, 321–343. DOI: [10.1016/0022-1694\(90\)90131-G](https://doi.org/10.1016/0022-1694(90)90131-G)
- Hooper, R.P., 2001. Applying the scientific method to small catchment studies: a review of the Panola Mountain experience. *Hydrol. Processes* 15, 2039–2050. DOI: [10.1002/hyp.255](https://doi.org/10.1002/hyp.255)

- Hooper, R.P., 2003. Diagnostic tools for mixing models of stream water chemistry. *Water Resour. Res.* 39, 1055. DOI: [10.1029/2002WR001528](https://doi.org/10.1029/2002WR001528)
- Hugenschmidt, C., Ingwersen, J., Sangchan, W., Sukvanachaiikul, Y., Duffner, A., Uhlenbrook, S., Streck, T., 2014. A three-component hydrograph separation based on geochemical tracers in a tropical mountainous headwater catchment in northern Thailand. *Hydrol. Earth Syst. Sci.* 18, 525–537. DOI: [10.5194/hess-18-525-2014](https://doi.org/10.5194/hess-18-525-2014)
- IAEA (International Atomic Energy Agency), 2007. Reference Sheet for Reference Material. GISP. IAEA, Vienna.
- Inamdar, S., 2011. The use of geochemical mixing models to derive runoff sources and hydrologic flow paths, in: Levia, D.F., Carlyle-Moses, D., Tanaka, T. (Eds.), *Forest hydrology and biogeochemistry. Synthesis of past research and future directions.* Springer, pp. 163–183.
- Inamdar, S., Dhillon, G., Singh, S., Dutta, S., Levia, D., Scott, D., Mitchell, M., Van Stan, J., McHale, P., 2013. Temporal variation in end-member chemistry and its influence on runoff mixing patterns in a forested, Piedmont catchment. *Water Resour. Res.* 49, 1828–1844. DOI: [10.1002/wrcr.20158](https://doi.org/10.1002/wrcr.20158)
- IUSS Working Group WRB, 2014. World Reference Base for Soil Resources 2014. International soil classification system for naming soils and creating legends for soil maps. World Soil Resources Reports No. 106. FAO, Rome.
- Jeong, K.-Y., Lee, D.-R., Moon, J.-W., 2003. Analysis of seasonal water quality and quantity characteristics for Seolmacheon experimental watershed. *Proc. Joint Conf. Korea Water Environ. Assoc.*, 185–188. (in Korean)
- Jeong, J.-J., Bartsch, S., Fleckenstein, J.H., Matzner, E., Tenhunen, J.D., Lee, S.D., Park, S.K., Park, J.-H., 2012. Differential storm responses of dissolved and particulate organic carbon in a mountainous headwater stream, investigated by high-frequency, in situ optical measurements. *J. Geophys. Res.* 117, G03013. DOI: [10.1029/2012JG001999](https://doi.org/10.1029/2012JG001999)
- Jeong, S.-J., Ho, C.-H., Choi, S.-D., Kim, J., Lee, E.-J., Gim, H.-J., 2013. Satellite data-based phenological evaluation of the nationwide reforestation of South Korea. *PLoS ONE* 8, e58900. DOI: [10.1371/journal.pone.0058900](https://doi.org/10.1371/journal.pone.0058900)
- Joerin, C., Beven, K.J., Iorgulescu, I., Musy, A., 2002. Uncertainty in hydrograph separations based on geochemical mixing models. *J. Hydrol.* 255, 90–106. DOI: [10.1016/S0022-1694\(01\)00509-1](https://doi.org/10.1016/S0022-1694(01)00509-1)
- Jung, E.-Y., Otieno, D., Lee, B., Lim, J.H., Kang, S.K., Schmidt, M.W.T., Tenhunen, J., 2010. Up-scaling to stand transpiration of an Asian temperate mixed-deciduous forest from single tree sapflow measurements. *Plant Ecol.* 212, 383–395. DOI: [10.1007/s11258-010-9829-3](https://doi.org/10.1007/s11258-010-9829-3)
- Jung, B.-J., Lee, H.-J., Jeong, J.-J., Owen, J., Kim, B., Meusburger, K., Alewell, C., Gebauer, G., Shope, C., Park, J.-H., 2012. Storm pulses and varying sources of hydrologic carbon export from a mountainous watershed. *J. Hydrol.* 440–441, 90–101. DOI: [10.1016/j.jhydrol.2012.03.030](https://doi.org/10.1016/j.jhydrol.2012.03.030)

- Jung, Y.-Y., Koh, D.-C., Lee, J., Ko, K.-S., 2013. Applications of isotope ratio infrared spectroscopy (IRIS) to analysis of stable isotopic compositions of liquid water. *Econ. Environ. Geol.* 46, 495–508. DOI: [10.9719/EEG.2013.46.6.495](https://doi.org/10.9719/EEG.2013.46.6.495) (in Korean)
- Kang, S., Tenhunen, J., 2010. Complex terrain and ecological heterogeneity (TERRECO): evaluating ecosystem services in production versus water quantity/quality in mountainous landscapes. *Korean J. Agric. For. Meteorol.* 12, 307–316. DOI: [10.5532/KJAFM.2010.12.4.307](https://doi.org/10.5532/KJAFM.2010.12.4.307) (in Korean)
- Katsuyama, M., Ohte, N., Kobashi, S., 2001. A three-component end-member analysis of streamwater hydrochemistry in a small Japanese forested headwater catchment. *Hydrol. Processes* 15, 249–260. DOI: [10.1002/hyp.155](https://doi.org/10.1002/hyp.155)
- Katsuyama, M., Kabeya, N., Ohte, N., 2009. Elucidation of the relationship between geographic and time sources of stream water using a tracer approach in a headwater catchment. *Water Resour. Res.* 45, W06414. DOI: [10.1029/2008WR007458](https://doi.org/10.1029/2008WR007458)
- Kim, S.-J., Lee, D., Kim, J., Kim, S., 2007. Hydro-biogeochemical approaches to understanding of water and carbon cycling in the Gwangneung forest catchment. *Korean J. Agric. For. Meteorol.* 9, 109–120. DOI: [10.5532/KJAFM.2007.9.2.109](https://doi.org/10.5532/KJAFM.2007.9.2.109)
- Kim, K., Yoo, J.-Y., 2007. Hydrograph separation using geochemical tracers by three-component mixing model for the coniferous forested catchment in Gwangneung Gyeonggi-do, Republic of Korea. *J. Korean For. Soc.* 96, 561–566.
- Kim, S.-J., Lee, D., Kim, S., 2009. Use of isotope data to determine mean residence time (MRT) of water in a forest catchment: ³⁵S and ³H-based estimates. *Asia-Pacific J. Atmos. Sci.* 45, 165–173.
- Kim, J.H., Jin, G., Chung, S.H., 2015. Stand development patterns of forest cover types in the natural forests of northern Baekdudaegan in South Korea. *J. For. Res.* 26, 381–390. DOI: [10.1007/s11676-015-0044-x](https://doi.org/10.1007/s11676-015-0044-x)
- KMA (Korea Meteorological Administration), 2013. Annual climatological report 2013. KMA, Seoul.
- Koh, Y., Bae, D., Kim, C., Kim, K., Chung, H., Kim, S., 2001. Consideration of the groundwater recharge based on environmental isotopic characteristics of the small basin in the Yeosu area. *J. Korean Soc. Soil Groundw. Env.* 6, 93–106. (in Korean)
- Kottek, M., Grieser, J., Beck, C., Rudolf, B., Rubel, F., 2006. World map of the Köppen-Geiger climate classification updated. *Meteorol. Z.* 15, 259–263. DOI: [10.1127/0941-2948/2006/0130](https://doi.org/10.1127/0941-2948/2006/0130)
- Kwon, H., Lee, J.-H., Lee, Y.-K., Lee, J.W., Jung, S.W., Kim, J., 2009. Seasonal variations of evapotranspiration observed in a mixed forest in the Seolmacheon catchment. *Korean J. Agric. For. Meteorol.* 11, 39–47. DOI: [10.5532/KJAFM.2009.11.1.039](https://doi.org/10.5532/KJAFM.2009.11.1.039) (in Korean)
- Lee, D., Kim, J., Kim, S.-J., Moon, S.-K., Lee, J., Lim, J.-H., Son, Y., Kang, S., Kim, S., Kim, K., Woo, N., Lee, B., Kim, S., 2007. Lessons from cross-scale studies of water and carbon cycles in the Gwangneung forest catchment in a complex landscape of monsoon Korea. *Korean J. Agric. For. Meteorol.* 9, 149–160. DOI: [10.5532/KJAFM.2007.9.2.149](https://doi.org/10.5532/KJAFM.2007.9.2.149)

- Lee, S.R., Cho, K., 2012. Precambrian crustal evolution of the Korean peninsula. *J. Petrol. Soc. Korea* 21, 89–112. (in Korean)
- Lee, H.-J., Chun, K.-W., Shope, C.L., Park, J.-H., 2015. Multiple time-scale monitoring to address dynamic seasonality and storm pulses of stream water quality in mountainous watersheds. *Water* 7, 6117–6138. DOI: [10.3390/w7116117](https://doi.org/10.3390/w7116117)
- Lee, M.-H., 2016. Dynamics of dissolved and particulate organic carbon and nitrogen in forest ecosystems. University of Bayreuth, Bayreuth.
- Lischeid, G., 2008. Combining hydrometric and hydrochemical data sets for investigating runoff generation processes: tautologies, inconsistencies and possible explanations. *Geogr. Compass* 2, 255–280. DOI: [10.1111/j.1749-8198.2007.00082.x](https://doi.org/10.1111/j.1749-8198.2007.00082.x)
- McDonnell, J.J., Bonell, M., Stewart, M., Pearce, A., 1990. Deuterium variations in storm rainfall: implications for stream hydrograph separation. *Water Resour. Res.* 26, 455–458. DOI: [10.1029/WR026i003p00455](https://doi.org/10.1029/WR026i003p00455)
- Ohte, N., Tokuchi, N., Fujimoto, M., 2010. Seasonal patterns of nitrate discharge from forested catchments: information derived from Japanese case studies. *Geogr. Compass* 4, 1358–1376. DOI: [10.1111/j.1749-8198.2010.00377.x](https://doi.org/10.1111/j.1749-8198.2010.00377.x)
- Park, J.-H., Duan, L., Kim, B., Mitchell, M.J., Shibata, H., 2010. Potential effects of climate change and variability on watershed biogeochemical processes and water quality in Northeast Asia. *Environ. Int.* 36, 212–225. DOI: [10.1016/j.envint.2009.10.008](https://doi.org/10.1016/j.envint.2009.10.008)
- Pinder, G.F., Jones, J.F., 1969. Determination of the ground-water component of peak discharge from the chemistry of total runoff. *Water Resour. Res.* 5, 438–445. DOI: [10.1029/WR005i002p00438](https://doi.org/10.1029/WR005i002p00438)
- Preisendorfer, R.W., Zwiers, F.W., Barnett, T.P., 1981. Foundations of principal component selection rules. SIO Reference Series 81–4. Scripps Institute of Oceanography, La Jolla.
- Rice, K.C., Hornberger, G.M., 1998. Comparison of hydrochemical tracers to estimate source contributions to peak flow in a small, forested, headwater catchment. *Water Resour. Res.* 34, 1755–1766. DOI: [10.1029/98WR00917](https://doi.org/10.1029/98WR00917)
- Schoeneberger, P.J., Wysocki, D.A., Benham, E.C. (Eds.), 2011. Field book for describing and sampling soils, version 3.0. Natural Resources Conservation Service, National Soil Survey Center, Lincoln.
- Schultz, N.M., Griffis, T.J., Lee, X., Baker, J.M., 2011. Identification and correction of spectral contamination in $^2\text{H}/^1\text{H}$ and $^{18}\text{O}/^{16}\text{O}$ measured in leaf, stem, and soil water. *Rapid Commun. Mass Spectrom.* 25, 3360–3368. DOI: [10.1002/rcm.5236](https://doi.org/10.1002/rcm.5236)
- Seo, K.-H., Son, J.-H., Lee, J.-Y., 2011. A new look at Changma. *Atmos.* 21, 109–121. (in Korean)
- Shin, J.-H., 2002. Ecosystem geography of Korea, in: Lee, D.W., Jin, V., Choe, J.C., Son, Y.H., Lee, H.-Y., Hong, S.K., Ihm, B.-S. (Eds.), *Ecology of Korea*. Bumwoo, Seoul, pp.19–46.
- Shope, C.L., Bartsch, S., Kim, K., Kim, B., Tenhunen, J., Peiffer, S., Park, J.-H., Ok, Y.S., Fleckenstein, J., Koellner, T., 2013. A weighted, multi-method approach for accurate

- basin-wide streamflow estimation in an ungauged watershed. *J. Hydrol.* 494, 72–82. DOI: [10.1016/j.jhydrol.2013.04.035](https://doi.org/10.1016/j.jhydrol.2013.04.035)
- Sidele, R.C., Tsuboyama, Y., Noguchi, S., Hosoda, I., Fujieda, M., Shimizu, T., 1998. Progress towards understanding stormflow generation in headwater catchments, in: Sassa, K. (Ed.), *Environmental Forest Science*. Springer, pp. 483–498.
- Sidele, R.C., Tsuboyama, Y., Noguchi, S., Hosoda, I., Fujieda, M., Shimizu, T., 2000. Stormflow generation in steep forested headwaters: a linked hydrogeomorphic paradigm. *Hydrol. Processes* 14, 369–385. DOI: [10.1002/\(SICI\)1099-1085\(20000228\)14:3<369::AID-HYP943>3.0.CO;2-P](https://doi.org/10.1002/(SICI)1099-1085(20000228)14:3<369::AID-HYP943>3.0.CO;2-P)
- Sidele, R.C., Noguchi, S., Tsuboyama, Y., Laursen, K., 2001. A conceptual model of preferential flow systems in forested hillslopes: evidence of self-organization. *Hydrol. Processes* 15, 1675–1692. DOI: [10.1002/hyp.233](https://doi.org/10.1002/hyp.233)
- Sklash, M.G., Farvolden, R.N., Fritz, P., 1976. A conceptual model of watershed response to rainfall, developed through the use of oxygen-18 as a natural tracer. *Canadian J. Earth Sci.* 13, 271–283. DOI: [10.1139/e76-029](https://doi.org/10.1139/e76-029)
- Sklash, M.G., Farvolden, R.N., 1979. The role of groundwater in storm runoff. *J. Hydrol.* 43, 45–65. DOI: [10.1016/0022-1694\(79\)90164-1](https://doi.org/10.1016/0022-1694(79)90164-1)
- Tallaksen, L., 1995. A review of baseflow recession analysis. *J. Hydrol.* 165, 349–370. DOI: [10.1016/0022-1694\(94\)02540-R](https://doi.org/10.1016/0022-1694(94)02540-R)
- Tani, M., 1997. Runoff generation processes estimated from hydrological observations on a steep forested hillslope with a thin soil layer. *J. Hydrol.* 200, 84–109. DOI: [10.1016/S0022-1694\(97\)00018-8](https://doi.org/10.1016/S0022-1694(97)00018-8)
- Taylor, J.R., 1997. *An introduction to error analysis—The study of uncertainties in physical measurements*, second ed. University Science Books, Sausalito.
- Tsuboyama, Y., 2006. An experimental study on temporal and spatial variability of flow pathways in a small forested catchment. *Bull. FFPRI* 5, 135–174.
- Uchida, T., Kosugi, K., Mizuyama, T., 2002. Effects of pipe flow and bedrock groundwater on runoff generation in a steep headwater catchment in Ashiu, central Japan. *Water Resour. Res.* 38, 1119. DOI: [10.1029/2001WR000261](https://doi.org/10.1029/2001WR000261)
- Uchida, T., Asano, Y., Ohte, N., Mizuyama, T., 2003. Analysis of flowpath dynamics in a steep unchannelled hollow in the Tanakami Mountains of Japan. *Hydrol. Processes* 17, 417–430. DOI: [10.1002/hyp.1133](https://doi.org/10.1002/hyp.1133)
- Uchida, T., McDonnell, J.J., Asano, Y., 2006. Functional intercomparison of hillslopes and small catchments by examining water source, flowpath and mean residence time. *J. Hydrol.* 327, 627–642. DOI: [10.1016/j.jhydrol.2006.02.037](https://doi.org/10.1016/j.jhydrol.2006.02.037)
- van Genuchten, M.T., 1980. A closed-form equation for predicting the hydraulic conductivity of unsaturated soils. *Soil Sci. Soc. Am. J.* 44, 892–898. DOI: [10.2136/sssaj1980.03615995004400050002x](https://doi.org/10.2136/sssaj1980.03615995004400050002x)

- Weihermüller, L., Siemens, J., Deurer, M., Knoblauch, S., Rupp, H., Göttlein, A., Pütz, T., 2007. In situ soil water extraction: a review. *J. Environ. Qual.* 36, 1735–1748. DOI: [10.2134/jeq2007.0218](https://doi.org/10.2134/jeq2007.0218)
- West, A.G., Goldsmith, G.R., Brooks, P.D., Dawson, T.E., 2010. Discrepancies between isotope ratio infrared spectroscopy and isotope ratio mass spectrometry for the stable isotope analysis of plant and soil waters. *Rapid Commun. Mass Spectrom.* 24, 1948–1954. DOI: [10.1002/rcm.4597](https://doi.org/10.1002/rcm.4597)
- WMO (World Meteorological Organization), 2009. *Guide to Hydrological Practices Volume II. Management of Water Resources and Application of Hydrological Practices*, sixth ed. WMO-No. 168. WMO, Geneva.
- WMO (World Meteorological Organization), 2010. *Manual on Stream Gauging. Volume II – Computation of Discharge*. WMO-No. 1044. WMO, Geneva.
- Zhao, L., Xiao, H., Zhou, J., Wang, L., Cheng, G., Zhou, M., Yin, L., McCabe, M.F., 2011. Detailed assessment of isotope ratio infrared spectroscopy and isotope ratio mass spectrometry for the stable isotope analysis of plant and soil waters. *Rapid Commun. Mass Spectrom.* 25, 3071–3082. DOI: [10.1002/rcm.5204](https://doi.org/10.1002/rcm.5204)

Chapter 3

Water fluxes and quality of a forested catchment over two hydrologically contrasting years of the East Asian summer monsoon

Jean-Lionel Payeur-Poirier¹, Mi-Hee Lee², Luisa Hopp¹, Stefan Peiffer¹

¹ Department of Hydrology, Bayreuth Center of Ecology and Environmental Research (BayCEER), University of Bayreuth, Bayreuth, Germany

² Department of Soil Ecology, Bayreuth Center of Ecology and Environmental Sciences (BayCEER), University of Bayreuth, Bayreuth, Germany

Correspondence: jean.lionel.payeur.poirier@gmail.com (J.-L. Payeur-Poirier)

Status: in preparation

Abstract

At a forested headwater catchment of South Korea, the East Asian summer monsoon (EASM) of 2013 yielded 826 mm of precipitation and lasted 49 days while, in 2014, the EASM yielded 94 mm of precipitation and lasted 28 days. We studied the hydrological dynamics of this catchment over these two oppositely extreme years of the EASM, which corresponded to some of the future predicted extremes in hydroclimatic conditions. High-frequency hydrometric, hydrochemical, isotopic, and meteorological measurements were conducted, and tracer-based hydrograph separations were performed. For the 2013 EASM, water storage increased by 48 mm and the overall runoff coefficient was 74.7%. For the 2014 EASM, water storage decreased by 21 mm and the runoff coefficient was 11.7%. A threshold response of runoff to the sum of antecedent soil moisture and precipitation was observed, but only reached and exceeded in 2013. Above the threshold, subsurface flow was enhanced and simultaneously contributed to runoff and the recharge of the saturated zone. Runoff for the 2013 EASM had a much greater proportion of soil water than in 2014. The time-series of stream water solute concentrations substantially differed between both years of the EASM, and the total solute fluxes in runoff were over one order of magnitude greater in 2013 than in 2014. The total fluxes of dissolved organic carbon (DOC) displayed the greatest relative difference between both years of the EASM and the total fluxes of nitrate (NO₃-), the smallest relative difference, likely reflecting the differing contributions of throughfall and groundwater to runoff. These results should be useful to incorporate the effects of extreme EASMs in regional hydrological models, and should contribute to the ongoing efforts to estimate and predict the water balance and quality of the Lake Soyang watershed.

Keywords: extreme hydroclimatic conditions, runoff generation processes, hydrological dynamics, headwaters, groundwater, South Korea

3.1. Introduction

In South Korea, the averages and extremes of temperature and precipitation have been increasing for the last few decades (Chang and Kwon, 2007; Choi et al., 2008; Jung et al., 2002). The trends in precipitation are most pronounced during the months of July and August and are linked to the occurrence of the East Asian summer monsoon (EASM) and to the post-

EASM period, as defined by Ha et al. (2012) and Seo et al. (2011). These trends are towards a higher total summer precipitation, a shift in the peak period of precipitation from July to August, and a higher frequency, intensity and duration of heavy rainfall events (Choi et al., 2010a; Chung et al., 2004; Ha et al., 2012; Ho et al., 2003; Lee et al., 2010). Choi et al. (2008) reported that, in the region of the Lake Soyang watershed, the precipitation of extremely wet days increased by 61 to 80 mm per decade over the period from 1973 to 2007. The trends in precipitation are predicted to continue and to display high spatial and temporal variability (Bae et al., 2011; Im et al., 2008; Kim et al., 2011a). On the other hand, South Korea has also been experiencing drought at regional and large scales (Kim et al., 2011b). Insufficient precipitation during the EASM and the post-EASM period results in particularly long and severe droughts, as these periods are followed by the dry season (Choi et al., 2010a; Kim et al., 2011b). The occurrence and severity of drought are predicted to increase, which, along with the trends in precipitation, would result in the increased occurrence of extreme hydroclimatic conditions (Im et al., 2016; Nam et al., 2015; Seo et al., 2013).

Changes in temperature and in the precipitation regime of the EASM have induced changes in the water fluxes of South Korean watersheds. Increases in monthly runoff and in maximum discharge were reported for the wet season, while decreases in runoff were reported for the dry season (Bae et al., 2008a; Kang et al., 2015). Along with the current agricultural, farming and deforestation practices, the changes in fluxes of the wet season have caused the deterioration of water quality (Park et al., 2010). For the Han River basin, Ahn and Kim (2016) and Bae et al. (2008b) predicted substantial increases in annual runoff and evapotranspiration of a maximum of ~35% and ~45% compared to the baseline period, for the end of the century, respectively.

As forested catchments are subjected to changes in their input of precipitation induced by climate change (Lim et al., 2006; NIER, 2010), their water fluxes and quality may likely be altered and, hence, the input of water to downstream regions. The knowledge and comprehension of the hydrological dynamics of forested catchments, under the current and predicted conditions of the EASM, are essential elements for the sustainable management of water in South Korea, since this country is mainly covered by forests (Kang and Park, 2015; Yang, 2007). We argue that the studies required to enhance these elements should be conducted over periods that closely approximate the predicted conditions. These studies should not only focus on the water balance and quality of forested catchments, but also on the processes influencing them.

In a companion article, Payeur-Poirier et al. (in preparation) reported on the dynamics of water sources and flow paths at a forested catchment as induced by the EASM, and on its influence on runoff generation. Their findings are based on observations made during the 2013 EASM, of which the precipitation was 206% of the average regional EASM precipitation of the previous 40 years. In contrast, the precipitation of the 2014 EASM was only 32% of this average, as South Korea experienced a severe drought (Wilcox et al., 2015). In the current article, we report on the water fluxes and quality of this forested catchment over the 2013 and the 2014 EASM, which were representative of the observed and future predicted extremes in the precipitation regime of this climate subsystem. We extend the findings of Payeur-Poirier et al. (in preparation) to the influence on water quality of the inter-annual variability in water sources and flow paths, and associated runoff generation processes. Our objectives were (1) to quantify the major fluxes of water, the major hydrological conditions, and the fluxes of solutes in runoff, (2) to estimate the contributions to runoff of its most likely sources, and (3) to identify some of the major differences in hydrological dynamics between these two oppositely extreme years of the EASM. The EASM is hereinafter referred to as the summer monsoon.

3.2. Materials and methods

3.2.1. Site description

This study was conducted at a site located in the northern part of the Lake Soyang watershed, which is located in the north-east of South Korea and is part of the Han River basin (Fig. 3.1). Average annual precipitation and temperature measured in close proximity to the site are 1273 mm and 9.9 °C (1997–2014). The precipitation from June through August accounts on average for $60.1 \pm 10.9\%$ of the annual precipitation. In this region, the summer monsoon occurs over an average period of 32 days, usually from late June to late July (Seo et al., 2011).

The site consists of a small (0.16 km^2) forested headwater catchment. It comprises a narrow riparian area and steep hillslopes, which is typical of this mountainous region. The mean elevation and slope are 529 m and 23.9° . The site is drained by a perennial stream of variable extent (minimum of 65 m and maximum of 226 m stream length, from the catchment

outflow). Two intermittent springs were observed to flow directly to the stream during and following major rainfall events. The site is underlain by orthogneiss belonging to the Gyeonggi gneiss complex (Lee and Cho, 2012). The soil is a shallow Eutric Cambisol (following IUSS Working Group WRB, 2014) of loam texture (Lee, 2016) characterized as well to excessively drained (following Schoeneberger et al., 2011). The site is covered at 61.3% by a purely deciduous stand and at 38.7% by a purely coniferous stand. See Payeur-Poirier et al. (in preparation) for a detailed description of the study site.

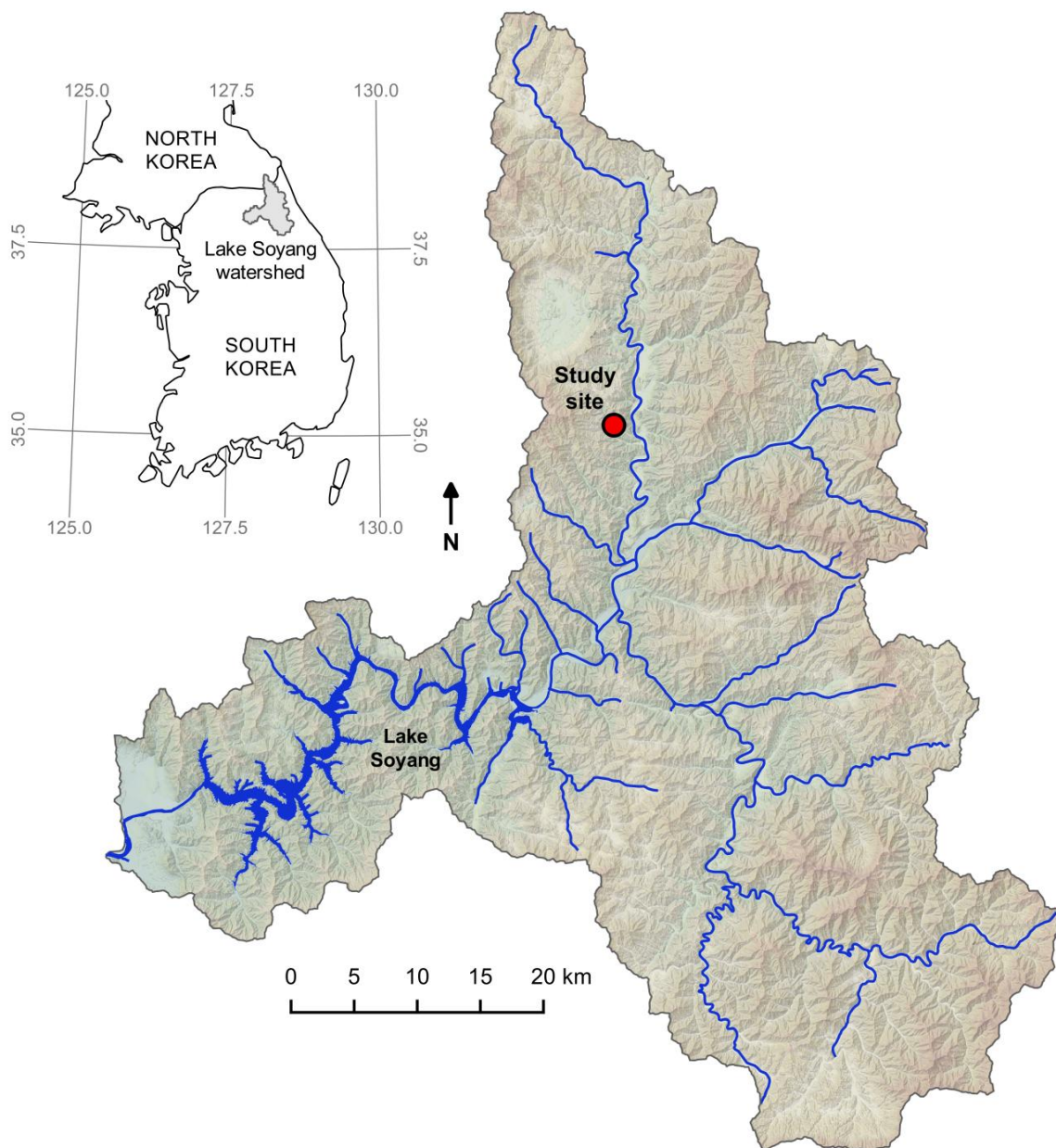


Figure 3.1. Location and detailed map of the Lake Soyang watershed, including Lake Soyang, the major rivers and the study site location. The relief is vertically exaggerated by a factor of 1.5. See Payeur-Poirier et al. (in preparation) for a detailed map of the study site.

3.2.2. Regional characteristics of the 2013 and the 2014 summer monsoon

In this region, the 2013 summer monsoon yielded 817 mm of precipitation and lasted 49 days (from June 17 to August 4), and the 2014 summer monsoon yielded 126 mm of precipitation and lasted 28 days (from July 2 to July 29; GRMA, 2013, 2014). These years of the summer monsoon were, respectively, the longest and the shortest that had occurred since 1973 (earliest available records). The summer monsoon precipitation was 206 and 32% of the average since 1973, respectively (396 mm; GRMA, 2014). For the period from June through August, the precipitation in 2014 was the lowest on record since 1973, and South Korea experienced a severe drought (Wilcox et al., 2015). Air temperature for this period averaged 25.0 and 23.8 °C in 2013 and 2014, respectively, and was higher than the average since 1973 (23.1 °C; GRMA, 2013, 2014). For this period, 2013 was the warmest year since 1973. To summarize, the 2013 summer monsoon was long, wet and hot, and the 2014 summer monsoon was short, dry and somewhat warmer than on average. Annual precipitation measured in close proximity to the site was 1313 and 699 mm in 2013 and 2014, respectively.

3.2.3. Meteorological measurements

Meteorological measurements were made at a 5-min frequency from June 1 to August 31, 2013, and from June 12 to August 11, 2014, and consisted of: temperature (°C), relative humidity (%) and throughfall (mm). The measurements were made using a weather station installed under the canopy at a 3-m height, close to the catchment outflow (WS-GP1, Delta-T Devices Ltd., Cambridge, UK). In addition, throughfall was measured with four passive collectors randomly distributed within the site, and precipitation (mm) was measured with a passive collector installed in an open area located 850 m south-east of the site. Rainfall depths were measured following every rainfall event over the same periods, and catchment-scale throughfall was estimated as the average of all throughfall measurements. Individual rainfall events were identified following Payeur-Poirier et al. (in preparation), and the return period of every event was estimated with an intensity-duration-frequency curve derived by Kim (2008). The automated weather station (AWS) number 594 of the Korea Meteorological Administration was located 3 km north-east of the site in a valley bottom and measured temperature and precipitation at a frequency of 1 min and a height of 2 m over the same periods. Data of daily temperature and precipitation measured by this AWS were also

acquired for the period from January 1, 1997, to December 31, 2014 (totality of available data).

3.2.4. Hydrometric measurements

Water stage (cm) and temperature (°C) were measured in a V-notch weir at the outflow of the catchment at a 5-min frequency from June 1 to August 31, 2013, and from June 1 to August 16, 2014, using a pressure transducer (Levelogger Gold M10, Solinst Canada Ltd., Georgetown, Canada) that was barometrically compensated with a barometric pressure transducer (Barologger Gold M1.5, Solinst Canada Ltd.) installed at the weir. Specific discharge (mm h^{-1}) was calculated following WMO (2010). Electrical conductivity (EC, $\mu\text{S cm}^{-1}$ at 25 °C) was measured at the same location and frequency from June 1 to August 16, 2013, and from June 10 to August 13, 2014, using a handheld meter with datalogger (Cond 340i, WTW GmbH, Weilheim, Germany). Water temperature was measured at seven additional upstream locations including the locations where intermittent springs flowed directly to the stream, at the same frequency from June 26 to August 16, 2013, and from June 25 to August 10, 2014 (HOBO Pendant UA-002-08, Onset Computer Corp., Bourne, USA).

Piezometric head (cm) was measured at three plots which formed a 50-m long transect from the hillslope, to the toeslope, to the riparian area of the catchment, at a 5-min frequency from June 1 to August 31, 2013, and from June 9 to August 16, 2014, using pressure transducers (Levelogger Junior Model 3001, Solinst Canada Ltd.) that were barometrically compensated with a barometric pressure transducer (Barologger Gold M1.5, Solinst Canada Ltd.) installed at the toeslope plot. The piezometers were installed at until-tool-refusal-depth. Piezometric head was also measured in the lower part of the riparian area, where an intermittent spring flowed directly to the stream. Volumetric soil-water content (θ_v , $\text{m}^3 \text{m}^{-3}$; hereinafter referred to as soil moisture) was measured at each plot at depths of 10, 30 and 50 cm at the same frequency from June 1 to August 24, 2013, and from June 11 to August 11, 2014, using multisensors (5TE, Decagon Devices Inc., Pullman, USA). Catchment-scale θ_v was estimated following Haga et al. (2005). An antecedent soil moisture index (ASMI) was derived for each rainfall event, by integrating the soil moisture measurements at the onset of an event into an estimation of water storage in the soil profile, following Haga et al. (2005) and using the hillslope and riparian areas as subareas of the catchment. See Payeur-Poirier et al. (in preparation) for a more detailed description of the experimental setup and measurements.

3.2.5. Water sampling, chemical analysis and isotopic analysis

Stream water, groundwater, spring water, soil water, and throughfall were sampled from June 3 to August 16, 2013, and from June 11 to August 17, 2014, following the procedures detailed by Payeur-Poirier et al. (in preparation). Stream water was sampled in the V-notch weir at least once per 2 days over the whole periods and, during and following major rainfall events, at least every 2 hours. Samples collected in the streambed at an upstream location where water emerged over a short length, during the period of lowest flow preceding the first event of the summer monsoon of each year, were considered as groundwater. Spring water was sampled from both intermittent springs following their activation. Soil water was sampled at several depths at the hillslope, the toeslope and the riparian plot using suction lysimeters, at least once per 2 days over the whole periods. Throughfall was sampled from the passive collectors directly following every rainfall event. In terms of chemistry and isotopic abundance, each throughfall sample was considered as the average for an event and a volumetric-weighted average for a particular event was calculated to obtain a catchment-scale value. At the time of collection, each sample was split into two parts, one for chemical analysis and one for isotopic analysis. The samples were stored in a dark environment at a temperature of 4 °C until analyses.

The concentrations (mg l^{-1}) of calcium (Ca^{2+}), magnesium (Mg^{2+}), potassium (K^+), sodium (Na^+), chloride (Cl^-), nitrate (NO_3^-), sulphate (SO_4^{2-}) and silica (SiO_2), as well as EC and the relative abundance of deuterium ($\delta^2\text{H}$, ‰ in relation to VSMOW) of the samples were measured. The concentrations of Ca^{2+} , Mg^{2+} , K^+ , Na^+ and SiO_2 were measured by inductively coupled plasma optical emission spectrometry (Optima 3200 XL, PerkinElmer LAS GmbH, Rodgau, Germany), and those of Cl^- , NO_3^- and SO_4^{2-} were measured by ion chromatography (Metrohm IC Separation Center with Suppressor Module, Metrohm AG, Herisau, Switzerland). The concentration of NO_3^- is hereinafter expressed either as NO_3^- or $\text{NO}_3\text{-N}$. EC was measured at the time of sample collection using a handheld meter (Cond 340i, WTW GmbH). The $\delta^2\text{H}$ measurements for the samples of stream water and throughfall collected in 2013 were realized using a mass spectrometer (DELTA V Advantage, Thermo Fisher Scientific GmbH, Bremen, Germany) coupled to a high-temperature pyrolysis reactor (HTO, HEKAtech GmbH, Wegberg, Germany) and a continuous flow interface (ConFlo IV, Thermo Fisher Scientific GmbH). For the rest of the samples, $\delta^2\text{H}$ was measured by off-axis integrated cavity output spectroscopy (TIWA-45EP, Los Gatos Research Inc., Mountain View, USA).

The spring water samples were not analyzed for $\delta^2\text{H}$. See Payeur-Poirier et al. (in preparation) for a more detailed description of the analyses. The concentrations of dissolved organic carbon (DOC, mg C l^{-1}) and total dissolved nitrogen (TDN, mg N l^{-1}) were measured for a subset of stream water samples of each year. The samples were pre-filtered with a cellulose acetate membrane or nylon filter ($0.45 \mu\text{m}$) and the concentrations were measured using a total organic carbon analyzer (TOC-V, Shimadzu Corporation, Kyoto, Japan).

3.2.6. Data analysis

3.2.6.1. Runoff and solute fluxes

Total runoff for individual rainfall events was calculated as runoff from the start of the event to when discharge on the receding limb was measured or calculated as equal to its initial value. A recession analysis of the 2013 hydrograph was performed by Payeur-Poirier et al. (in preparation), in order to calculate total runoff for the events with recession periods interrupted by the occurrence of subsequent events. The runoff coefficient of each event was then calculated following WMO (2009). These calculations were also applied for the summer monsoon of each year. Solute fluxes in runoff were calculated by first averaging stream solute concentrations and discharge between sample collection times, and then multiplying the concentration and discharge values. The flux values were summed to derive total values for the summer monsoon.

3.2.6.2. Evapotranspiration

Daily potential evapotranspiration (ET_p) was estimated with the Priestley-Taylor equation (Priestley and Taylor, 1972). The daily net radiation variable of the equation was estimated following Archibald and Walter (2014) with the temperature values measured by the AWS. This estimation was separately realized for the coniferous and deciduous stands of the site, using an albedo of 0.09 for the former and 0.13 for the latter. These values were reported by Cescatti et al. (2012), Choi et al. (2005) and Ryu et al. (2008) for a coniferous and a deciduous stand located in South Korea and similar to the stands of the site in terms of vegetation characteristics and climate. Priestley-Taylor coefficients (α) of 0.47 and 0.91 were used for the coniferous and deciduous stands, respectively. These values were derived from Komatsu (2005) for a coniferous stand with a canopy height of 23 m and for a temperate broad-leaved stand, and were multiplied by 1.11 to estimate whole-day values. The values

proposed by Komatsu (2005) are based on dry-canopy evapotranspiration measurements and are likely higher for wet-canopy conditions (Kwon, 2011). For the 2013 summer monsoon, soil moisture was not considered a limiting factor since values were not in the ranges considered as water stress or high water content conditions (Khatun et al., 2011a). Therefore, daily actual evapotranspiration (ET_d) was considered equal to ET_p . For the 2014 summer monsoon, the strength of this inference was limited since soil moisture could have limited ET_d in the driest period. The soil heat flux variable of the equation was considered null on a daily basis, and the values of ET_d were summed to derive total values for the summer monsoon.

3.2.6.3. Hydrograph separation

Tracer-based mass balance hydrograph separations coupled with principal component analyses (PCA) and end-member mixing analyses (EMMA) were performed following the procedures detailed by Payeur-Poirier et al. (in preparation), based on the procedures proposed by Christophersen and Hooper (1992), Hooper (2003) and Sklash and Farvolden (1979). The potential end-members were throughfall, groundwater, and soil water at several depths at the hillslope, the toeslope, and the riparian area of the catchment. The relative contributions to runoff of the most likely end-members were estimated for each stream water sample, daily averages were calculated, and averages for the periods before, during and after the summer monsoon were finally calculated. For this study, the contributions of soil water at several depths were aggregated per area.

For both years, Ca^{2+} , Mg^{2+} , EC and δ^2H were considered as conservative tracers. For 2013, only Ca^{2+} , EC and δ^2H were used in the mixing models and the dataset was divided into two parts, i.e. the initial (before DOY 190) and the major (after DOY 190) period, in order to maximize the satisfaction of the assumptions underlying the hydrograph separation technique (Payeur-Poirier et al., in preparation). Mixing models were separately applied for each part of the 2013 dataset and explained 88.2 and 83.8% of the variation in the datasets. The most likely end-members were identified as groundwater and soil water at the hillslope, the toeslope and the riparian area. For 2014, only EC and δ^2H were used in the mixing model since only three end-members were identified. Ca^{2+} and Mg^{2+} were used to test the model, which was applied for the entire dataset. The mixing subspace was defined by the first principal component, and the mixing model explained 92.9% of the variation in the dataset. The most likely end-members were identified as groundwater and soil water at the toeslope and the riparian area. Except for the assumption of spatial invariance of end-member tracer

values, which was not possible to test due to the restricted extent of the sampling setup, the assumptions underlying this technique (Buttle, 1994; Inamdar, 2011) were considered to be satisfied for the 2013 and the 2014 dataset. The three separate mixing models were fairly successful in reproducing the measured stream water tracer values, which is a good indication that the mixing models were valid (Hooper, 2003; Inamdar, 2011). The relative root-mean-square errors (RRMSEs) of the residuals between the predicted and the measured values were < 11% for all conservative tracers.

In order to compare both years in terms of the ratios of stream water tracer values, the values of Ca^{2+} , EC and $\delta^2\text{H}$ of 2014 were standardized to those of 2013 and projected into the one-dimensional mixing subspace of the 2013 values, following Hooper (2003). For each tracer, the residuals between the projected and the measured values of 2014 were plotted against the latter, their pattern was analyzed and the RRMSE was calculated.

3.3. Results

3.3.1. Water fluxes and hydrological conditions

3.3.1.1. Precipitation and throughfall

The 2013 summer monsoon yielded 826 mm of precipitation of which 95.4% fell as throughfall, and the 2014 summer monsoon yielded 94 mm of precipitation of which 83.0% fell as throughfall (Table 3.1). During the former, sixteen individual rainfall events occurred and ranged from 8 to 127 mm in precipitation, while only three events which ranged from 15 to 45 mm in precipitation occurred during the latter. The three most important events in terms of precipitation occurred in 2013 and had return periods of 3.41, 2.17 and 1.25 years, while the other events had return periods below one year. Although most of the events of the 2013 summer monsoon occurred within a period of only 16 days (Fig. 3.2, from day of year (DOY) 189 to 204), the events were more evenly distributed in time than in 2014. As a matter of fact, a period of 15 days elapsed between the 2nd and the 3rd rainfall event of the 2014 summer monsoon (Fig. 3.2, from DOY 191 to 205).

Table 3.1. Selected characteristics of the 2013 and the 2014 summer monsoon, and major hydrological fluxes and conditions at the study site.

	2013 summer monsoon	2014 summer monsoon
Period (Julian day) ^a	168–216	183–210
Period length (day)	49	28
Precipitation (mm)	826	94
Throughfall (mm)	788	78
Ratio of throughfall to precipitation (%)	95.4	83.0
Runoff (mm)	617	11
Runoff coefficient (%)	74.7	11.7
Flow regime coefficient ^b	444.0	6.4
Evapotranspiration (mm)	161	104
Water balance (mm)	48	-21
Number of individual rainfall events	16	3
Stream water temperature mean (°C) ^c	10.8	14.3
Maximum extent of the stream (m) ^d	226	65

^a GRMA (2013, 2014).

^b Ratio of maximum discharge to minimum discharge.

^c At the catchment outflow.

^d From the catchment outflow.

3.3.1.2. Runoff

Total runoff for the summer monsoon was over one order of magnitude greater in 2013 than in 2014 (Table 3.1). During the 2013 summer monsoon, hourly specific discharge ranged from 0.02 to 8.88 mm hr⁻¹ and averaged 0.50 ± 0.86 mm hr⁻¹ (Fig. 3.2). It reached its lowest value shortly following the onset of the summer monsoon, and subsequently varied with the occurrence of rainfall events. Both intermittent springs were responsive to major rainfall events and flowed for periods ranging from hours to several days following the end of an event. During the 2014 summer monsoon, hourly specific discharge ranged from 0.008 to 0.051 mm hr⁻¹ and averaged 0.016 ± 0.008 mm hr⁻¹. It was relatively low until shortly before the end of the summer monsoon, when it substantially increased in response to the 3rd rainfall event (Fig. 3.2, DOY 206). The most upstream spring was first activated on the 3rd event and flowed for only a few hours following the end of the event, while the other spring was never

activated. At the onset of the 2013 and the 2014 summer monsoon, daily specific discharge was 0.56 and 0.38 mm d^{-1} , respectively.

The 2013 and the 2014 summer monsoon greatly differed in terms of runoff coefficient, which was more than six times higher in 2013 than in 2014 (Table 3.1). In 2013, the runoff coefficients of individual rainfall events of the summer monsoon ranged from 9.4 to 124.7% and averaged $60.5 \pm 33.5\%$, while in 2014 they ranged from 6.0 to 14.7% and averaged $10.7 \pm 3.6\%$. Three clusters were derived from the entire set of runoff coefficients (5 to 15%, 25 to 40%, 65% and above).

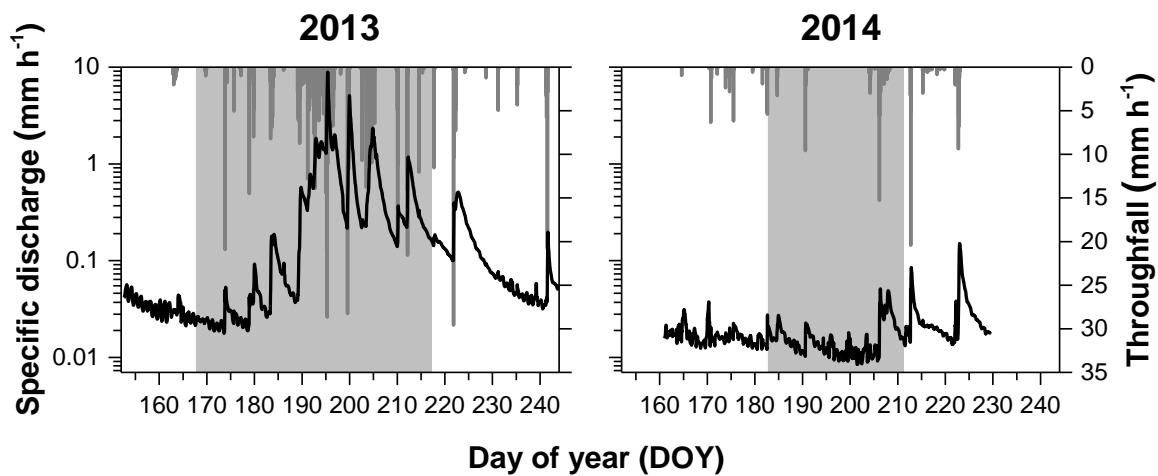


Figure 3.2. Specific discharge (hourly mean) and throughfall (hourly) as a function of time for the period from June 1 to August 31 of 2013 and 2014. The shaded areas correspond to the summer monsoon.

3.3.1.3. Evapotranspiration

Total actual evapotranspiration for the 2013 and the 2014 summer monsoon was 161 and 104 mm, respectively (Table 3.1). Daily values (ET_d) ranged from 0.5 to 4.8 mm and averaged 3.3 ± 1.4 mm for the former and 3.7 ± 1.0 mm for the latter. At clear-sky conditions, ET_d averaged $4.5 \pm 0.2 \text{ mm d}^{-1}$. The values fell within the ranges reported for the same period of the year for analogous sites in South Korea (Khatun et al., 2011b; Shin et al., 2012; Yeom et al., 2015).

3.3.1.4. Soil moisture and water table

The ranges in daily average soil moisture (θ_v) for the 2014 summer monsoon did not overlap those for the 2013 summer monsoon, except for one value at 10-cm depth (Fig. 3.3). The greatest range in values was observed in 2013, at 50-cm depth (15.7 to 26.8%), and the smallest range in values was observed at the same depth in 2014 (9.4 to 12.6%). θ_v did not exceed the value of field capacity proposed by Saxton and Rawls (2006) for a soil of loam texture. However, we believe that the average value of field capacity was much lower at the site, due to the high fraction of coarse gravel and stones of the soil (Payeur-Poirier et al., in preparation). While θ_v at 50-cm depth was lower than at shallower depths at the onset of the 2013 summer monsoon, it substantially increased during the first half of the summer monsoon to finally exceed the values at shallower depths. During the second half of the summer monsoon, relatively high values of soil moisture were sustained at all depths. In 2014, soil moisture at the onset of the summer monsoon was lower than at the onset of the 2013 summer monsoon at all depths (Fig. 3.3). It slightly increased in response to the 1st and 2nd rainfall events, but thereafter decreased until it reached its lowest values before the occurrence of the 3rd event. This event induced a substantial increase in soil moisture and values slightly exceeded the respective value at the onset of the summer monsoon. The ASMI of individual rainfall events ranged between 96 and 138 mm in 2013 and between 67 and 81 mm in 2014.

Over both years of the summer monsoon, a water table was observed only once for a period of 12 hours, in 2013. It occurred in the lower part of the riparian area and was associated with the flow of an intermittent spring. The water table had a maximum depth of 38 cm and did not intersect the soil surface.

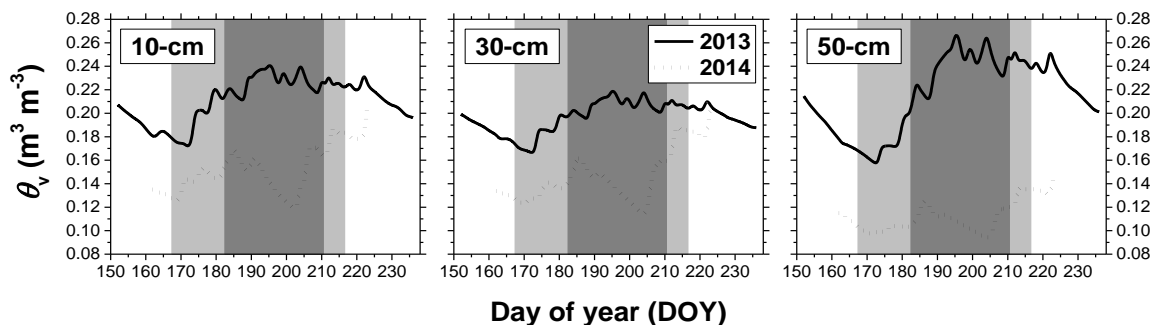


Figure 3.3. Soil moisture (θ_v , daily mean) at 10-, 30- and 50-cm depth at the catchment scale as a function of time for the period from June 1 to August 24 of 2013 and 2014. The light grey areas correspond to the 2013 summer monsoon; the dark grey areas correspond to the 2014 summer monsoon.

3.3.2. Water quality and solute fluxes

A visual analysis of the Piper diagrams of the sampled water revealed that the proportions of cations were similar between both years and between stream water, spring water and groundwater (Fig. 3.4). From 2013 to 2014, except for throughfall, the composition of water shifted towards higher proportion of NO_3^- and lower proportions of SO_4^{2-} and Cl^- . The time-series of stream water quality displayed marked differences between both years for EC, $\delta^2\text{H}$ and most solutes (Fig. 3.5). Until the approximate period corresponding to the onset of the 2014 summer monsoon, the concentrations of all solutes were similar between both years and were relatively stable or slightly increasing. Then, in 2013, the occurrence of six major rainfall events within a period of 6 days resulted in substantial decreases in the concentrations of most solutes, although some of the events induced temporary increases in the concentration of K^+ , $\text{NO}_3\text{-N}$, SO_4^{2-} and TDN. Thereafter, the concentrations of most solutes either remained below their level at the onset of the summer monsoon or gradually increased to reach it. In 2014, following the onset of the summer monsoon and until the 3rd rainfall event, solute concentrations were generally stable or slightly increasing except for $\text{NO}_3\text{-N}$ and TDN (Fig. 3.5). Their concentrations first increased in response to the 1st and 2nd rainfall events, and then decreased to their approximate value at the onset of the summer monsoon. For most solutes, the 3rd rainfall event induced some slight decrease but a general and substantial increase in concentration. The concentrations of Ca^{2+} , Mg^{2+} , K^+ , $\text{NO}_3\text{-N}$, SO_4^{2-} , SiO_2 and TDN remained generally high following the end of the summer monsoon and temporarily increased in response to subsequent rainfall events. Over both years of the summer monsoon, the concentration of DOC temporarily increased during major events but did not decrease below its approximate value at the onset of the summer monsoon, and the concentration of Cl^- did not follow any clear pattern. The general, temporal patterns of solute concentrations and their differences between both years were well represented in the time-series of EC (Fig. 3.5). Although the temporal pattern of $\delta^2\text{H}$ in 2013 was not as clear as the general pattern of stream water chemistry, temporary increases during major events and a general shift towards higher values were observed. In 2014, the values were initially stable and only slightly increased in response to the 3rd rainfall event.

Total solute fluxes in runoff for the 2013 and the 2014 summer monsoon are presented in Table 3.2. The fluxes of all solutes were over one order of magnitude greater in 2013 than in 2014. The fluxes of DOC displayed the greatest relative difference between both years and

the fluxes of $\text{NO}_3\text{-N}$ the smallest relative difference. In 2013, the fluxes of the measured solutes were in the order $\text{SO}_4^{2-} > \text{Ca}^{2+} > \text{SiO}_2 > \text{Cl}^- > \text{TDN} > \text{DOC} > \text{NO}_3\text{-N} > \text{Mg}^{2+} > \text{K}^+ > \text{Na}^+$. In 2014, the fluxes were in the order $\text{Ca}^{2+} > \text{SO}_4^{2-} > \text{SiO}_2 > \text{TDN} > \text{NO}_3\text{-N} > \text{Mg}^{2+} > \text{DOC} > \text{Cl}^- > \text{K}^+ > \text{Na}^+$ (Table 3.2).

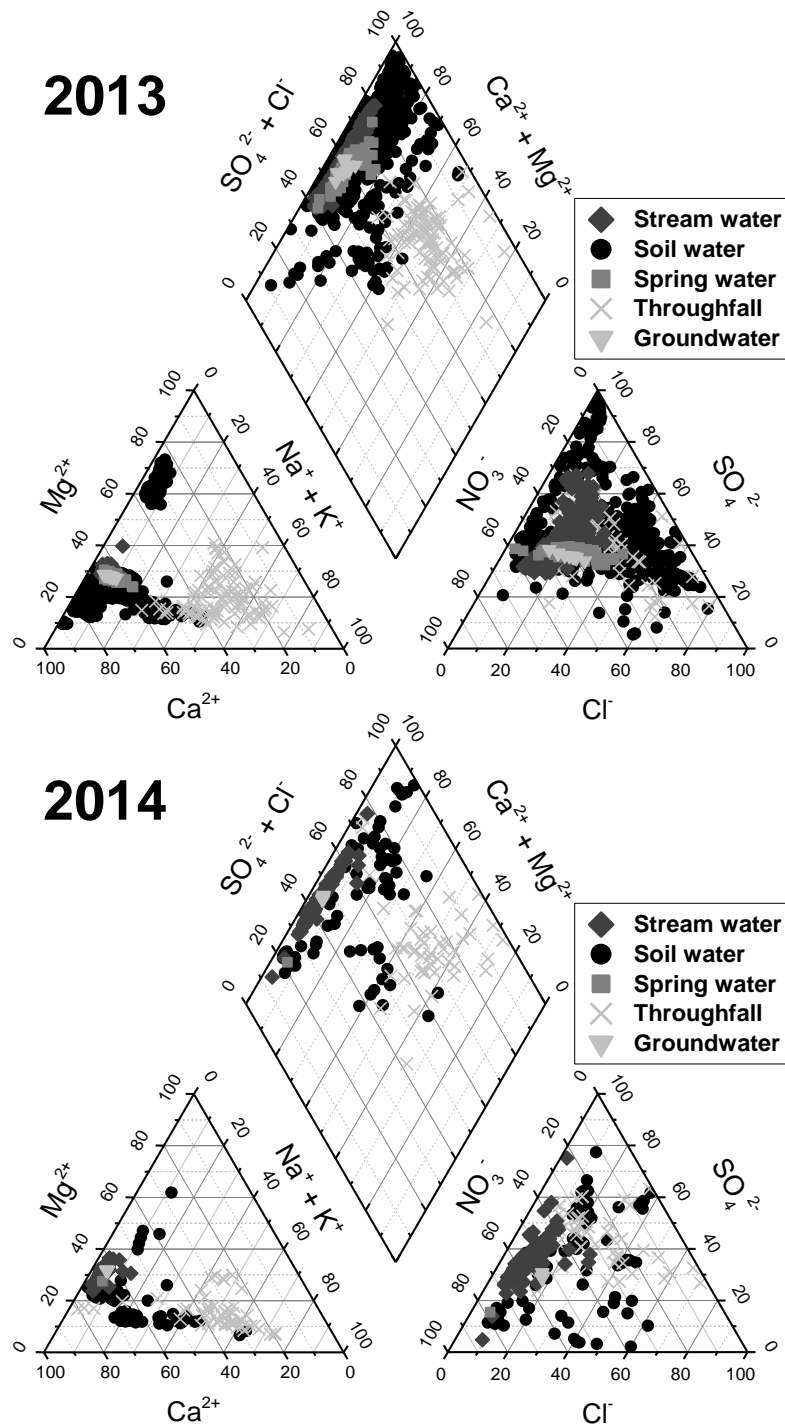


Figure 3.4. Piper diagrams of stream water, soil water, spring water, throughfall and groundwater for the 2013 and the 2014 study period. Data are in units of % meq l^{-1} .

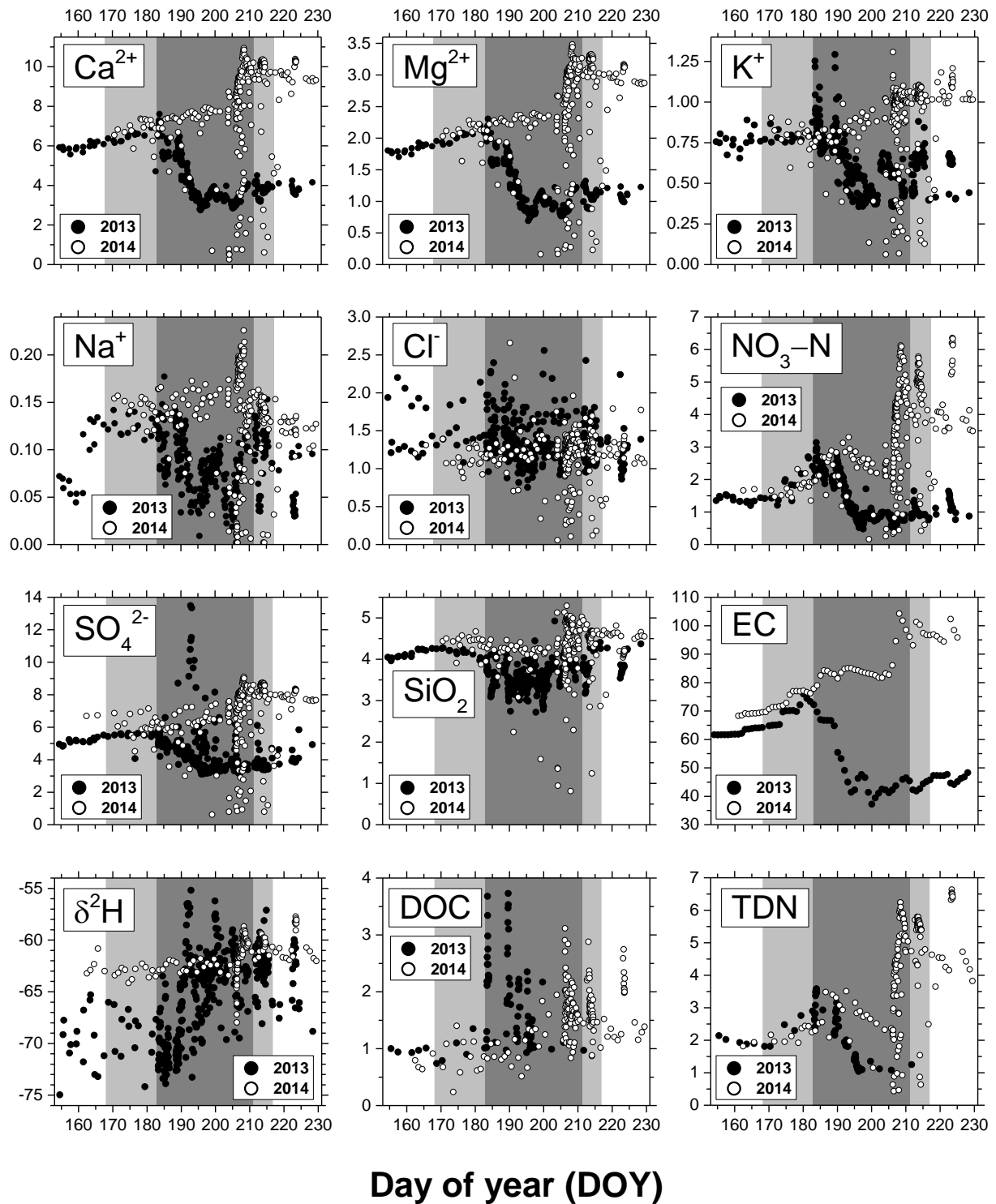


Figure 3.5. Stream water solute concentrations, electrical conductivity (EC) and relative abundance of deuterium ($\delta^2\text{H}$) as a function of time for the 2013 and the 2014 study period. The light grey areas correspond to the 2013 summer monsoon; the dark grey areas correspond to the 2014 summer monsoon. Ions and the compound are in units of mg l⁻¹, EC is in units of $\mu\text{S cm}^{-1}$ at 25 °C (daily mean), $\delta^2\text{H}$ is in units of ‰ in relation to VSMOW, DOC is in units of mg C l⁻¹, TDN is in units of mg N l⁻¹.

Table 3.2. Total solute fluxes in runoff for the 2013 and the 2014 summer monsoon.

Solute	2013 summer monsoon	2014 summer monsoon
Ca ²⁺ (kg ha ⁻¹)	21.13	0.79
Mg ²⁺ (kg ha ⁻¹)	5.89	0.24
K ⁺ (kg ha ⁻¹)	3.21	0.09
Na ⁺ (kg ha ⁻¹)	0.36	0.01
Cl ⁻ (kg ha ⁻¹)	8.84	0.13
NO ₃ -N (kg ha ⁻¹)	6.13	0.30
SO ₄ ²⁻ (kg ha ⁻¹)	27.74	0.64
SiO ₂ (kg ha ⁻¹)	21.01	0.45
DOC (kg C ha ⁻¹)	8.16	0.14
TDN (kg N ha ⁻¹)	8.30	0.35

3.3.3. Runoff sources

A decrease in the average relative contribution of groundwater to runoff from the period before to the period following the summer monsoon occurred in both years (Table 3.3). This decrease was much more important in 2013 than in 2014 (78.2 ± 5.8 to $16.7 \pm 18.4\%$ versus 89.2 ± 4.5 to $63.8 \pm 4.8\%$). In 2013, the decrease was accompanied by a gradual and substantial increase in the contributions of hillslope and riparian soil water. Following the summer monsoon, runoff mainly consisted of hillslope soil water ($50.3 \pm 9.3\%$). In 2014, the decrease was accompanied by an increase in the contribution of toeslope soil water, and groundwater remained the major source of runoff throughout the study period (Table 3.3). In contrast to 2013, soil water from the hillslope area did not substantially contribute to runoff in 2014. Before the summer monsoon, the contribution to runoff of riparian soil water was much higher in 2014 than in 2013. During the summer monsoon, its contribution was similar between both years and, following the summer monsoon, it was much higher in 2013 than in 2014 (Table 3.3).

The orthogonal projections of the 2014 stream water tracer values only partially fitted the one-dimensional mixing subspace defined by those of 2013 (Fig. 3.6; the subspace was plotted in two dimensions for ease of viewing). For the samples collected before the summer monsoon, all of the projections of the 2014 values fell within the range of those of the 2013 values. For the samples collected during the summer monsoon, 96% of the projections of the 2014 values had positive values of the first principal component ($U1$). However, only 52% of

the projections of the 2014 values fell within the range of those of the 2013 values. For the samples collected after the summer monsoon, 96% of the projections of the 2014 values exceeded the range of those of the 2013 values (Fig. 3.6). Clear patterns were observed in the residuals between the projected and the measured values plotted against the latter, and the RRMSEs of the residuals were 19.7, 24.0 and 31.2% for $\delta^2\text{H}$, Ca^{2+} and EC, respectively.

Table 3.3. Relative contributions of water sources to runoff for the periods before, during and after the 2013 and the 2014 summer monsoon. Values are followed by the respective standard deviations (SD).

Source	Average daily mean contribution to runoff (%)					
	Before the summer monsoon ^a		During the summer monsoon ^b		After the summer monsoon ^c	
	2013	2014	2013	2014	2013	2014
Groundwater	78.2 ± 5.8	89.2 ± 4.5	60.1 ± 8.3	82.3 ± 10.2	16.7 ± 18.4	63.8 ± 4.8
Hillslope soil water	3.3 ± 5.0	–	20.7 ± 6.2	–	50.3 ± 9.3	–
Toeslope soil water	16.6 ± 3.7	0	8.5 ± 3.9	6.7 ± 14.5	–	35.8 ± 4.1
Riparian soil water	1.9 ± 1.0	10.8 ± 4.5	10.7 ± 8.9	11.0 ± 5.6	33.0 ± 9.3	0.4 ± 1.6

^a In 2013, from day of year (DOY) 154 to 167, period of 14 days. In 2014, from DOY 162 to 182, period of 21 days.

^b In 2013, from DOY 168 to 216, period of 49 days. In 2014, from DOY 183 to 210, period of 28 days.

^c In 2013, from DOY 217 to 228, period of 12 days. In 2014, from DOY 211 to 229, period of 19 days.

3.4. Discussion

3.4.1. Water fluxes and runoff generation

The difference of almost one order of magnitude in precipitation between the 2013 and the 2014 summer monsoon induced definite differences in the amount and sources of runoff, in associated runoff generation processes and, at a lesser extent, in the water balance of the catchment. In 2013, the water balance for the summer monsoon resulted in an increase in storage of 48 mm, while in 2014 it resulted in a decrease in storage of 21 mm (Table 3.1). Runoff accounted for most of the water output in 2013 and evapotranspiration was the major

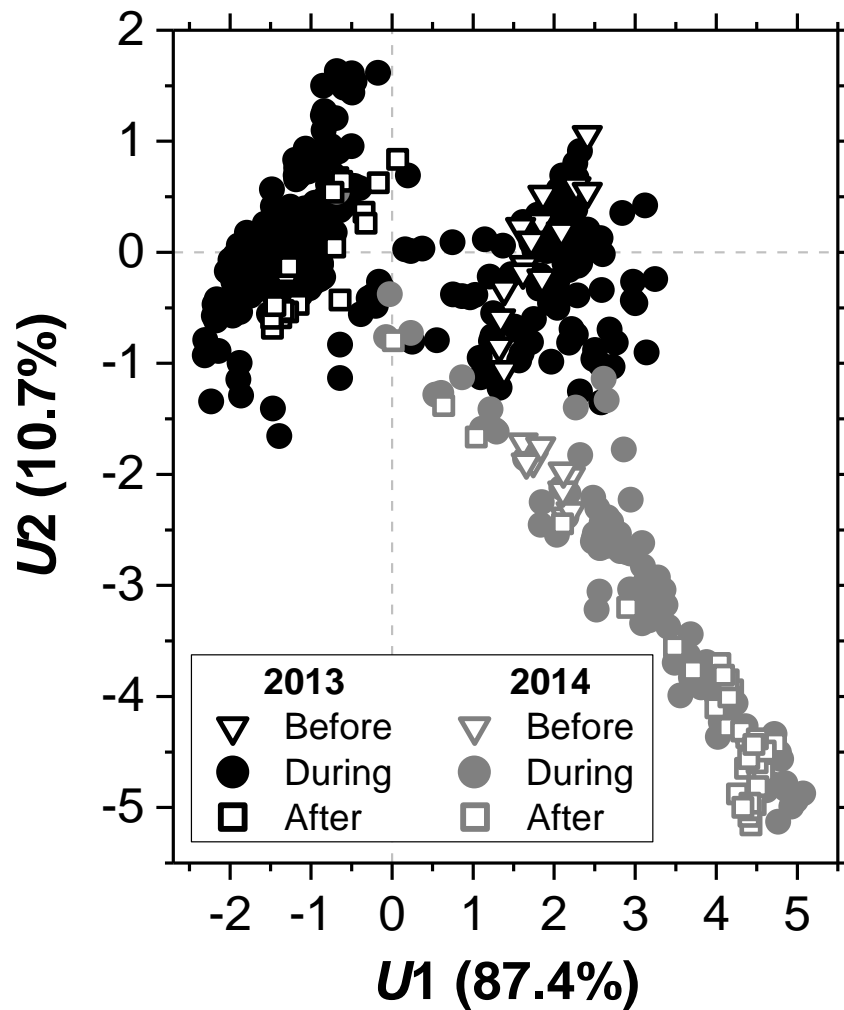


Figure 3.6. Orthogonal projections of stream water tracer values for the periods before, during and after the 2013 and the 2014 summer monsoon, in the mixing subspace of the 2013 values. The percentage of variation explained by each principal component (U_x) follows the order of the component in parentheses. $U2$ was not retained but plotted for ease of viewing.

water output in 2014. However, a decoupling of potential and actual evapotranspiration may have occurred in 2014, as soil moisture temporarily decreased to values close to the range considered as water stress conditions (Khatun et al., 2011a). Hence, it is possible that a lesser decrease or even an increase in storage occurred in 2014, which would reduce the absolute difference in the water balance. Nevertheless, this difference is relatively small in comparison to the difference in precipitation between both years of the summer monsoon. Likely responsible for this is the low storage capacity of the catchment, which is a common feature of steep catchments with shallow soils. We also deduced a low storage capacity from the observation that the stream had ceased to flow in the month of July 2015, as the drought in

South Korea persisted. While the input of an additional 732 mm of precipitation was more than enough to sustain a higher total evapotranspiration in 2013, most of the precipitation was converted to runoff and the catchment could only store an additional 48 mm of water. In this sense, the 2013 and the 2014 summer monsoon differed much more in terms of water fluxes than in terms of water balance. Whether most of the precipitation was converted to runoff or evapotranspiration, the absolute increase or decrease in storage remained relatively low.

The large range in runoff coefficients of individual rainfall events (6.0 to 124.7%) suggested that the proportion of precipitation converted to runoff varied between events. Choi et al. (2010b) reported low runoff coefficients for events preceded by dry conditions, and higher coefficients for events preceded by wet conditions. As explained by Payeur-Poirier et al. (in preparation) for the events of 2013, low runoff coefficients were associated to the increase in soil moisture storage, and high coefficients were associated to the likely occurrence of transient saturation and subsequent fast subsurface flow by the high input of precipitation. Soil moisture and precipitation have been known to greatly influence the generation of runoff (Choi et al., 2010b; Haga et al., 2005; Sidle, 2006). We attempted to establish correlations between runoff, antecedent soil moisture index (ASMI) and precipitation of individual rainfall events to quantify the conditions of runoff generation (Fig. 3.7). As function of ASMI, runoff greatly increased above a certain threshold (except for two events), but the correlations below and above this threshold were not significant. A significant correlation was found between runoff and precipitation. However, what best differentiated the events of low and medium runoff coefficients from the events of high coefficients was a threshold in the sum of ASMI and precipitation for each event (Fig. 3.7). Below the threshold, runoff did not significantly increase with this sum, and above the threshold, runoff substantially increased with this sum. The threshold of 157 mm was reached and exceeded in 2013, but not in 2014, as the runoff coefficients of the 2014 events fell within the cluster of low values. We believe the clustering of runoff coefficients into low (5 to 15%), medium (25 to 40%) and high values (65% and above) reflects the proportions of precipitation converted to runoff, evapotranspiration or storage, the medium values corresponding to a transitional state in these proportions. In 2013, the threshold was reached when the most intense period in terms of rainfall events began (Fig. 3.2, from DOY 189 to 204), during which events of high return periods yielded high amounts of precipitation. This coincided with the first day of the study period that daily runoff exceeded daily evapotranspiration, which did not occur over the

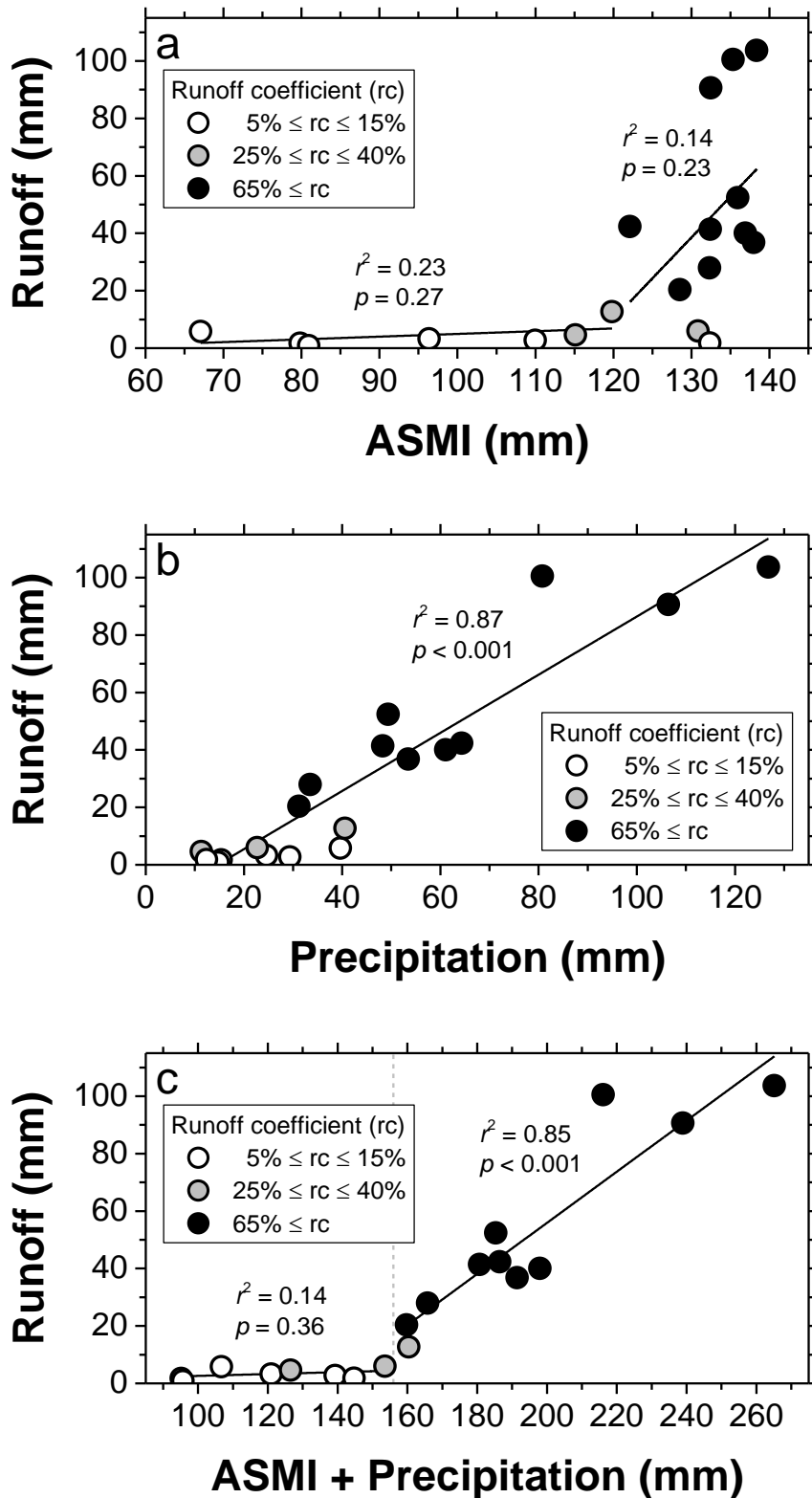


Figure 3.7. Total runoff for individual rainfall events of the 2013 and the 2014 summer monsoon as a function of (a) antecedent soil moisture index (ASMI), (b) precipitation and (c) the sum of ASMI and precipitation. The runoff coefficients of events (rc) are identified per cluster. In plot (c), linear regressions were separately calculated for the events below and the events above the threshold value; the vertical dashed line corresponds to the threshold value.

2014 study period. This suggests that, below the threshold, most of the throughfall replenished soil moisture deficits that were at least partly caused by evapotranspiration. Above the threshold, most of the throughfall either directly contributed to runoff through subsurface flow from the hillslope area or recharged the saturated zone, as explained by Payeur-Poirier et al. (in preparation). This is also consistent with the relative contributions to runoff of its most likely sources, as a substantial contribution to runoff of soil water from the 2014 study period. This suggests that, below the threshold, most of the throughfall replenished soil moisture deficits that were at least partly caused by evapotranspiration. Above the threshold, most of the throughfall either directly contributed to runoff through hillslope area only occurred in 2013 (Table 3.3). In 2014, only the contribution from toeslope soil water significantly increased from the period before to the period after the summer monsoon, and this increase occurred during the 3rd rainfall event. We believe that it likely contributed to runoff through lateral unsaturated flow, as explained by Payeur-Poirier et al. (in preparation). In fact, before this event, soil water could only be sampled at the riparian area.

The threshold of 135 mm derived from the sum of ASMI and cumulative precipitation by Haga et al. (2005) was similar to our threshold value, and was related to the subsurface flow of water from the upslope to the spring area. Threshold responses of runoff were also observed in other temperate forested catchments and hillslopes (Detty and McGuire, 2010; Graham et al., 2010; James and Roulet, 2007; Sidle et al., 1995; Tani, 1997; Tromp-van Meerveld and McDonnell, 2006), and were related to the activation of saturated, subsurface flow. In 2014, only one of the two intermittent springs was activated for a few hours, and the stream did not extend upstream from its initial extent. The fact that the stream extended further upstream in 2013 than in 2014 (Table 3.1) supported the inference of a direct contribution to runoff of hillslope soil water. The importance of subsurface flow above a certain threshold has been emphasized by many authors (Choi et al., 2010b; Fujimoto et al., 2008; Gomi et al., 2010). Tsuboyama (2006) proposed that a certain degree of wetness, represented by piezometric head and discharge, must be reached for upslope areas to substantially contribute to stormflow through preferential flow paths. The conceptual model of stormflow generation within headwater catchments developed by Sidle (2006) is partly based on the activation of preferential flow paths above a threshold of soil moisture, through which upslope areas contribute to stormflow. Uchida et al. (2002) also reported a threshold response to precipitation of preferential flow from upslope to downslope areas. Our results agree with the aforementioned findings. The contribution from rapid, subsurface flow

influenced the shape of the flow-duration curve of both years of the summer monsoon (Table 3.4 and Fig. 3.8).

Table 3.4. Percentile exceedance specific discharge (hourly mean) for the period from June 1 to August 16 of 2013 and 2014. Both periods include the summer monsoon.

Percentile	2013	2014
q_1 (mm h ⁻¹)	3.503	0.079
q_5 (mm h ⁻¹)	1.583	0.065
q_{50} (mm h ⁻¹)	0.117	0.018
q_{95} (mm h ⁻¹)	0.022	0.010
q_{99} (mm h ⁻¹)	0.019	0.009

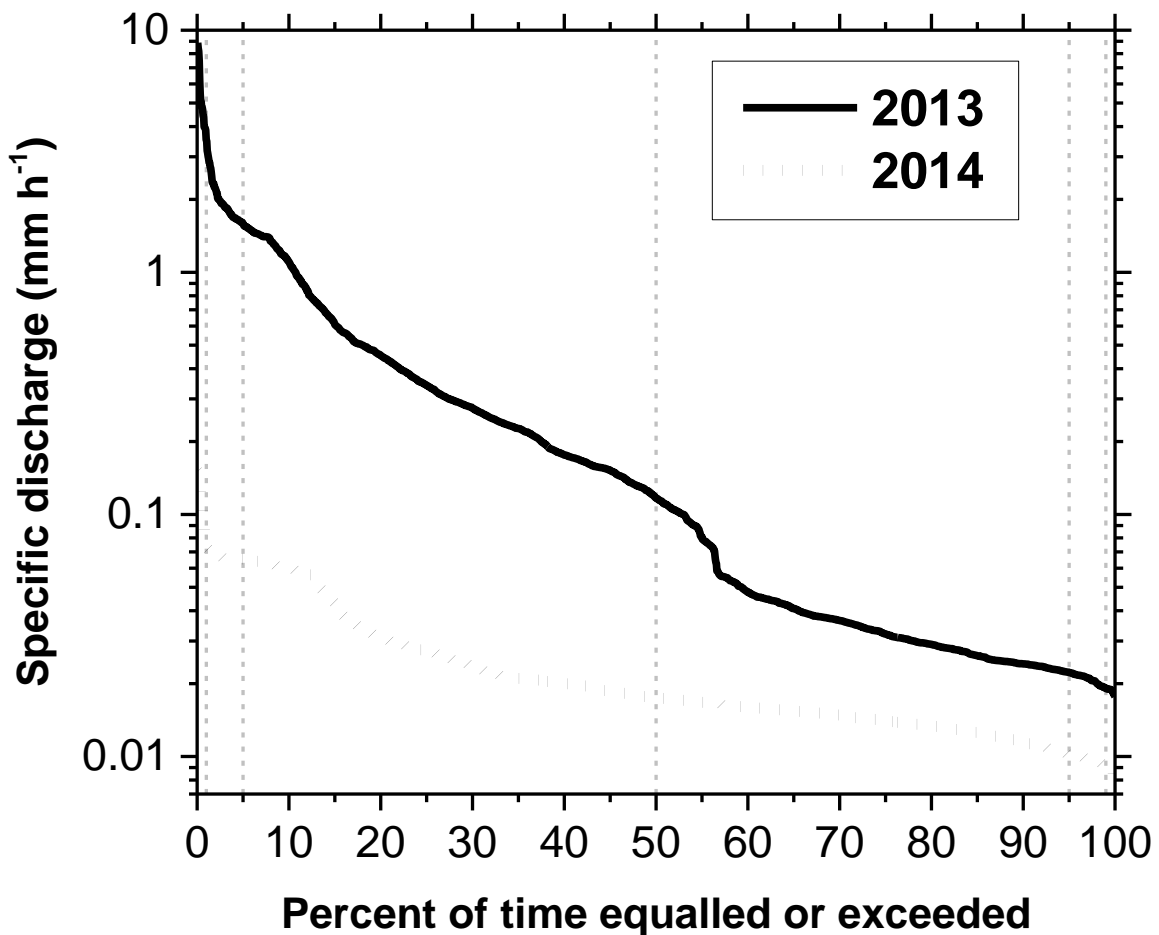


Figure 3.8. Flow-duration curves of specific discharge (hourly mean) for the period from June 1 to August 16 of 2013 and 2014 (measurement period common to both years, which includes the summer monsoon). Vertical dashed lines correspond to the 1st, 5th, 50th, 95th and 99th percentiles.

3.4.2. Water quality

In terms of stream water chemistry, the catchment was comparable to other catchments of the East Asian summer monsoon region (Asano et al., 2009; Tsujimura et al., 2001). Even though the time-series of concentration of most ions differed between the 2013 and the 2014 summer monsoon, the proportions of ions were similar between both years (Figs. 3.4 and 3.5). An exception would be NO_3^- , of which the higher proportion in 2014 could be due to a higher rate of production associated with a higher average stream water temperature (Table 3.1). However, similar proportions suggest that the substantial decrease in concentrations that occurred approximately halfway through the 2013 summer monsoon was likely due to a dilution effect (Fig. 3.5). At this period, the consecutive occurrence of six major rainfall events resulted in the massive input of throughfall to the catchment, and the likely dilution of stream water. This was also the period when the threshold in runoff generation was reached and exceeded. In 2014, the occurrence of only one major rainfall event did not suffice to induce such a dilution effect. Instead, EC and the concentration of most solutes increased in response to the rainfall events, especially in response to the 3rd event. This may be explained by the initial flushing of solutes from the soil to the stream. This initial flushing also occurred during the first few events of 2013, but the increases in values were less pronounced because discharge at this period was higher (Fig. 3.2). Lee et al. (2015) have inferred that the initial flushing of major anions was later overcome by a dilution effect induced by rainfall events.

Although the proportions of most ions were similar between both years, the proportions in the values of Ca^{2+} , EC and $\delta^2\text{H}$ were not similar between both years. In 2013, values of Ca^{2+} and EC were negatively correlated with values of $\delta^2\text{H}$ while, in 2014, values of Ca^{2+} and EC were positively correlated with values of $\delta^2\text{H}$. This resulted in the stream water values of 2014 not fitting in the mixing subspace of the 2013 values (Fig. 3.6), and agreed with a higher contribution of groundwater to runoff in 2014 (Table 3.3).

The difference in the concentration and in the total fluxes of DOC may be attributable to the difference in water sources. As Kim et al. (2007) reported, DOC concentration in the surface soil is higher than in groundwater, which is consistent with a higher contribution to runoff of hillslope soil water in 2013 (Table 3.3). In 2013, as discharge first increased, the concentration of DOC also increased, but then it decreased with the dilution by the high input of precipitation (Fig. 3.9).

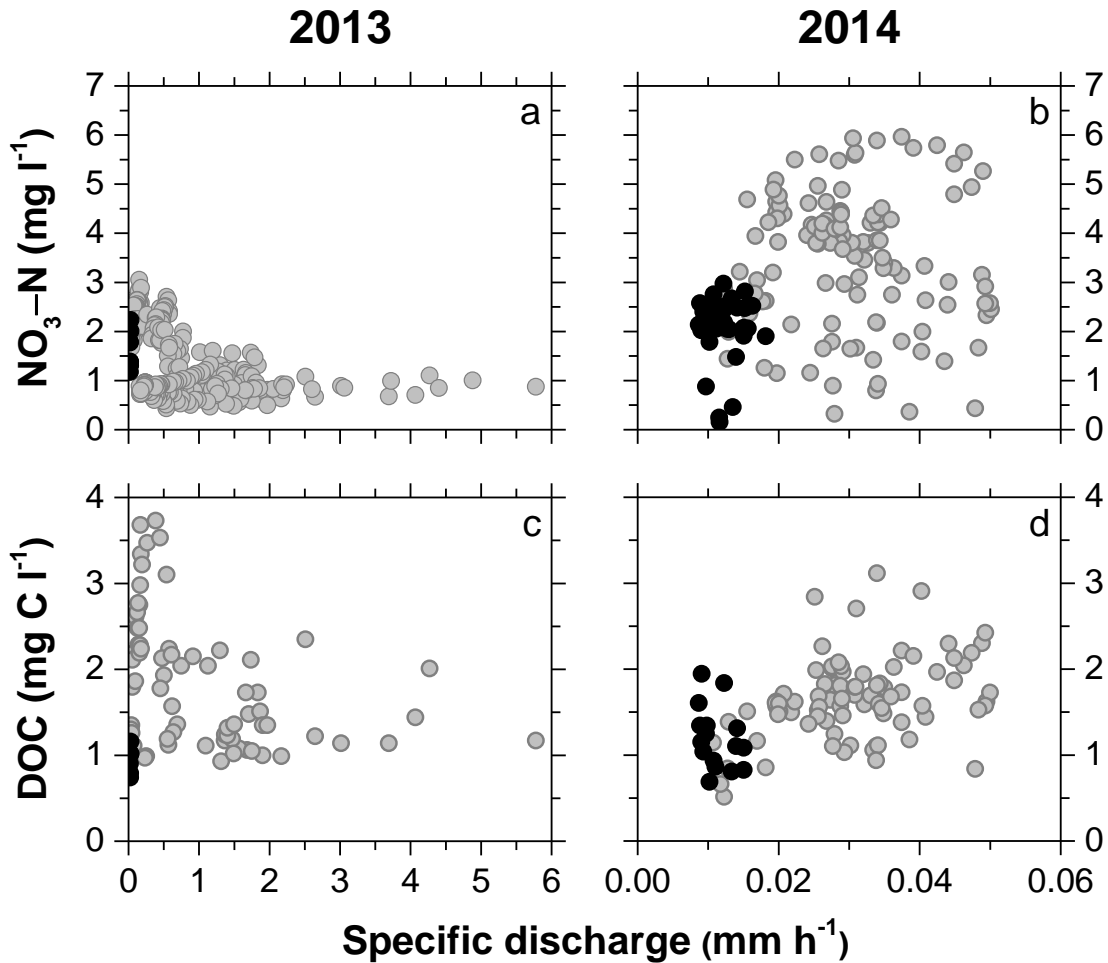


Figure 3.9. Stream water concentrations of $\text{NO}_3\text{-N}$ and dissolved organic carbon (DOC) as a function of specific discharge for (a, c) the 2013 and (b, d) the 2014 summer monsoon. Black data points correspond to samples collected at low-flow conditions and grey data points correspond to samples collected during and following rainfall events. Two data points exceed the range of the abscissa of plots (a) and (c).

3.5. Conclusions

This study has compared the water fluxes and quality of a forested headwater catchment and examined their linkages with runoff generation processes over two hydrologically contrasting years of the East Asian summer monsoon (EASM). In relation to the average conditions of the EASM, the 2013 EASM was comparable to a “natural flood experiment” and the 2014 EASM was comparable to a “natural drought experiment”, and they closely approximated some of the future predicted conditions of this climate subsystem. As demonstrated in this study, extremely differing years of the EASM can result in extremely differing fluxes of water and solutes, contributions to runoff, and water quality from forested

catchments. The results could be useful for modelling the hydrological dynamics of forested catchments over future conditions in the EASM, and improve the “transient” feature of process-based hydrological models, as proposed by Fatichi et al. (2016).

Acknowledgements

We greatly acknowledge support from the International Research Training Group TERRECO (Kang and Tenhunen, 2010), which was funded by the German Research Foundation (DFG) at the University of Bayreuth, Bayreuth, Germany, and the Korea Research Foundation (KRF) at Kangwon National University, Chuncheon, South Korea. The isotopic analyses by the laboratory of the Institute of Landscape Ecology, University of Münster, Münster, Germany, supervised by Dr. Klaus-Holger Knorr, are also appreciated.

References

- Ahn, S.R., Kim, S.J., 2016. Assessment of climate change impacts on the future hydrologic cycle of the Han River basin in South Korea using a grid-based distributed model. *Irrig. Drain.* 65, 11–21. DOI: [10.1002/ird.1963](https://doi.org/10.1002/ird.1963)
- Archibald, J.A., Walter, M.T., 2014. Do energy-based PET models require more input data than temperature-based models?—An evaluation at four humid Fluxnet sites. *J. Am. Water Resour. Assoc.* 50, 497–508. DOI: [10.1111/jawr.12137](https://doi.org/10.1111/jawr.12137)
- Asano, Y., Uchida, T., Mimasu, Y., Ohte, N., 2009. Spatial patterns of stream solute concentrations in a steep mountainous catchment with a homogeneous landscape. *Water Resour. Res.* 45, W10432. DOI: [10.1029/2008WR007466](https://doi.org/10.1029/2008WR007466)
- Bae, D.-H., Jung, I.-W., Chang, H., 2008a. Long-term trend of precipitation and runoff in Korean river basins. *Hydrol. Process.* 22, 2644–2656. DOI: [10.1002/hyp.6861](https://doi.org/10.1002/hyp.6861)
- Bae, D.-H., Jung, I.-W., Chang, H., 2008b. Potential changes in Korean water resources estimated by high-resolution climate simulation. *Clim. Res.* 35, 213–226. DOI: [10.3354/cr00704](https://doi.org/10.3354/cr00704)
- Bae, D.-H., Jung, I.-W., Lee, B.-J., Lee, M.-H., 2011. Future Korean water resources projection considering uncertainty of GCMs and hydrological models. *J. Korea Water Resour. Assoc.* 44, 389–406. DOI: [10.3741/JKWRA.2011.44.5.389](https://doi.org/10.3741/JKWRA.2011.44.5.389) (in Korean)
- Buttle, J.M., 1994. Isotope hydrograph separations and rapid delivery of pre-event water from drainage basins. *Prog. Phys. Geogr.* 18, 16–41. DOI: [10.1177/030913339401800102](https://doi.org/10.1177/030913339401800102)
- Cescatti, A., Marcolla, B., Vannan, S.K.S., Pan, J.Y., Román, M.O., Yang, X., Ciais, P., Cook, R.B., Law, B.E., Matteucci, G., Migliavacca, M., Moors, E., Richardson, A.D., Seufert, G., Schaaf, C.B., 2012. Intercomparison of MODIS albedo retrievals and in situ measurements across the global FLUXNET network. *Remote Sens. Environ.* 121, 323–334. DOI: [10.1016/j.rse.2012.02.019](https://doi.org/10.1016/j.rse.2012.02.019)
- Chang, H., Kwon, W.-T., 2007. Spatial variations of summer precipitation trends in South Korea, 1973–2005. *Env. Res. Lett.* 2, 045012. DOI: [10.1088/1748-9326/2/4/045012](https://doi.org/10.1088/1748-9326/2/4/045012)
- Choi, T., Lim, J.-H., Chun, J.-H., Lee, D., Kim, J., 2005. Microclimatological characteristics observed from the flux tower in Gwangneung forest watershed. *Korean J. Agric. For. Meteorol.* 7, 35–44. (in Korean)
- Choi, G., Kwon, W.-T., Boo, K.-O., Cha, Y.-M., 2008. Recent spatial and temporal changes in means and extreme events of temperature and precipitation across the Republic of Korea. *J. Korean Geogr. Soc.* 43, 681–700. (in Korean)
- Choi, K.-S., Moon, J.-Y., Kim, D.-W., Byun, H.-R., Kripalani, R., 2010a. The significant increase of summer rainfall occurring in Korea from 1998. *Theor. and Appl. Climatol.* 102, 275–286. DOI: [10.1007/s00704-010-0256-0](https://doi.org/10.1007/s00704-010-0256-0)
- Choi, H.T., Kim, K., Lee, C.H., 2010b. The effect of antecedent moisture conditions on the contributions of runoff components to stormflow in the coniferous forest catchment. *J. Korean For. Soc.* 99, 755–761.

- Christophersen, N., Hooper, R.P., 1992. Multivariate analysis of stream water chemical data: the use of principal components analysis for the end-member mixing problem. *Water Resour. Res.* 28, 99–107. DOI: [10.1029/91WR02518](https://doi.org/10.1029/91WR02518)
- Chung, Y.-S., Yoon, M.-B., Kim, H.-S., 2004. On climate variations and changes observed in South Korea. *Clim. Change* 66, 151–161. DOI: [10.1023/B:CLIM.0000043141.54763.f8](https://doi.org/10.1023/B:CLIM.0000043141.54763.f8)
- Detty, J., McGuire, K., 2010. Threshold changes in storm runoff generation at a till-mantled headwater catchment. *Water Resour. Res.* 46, W07525. DOI: [10.1029/2009WR008102](https://doi.org/10.1029/2009WR008102)
- Fatichi, S., Vivoni, E.R., Ogden, F.L., Ivanov, V.Y., Mirus, B., Gochis, D., Downer, C.W., Camporese, M., Davison, J.H., Ebel, B., others, 2016. An overview of current applications, challenges, and future trends in distributed process-based models in hydrology. *J. Hydrol.* 537, 45–60. DOI: [10.1016/j.jhydrol.2016.03.026](https://doi.org/10.1016/j.jhydrol.2016.03.026)
- Fujimoto, M., Ohte, N., Tani, M., 2008. Effects of hillslope topography on hydrological responses in a weathered granite mountain, Japan: comparison of the runoff response between the valley-head and the side slope. *Hydrol. Process.* 22, 2581–2594. DOI: [10.1002/hyp.6857](https://doi.org/10.1002/hyp.6857)
- Gomi, T., Asano, Y., Uchida, T., Onda, Y., Sidle, R.C., Miyata, S., Kosugi, K., Mizugaki, S., Fukuyama, T., Fukushima, T., 2010. Evaluation of storm runoff pathways in steep nested catchments draining a Japanese cypress forest in central Japan: a geochemical approach. *Hydrol. Process.* 24, 550–566. DOI: [10.1002/hyp.7550](https://doi.org/10.1002/hyp.7550)
- Graham, C.B., Woods, R.A., McDonnell, J.J., 2010. Hillslope threshold response to rainfall: (1) A field based forensic approach. *J. Hydrol.* 393, 65–76. DOI: [10.1016/j.jhydrol.2009.12.015](https://doi.org/10.1016/j.jhydrol.2009.12.015)
- GRMA (Gangwon Regional Meteorological Administration), 2013. Gangwon province summer months (June-August) meteorological characteristics. KMA, Seoul. (in Korean)
- GRMA (Gangwon Regional Meteorological Administration), 2014. Gangwon province summer months (June-August) meteorological characteristics. KMA, Seoul. (in Korean)
- Ha, K.-J., Heo, K.-Y., Lee, S.-S., Yun, K.-S., Jhun, J.-G., 2012. Variability in the East Asian Monsoon: a review. *Meteorol. Appl.* 19, 200–215. DOI: [10.1002/met.1320](https://doi.org/10.1002/met.1320)
- Haga, H., Matsumoto, Y., Matsutani, J., Fujita, M., Nishida, K., Sakamoto, Y., 2005. Flow paths, rainfall properties, and antecedent soil moisture controlling lags to peak discharge in a granitic unchanneled catchment. *Water Resour. Res.* 41, W12410. DOI: [10.1029/2005WR004236](https://doi.org/10.1029/2005WR004236)
- Ho, C.-H., Lee, J.-Y., Ahn, M.-H., Lee, H.-S., 2003. A sudden change in summer rainfall characteristics in Korea during the late 1970s. *Int. J. Climatol.* 23, 117–128. DOI: [10.1002/joc.864](https://doi.org/10.1002/joc.864)
- Hooper, R.P., 2003. Diagnostic tools for mixing models of stream water chemistry. *Water Resour. Res.* 39, 1055. DOI: [10.1029/2002WR001528](https://doi.org/10.1029/2002WR001528)
- Im, E.-S., Ahn, J.-B., Kwon, W.-T., Giorgi, F., 2008. Multi-decadal scenario simulation over Korea using a one-way double-nested regional climate model system. Part 2: future climate projection (2021–2050). *Clim. Dyn.* 30, 239–254. DOI: [10.1007/s00382-007-0282-5](https://doi.org/10.1007/s00382-007-0282-5)

- Im, E.-S., Choi, Y.-W., Ahn, J.-B., 2016. Robust intensification of hydroclimatic intensity over East Asia from multi-model ensemble regional projections. *Theor. Appl. Climatol.* DOI: [10.1007/s00704-016-1846-2](https://doi.org/10.1007/s00704-016-1846-2)
- Inamdar, S., 2011. The use of geochemical mixing models to derive runoff sources and hydrologic flow paths, in: Levia, D.F., Carlyle-Moses, D., Tanaka, T. (Eds.), *Forest hydrology and biogeochemistry. Synthesis of past research and future directions.* Springer, pp. 163–183.
- IUSS Working Group WRB, 2014. *World Reference Base for Soil Resources 2014. International soil classification system for naming soils and creating legends for soil maps.* World Soil Resources Reports No. 106. FAO, Rome.
- James, A.L., Roulet, N.T., 2007. Investigating hydrologic connectivity and its association with threshold change in runoff response in a temperate forested watershed. *Hydrol. Process.* 21, 3391–3408. DOI: [10.1002/hyp.6554](https://doi.org/10.1002/hyp.6554)
- Jung, H.-S., Choi, Y., Oh, J.-H., Lim, G.-H., 2002. Recent trends in temperature and precipitation over South Korea. *Int. J. Climatol.* 22, 1327–1337. DOI: [10.1002/joc.797](https://doi.org/10.1002/joc.797)
- Kang, S., Tenhunen, J., 2010. Complex terrain and ecological heterogeneity (TERRECO): evaluating ecosystem services in production versus water quantity/quality in mountainous landscapes. *Korean J. Agric. For. Meteorol.* 12, 307–316. DOI: [10.5532/KJAFM.2010.12.4.307](https://doi.org/10.5532/KJAFM.2010.12.4.307) (in Korean)
- Kang, H.-Y., Lee, S.-H., Kim, J.-S., Moon, Y.-I., 2015. Characterizing changes of hydrologic variability at multi-purpose dams in Korea. *J. Korean Soc. Hazard Mitig.* 15, 123–130. DOI: [10.9798/KOSHAM.2015.15.1.123](https://doi.org/10.9798/KOSHAM.2015.15.1.123) (in Korean)
- Kang, M.G., Park, S.W., 2015. An adaptive watershed management assessment based on watershed investigation data. *Environ. Manage.* 55, 1006–1021. DOI: [10.1007/s00267-014-0442-4](https://doi.org/10.1007/s00267-014-0442-4)
- Khatun, R., Ohta, T., Kotani, A., Asanuma, J., Gamo, M., Han, S., Hirano, T., Nakai, Y., Saigusa, N., Takagi, K., Wang, H., Yoshifuji, N., 2011a. Spatial variations in evapotranspiration over East Asian forest sites. II. Surface conductance and aerodynamic conductance. *Hydrol. Res. Lett.* 5, 88–92. DOI: [10.3178/HRL.5.88](https://doi.org/10.3178/HRL.5.88)
- Khatun, R., Ohta, T., Kotani, A., Asanuma, J., Gamo, M., Han, S., Hirano, T., Nakai, Y., Saigusa, N., Takagi, K., Wang, H., Yoshifuji, N., 2011b. Spatial variations in evapotranspiration over East Asian forest sites. I. Evapotranspiration and decoupling coefficient. *Hydrol. Res. Lett.* 5, 83–87. DOI: [10.3178/HRL.5.83](https://doi.org/10.3178/HRL.5.83)
- Kim, S., Lee, D., Kim, J., Kim, S., 2007. Hydro-biogeochemical approaches to understanding of water and carbon cycling in the Gwangneung forest catchment. *Korean J. Agric. For. Meteorol.* 9, 109–120. DOI: [10.5532/KJAFM.2007.9.2.109](https://doi.org/10.5532/KJAFM.2007.9.2.109)
- Kim, K., 2008. Application of intensity-duration-frequency curve for Korean rainfall data using cumulative distribution function. Yonsei University, Yonsei.
- Kim, B.-S., Kim, B.-K., Kwon, H.-H., 2011a. Assessment of the impact of climate change on the flow regime of the Han River basin using indicators of hydrologic alteration. *Hydrol. Process.* 25, 691–704. DOI: [10.1002/hyp.7856](https://doi.org/10.1002/hyp.7856)

- Kim, D.-W., Byun, H.-R., Choi, K.-S., Oh, S.-B., 2011b. A spatiotemporal analysis of historical droughts in Korea. *J. Appl. Meteorol. Climatol.* 50, 1895–1912. DOI: [10.1175/2011JAMC2664.1](https://doi.org/10.1175/2011JAMC2664.1)
- Komatsu, H., 2005. Forest categorization according to dry-canopy evaporation rates in the growing season: comparison of the Priestley-Taylor coefficient values from various observation sites. *Hydrol. Processes* 19, 3873–3896. DOI: [10.1002/hyp.5987](https://doi.org/10.1002/hyp.5987)
- Kwon, H., 2011. Measurements of wet canopy evaporation in forests: a review. *Korean J. Agric. For. Meteorol.* 13, 56–68. DOI: [10.5532/KJAFM.2010.13.2.056](https://doi.org/10.5532/KJAFM.2010.13.2.056)
- Lee, S.-S., Vinayachandran, P., Ha, K.-J., Jhun, J.-G., 2010. Shift of peak in summer monsoon rainfall over Korea and its association with El Niño-Southern Oscillation. *J. Geophys. Res.* 115, D02111. DOI: [10.1029/2009JD011717](https://doi.org/10.1029/2009JD011717)
- Lee, S.R., Cho, K., 2012. Precambrian Crustal Evolution of the Korean Peninsula. *J. Petrol. Soc. Korea* 21, 89–112. (in Korean)
- Lee, H.-J., Chun, K.-W., Shope, C.L., Park, J.-H., 2015. Multiple Time-Scale Monitoring to Address Dynamic Seasonality and Storm Pulses of Stream Water Quality in Mountainous Watersheds. *Water* 7, 6117–6138. DOI: [10.3390/w7116117](https://doi.org/10.3390/w7116117)
- Lee, M.-H., 2016. Dynamics of dissolved and particulate organic carbon and nitrogen in forest ecosystems. University of Bayreuth, Bayreuth.
- Lim, J.-H., Shin, J.-H., Lee, D.-K., Suh, S.-J., 2006. Climate change impacts on forest ecosystems: research status and challenges in Korea. *Korean J. Agric. For. Meteorol.* 8, 199–207.
- Nam, W.-H., Hayes, M.J., Svoboda, M.D., Tadesse, T., Wilhite, D.A., 2015. Drought hazard assessment in the context of climate change for South Korea. *Agric. Water Manage.* 160, 106–117. DOI: [10.1016/j.agwat.2015.06.029](https://doi.org/10.1016/j.agwat.2015.06.029)
- NIER (National Institute of Environmental Research), 2010. Korean climate change assessment report 2010. National Institute of Environmental Research, Seoul.
- Park, J.-H., Duan, L., Kim, B., Mitchell, M.J., Shibata, H., 2010. Potential effects of climate change and variability on watershed biogeochemical processes and water quality in Northeast Asia. *Environ. Int.* 36, 212–225. DOI: [10.1016/j.envint.2009.10.008](https://doi.org/10.1016/j.envint.2009.10.008)
- Payeur-Poirier, J.-L., Hopp, L., Peiffer, S., in preparation. A sudden shift in runoff generation processes at a forested catchment as induced by the East Asian summer monsoon.
- Priestley, C.H.B., Taylor, R.J., 1972. On the assessment of surface heat flux and evaporation using large-scale parameters. *Mon. Weather Rev.* 100, 81–92. DOI: [10.1175/1520-0493\(1972\)100<0081:OTAOSH>2.3.CO;2](https://doi.org/10.1175/1520-0493(1972)100<0081:OTAOSH>2.3.CO;2)
- Ryu, Y., Kang, S., Moon, S.-K., Kim, J., 2008. Evaluation of land surface radiation balance derived from moderate resolution imaging spectroradiometer (MODIS) over complex terrain and heterogeneous landscape on clear sky days. *Agric. For. Meteorol.* 148, 1538–1552. DOI: [10.1016/j.agrformet.2008.05.008](https://doi.org/10.1016/j.agrformet.2008.05.008)

- Saxton, K., Rawls, W., 2006. Soil water characteristic estimates by texture and organic matter for hydrologic solutions. *Soil Sci. Soc. Am. J.* 70, 1569–1578. DOI: [10.2136/sssaj2005.0117](https://doi.org/10.2136/sssaj2005.0117)
- Schoeneberger, P.J., Wysocki, D.A., Benham, E.C. (Eds.), 2011. Field book for describing and sampling soils, version 3.0. Natural Resources Conservation Service, National Soil Survey Center, Lincoln.
- Seo, K.-H., Son, J.-H., Lee, J.-Y., 2011. A new look at Changma. *Atmos.* 21, 109–121. (in Korean)
- Seo, K.-H., Ok, J., Son, J.-H., Cha, D.-H., 2013. Assessing future changes in the East Asian summer monsoon using CMIP5 coupled models. *J. Clim.* 26, 7662–7675. DOI: [10.1175/JCLI-D-12-00694.1](https://doi.org/10.1175/JCLI-D-12-00694.1)
- Shin, H., Park, M., Kim, S., 2012. Evaluation of forest watershed hydro-ecology using measured data and RHESSYS model for the Seolmacheon catchment. *J. Korea Water Resour. Assoc.* 45, 1293–1307. DOI: [10.3741/JKWRA.2012.45.12.1293](https://doi.org/10.3741/JKWRA.2012.45.12.1293) (in Korean)
- Sidele, R.C., Tsuboyama, Y., Noguchi, S., Hosoda, I., Fujieda, M., Shimizu, T., 1995. Seasonal hydrologic response at various spatial scales in a small forested catchment, Hitachi Ohta, Japan. *J. Hydrol.* 168, 227–250. DOI: [10.1016/0022-1694\(94\)02639-S](https://doi.org/10.1016/0022-1694(94)02639-S)
- Sidele, R.C., 2006. Stormflow generation in forest headwater catchments: a hydrogeomorphic approach. *For. Snow Landsc. Res.* 80, 115–128.
- Sklash, M.G., Farvolden, R.N., 1979. The role of groundwater in storm runoff. *J. Hydrol.* 43, 45–65. DOI: [10.1016/0022-1694\(79\)90164-1](https://doi.org/10.1016/0022-1694(79)90164-1)
- Tani, M., 1997. Runoff generation processes estimated from hydrological observations on a steep forested hillslope with a thin soil layer. *J. Hydrol.* 200, 84–109. DOI: [10.1016/S0022-1694\(97\)00018-8](https://doi.org/10.1016/S0022-1694(97)00018-8)
- Tromp-van Meerveld, H., McDonnell, J.J., 2006. Threshold relations in subsurface stormflow: 2. The fill and spill hypothesis. *Water Resour. Res.* 42, W02411. DOI: [10.1029/2004WR003778](https://doi.org/10.1029/2004WR003778)
- Tsuboyama, Y., 2006. An experimental study on temporal and spatial variability of flow pathways in a small forested catchment. *Bull. FFPRI* 5, 135–174.
- Tsujimura, M., Onda, Y., Ito, J., 2001. Stream water chemistry in a steep headwater basin with high relief. *Hydrol. Process.* 15, 1847–1858. DOI: [10.1002/hyp.243](https://doi.org/10.1002/hyp.243)
- Uchida, T., Kosugi, K., Mizuyama, T., 2002. Effects of pipe flow and bedrock groundwater on runoff generation in a steep headwater catchment in Ashiu, central Japan. *Water Resour. Res.* 38, 1119. DOI: [10.1029/2001WR000261](https://doi.org/10.1029/2001WR000261)
- Wilcox, L., Dong, B., Sutton, R., Highwood, E., 2015. The 2014 hot, dry summer in northeast Asia. *Bull. Am. Meteorol. Soc.* 96, S105–S110. DOI: [10.1175/BAMS-D-15-00123.1](https://doi.org/10.1175/BAMS-D-15-00123.1)
- WMO (World Meteorological Organization), 2009. Guide to Hydrological Practices Volume II. Management of Water Resources and Application of Hydrological Practices, sixth ed. WMO-No. 168. WMO, Geneva.

- WMO (World Meteorological Organization), 2010. Manual on Stream Gauging. Volume II – Computation of Discharge. WMO-No. 1044. WMO, Geneva.
- Yang, H., 2007. Water balance change of watershed by climate change. J. Korean Geogr. Soc. 42, 405–420. (in Korean)
- Yeom, J.-M., Lee, C.-S., Park, S.-J., Ryu, J.-H., Kim, J.-J., Kim, H.-C., Han, K.-S., 2015. Evapotranspiration in Korea estimated by application of a neural network to satellite images. Remote Sens. Lett. 6, 429–438. DOI: [10.1080/2150704X.2015.1041169](https://doi.org/10.1080/2150704X.2015.1041169)

Chapter 4

Variability in runoff fluxes of dissolved and particulate carbon and nitrogen from two watersheds of different tree species during intense storm events

Mi-Hee Lee¹, Jean-Lionel Payeur-Poirier², Ji-Hyung Park³, Egbert Matzner¹

¹ Department of Soil Ecology, Bayreuth Center of Ecology and Environmental Research (BayCEER), University of Bayreuth, Bayreuth, Germany

² Department of Hydrology, Bayreuth Center of Ecology and Environmental Research (BayCEER), University of Bayreuth, Bayreuth, Germany

³ Department of Environmental Science and Engineering, Ewha Womans University, Seoul, South Korea

Correspondence: egbert.matzner@uni-bayreuth.de (E. Matzner)

Status: published in *Biogeosciences*

Citation: Lee, M.-H., Payeur-Poirier, J.-L., Park, J.-H., Matzner, E., 2016. Variability in runoff fluxes of dissolved and particulate carbon and nitrogen from two watersheds of different tree species during intense storm events. *Biogeosciences* 13, 5421-5432. DOI: [10.5194/bg-13-5421-2016](https://doi.org/10.5194/bg-13-5421-2016)

Abstract

Heavy storm events may increase the amount of organic matter in runoff from forested watersheds as well as the relation of dissolved to particulate organic matter. This study evaluated the effects of monsoon storm events on the runoff fluxes and on the composition of dissolved ($< 0.45 \mu\text{m}$) and particulate ($0.7 \mu\text{m}$ to 1 mm) organic carbon and nitrogen (DOC, DON, POC, PON) in a mixed coniferous/deciduous (mixed watershed) and a deciduous forested watershed (deciduous watershed) in South Korea. During storm events, DOC concentrations in runoff increased with discharge, while DON concentrations remained almost constant. DOC, DON and $\text{NO}_3\text{-N}$ fluxes in runoff increased linearly with discharge pointing to changing flow paths from deeper to upper soil layers at high discharge, whereas nonlinear responses of POC and PON fluxes were observed likely due to the origin of particulate matter from the erosion of mineral soil along the stream benches. The integrated C and N fluxes in runoff over the 2 months study period were in the order; $\text{DOC} > \text{POC}$ and $\text{NO}_3\text{-N} > \text{DON} > \text{PON}$. The integrated DOC fluxes in runoff during the study period were much larger at the deciduous watershed (16 kg C ha^{-1}) than at the mixed watershed (7 kg C ha^{-1}), while the integrated $\text{NO}_3\text{-N}$ fluxes were higher at the mixed watershed (5.2 kg N ha^{-1}) than at the deciduous watershed (2.9 kg N ha^{-1}). The latter suggests a larger N uptake by deciduous trees. Integrated fluxes of POC and PON were similar at both watersheds. The composition of organic matter in soils and runoff indicate that the contribution of near surface flow to runoff was larger at the deciduous than at the mixed watershed. Our results demonstrate different responses of particulate and dissolved C and N in runoff to storm events as a combined effect of tree species composition and watershed specific flow paths.

Keywords: dissolved organic carbon, dissolved organic nitrogen, particulate organic carbon, particulate organic nitrogen, monsoon storm, forested watershed

4.1. Introduction

As much of the dissolved organic matter (DOM) in aquatic systems originates from soil derived organic matter, the export of terrestrial carbon (C) and nitrogen (N) into aquatic environments is a primary link between these systems (Bauer and Bianchi, 2011; Bianchi, 2011; Camino-Serrano et al., 2014; Canham et al., 2012). The export of terrestrial C and N

occurs in the form of dissolved and particulate organic carbon and nitrogen (DOC, DON, POC, PON). Particulate organic matter (POM) can be operationally classified into fine (0.1 to 63 μm) and coarse (63 μm to 2 mm) fractions (Richey, 2005). The export of POC was in some cases the major C export in stream (Dhillon and Inamdar, 2013; Jung et al., 2012; Kim et al., 2010; Lloret et al., 2013). On the contrary, DOC was reported as the dominant organic C form in a temperate headwater catchment (Johnson et al., 2006), a tropical rainforest catchment (Bass et al., 2011) and for several large tropical watersheds such as Amazon, Orinoco, Parana and Mengong (Lloret et al., 2013).

In regions with seasonally large differences in precipitation, most of the annual organic C export from forested watersheds to streams is driven by heavy storm events with cyclones and hurricane (Dhillon and Inamdar, 2013; Lloret et al., 2013). Such conditions are pronounced in the Korean peninsula in which the monsoon season (Jeong et al., 2012; Kim et al., 2010), represented 52% and 83% of the annual DOC and POC runoff fluxes. During storm events, a change in hydrological flow paths in watersheds has been often observed from deeper to upper soil layers (Bass et al., 2011; Sanderman et al., 2009; Singh et al., 2014). Surface flow-inducing storm events can alter the fluxes and concentrations of DOC and POC in runoff by shifting preferential flows through macropores, surface runoff and lateral flow (Katsuyama and Ohte, 2002; Kim et al., 2010; McGlynn and McDonnell, 2003).

In case of organic N export, DON was the major form of N in runoff from pristine forested watersheds (Alvarez-Cobelas et al., 2008; Frank et al., 2000; Kaushal and Lewis, 2003; Pellerin et al., 2006; Yates and Johnes, 2013). Only few data are available on the partitioning of DON and PON fluxes in runoff from forested watersheds, like Inamdar et al. (2015). They reported that particulate N composed 39-87% of the storm event N export. The question remains open, if organic N in runoff – either dissolved or particulate – from forested watersheds behaves similar to organic C or not. Some studies reported that concentrations of DON and DOC correlated strongly (von Schiller et al., 2015), but also weak relationships were found (Singh et al., 2015).

Considering an effect of watershed characteristic, tree species might influence the export of DOM from forested watersheds. DOM from coniferous litter generally comprises more refractory (e.g. hydrophobic acid, lignin) and aromatic compounds, and a relatively larger proportion of high molecular weight compounds than DOM from deciduous litter. It is also more acidic than DOM from deciduous litter (Don and Kalbitz, 2005; Hansson et al.,

2011; Kiikkilä et al., 2013). Moreover, higher DOC and DON concentrations were found in oak, beech, and silver birch forest floors compared to Norway spruce, Douglas fir, and Scots pine (Smolander and Kitunen, 2011; Trum et al., 2011). Amiotte-Suchet et al. (2007) found higher annual DOC concentrations and fluxes in runoff at a deciduous forested watershed than at a watershed dominated by coniferous species.

As a result of global warming, heavy storm events have occurred more frequently and became stronger in recent decades (IPCC, 2013). Furthermore, forest management, namely the selection of tree species, might influence the export of organic matter from forested watersheds. Understanding the influence of both drivers is needed for a better prediction of the link between terrestrial and aquatic ecosystems and to support an efficient downstream water quality management. The goal of this study was thus to investigate the influence of tree species and heavy storm events on the fluxes of dissolved and particulate forms of C and N from a mixed coniferous/deciduous and a deciduous forested watershed in South Korea during the 2013 monsoon season.

4.2. Materials and methods

4.2.1. Study area and site

The Lake Soyang basin area (Figure 4.1) is located in the upstream region of the Han River, which is the main source of drinking water for about 23 million citizens of South Korea (Lee et al., 2013; Park et al., 2010). The average annual temperature of the Lake Soyang watershed in western Gangwon-province is 11°C with monthly average temperature ranging from -5°C in January to 24°C in August (Korea Meteorological Administration, 2016). Annual precipitation ranges from 1200 to 1500 mm and the summer monsoon usually accounts for 50 to 60% of the annual precipitation (Park et al., 2010; Seo et al., 2011). Korean mountainous forests are mostly composed of deciduous forests representing 47% of the total forested area (38% coniferous forest, 12% mixed coniferous and deciduous forest) and most of the broadleaved forests of South Korea are distributed within the Gangwon province (Korea Forest Research Institute, 2013).

The mixed coniferous/deciduous forested watershed (mixed watershed; Figure 4.1) is located in Seohwa, the Gangwon province (38°12'N, 128°11'E, 368 to 682 m above sea

level). The area of the mixed watershed (Table 4.1) is 15.6 ha with 6.1 ha of coniferous forest (39%) and 9.5 ha of deciduous forest (61%). Two research plots as one in the coniferous part (MC plot) and the other one in the deciduous part (MD plot) were established. The slope of the mixed watershed as obtained from a digital elevation model ranges from 4.0 to 41° with an average of 28°. The lower part of the mixed watershed is dominated by coniferous species, including *Larix kaempferi* (Lamb.) Carr. (Japanese larch) and *Pinus densiflora* Siebold & Zucc. (Japanese red pine). The upper part of the mixed watershed is dominated by deciduous species, such as *Juglans mandshurica* Maxim. (Manchurian walnut), *Acer pictum* subsp. *mono* (Maxim.) H. Ohashi (Mono maple), *Quercus dentata* Thunb. (Daimyo oak), *Tilia amurensis* Kom. (Lime tree) and *Ulmus davidiana* var. *japonica* (Rehder) Nakai (Japanese elm).

The slope direction of the coniferous part at the mixed watershed is towards the MD plot. Lateral flow from the coniferous part to the MD plot can only influence deeper soil solution characteristics as near surface flow was never observed. Our data (see results) indicate significant quality differences of soil solutions between the MD and MC plots which suggest only a minor influence on soil solution chemistry at the MD plot from lateral flows. Furthermore, the quality parameters of soil solutions at the MD plot were similar to those of the DD plot, the latter being not influenced by lateral flows from coniferous sites. Thus, it is unlikely that the MC plot did affect the MD plot.

The deciduous forested watershed (deciduous watershed; Figure 4.1) is located in Haean, the Gangwon province (38°15'N, 128°7'E, 586 to 1005 m above sea level). The area of the deciduous watershed (Table 4.1) is 39.0 ha and is covered by various deciduous species. A research plot as deciduous plot (DD plot) was established in this watershed. The slope of the deciduous watershed ranges from 4 to 53° with an average of 24°. The dominant tree species are *Juglans mandshurica* Maxim. (Manchurian walnut), *Acer pictum* subsp. *mono* (Maxim.) Ohashi (Mono maple), *Quercus dentata* (Daimyo oak), *Quercus mongolica* (Mongolian oak) and *Fraxinus rhynchophylla* (Korean/Chinese ash). The average age of trees in the two watersheds is about 35 years. The distance between the two watersheds is ca. 6 km.

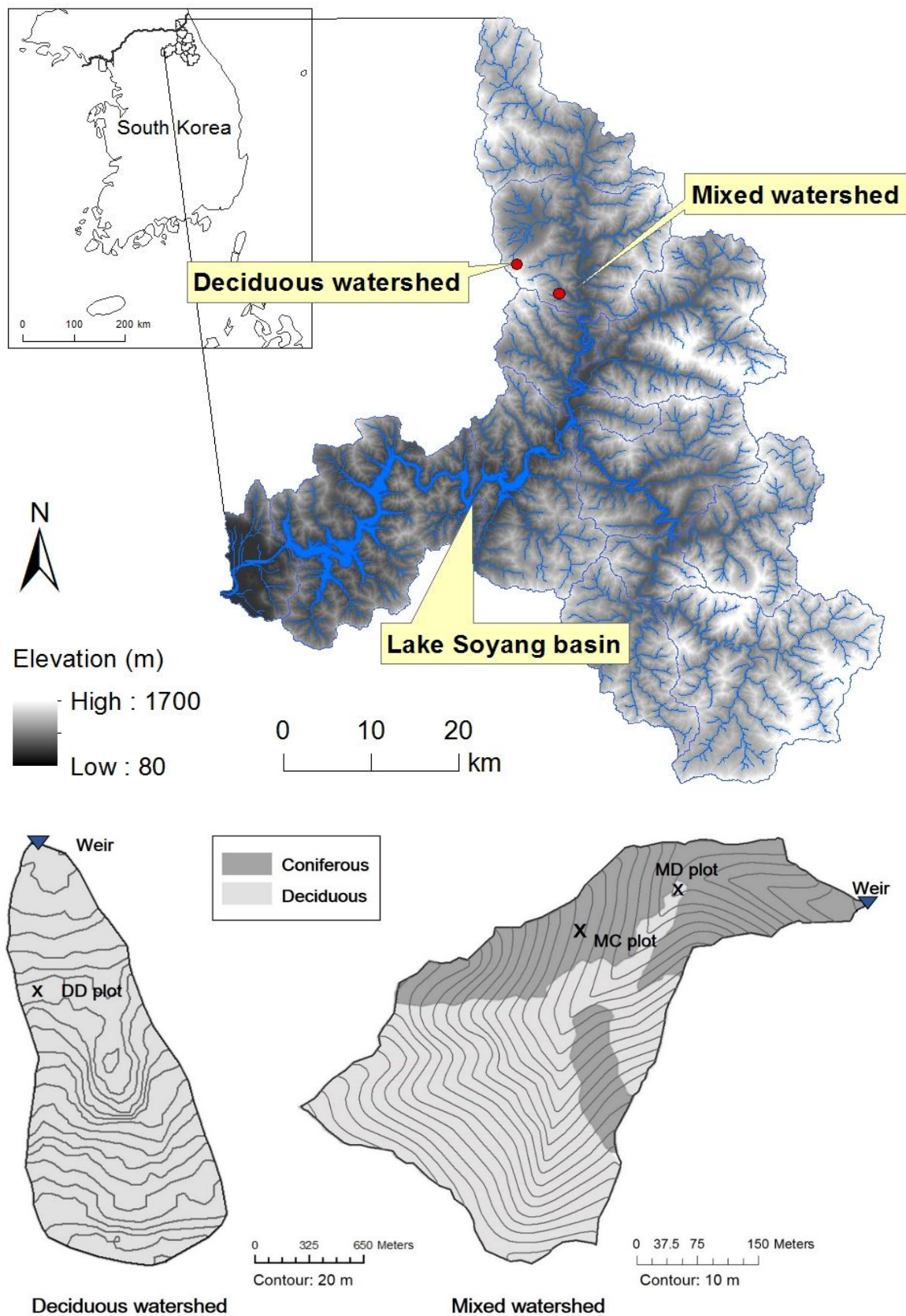


Figure 4.1. Location and tree species composition of the two studied forested watersheds. Lake Soyang map was modified from Jung et al. (2015).

Table 4.1. Tree species composition and geomorphological characteristics of the studied forested watersheds.

Watershed	Major tree species	Area (ha)	Average slope (°)	Altitude (m a.s.l.)
Mixed		15.6	23.9	368–682
Coniferous	Larch and Pine	6.1	–	–
Deciduous	Walnut, Maple, Oak, Lime, Elm	9.5	–	–
Deciduous	Walnut, Maple, Oak, Ash	39.0	24.0	586–1005

a.s.l.: above sea level.

4.2.2. Experimental design

4.2.2.1. Water sampling

Bulk precipitation samplers (n=2) were installed at each watershed in an open area located ~100 m from the plots. Throughfall collectors (n=5) under the canopy were equipped with filters to prevent large particles from entering. Forest floor leachate was collected beneath the organic layer along the slope side using zero tension lysimeters (n=5) of 185 cm² made of acrylic material. Soil solution was collected at a depth of ~50 cm with suction lysimeters (n=5) made of ceramic cups.

Before storm events in June 2013, throughfall, forest floor leachate and soil solution were collected at about weekly intervals, and runoff samples were collected 2-3 times per week. During storm events in July 2013, throughfall, forest floor leachate and soil solution was collected after each storm event so that these samples represent cumulative water samples during the entire storm event. In case of runoff, samples were taken in July 2013 at the weir using automatic collectors (6712 Portable Sampler, Teledyne Isco Inc., Lincoln, NE, USA) before, during, and after each rain event at intervals of 1 or 2 h. Discharge at the outlet of the watersheds was measured by a V-notch weir. During routine runoff sampling, water temperature, pH and electrical conductivity was measured in situ. Water samples were cooled at 4°C and then were filtered (see 2.4) within 2 days after sampling. Filtered solution samples were frozen for 1 month until further analysis of water quality and quantity.

Precipitation data (total and hour unit; Table 4.2) at the study area were used from the automatic weather station of the Korea Meteorological Administration at the point ‘Seohwa 594’ and ‘Haean 518’ for the mixed watershed and for the deciduous watershed, respectively. Those data were also comparable to ours from bulk precipitation measurements at the field sites.

4.2.2.2. Soil sampling

The total stock of organic horizons (Oi: slightly decomposed recognizable litter, Oe: moderately decomposed fragmented litter, Oa: highly decomposed humic material) was collected at each plot in a 20 × 20 cm frame with 10 replicates. The average thickness of Oi and Oe+Oa was 1.2 and 1.5 cm at the MC plot, 2.5 and 3 cm at the MD plot, and 2.3 and 2 cm at the DD plot, respectively. Mineral soil samples were collected from 3 pits at each plot in 10 cm depth layers down to 50 cm depth. In case of the DD plot, the sampling of mineral soil was not possible deeper than 40 cm depth due to massive rock. Before the analyses, soil samples were air-dried and crushed to pass through a 2 mm sieve. Soil pH was measured from a solution of a soil to solution (0.01 M CaCl₂) ratio of 1:2.5 after shaking for 2 hours. Total C and N contents were analyzed using an elemental analyzer (vario MAX CN, Elemental, Germany). Soil texture was determined by sedimentation.

4.2.3. Calculations

4.2.3.1. Fluxes of C and N in runoff

In June 2013, before the monsoon storm events, the fluxes of DOC were calculated on a weekly basis by multiplying the DOC weekly mean concentration in runoff by the weekly mean discharge. The concentrations of DON, NO₃-N, POC and PON in runoff were partly below the detection limit. Concentrations less than detection limit were observed in 5-8% of the measurements in runoff during the July events. The detection limits were applied to the calculation of export fluxes as 0.03 mg DON L⁻¹, 0.5 mg NO₃-N L⁻¹, 0.003 mg POC L⁻¹, 0.0003 mg PON L⁻¹. During the period of storm events in July 2013, the fluxes of DOC, DON, NO₃-N, POC and PON in runoff were computed at 1 or 2 h intervals by multiplying the measured concentrations with the corresponding discharge. During the monsoon season the rainfall was not continuous on all days but with intermittent gaps. The most lasting rainfall

events were identified as storm events with more than a day interval between each storm event.

4.2.3.2. Statistics for origin of DOM and POM

The normality of data was tested with the Shapiro-Wilk Test. When the normality was assured, the Holm-Sidak Test was used for both pairwise comparisons and comparisons versus a control group. When the normality test failed, the Dunn's Test was used for all pairwise comparisons and comparisons against a control group with rank-based-ANOVA.

4.2.4. Chemical analyses

After filtration through a pre-rinsed cellulose acetate membrane filter (0.45 μm , Whatman), the concentrations of DOC and total dissolved nitrogen (TDN) in water samples were measured by a total organic carbon analyzer (TOC-CPH, Shimadzu, Japan). DON concentration was calculated as the difference between total nitrogen and mineral-N ($\text{NO}_3^- + \text{NH}_4^+$). Nitrate and ammonium concentrations were measured by flow injection (FIA-LAB; MLE, Dresden, Germany). Nitrite was not measured because concentrations were negligible in soil solutions and runoff.

In this study, the POC and PON fraction is defined as the size class 0.7 μm to 1 mm. Samples were filtered through a 1 mm mesh to remove larger particulate materials and then finally filtered through a pre-rinsed 0.7 μm pore size glass filter (GF/F, Whatman). Before using the glass filters, the filters were pre-combusted at 450°C to remove any organic material. The residues of particulate material on the GF/F filters were analysed for POC and PON after drying at 65°C using an elemental analyser (Carlo Erba 1108, Milano, Italy) coupled to a ConFlo III interface and an isotope ratio mass spectrometer (Finnigan MAT, Bremen, Germany). DOC and POC cutoff limits as 0.45 and 0.7 μm were unmatched in this study because of practical reasons and the unmatched fraction is considered negligible.

The absorption spectra of DOM were obtained at wavelengths from 200 to 600 nm using a UV-visible spectrophotometer (DR5000, HACH). Specific ultraviolet absorbance (SUVA_{280}) values were determined by UV absorbance at 280 nm divided by the DOC concentrations and multiplied by 100.

For fluorescence excitation-emission matrices, fluorescence intensities were recorded with a luminescence spectrometer (LS-55, Perkin-Elmer, USA) following the method of

Baker (2001), Chen et al. (2007), and Hur and Cho (2012). Excitation and emission slits were both adjusted to 10 nm. DOM samples were diluted under the ultraviolet absorbance of 0.1 at 280 nm to avoid inner-filter correction, and then were adjusted to pH 3.0 for the fluorescence measurements. The fluorescence intensities of all samples were normalized to units of quinine sulfate equivalents. The humification index (HIXem) was calculated by dividing the emission intensity from 435 to 480 nm region by intensity from 300 to 345 nm (Zsolnay et al., 1999). Fluorescence characteristics of water samples were interpreted as fulvic-like fluorescence (FLF), humic-like fluorescence (HLF) and protein-like fluorescence (PLF) (Fellman et al., 2010; Singh et al., 2014).

After filtration (0.45 μm , Whatman), water samples were freeze-dried to measure ^{13}C and ^{15}N isotope abundances of DOC and TDN using an elemental analyzer (Carlo Erba 1108, Milano, Italy) coupled to a ConFlo III interface and an isotope ratio mass spectrometer (Finnigan MAT, Bremen, Germany).

4.3. Results

4.3.1. Soil and hydrological characteristics

The morphology of the organic layers at the MC, MD, and DD plots were similar, representing a moder-like organic layer, with distinct Oi-layers and less distinct Oe and Oa-layers. However, the depth of O-layer in the MC plot (ca. 3 cm) was thinner than in the MD and DD plot (ca. 4-5 cm). The typical soil type at both watersheds is Eutric Cambisol (FAO, 2014). Soil texture at all plots ranged from 40-44%, 30-38% and 18-22% for sand, silt and clay, respectively. The C content of the organic layers at all plots ranged from 45 to 48% in the Oi and from 34 to 38% in the Oe+Oa layers. The C/N ratio at all plots decreased from the organic layer (20-29) to the mineral soil (10-12) down to 40-50 cm depth. The soil $\delta^{13}\text{C}$ and soil $\delta^{15}\text{N}$ values significantly increased with soil depth from -29 to -24‰ and from 0 to 8‰, respectively (Figure 4.2).

The average discharge in June 2013 before storm events was 0.03 mm h^{-1} at the mixed watershed and 0.06 mm h^{-1} at the deciduous watershed (data not shown). The total amount of precipitation in July was slightly higher at the deciduous watershed (367 mm) than at the mixed watershed (313 mm; Table 4.2). Also, the intensity of precipitation in July was larger

at the deciduous watershed than at the mixed watershed. Similar to precipitation data, the mixed watershed had less maximum discharge and also slightly lower discharge before start of a storm event than the deciduous watershed.

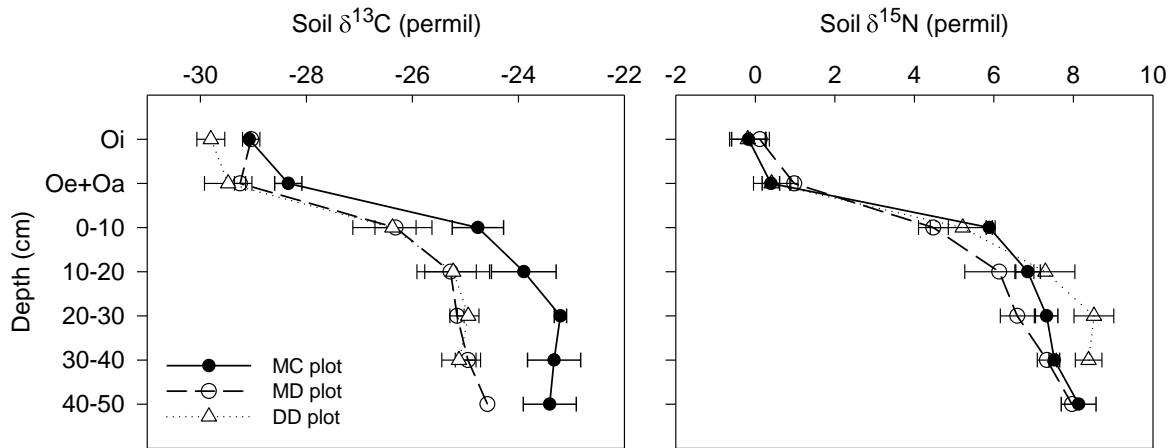


Figure 4.2. Soil profiles of ^{13}C and ^{15}N isotope abundance at the MC, MD, and DD plot. Error bars represent standard deviation (n=3).

Table 4.2. Hydrological characteristics of sampled storm events and maximum concentration of dissolved organic carbon (DOC) and nitrogen (DON), particulate organic carbon (POC) and nitrogen (PON) in runoff. All dates are in 2013.

Watershed	Start date	Duration (h)	Number of samples	Total precip. (mm)	Max. precip. intensity (mm h ⁻¹)	Avg. precip. intensity (mm h ⁻¹)	Max. discharge (mm h ⁻¹)	Initial discharge (mm h ⁻¹)	Max. DOC (mg C L ⁻¹)	Max. DON (mg N L ⁻¹)	Max. POC (mg C L ⁻¹)	Max. PON (mg N L ⁻¹)
Mixed	July 02	15	16	40.0	8.5	2.7	0.17	0.03	3.7	0.1	0.04	0.002
	July 08	24	15	56.5	10.0	2.3	0.55	0.04	3.7	0.4	0.06	0.004
	July 11	12	12	44.5	10.0	3.7	1.47	0.52	2.1	0.2	0.03	0.003
	July 14	41	26	172.5	34.0	4.2	8.89	1.21	2.4	0.2	10.70	0.730
				(total 313.5)	(avg. 15.6)	(avg. 3.2)	(avg. 2.77)	(avg. 0.45)				
Deciduous	July 08	32	21	117.5	20.0	3.6	3.16	0.10	6.9	0.6	8.60	0.580
	July 11	15	20	43.5	8.0	2.9	3.07	0.58	5.0	0.2	0.30	0.020
	July 14	42	23	148.5	32.0	3.5	7.39	1.07	5.1	0.2	3.20	0.210
	July 18	9	10	58.0	20.5	6.4	6.61	0.32	5.2	0.2	1.10	0.080
				(total 367.5)	(avg. 20.1)	(avg. 4.1)	(avg. 5.06)	(avg. 0.52)				

precip.: precipitation

4.3.2. Concentrations of carbon and nitrogen in runoff during storm events

The increase of the DOC concentrations in runoff with discharge was steeper at the deciduous watershed (e.g. 1.9 to 6.9 mg C L⁻¹ on July 8th, 2013) than at the mixed watershed (e.g. 1.0 to 3.7 mg C L⁻¹ on July 8th, 2013) (Figure 4.3a). In contrast, the DON concentrations in runoff from both watersheds were independent of discharge (Figure 4.3b). The highest concentration of DOC and DON in runoff was observed during the earlier storm events (Table 4.2). The NH₄-N concentrations were at any time negligible (< 0.05 mg N L⁻¹).

At discharges from ~1 to 9 mm h⁻¹, higher concentrations of POC and PON in runoff were found (Figure 4.3d, e). For example, the POC concentration in runoff from the mixed watershed was as high as 10.7 mg C L⁻¹ at the largest discharge of 9 mm h⁻¹. At the deciduous watershed, the POC concentration in runoff reached a maximum of 8.6 mg C L⁻¹ already at 3 mm h⁻¹ discharge during the first storm event (Figure 4.3d, Table 4.2). The following more intense storms did result in lower POC concentrations. The pattern of POC concentration coincided with those of PON ($r=0.99$).

The runoff DOC concentrations in response to discharge had a clockwise hysteretic loop with higher concentrations on the rising than on the falling limb (Figure 4.3a). No hysteretic loops were observed for DON, POC and PON (Figure 4.3b, d, e).

The DOC/DON ratio in runoff ranged from 5 to 60 (Figure 4.3c). The DON concentrations lower than 0.05 mg N L⁻¹ were not considered for calculation of the DOC/DON ratios. In response to increased discharge, the DOC/DON ratios were stable at the mixed watershed, while there was a tendency for increasing in the DOC/DON ratios with discharge at the deciduous watershed. On the contrary, there was no response of the POC/PON ratio to discharge. Unlike to the DOC/DON ratio, the POC/PON ratio ranged narrowly from 10 to 20 at both watersheds (Figure 4.3f) with an average of 12 at the mixed and 13 at the deciduous watershed.

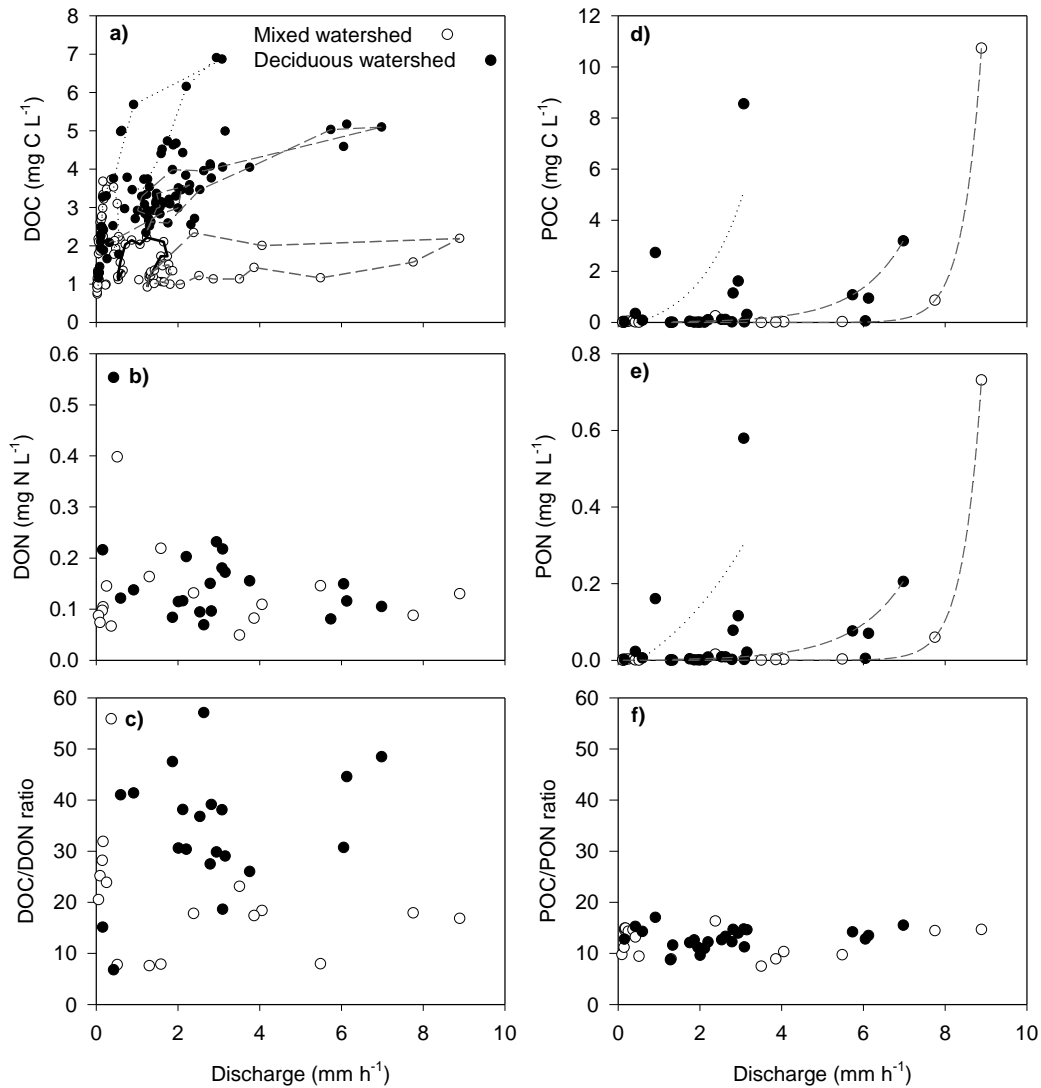


Figure 4.3. Concentrations of a) dissolved organic carbon (DOC) and b) nitrogen (DON), d) particulate organic carbon (POC) and e) nitrogen (PON) and the ratios of c) DOC/DON and f) POC/PON in runoff with discharge during monsoon storm events. Dotted, solid and dashed lines correspond to the storm event of July 8th 2013, July 11th 2013 and July 14th 2013, respectively.

4.3.3. Fluxes of carbon and nitrogen

The fluxes of DOC, DON and NO₃-N in runoff were linearly correlated to discharge at both watersheds (Figure 4.4). The DOC fluxes at the deciduous watershed increased with a much steeper slope in response to discharge than at the mixed, while the NO₃-N fluxes at the mixed watershed more steeply increased with increasing discharge than at the deciduous. The POC fluxes were generally much lower than the DOC fluxes, but the POC and PON fluxes increased in a non-linear response to discharge. Only at a single peak flow event on July 14th

2013, the POC fluxes at the mixed watershed were 5 times greater than the DOC fluxes. The same trend was found for the PON and DON fluxes. At the deciduous watershed, only one event caused slightly larger POC than DOC fluxes.

The integrated C and N fluxes over the study period from both watersheds were in the order; DOC > POC and NO₃-N > DON > PON (Table 4.3). The DOC fluxes as the dominant C flux form contributed 75% and 92% of the total organic C flux at the mixed and the deciduous watersheds, respectively. The integrated fluxes of DOC and DON were higher at the deciduous (16 kg C ha⁻¹ and 0.5 kg N ha⁻¹) than at the mixed watershed (6.7 kg C ha⁻¹ and 0.26 kg N ha⁻¹). The integrated fluxes of POC and PON were small at both watersheds with only minor differences. Before storm events in June 2013, POC and PON were almost not exported at both watersheds. However, the integrated fluxes of POC and PON increased extremely during heavy storm events in July 2013. The NO₃-N fluxes as the dominant N flux form represented 93% and 82% of the total N flux in runoff at the mixed and the deciduous watershed, respectively. The integrated fluxes of NO₃-N were about twice as high (5.2 kg N ha⁻¹) at the mixed watershed than at the deciduous watershed (2.9 kg N ha⁻¹).

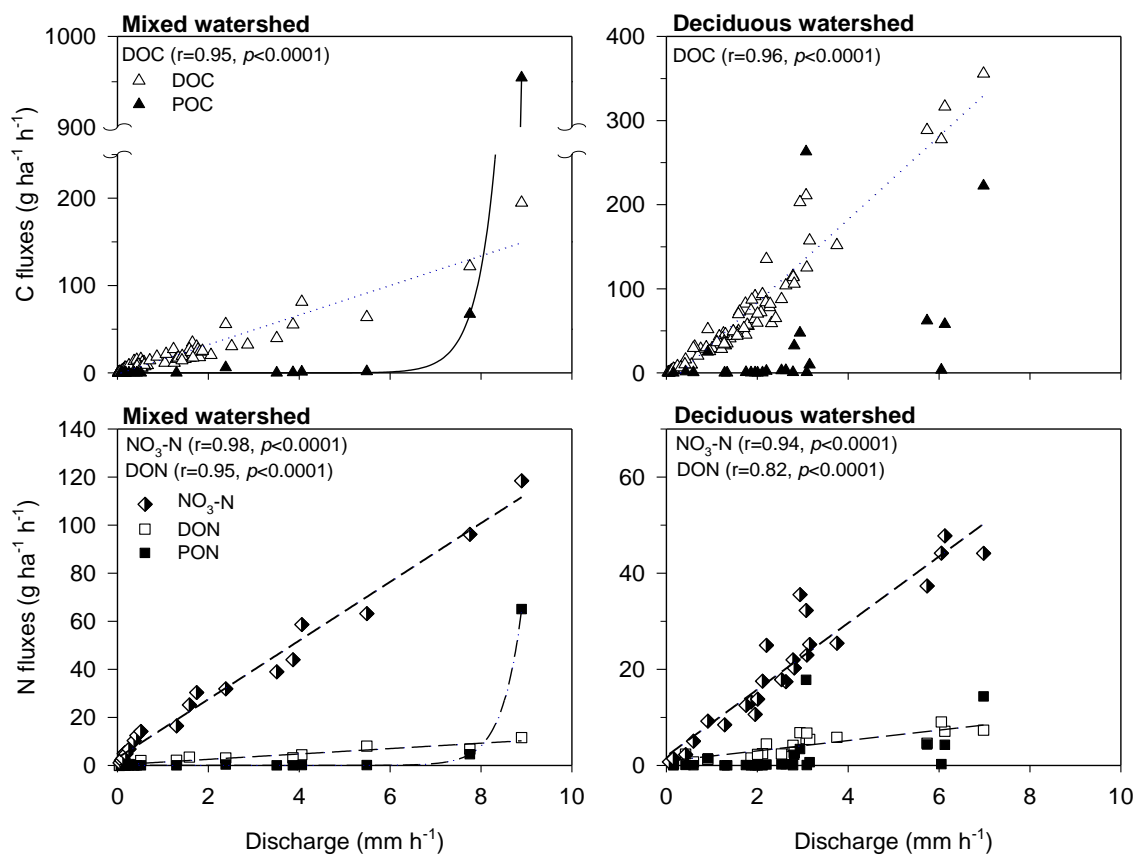


Figure 4.4. Fluxes of DOC, POC, DON, PON and NO₃-N in runoff with discharge during monsoon storm events.

Table 4.3. Total precipitation, total runoff and integrated fluxes of dissolved organic carbon (DOC) and nitrogen (DON), nitrate (NO₃-N), particulate organic carbon (POC) and nitrogen (PON) in June and July 2013.

Watershed	Period	Total precip. (mm)	Total runoff (mm)	DOC fluxes (kg C ha ⁻¹)	DON fluxes (kg N ha ⁻¹)	NO ₃ -N fluxes (kg N ha ⁻¹)	POC fluxes (kg C ha ⁻¹)	PON fluxes (kg N ha ⁻¹)
Mixed	June ^a	86.0	21.8	0.22	0.02	0.43	0.001	0.0001
	July ^b	508.0	380.7	6.74	0.26	5.20	2.220	0.1500
Deciduous	June ^a	70.5	52.4	0.85	0.10	0.52	0.010	0.0010
	July ^b	498.0	439.5	16.13	0.52	2.87	1.460	0.1100

precip.: precipitation

^a Before heavy storm events, from June 1st to June 30th, 2013.

^b Heavy storm events from July 1st to July 20th, 2013.

4.3.4. Chemical properties of DOM and POM in runoff

The chemical properties of DOM changed with increased discharge at the deciduous watershed, while no significant changes were observed at the mixed watershed (Figure 4.5). At the deciduous watershed, SUVA₂₈₀ and HIX_{em} increased with increased discharge, while PLF/FLF, PLF/HLF, $\delta^{13}\text{C}_{\text{DOC}}$ and $\delta^{15}\text{N}_{\text{TDN}}$ decreased.

At the mixed watershed, the ranges of the DOC/DON ratio, SUVA₂₈₀ and HIX_{em} in runoff were similar to those in throughfall and soil solution, while PLF/FLF and PLF/HLF in runoff corresponded more to those in forest floor percolates (Figure 4.6). In contrast, at the deciduous watershed, these parameters in runoff were closely related to the quality of forest floor leachates. Also, the ¹³C data in runoff, being more negative at the deciduous watershed, point to a larger proportion of forest floor leachates in runoff than at the coniferous watershed.

The patterns of DOC/DON ratios in response to discharge were also different at the two watersheds (Figure 4.3c). Large DOC/DON ratios at high discharge at the deciduous watershed resulted from the positive response of DOC concentration and the stable DON concentration to discharge. The DOC/DON ratios at the coniferous watershed were stable in response to discharge.

The range of the POC/PON ratio in runoff was similar to that of the POC/PON ratio of mineral soil layers at both watersheds (Figure 4.7). The same holds for the $\delta^{13}\text{C}_{\text{POC}}$ values. The $\delta^{15}\text{N}_{\text{PON}}$ in runoff had a huge variation, with averages being larger than those of the forest floor, but less than those of the mineral soil.

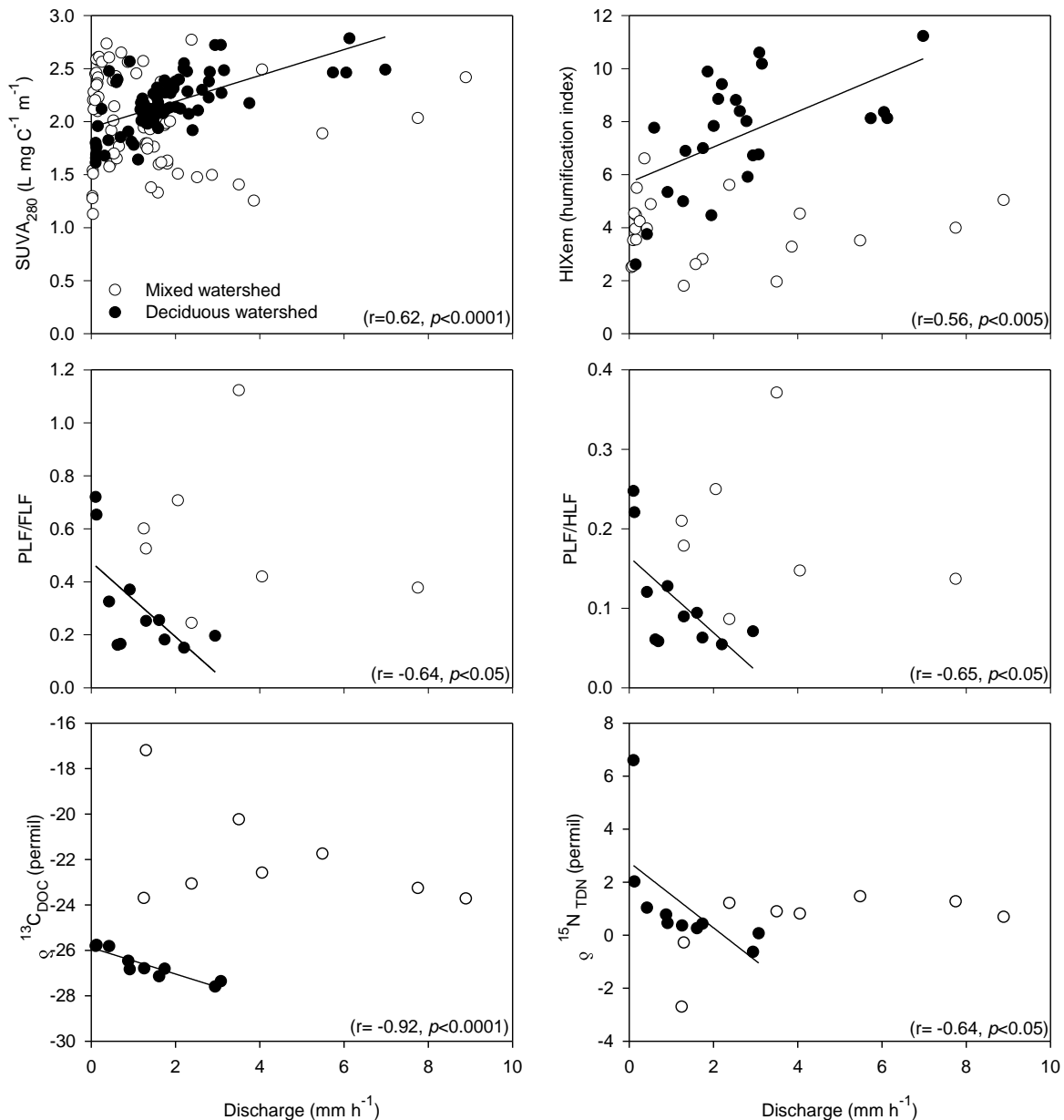


Figure 4.5. Specific ultraviolet absorbance (SUVA_{280}), humification index (HIXem), protein-like fluorescence/humic-like fluorescence (PLF/HLF), protein-like fluorescence/fulvic-like fluorescence (PLF/FLF), ^{13}C isotope abundance of dissolved organic carbon ($\delta^{13}\text{C}_{\text{DOC}}$) and ^{15}N isotope abundance of total dissolved nitrogen ($\delta^{15}\text{N}_{\text{TDN}}$) in runoff with discharge during monsoon storm events. Only significant regressions are shown.

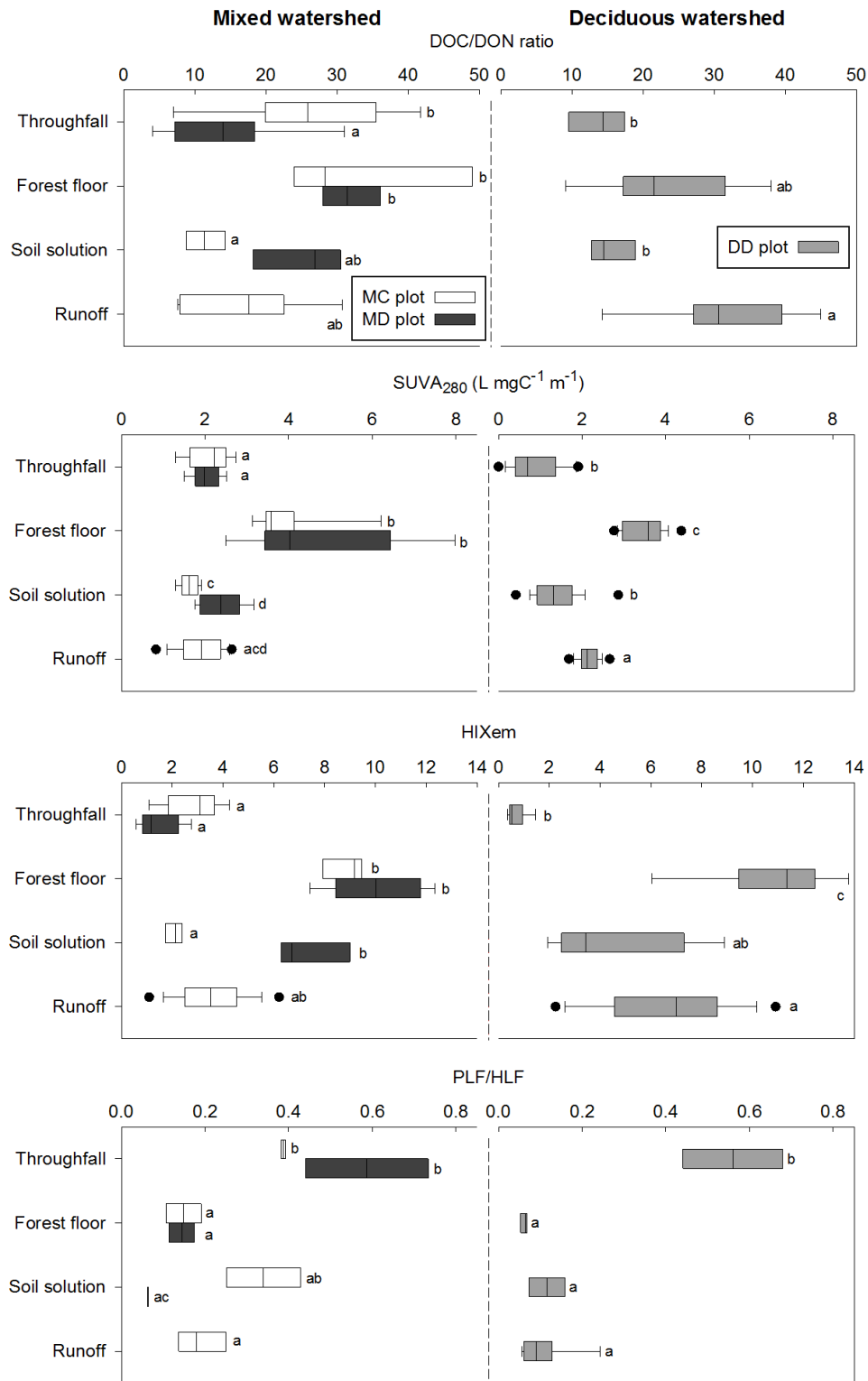


Figure 4.6. Range of dissolved organic carbon and nitrogen ratio (DOC/DON ratio), specific ultraviolet absorbance (SUVA₂₈₀), humification index (HIXem), and protein-like fluorescence/humic-like fluorescence (PLF/HLF) of throughfall, forest floor leachates, soil solution, and runoff during monsoon storm events. Box plots display minimum, lower quartile, median, upper quartile, maximum and outliers. Statistically significant differences between sample types (throughfall, forest floor leachates, soil solution, and runoff) are indicated by different letters in the box plots, significance level of $p < 0.05$.

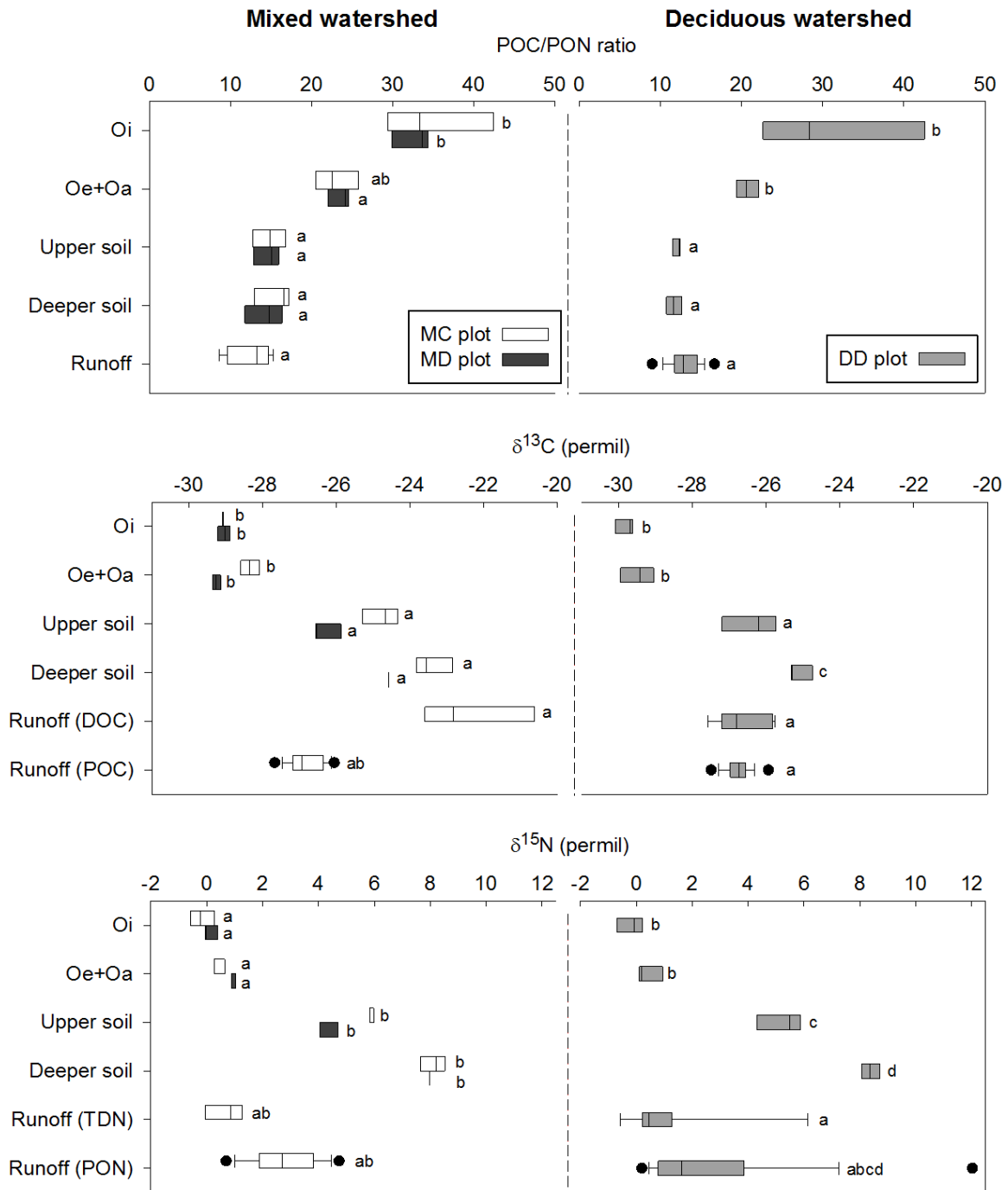


Figure 4.7. Range of particulate organic carbon and nitrogen ratio (POC/PON ratio), $\delta^{13}C$ and $\delta^{15}N$ in Oi, Oe+Oa, upper soil (0-10 cm depth), deeper soil (40-50 cm depth at the MC and MD plot, 30-40 cm depth at the DD plot), and runoff. Box plots display minimum, lower quartile, median, upper quartile, maximum and outliers. Statistically significant differences between sample types (Oi, Oe+Oa, upper soil, deeper soil, and runoff) are indicated by different letters in the box plots, significance level of $p < 0.05$.

4.4. Discussion

4.4.1. Different response of DOC to increased discharge at the mixed and the deciduous watershed

We intensively sampled 4 heavy rainfall events during the monsoon season, the events representing a substantial proportion of the annual precipitation in the region. While the number of events was rather small, consistent patterns emerged documenting the response of N and C fluxes to precipitation and discharge changes. The increase of DOC concentrations and fluxes in runoff induced by heavy storm events with increased discharge is consistent with the findings of previous studies (Dhillon and Inamdar, 2013; Jeong et al., 2012; Johnson et al., 2006; Lloret et al., 2013). In our study, the response to discharge and the integrated fluxes of DOC in runoff were much larger at the deciduous than at the mixed watershed. Similar to our results, larger annual DOC fluxes at a deciduous forested catchment than at a mixed coniferous catchment were reported by Amiotte-Suchet et al. (2007).

The different response of DOM in runoff to discharge between the two watersheds, such as the large response of runoff DOC concentration to discharge at the deciduous watershed (Figure 3a) and the significant change in runoff DOC quality parameters (Figure 5), are likely caused by a shift of hydrological flow paths to more surficial layers at the deciduous watershed. Also, the comparison of DOC quality parameters in runoff with those in forest floor leachates and soil solution at the deciduous watershed (Figure 6) indicated that a larger proportion of the DOC in runoff from forest floor leachates at the deciduous. Previous studies have also reported a positive relationships between discharge and DOM concentrations in runoff as a consequence of changing hydrologic flow paths from deeper soil to upper soil layers and forest floors at high discharge (Aitkenhead-Peterson et al., 2005; Bass et al., 2011; Sanderman et al., 2009). As several watershed characteristics (slope and soil textures) and the precipitation regime at both watersheds were similar, the differences between the watersheds are likely due to the tree species effects on the infiltration of precipitation water into the soil and on the mobilization of DOM. The tree species effect became obvious although the proportion of coniferous tree species was only 39% of the watershed area. Several processes might be involved to explain the tree species effect: i) In the deciduous litter layer the leaves are overlapping and partly impermeable, which may cause more surface near flow than in coniferous litter layers with relatively large pore spaces in

between needles. ii) The relatively higher level of hydrophobicity of coniferous forest floors compared to deciduous forest floors (Butzen et al., 2014) can result in less DOC release from coniferous forest floors. iii) The mobilization of DOC in soils depends on throughfall chemistry (Kalbitz et al., 2000). Throughfall at the MC plot was more acidic (pH 4.7 ± 0.4) and had a higher ionic strength ($15.9 \pm 11.3 \mu\text{S cm}^{-1}$) than at the DD plot (pH 6.1 ± 0.2 , $10.3 \pm 6.3 \mu\text{S cm}^{-1}$) and the MD plot (pH 5.8 ± 0.4 , $9.0 \pm 6.3 \mu\text{S cm}^{-1}$). Acidity and ionic strength are negatively related to DOC release from soils (Clark et al., 2011; Michalzik et al., 2001; Moldan et al., 2012). iv) In stream generation of DOC from litter might be involved (Johnson et al., 2006) if more leaf than needle litter enters the stream. v) As the deciduous watershed is located at a higher altitude the soils might generally be shallower than at the mixed watershed, which will add to the larger near surface flow paths under high precipitation. vi) Faster decomposition of the deciduous litter leaches relatively more DOM resulting in higher DOC export fluxes at the deciduous than at the mixed watershed. Based on our data set of this study, one cannot quantify the relative importance of these factors causing the differences between the watersheds.

4.4.2. Organic and inorganic nitrogen in runoff

At both watersheds, $\text{NO}_3\text{-N}$ was the dominant form of total N flux in runoff (Table 4.3). Several studies have reported that DON accounted for the dominant fraction of N flux in undisturbed forested watersheds (Alvarez-Cobelas et al., 2008; Frank et al., 2000; Kaushal and Lewis, 2003; Pellerin et al., 2006). Substantial fluxes of $\text{NO}_3\text{-N}$ and the dominance of $\text{NO}_3\text{-N}$ over DON in runoff are likely due to a certain degree of N-saturation (N supply > N demand) of these forested watersheds (Aber et al., 1998; Compton et al., 2003). Hence, the finding of the dominant $\text{NO}_3\text{-N}$ of total N flux implies that the N deposition in the area seems quite high (estimated between $24\text{-}51 \text{ kg N ha}^{-1} \text{ yr}^{-1}$; Berger et al., 2013). In July 2013, the integrated N flux in throughfall was however similar at the both watersheds (data not shown). Hence, the differences in N deposition between the two watersheds unlikely explain higher $\text{NO}_3\text{-N}$ fluxes in runoff at the mixed than at the deciduous watershed (Table 4.3). The C/N ratio of the forest floor was found to be a good indicator of $\text{NO}_3\text{-N}$ release with increasing fluxes at low C/N ratios (Borken and Matzner, 2004; MacDonald et al., 2002). However, the C/N ratio of the organic layer at the mixed watershed (20-28) was higher than at the deciduous watershed (19-21), which does not agree with the findings of MacDonald et al.

(2002). Overall, it seems that a larger N uptake by the deciduous trees at the deciduous watershed could explain the differences in the NO₃-N fluxes.

4.4.3. Particulate organic matter in runoff

The integrated fluxes of POC and PON during the study period were much less than those of the dissolved elements and did not differ significantly between the watersheds. POC and PON fluxes exceeded their dissolved fractions only for short time during heavy storm events with more than 100 mm precipitation except one storm event at the deciduous watershed on 2013 July 14 (Table 4.2). Previous studies in the nearby region considered 100 mm precipitation as a threshold that would induce large POC fluxes (Jeong et al., 2012; Jung et al., 2012). Our finding indicates that POM fluxes from forested watershed are unlikely regulated solely by precipitation amount, but slope and river bench characteristics will interfere. The small proportion of particulate fluxes in our study seems to be mainly caused by the relatively moderate precipitation events during the study period. The POC/PON ratios in runoff as well as the $\delta^{13}\text{C}_{\text{POC}}$ and $\delta^{15}\text{N}_{\text{PON}}$ were similar to those of the mineral soil and different to those of the forest floor. This indicates that the particulate matter originated from the erosion of mineral soil along the stream benches. Higher annual POC fluxes than DOC fluxes were observed in some mountainous forested watersheds (Kao and Liu, 1997; Kim et al., 2010; Lloret et al., 2013), which does not agree with our finding and some other studies (Dhillon and Inamdar, 2013; Inamdar et al., 2011; Jeong et al., 2012). The differences in findings may be related to the topography of forested watershed because steeper slopes induce higher fluxes of POC (Hilton et al., 2012; Janeau et al., 2014; Jung et al., 2012).

4.5. Conclusions

Our study emphasized the role of heavy precipitation events and vegetation cover for the export fluxes of particulate and dissolved organic C and N with runoff from forested watersheds. Our results suggest that changes of the precipitation regime, with more severe monsoon storms in the future as predicted, will increase the export of dissolved and particulate organic matter from these watersheds. The proportion of coniferous tree species at the mixed watershed was sufficient to induce less DOC fluxes and larger NO₃-N fluxes with runoff as compared to the deciduous watershed. Differences in the flow paths between the

watersheds are seen as the major trigger for the differences in runoff with a larger proportion of near surface flow at the deciduous watershed. A larger proportion of coniferous forests will likely lead to less inputs of organic carbon and larger inputs of inorganic nitrogen to the receiving surface water bodies.

Acknowledgements

This study was accomplished within the framework of the International Research Training Group TERRECO (GRK 1565/1) and funded by the German Research Foundation (Deutsche Forschungsgemeinschaft; DFG) at the University of Bayreuth and the Korean Research Foundation (KRF) at Kangwon National University. We acknowledge the BayCEER Laboratory of Isotope Biogeochemistry for the isotope abundance analysis and the Central Analytical Department of BayCEER for mineral-N measurement at the University of Bayreuth. We are grateful to other TERRECO colleagues for the comprehensive support and to Uwe Hell for the sampler installation of soil solution. We also appreciate the international collaboration with Bomchul Kim, Youngsoon Choi and Jaesung Eum from Kangwon National University (Chuncheon) and with Jin Hur and Bomi Lee from Sejong University (Seoul).

References

- Aber, J., McDowell, W., Nadelhoffer, K., Magill, A., Berntson, G., Kamakea, M., McNulty, S., Currie, W., Rustad, L., Fernandez, I., 1998. Nitrogen saturation in temperate forest ecosystems. *Biosci.* 48, 921–934. DOI: [10.2307/1313296](https://doi.org/10.2307/1313296)
- Aitkenhead-Peterson, J.A., Alexander, J.E., Clair, T.A., 2005. Dissolved organic carbon and dissolved organic nitrogen export from forested watersheds in Nova Scotia: Identifying controlling factors. *Global Biogeochem. Cycles* 19, 1–8. DOI: [10.1029/2004GB002438](https://doi.org/10.1029/2004GB002438)
- Alvarez-Cobelas, M., Angeler, D.G., Sánchez-Carrillo, S., 2008. Export of nitrogen from catchments: A worldwide analysis. *Environ. Pollut.* 156, 261–269. DOI: [10.1016/j.envpol.2008.02.016](https://doi.org/10.1016/j.envpol.2008.02.016)
- Amiotte-Suchet, P., Linglois, N., Leveque, J., Andreux, F., 2007. ¹³C composition of dissolved organic carbon in upland forested catchments of the Morvan Mountains (France): Influence of coniferous and deciduous vegetation. *J. Hydrol.* 335, 354–363. DOI: [10.1016/j.jhydrol.2006.12.002](https://doi.org/10.1016/j.jhydrol.2006.12.002)
- Baker, A., 2001. Fluorescence excitation–Emission matrix characterization of some sewage-impacted rivers. *Environ. Sci. Technol.* 35, 948–953. DOI: [10.1021/es000177t](https://doi.org/10.1021/es000177t)
- Bass, A.M., Bird, M.I., Liddell, M.J., Nelson, P.N., 2011. Fluvial dynamics of dissolved and particulate organic carbon during periodic discharge events in a steep tropical rainforest catchment. *Limnol. Oceanogr.* 56, 2282–2292. DOI: [10.4319/lo.2011.56.6.2282](https://doi.org/10.4319/lo.2011.56.6.2282)
- Bauer J.E., Bianchi T.S., 2011. Dissolved organic carbon cycling and transformation, in: Wolanski, E., McLusky, D.S. (Eds.), *Treatise on Estuarine and Coastal Science*, Vol. 5. Elsevier, pp. 7–67.
- Berger, S., Jung, E., Köpp, J., Kang, H., Gebauer, G., 2013. Monsoon rains, drought periods and soil texture as drivers of soil N₂O fluxes—Soil drought turns East Asian temperate deciduous forest soils into temporary and unexpectedly persistent N₂O sinks. *Soil Biol. Biochem.* 57, 273–281. DOI: [10.1016/j.soilbio.2012.09.026](https://doi.org/10.1016/j.soilbio.2012.09.026)
- Bianchi, T. S., 2011. The role of terrestrially derived organic carbon in the coastal ocean: A changing paradigm and the priming effect. *Proc. Natl. Acad. Sci.* 108, 19473–19481. DOI: [10.1073/pnas.1017982108](https://doi.org/10.1073/pnas.1017982108)
- Borken, W., Matzner, E., 2004. Nitrate leaching in forest soils: an analysis of long-term monitoring sites in Germany. *J. Plant Nutr. Soil Sci.* 167, 277–283. DOI: [10.1002/jpln.200421354](https://doi.org/10.1002/jpln.200421354)
- Butzen, V., Seeger, M., Wirtz, S., Huemann, M., Mueller, C., Casper, M., Ries, J. B., 2014. Quantification of Hortonian overland flow generation and soil erosion in a Central European low mountain range using rainfall experiments, *Catena* 113, 202–212. DOI: [10.1016/j.catena.2013.07.008](https://doi.org/10.1016/j.catena.2013.07.008)
- Camino-Serrano, M., Gielen, B., Luysaert, S., Ciais, P., Vicca, S., Guenet, B., de Vos, B., Cools, N., Ahrens, B., Arain, M.A., Borken, W., Clarke, N., Clarkson, B., Cummins, T., Don, A., Pannatier, E.G., Laudon, H., Moore, T., Nieminen, T.M., Nilsson, M.B., Peichl, M., Schwendenmann, L., Siemens, J., Janssens, I., 2014. Linking variability in

- soil solution dissolved organic carbon to climate, soil type, and vegetation type. *Global Biogeochem. Cycles* 28, 497–509. DOI: [10.1002/2013GB004726](https://doi.org/10.1002/2013GB004726)
- Canham, C.D., Pace, M.L., Weathers, K.C., McNeil, E.W., Bedford, B.L., Murphy, L., Quinn, S., 2012. Nitrogen deposition and lake nitrogen concentrations: a regional analysis of terrestrial controls and aquatic linkages. *Ecosphere* 3, 66. DOI: [10.1890/ES12-00090.1](https://doi.org/10.1890/ES12-00090.1)
- Chen, Z., Hu, C., Conmy, R. N., Muller-Karger, F., Swarzenski, P., 2007. Colored dissolved organic matter in Tampa Bay, Florida. *Mar. Chem.* 104, 98–109. DOI: [10.1016/j.marchem.2006.12.007](https://doi.org/10.1016/j.marchem.2006.12.007)
- Clark, J.M., Van Der Heijden, G.M.F., Palmer, S.M., Chapman, P.J., Bottrell, S.H., 2011. Variation in the sensitivity of DOC release between different organic soils following H₂SO₄ and sea-salt additions. *Eur. J. Soil Sci.* 62, 267–284. DOI: [10.1111/j.1365-2389.2010.01344.x](https://doi.org/10.1111/j.1365-2389.2010.01344.x)
- Compton, J.E., Church, M.R., Larned, S.T., Hogsett, W.E., 2003. Nitrogen export from forested watersheds in the oregon coast range: The role of N₂-fixing Red alder. *Ecosystems* 6, 773–785. DOI: [10.1007/s10021-002-0207-4](https://doi.org/10.1007/s10021-002-0207-4)
- Dhillon, G. S. and Inamdar, S.: Extreme storms and changes in particulate and dissolved organic carbon in runoff: Entering uncharted waters?, *Geophys. Res. Lett.*, 40(7), 1322–1327, doi:10.1002/grl.50306, 2013.
- Don, A., Kalbitz, K., 2005. Amounts and degradability of dissolved organic carbon from foliar litter at different decomposition stages. *Soil Biol. Biochem.* 37, 2171–2179. DOI: [10.1016/j.soilbio.2005.03.019](https://doi.org/10.1016/j.soilbio.2005.03.019)
- FAO (Food and Agriculture Organization of the United Nations), 2014. World reference base for soil resources 2014 international soil classification system for naming soils and creating legends for soil maps. FAO, Rome.
- Fellman, J.B., Hood, E., Spencer, R.G.M., 2010. Fluorescence spectroscopy opens new windows into dissolved organic matter dynamics in freshwater ecosystems: A review. *Limnol. Oceanogr.* 55, 2452–2462. DOI: [10.4319/lo.2010.55.6.2452](https://doi.org/10.4319/lo.2010.55.6.2452)
- Frank, H., Patrick, S., Peter, W., Hannes, F., 2000. Export of dissolved organic carbon and nitrogen from Gleysol dominated catchments—The significance of water flow paths. *Biogeochem.* 50, 137–161. DOI: [10.1023/A:1006398105953](https://doi.org/10.1023/A:1006398105953)
- Hansson, K., Olsson, B.A., Olsson, M., Johansson, U., Kleja, D.B., 2011. Differences in soil properties in adjacent stands of Scots pine, Norway spruce and silver birch in SW Sweden. *For. Ecol. Manage.* 262, 522–530. DOI: [10.1016/j.foreco.2011.04.021](https://doi.org/10.1016/j.foreco.2011.04.021)
- Hilton, R.G., Galy, A., Hovius, N., Kao, S.-J., Horng, M.-J., Chen, H., 2012. Climatic and geomorphic controls on the erosion of terrestrial biomass from subtropical mountain forest. *Global Biogeochem. Cycles* 26, GB3014, DOI: [10.1029/2012GB004314](https://doi.org/10.1029/2012GB004314)
- Hur, J., Cho, J., 2012. Prediction of BOD, COD, and total nitrogen concentrations in a typical urban river using a fluorescence excitation-emission matrix with PARAFAC and UV Absorption Indices. *Sensors* 12, 972–986. DOI: [10.3390/s120100972](https://doi.org/10.3390/s120100972)
- Inamdar, S., Singh, S., Dutta, S., Levia, D., Mitchell, M., Scott, D., Bais, H., McHale, P., 2011. Fluorescence characteristics and sources of dissolved organic matter for stream

- water during storm events in a forested mid-Atlantic watershed. *J. Geophys. Res.* 116, G03043. DOI: [10.1029/2011JG001735](https://doi.org/10.1029/2011JG001735)
- Inamdar, S., Dhillon, G., Singh, S., Parr, T., Qin, Z., 2015. Particulate nitrogen exports in stream runoff exceed dissolved nitrogen forms during large tropical storms in a temperate, headwater, forested watershed. *J. Geophys. Res.* 120, 1548–1566. DOI: [10.1002/2015JG002909](https://doi.org/10.1002/2015JG002909)
- IPCC (Intergovernmental Panel on Climate Change), 2013. Summary for Policymakers, in: Stocker, T.F., Qin, D., Plattner, G.-K., Tignor, M., Allen, S.K., Doschung, J., Nauels, A., Xia, Y., Bex, V., Midgley, P.M. (Eds.), *Climate Change 2013–The Physical Science Basis*. Cambridge University Press, pp. 1–30.
- Janeau, J.-L., Gillard, L.-C., Grellier, S., Jouquet, P., Le, T.P.Q., Luu, T.N.M., Ngo, Q.A., Orange, D., Pham, D.R., Tran, D.T., Tran, S.H., Trinh, A.D., Valentin, C., Rochelle-Newall, E., 2014. Soil erosion, dissolved organic carbon and nutrient losses under different land use systems in a small catchment in northern Vietnam. *Agric. Water Manag.* 146, 314–323. DOI: [10.1016/j.agwat.2014.09.006](https://doi.org/10.1016/j.agwat.2014.09.006)
- Jeong, J.J., Bartsch, S., Fleckenstein, J.H., Matzner, E., Tenhunen, J.D., Lee, S.D., Park, S.K., Park, J.-H., 2012. Differential storm responses of dissolved and particulate organic carbon in a mountainous headwater stream, investigated by high-frequency, in situ optical measurements. *J. Geophys. Res.* 117, 1–13. DOI: [10.1029/2012JG001999](https://doi.org/10.1029/2012JG001999)
- Johnson, M.S., Lehmann, J., Selva, E.C., Abdo, M., Riha, S., Couto, E.G., 2006. Organic carbon fluxes within and streamwater exports from headwater catchments in the southern Amazon. *Hydrol. Process.* 20, 2599–2614. DOI: [10.1002/hyp.6218](https://doi.org/10.1002/hyp.6218)
- Jung, B.J., Lee, H.J., Jeong, J.J., Owen, J., Kim, B., Meusbürger, K., Alewell, C., Gebauer, G., Shope, C., Park, J.-H., 2012. Storm pulses and varying sources of hydrologic carbon export from a mountainous watershed. *J. Hydrol.* 440–441, 90–101. DOI: [10.1016/j.jhydrol.2012.03.030](https://doi.org/10.1016/j.jhydrol.2012.03.030)
- Jung, B.-J., Jeanneau, L., Alewell, C., Kim, B., Park, J.-H., 2015. Downstream alteration of the composition and biodegradability of particulate organic carbon in a mountainous, mixed land-use watershed. *Biogeochem.* 122, 79–99. DOI: [10.1007/s10533-014-0032-9](https://doi.org/10.1007/s10533-014-0032-9)
- Kalbitz, K., Solinger, S., Park, J.-H., Michalzik, B., Matzner, E., 2000. Controls on the dynamics of dissolved organic matter in soils: a review. *Soil Sci.* 165, 277–304. DOI: [10.1097/00010694-200004000-00001](https://doi.org/10.1097/00010694-200004000-00001)
- Kao, S.-J., Liu, K.-K., 1997. Fluxes of dissolved and nonfossil particulate organic carbon from an Oceania small river (Lanyang Hsi) in Taiwan. *Biogeochem.* 39, 255–269. DOI: [10.1023/A:1005864605382](https://doi.org/10.1023/A:1005864605382)
- Katsuyama, M., Ohte, N., 2002. Determining the sources of stormflow from the fluorescence properties of dissolved organic carbon in a forested headwater catchment. *J. Hydrol.* 268, 192–202. DOI: [10.1016/S0022-1694\(02\)00175-0](https://doi.org/10.1016/S0022-1694(02)00175-0)
- Kaushal, S.S., Lewis, W.M., 2003. Patterns in the chemical fractionation of organic nitrogen in Rocky Mountain streams. *Ecosystems* 6, 483–492. DOI: [10.1007/s10021-003-0175-3](https://doi.org/10.1007/s10021-003-0175-3)

- Kiikkilä, O., Smolander, A., Kitunen, V., 2013. Degradability, molecular weight and adsorption properties of Dissolved Organic Carbon and nitrogen leached from different types of decomposing litter. *Plant Soil* 373, 787–798. DOI: [10.1007/s11104-013-1837-3](https://doi.org/10.1007/s11104-013-1837-3)
- Kim, S.J., Kim, J., Kim, K., 2010. Organic carbon efflux from a deciduous forest catchment in Korea. *Biogeosci.* 7, 1323–1334. DOI: [10.5194/bg-7-1323-2010](https://doi.org/10.5194/bg-7-1323-2010)
- Korea Forest Research Institute, 2013. Distribution of main tree species in South Korea–1:5 000 based on the map of forest type. Available from: http://www.forest.go.kr/newkfsweb/html/HtmlPage.do?pg=/fgis/UI_KFS_5002_020100.html&mn=KFS_02_04_03_04_01&orgId=fgis (accessed 18.09.2016)
- KMA (Korea Meteorological Administration), 2016. Available from <http://web.kma.go.kr/> (accessed 12.06.2016)
- Lee, J.-Y., Kim, J.-K., Owen, J. S., Choi, Y., Shin, K., Jung, S., Kim, B., 2013. Variation in carbon and nitrogen stable isotopes in POM and zooplankton in a deep reservoir and relationship to hydrological characteristics. *J. Freshw. Ecol.* 28, 47–62. DOI: [10.1080/02705060.2012.689999](https://doi.org/10.1080/02705060.2012.689999)
- Lloret, E., Dessert, C., Pastor, L., Lajeunesse, E., Crispi, O., Gaillardet, J., Benedetti, M.F., 2013. Dynamic of particulate and dissolved organic carbon in small volcanic mountainous tropical watersheds. *Chem. Geol.* 351, 229–244. DOI: [10.1016/j.chemgeo.2013.05.023](https://doi.org/10.1016/j.chemgeo.2013.05.023)
- MacDonald, J.A., Dise, N.B., Matzner, E., Armbruster, M., Gundersen, P., Forsius, M., 2002. Nitrogen input together with ecosystem nitrogen enrichment predict nitrate leaching from European forests. *Glob. Chang. Biol.* 8, 1028–1033. DOI: [10.1046/j.1365-2486.2002.00532.x](https://doi.org/10.1046/j.1365-2486.2002.00532.x)
- McGlynn, B.L., McDonnell, J.J., 2003. Role of discrete landscape units in controlling catchment dissolved organic carbon dynamics. *Water Resour. Res.* 39, 1090. DOI: [10.1029/2002WR001525](https://doi.org/10.1029/2002WR001525)
- Michalzik, B., Kalbitz, K., Park, J.-H., Solinger, S., Matzner, E., 2001. Fluxes and concentrations of dissolved organic carbon and nitrogen—A synthesis for temperate forests, *Biogeochem.* 52, 173–205. DOI: [10.1023/A:1006441620810](https://doi.org/10.1023/A:1006441620810)
- Moldan, F., Hruška, J., Evans, C.D., Hauhs, M., 2012. Experimental simulation of the effects of extreme climatic events on major ions, acidity and dissolved organic carbon leaching from a forested catchment, Gårdsjön, Sweden. *Biogeochem.* 107, 455–469. DOI: [10.1007/s10533-010-9567-6](https://doi.org/10.1007/s10533-010-9567-6)
- Park, J.-H., Duan, L., Kim, B., Mitchell, M.J., Shibata, H., 2010. Potential effects of climate change and variability on watershed biogeochemical processes and water quality in Northeast Asia. *Environ. Int.* 36, 212–225. DOI: [10.1016/j.envint.2009.10.008](https://doi.org/10.1016/j.envint.2009.10.008)
- Pellerin, B.A., Kaushal, S.S., McDowell, W.H., 2006. Does anthropogenic nitrogen enrichment increase organic nitrogen concentrations in runoff from forested and human-dominated watersheds?. *Ecosystems* 9, 852–864. DOI: [10.1007/s10021-006-0076-3](https://doi.org/10.1007/s10021-006-0076-3)
- Richey, J.E., 2005. Global River Carbon Biogeochemistry, in: Anderson, M.G. (Ed.), *Encyclopedia of Hydrological Sciences*. John Wiley & Sons Ltd, pp. 1–13.

- Sanderman, J., Lohse, K.A., Baldock, J.A., Amundson, R., 2009. Linking soils and streams: Sources and chemistry of dissolved organic matter in a small coastal watershed. *Water Resour. Res.* 45, W03418. DOI: [10.1029/2008WR006977](https://doi.org/10.1029/2008WR006977)
- Seo, K.-H., Son, J.-H., Lee, J.-Y., 2011. A new look at Changma. *Atmos.* 21, 109–121. (in Korean)
- Singh, S., Inamdar, S., Mitchell, M., McHale, P., 2014. Seasonal pattern of dissolved organic matter (DOM) in watershed sources: influence of hydrologic flow paths and autumn leaf fall. *Biogeochem.* 118, 321–337. DOI: [10.1007/s10533-013-9934-1](https://doi.org/10.1007/s10533-013-9934-1)
- Singh, S., Inamdar, S., Mitchell, M., 2015. Changes in dissolved organic matter (DOM) amount and composition along nested headwater stream locations during baseflow and stormflow. *Hydrol. Process.* 29, 1505–1520. DOI: [10.1002/hyp.10286](https://doi.org/10.1002/hyp.10286)
- Smolander, A., Kitunen, V., 2011. Comparison of tree species effects on microbial C and N transformations and dissolved organic matter properties in the organic layer of boreal forests. *Appl. Soil Ecol.* 49, 224–233. DOI: [10.1016/j.apsoil.2011.05.002](https://doi.org/10.1016/j.apsoil.2011.05.002)
- Trum, F., Titeux, H., Ranger, J., Delvaux, B., 2011. Influence of tree species on carbon and nitrogen transformation patterns in forest floor profiles. *Ann. For. Sci.* 68, 837–847. DOI: [10.1007/s13595-011-0080-4](https://doi.org/10.1007/s13595-011-0080-4)
- von Schiller, D., Graeber, D., Ribot, M., Timoner, X., Acuña, V., Martí, E., Sabater, S., Tockner, K., 2015. Hydrological transitions drive dissolved organic matter quantity and composition in a temporary Mediterranean stream. *Biogeochem.* 123, 1–18. DOI: [10.1007/s10533-015-0077-4](https://doi.org/10.1007/s10533-015-0077-4)
- Yates, C.A., Johnes, P.J., 2013. Nitrogen speciation and phosphorus fractionation dynamics in a lowland Chalk catchment. *Sci. Total Environ.* 444, 466–479. DOI: [10.1016/j.scitotenv.2012.12.002](https://doi.org/10.1016/j.scitotenv.2012.12.002)
- Zsolnay, A., Baigar, E., Jimenez, M., Steinweg, B., Saccomandi, F., 1999. Differentiating with fluorescence spectroscopy the sources of dissolved organic matter in soils subjected to drying. *Chemosphere* 38, 45–50. DOI: [10.1016/S0045-6535\(98\)00166-0](https://doi.org/10.1016/S0045-6535(98)00166-0)

Appendix

List of additional contributions

Payeur-Poirier, J.-L., Nguyen, T. T., 2017. The Inclusion of Forest Hydrological Services in the Sustainable Development Strategy of South Korea. *Sustainability* 9, 1470. DOI: [10.3390/su9081470](https://doi.org/10.3390/su9081470).

Payeur-Poirier, J.-L., Hopp, L., Peiffer, S., 2015. The hydrological behaviour of a forested catchment during two contrasting summer monsoon seasons. *Geophysical Research Abstracts* 17, EGU2015–10041.

Payeur-Poirier, J.-L., Hopp, L., Peiffer, S., 2015. Water flow paths in a forested catchment of the East Asian monsoon region. *Geophysical Research Abstracts* 17, EGU2015–10187.

Payeur-Poirier, J.-L., Hopp, L., Peiffer, S., 2014. Water sources and flow paths in a forested catchment of the East Asian monsoon region. *Poster Proceedings of FRIEND-Water 2014*, 106–107.

Protocol for the collection and storage of water samples

Important notice: This protocol is intended for the collection and storage of stream water, soil water, throughfall and precipitation samples from, respectively, small streams, suction lysimeters and passive throughfall and precipitation collectors, followed by the analysis of chemical quality (electrical conductivity (EC) and the concentrations of calcium (Ca^{2+}), magnesium (Mg^{2+}), potassium (K^+), sodium (Na^+), chloride (Cl^-), nitrate (NO_3^-), sulphate (SO_4^{2-}) and silica (SiO_2)) and isotopic abundance ($\delta^2\text{H}$ and $\delta^{18}\text{O}$). The design of the passive throughfall and precipitation collectors includes a valve for the collection of samples. The design of the suction lysimeters includes a valve for the entry of air and one for the collection of water. Most of the contents of this protocol were inspired and derived from Bartram and Balance (1996), CCME (2011), Curley et al. (2011), Lane et al. (2003), U.S. Geological Survey (2006), Wilde (2004), Wilde (2005) and WMO (2008).

Preparation of equipment and bottles

- Equipment and bottles must be made of fluorocarbon polymers or polypropylene or polyethylene or polyvinyl chloride (PVC) or nylon (high density plastic). Not metal nor rubber.
- For the sampling of water followed by the analysis of isotopic abundance, equipment and bottles can also be made of glass.
- Bottles must have a volume of at least: 15 ml for the sampling of water followed by the analysis of chemical quality, 1.5 ml for the sampling of water followed by the analysis of isotopic abundance. Bottles must have hermetic sealing caps.
- Brushes must be uncolored.
- Sealable plastic bags must have uncolored closure strips.
- Washbasins must be white or uncolored.
- Deionized water (DIW) must have a maximum specific conductance of $1 \mu\text{S cm}^{-1}$.
- “Equipment and bottles should be cleaned in an area protected from airborne or other sources of contamination.” (U.S. Geological Survey, 2006)
- When cleaning and handling equipment and bottles, disposable, powderless gloves must be worn.

1. Verify equipment and bottle supplies. Inspect equipment and bottles for stains, cuts, or abrasions, even if they were never used. Replace as needed.
2. Prepare a contaminant-free space for cleaning and drying the equipment and bottles, with clean plastic sheeting over the work surface.
3. Rinse the inside of a washbasin with tap water until no particles are visible. Scrubbing with soft scrub brushes may be necessary to remove particles.
4. Fill the washbasin with equipment and bottles and then fill the washbasin with tap water.
5. Let the equipment and bottles soak for at least 2 hours. At least twice during the soaking period, put on disposable, powderless gloves and “mix” the equipment and bottles through the water for at least 15 seconds.
6. Empty the water from the washbasin. Repeat steps number 4, 5, and 6, once.

7. Put on disposable, powderless gloves.
8. Using a laboratory bottle with a squirting straw, rinse the interior of each individual piece of equipment and bottle with DIW water.
9. “Allow equipment and bottles to air-dry in an area free from potential airborne contaminants” (U.S. Geological Survey, 2006), preferably on the plastic sheeting.
10. Once dry, re-assemble equipment and bottles (caps on bottles) and store in sealable plastic bags.
11. Discard gloves.

Preparation for water sampling

- “The work plan delineates study activities and establishes the timeframe in which the activities are to be completed.” (U.S. Geological Survey, 2006)

1. Before heading out for the sampling site (if possible, the preceding day), write a work plan under the form of a checklist, which can also be used while gathering and preparing the required material such as equipment and bottles. Take the sampling frequency and weather forecast into account when writing the work plan. If *in situ* measurements are to be made, test the measuring devices.
2. Print all required forms.
3. Inform someone of your work plan.

Sampling of throughfall and precipitation

- Evaporation modifies the isotopic abundance of water, and therefore all precautions should be taken to minimize it.
- If it is raining at sampling time, all of the sampling procedures should be realized under shelter from precipitation.
- If oil is used in the passive collectors, be careful not to include it in the samples.
- Do not allow the sampled water to contact hands, even with gloves on.

1. Before heading out to the field, review the work plan.
2. Once at the sampling site, prepare the required equipment for sampling, including the field form(s). The bottles must be the last thing to be prepared.
3. Put on disposable, powderless gloves.
4. First, collect the sample for the analysis of isotopic abundance:
 - a. Flush the tubing at the bottom of the collector by quickly opening and closing the valve, letting some water flow through.
 - b. Connect a syringe to the valve. Open the valve, and collect more than 1.5 ml of water in the syringe. Close the valve.
 - c. Open the bottle and fill with water directly from the syringe. Fill the bottle to the brim.

- d. Immediately close the bottle and check if it contains any large air bubble and/or particle. If so, empty the bottle, rinse it (with DIW or water to be sampled), and repeat the sampling procedure.
 - e. Fill the bottle label and sampling form.
 - f. Store the bottle in a sealable plastic bag.
5. Second, collect the sample for the analysis of chemical quality:
 - a. If water is left in the syringe following the sampling for the analysis of isotopic abundance, empty it in the bottle.
 - b. If not, or if not enough is left, connect the syringe to the valve. Open the valve, and collect more than 15 ml of water in the syringe. Close the valve.
 - c. Open the bottle and fill with water directly from the syringe.
 - d. Immediately close the bottle.
 - e. Fill the bottle label and sampling form.
 - f. Store the bottle in a sealable plastic bag.
 - g. Discard the syringe (it can be washed and used again).
 6. If any other measurement must be made (e.g. temperature, electrical conductivity, etc.), make it following water sampling with water left in the collector.
 7. Empty the collector in a measuring cylinder and record water volume, taking into account the volume used for flushing and sampling.
 8. Using a laboratory bottle with a squirting straw, thoroughly rinse the interior of the collector and funnel with DIW water until no particles are visible. Scrubbing with soft scrub brushes may be necessary to remove particles and/or biofilms. Thoroughly empty the collector of any remaining water.
 9. Replace the collector at level.
 10. Discard gloves.

Sampling of stream water – grab

- “Samples may be collected at a single vertical at the centroid of streamflow if the section is known to be well mixed laterally and vertically with respect to concentrations of target analytes.” (U.S. Geological Survey, 2006). The centroid of streamflow is the point at which stream discharge is equal on either side of the vertical. At the outfall of the catchment, samples must be collected in the V-notch of the weir.
- Evaporation modifies the isotopic abundance of water, and therefore all precautions should be taken to minimize it.
- If the water depth is low, a suggestion is to dig a hole in the streambed, let the stream settle, and sample down to the top of the hole.
- Do not allow the sampled water to contact hands, even with gloves on.
- If it is raining at sampling time, all of the sampling procedures should be realized under shelter from precipitation.

1. Before heading out to the field, review the work plan.
2. Once at the sampling site, prepare the required equipment for sampling, including the field form(s). The bottles must be the last thing to be prepared.

3. Put on disposable, powderless gloves. After putting the gloves on, rinse them in water while gently rubbing hands together to remove any surface residue.
4. Partially fill and rinse the bottles with the water to be sampled (rinse water). To avoid suspended sand particles entering the bottles, collect water for rinsing at the edge of the stream in an area of low-flow turbidity, or in the V-notch of the weir. If further equipment is used for sampling, rinse it as well. Repeat the rinsing procedure once.
5. With the sample bottles in hand, wade to the centroid of streamflow, trying not to disturb the streambed. Place yourself facing upstream.
6. First, collect the sample for the analysis of isotopic abundance:
 - a. Open the bottle.
 - b. At the center of streamflow, or in the V-notch of the weir, quickly lower the bottle to the centroid of streamflow, with the bottle opening facing upstream.
 - c. Let the bottle fill to the brim.
 - d. Remove the bottle from the stream and close the bottle. Check if it contains any large air bubble and/or particle. If so, empty the bottle, rinse it (with DIW or water to be sampled), and repeat the sampling procedure.
 - e. Fill the bottle label and sampling form.
 - f. Store the bottle in a sealable plastic bag.
7. Second, collect the sample for the analysis of chemical quality following step 6. The bottle can contain air bubbles and/or particles.
8. If any other measurement must be made (e.g. stage, temperature, electrical conductivity, etc.), make it in the stream following water sampling.
9. Discard gloves.

Sampling of stream water – autosampler

- Evaporation modifies the isotopic concentration of water, and therefore all precautions should be taken to minimize it.
- Do not allow the sampled water to contact hands, even with gloves on.
- If it is raining at sampling time, all of the sampling procedures should be realized under shelter from precipitation.

1. Before heading out to the field, review the work plan. The work plan should be set so that the collection of samples from the autosampler occurs shortly after the sampling cycle of the autosampler is over.
2. Once at the sampling site, prepare the required equipment for sampling, including the field form(s). The bottles must be the last thing to be prepared.
3. Remove the upper part of the autosampler.
4. Put on disposable, powderless gloves. After putting the gloves on, rinse them in water while gently rubbing hands together to remove any surface residue.
5. Collect the samples for the analysis of chemical quality and isotopic abundance:

- a. Take a bottle from the autosampler. You may close its opening with your hand and shake it to mix the sampled water.
 - b. Open the bottle of the sample for the analysis of isotopic abundance and fill it to the brim by pouring water directly from the autosampler bottle.
 - c. Close the bottle of the sample for the analysis of isotopic abundance. Check if it contains any large air bubble and/or particle. If so, empty the bottle, rinse it (with DIW or water to be sampled), and repeat the sampling procedure.
 - d. Open the bottle of the sample for the analysis of chemical quality and fill it by pouring water directly from the autosampler bottle.
 - e. Close the bottle of the sample for the analysis of chemical quality.
 - f. Fill the bottle labels and sampling form.
 - g. Store the bottles in a sealable plastic bag.
 - h. Repeat the sampling procedures for all bottles of the autosampler.
 - i. Rinse all bottles of the autosampler with DIW.
6. If water is present in the bottom part of the autosampler, empty it.
 7. Replace the upper part of the autosampler.
 8. Discard gloves.

Sampling of soil water

- Evaporation modifies the isotopic concentration of water, and therefore all precautions should be taken to prevent it.
- Do not allow the sampled water to contact hands, even with gloves on.
- This protocol is intended for the collection of water from suction lysimeters which have two valves, one for the entry of air (labelled “AIR”) and one for the collection of water (labelled “H²O”).

1. Before heading out to the field, review the work plan.
2. Once at the sampling site, prepare the required equipment for sampling, including the field form(s). The bottles must be the last thing to be prepared.
3. Put on disposable, powderless gloves.
4. First, collect the sample for the analysis of isotopic abundance:
 - a. Connect a syringe to the valve of the lysimeter labeled “H²O”. Open the valve.
 - b. Open the valve of the lysimeter labeled “AIR”.
 - c. Fill the syringe with water from the lysimeter. Close the “H²O” valve and remove the syringe.
 - d. Open the bottle and fill it with water directly from the syringe. Fill the bottle to the brim.
 - e. Immediately close the bottle and check if it contains any large air bubble and/or particle. If so, empty the bottle, rinse it (with DIW), and repeat the sampling procedure.
 - f. Fill the bottle label and sampling form.
 - g. Store the bottle in a sealable plastic bag.
5. Second, collect the sample for the analysis of chemical quality:
 - a. If water is left in the syringe following the sampling for the analysis of isotopic abundance, empty it in the bottle.

- b. If not, or if not enough is left, connect the syringe to the “H²O” valve. Open the valve, and fill the syringe with water from the lysimeter. Close the “H²O” valve and remove the syringe.
- c. Open the bottle and fill it with water directly from the syringe.
- d. Immediately close the bottle.
- e. Fill the bottle label and sampling form.
- f. Store the bottle in a sealable plastic bag.
- g. Empty the lysimeter of water.
- h. Discard the syringe (it can be washed and used again).
- i. Connect a syringe to the “AIR” valve. Remove air from the lysimeter in order to create a negative pressure. Close the valve. Repeat if necessary.

6. Discard gloves.

Storage of water samples

- Evaporation modifies the isotopic concentration of water, and therefore all precautions should be taken to prevent it.
- Samples should be stored in an area protected from airborne or other sources of contamination.
- The samples must never be frozen.

1. Once collected, the samples should be either analysed as soon as possible or stored in a dark environment at ~4 °C, until analyses. Parafilm can be wrapped around the cap of the bottles to even more prevent evaporation.
2. If additional measurements are required (e.g. electrical conductivity), they should be realized before the samples are stored. It is important to thoroughly rinse measuring probes with DIW between samples.
3. Bottle labels should be protected from water by applying a piece of scotch tape over.
4. All information should be saved in sampling forms and/or files. The sampling forms should be kept and stored.

References

- Bartram, J., Ballance, R. (Eds.), 1996. Water quality monitoring: a practical guide to the design and implementation of freshwater quality studies and monitoring programmes. CRC Press, Boca Raton.
- CCME (Canadian Council of Ministers of the Environment), 2011. Protocols manual for water quality sampling in Canada. CCME, Ottawa.
- Curley, E., O’Flynn, M., McDonnell, K., 2011. The use of porous ceramic cups for sampling soil pore water from the unsaturated zone. *Int. J. Soil Sci.* 6, 1–11. DOI: [10.3923/ijss.2011.1.11](https://doi.org/10.3923/ijss.2011.1.11)
- Lane, S.L., Flanagan, S., Wilde, F.D., 2003. Selection of equipment for water sampling (ver. 2.0): U.S. Geological Survey Techniques of Water-Resources Investigations, book 9, chap. A2. U.S. Geological Survey, Reston.
- U.S. Geological Survey, 2006. Collection of water samples (ver. 2.0): U.S. Geological Survey Techniques of Water-Resources Investigations, book 9, chap. A4. U.S. Geological Survey, Reston.
- Wilde, F.D. (Ed.), 2004. Cleaning of Equipment for water sampling (ver. 2.0): U.S. Geological Survey Techniques of Water-Resources Investigations, book 9, chap. A3. U.S. Geological Survey, Reston.

- Wilde, F.D., 2005. Preparations for water sampling: U.S. Geological Survey Techniques of Water-Resources Investigations, book 9, chap. A1. U.S. Geological Survey, Reston.
- WMO (World Meteorological Organization), 2008. Guide to Hydrological Practices Volume I. Hydrology–From Measurement to Hydrological Information, sixth ed. WMO-No. 168. WMO, Geneva.

Guidelines for the installation of a V-notch weir

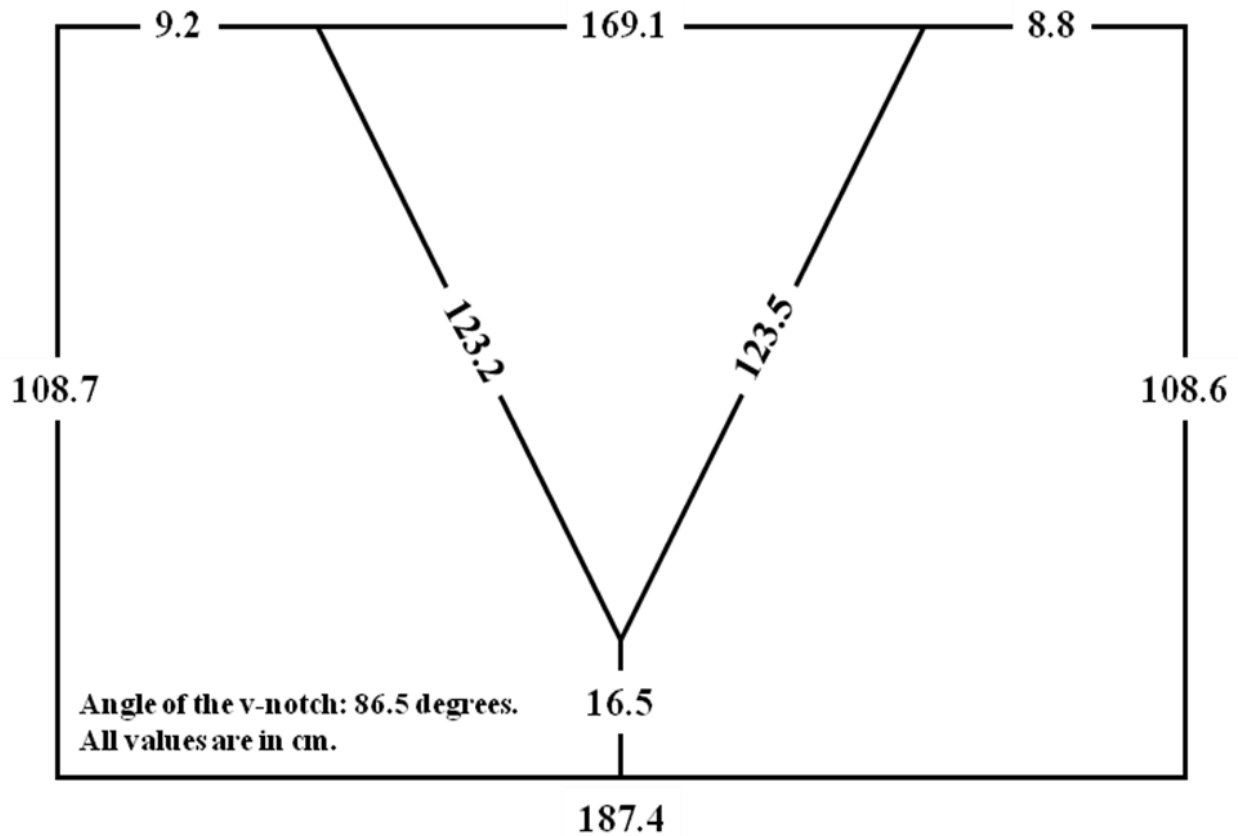
Important notice: These guidelines are intended for the installation of a V-notch weir in a small stream. They were derived from the observations of a forest engineer (the author of this dissertation) who took part in the installation of a V-notch weir in a small stream in South Korea. The installation was entirely supervised and coordinated by a civil engineer. Both engineers had previous experience in the installation of V-notch weirs in small streams. For more information on V-notch weirs, refer to WMO (2010a) and WMO (2010b). Photos of the PDF version are in color.

1. Build a rectangular or square frame for the V-notch plate to be installed, and build the V-notch plate as well. It is preferable to test the assembly of the frame and the V-notch plate before the installation, to be sure they fit each other. The frame must have external rods on the sides and bottom, which will hold the frame in concrete. The rods at the bottom must only be a few centimeters long. The frame and V-notch plate must be painted to prevent rust.





The angle of the V-notch must be between 20 and 100 degrees. The following image is an example of V-notch plate dimensions.



2. Clear the area where the weir will be installed of soil, debris and small rocks. It is highly recommended to dig down to bedrock. Gather rocks for their use in building the weir and classify them by size. Use water to rinse soil particles from rocks. Install a tube and bucket upstream of the area so that water can be gathered at all times (see picture below).



3. A tube must be installed in the stream so that water can flow through the base of the weir. Water flow should be directed to this tube using a plastic tarp. The tube must have a fitted end (downstream) where a cap will be screwed. The upstream end of the tube should be protected so that no concrete or rocks enter it during the installation. The base of the weir must be built over the tube. The first quantity of concrete must be laid directly on the ground, without pre-mixing. Water must be added successively, in several steps, while mixing the concrete with hands between steps. The base should be at level in both directions. Let the concrete dry completely before continuing work.



4. If possible, cut and carve through bedrock to make a base for the frame.



5. Dig ground and cut roots to make place for the concrete sidewalls. First, build a base for the walls. The first quantity of concrete must be laid directly on the ground, without pre-mixing. Water must be added successively, in several steps, while mixing the concrete with hands between steps. The next quantities of concrete must be mixed in a wide bucket before application. The base for the walls must extend until the “ground walls” and even a bit up these walls.



6. While the concrete of the sidewall base is still fresh, install the frame on the base of the weir. The frame must be installed at level in both directions, and as much as possible perpendicular to the stream bed. Stabilize the frame with rocks and branches and let concrete dry. Put concrete in the base for the frame (where bedrock was cut and carved). Let the concrete dry completely before continuing work.





7. Then, build the sidewalls of the weir using big, thick, flat rocks disposed horizontally on top of each other. Always put a thick layer of concrete between rocks (concrete must be pre-mixed in a wide bucket). It is not a bad idea to start with the part of the walls around the frame. The walls should extend downstream of the frame. When gathering rocks to be used for the construction of the sidewalls, it is better to take rocks downstream of the weir than upstream of the weir. The upstream portion of the streambed should be disturbed as less as possible.





Fill all the interstices with concrete and cover all rocks with concrete. This includes the interstice between the base of the weir and the frame, and any other interstice between the sidewalls and the frame. The finishing touch should be made with a large paint brush. All surfaces must be smooth. Let the concrete dry completely before continuing work.





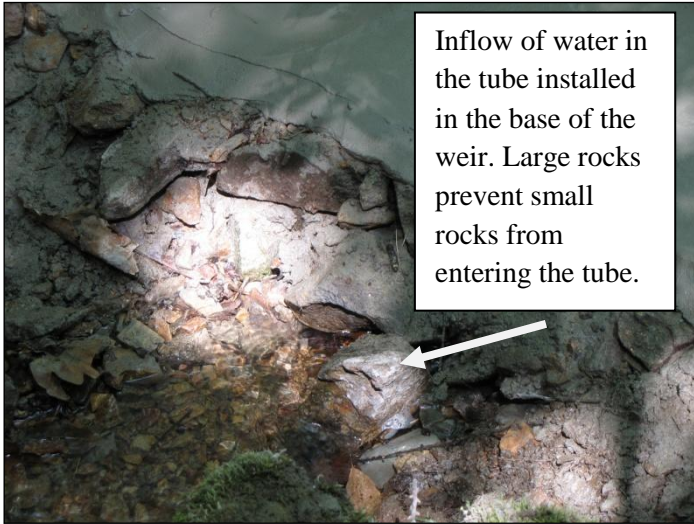
The area downstream of the frame should be cleared of rocks and debris and, as mentioned before, the walls should extend up to this area. Big rocks should be installed around the upstream and downstream parts of the tube installed in the base of the weir, in order to prevent small rocks from entering the tube.

8. Before installing the V-notch plate, clear the plate and the frame of particles. Then, apply silicone on the upstream side of the frame. Then, apply a rubber band over the silicone. Then, apply silicon on the rubber bands. Then, install the plate with bolts and nuts.



9. Cables to retain the frame and poles to retain debris and branches upstream of the weir can be installed as well.





The sidewalls are extending downstream of the weir. A big rock protects the downstream part of the tube.



10. Big rocks should be installed in the stream where flow will come out of the V-notch, to prevent erosion. Big rocks should also be installed downstream of the weir, against the V-notch plate, to support it even more (without concrete).
11. Ensure that the concrete is dry and close the tube in the base of the weir by screwing the cap to it (the cap should have an O-ring to ensure it is water-tight). The weir should then fill with water and, once water is flowing in the V-notch, the water level should stabilize.

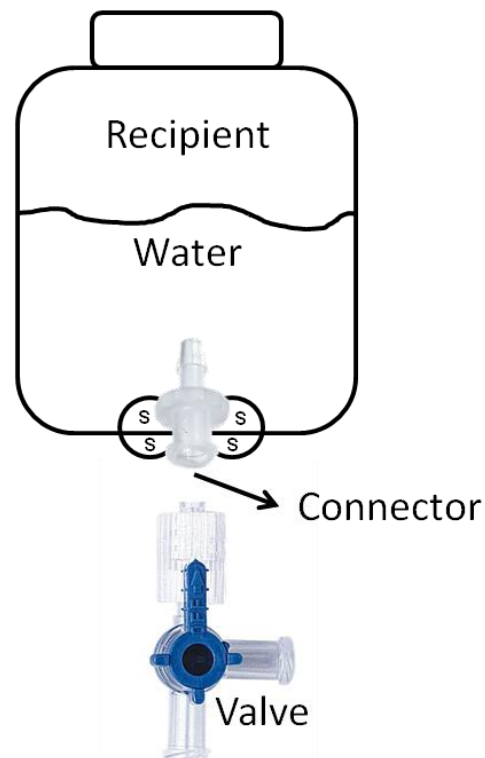
Notice: An addition to the weir can be made in order to prevent leaves, branches and debris from creating disturbances in the measurement of stage. At low stage, such debris can get stuck in the V-notch and make the water level in the weir rise. A half-cylinder shaped screen can be installed around the V-notch, in the upstream portion of the weir. The screen has to be highly perforated so that it does not create disturbance in discharge. It should be installed not too high above the crest of the V-notch, so that at high discharge (when it is almost impossible for debris to accumulate in the V-notch due to the strength of water flow) the water level will be over the screen. It is crucial that the weir be regularly checked and cleaned of debris.

References

- WMO (World Meteorological Organization), 2010a. Manual on Stream Gauging. Volume I – Fieldwork. WMO-No. 1044. WMO, Geneva.
- WMO (World Meteorological Organization), 2010b. Manual on Stream Gauging. Volume II – Computation of Discharge. WMO-No. 1044. WMO, Geneva.

Guidelines for the construction of a passive rainfall/throughfall collector with a valve for the collection of samples

1. Assemble a simple, passive rainfall/throughfall collector with a closed recipient and a funnel as shown in the images below. A piece of mosquito net can be installed at the wider opening of the funnel in order to prevent the entry of particles.



2. What is now needed are a laboratory valve, a male-female connector for the valve (see previous image), a drill and silicone.
3. At the bottom of the recipient, pierce a hole using the drill. The hole should be pierced where the bottom is flat or mostly flat. The hole should be wide enough to let the female part of the connector pass through, and narrow enough NOT to let the central ring of the connector and the screwing part of the valve pass through.
4. From inside the recipient, install the connector so that the male part is inside the recipient, the central ring sits on the bottom of the recipient, and the female part is outside the recipient (see previous image).
5. Connect the valve to the connector, only partially screwing both together.
6. Put silicone between the central ring of the connector and the bottom of the recipient, and tightly screw the connector and the valve together, so that the silicone is squeezed between the connector and the recipient. When screwing, center both parts in the hole, so that the inner rims of the parts lie on the edges of the recipient. Let it dry. The connector and valve should now be stable and attached to the edge of the recipient, the silicone used to make it water-tight. If the use of silicone is not recommended for the further analyses of water samples, use an alternative product.
7. Put silicone (more is better than less) around the connector both inside and outside the recipient (demarked as “S” on the previous image), taking care not to block the openings of the connector and/or the valve. If you wish to remove the valve for cleaning between sampling times, put silicone only on the connector and not on the valve, and let it dry before connecting the valve. Let everything dry.
8. Test whether the connector-valve connection is water-tight or not, and install plugs on the valve.
9. The water tightness of the connection should be checked and tested once in a while, while the collector is in use. Other standards of the use of such collectors are to be applied.

Notice: In order to reduce evaporation, a film of oil can be initially poured in the collector for it to lie over the collected water, or a ping-pong ball can be installed in the funnel. Whether or not the use of oil combined with the use of the valve-water-sampling technique can interfere with further analyses of water samples is up to the user.

Metadata of measurements, sampling and analyses

Measurements, sampling and analyses realized or requested by the author of this dissertation.

Geographic coordinates of the study site (decimal degrees of centre point): E 128.1816°,N 38.2051°

Measurements

Measurement	Medium	Location within site	1 st Period	2 nd Period
Stage	Water	At weir	01.06.2013 to 17.08.2014	–
Temperature	Water	At weir	01.06.2013 to 17.08.2014	–
Electrical conductivity	Water	At weir	16.05.2013 to 15.08.2013	10.06.2014 to 13.08.2014
Discharge	Water	At weir	Discrete	–
Temperature	Water	7 locations along the stream	26.06.2013 to 16.08.2013	25.06.2014 to 10.08.2014
Throughfall	Water	Near weir, under canopy	01.06.2013 to 01.09.2013	12.06.2014 to 11.08.2014
Temperature	Air	Near weir, under canopy	01.06.2013 to 01.09.2013	12.06.2014 to 11.08.2014
Relative humidity	Air	Near weir, under canopy	01.06.2013 to 01.09.2013	12.06.2014 to 11.08.2014
Radiation (downwelling)	Air	Near weir, under canopy	01.06.2013 to 01.09.2013	12.06.2014 to 11.08.2014
Barometric pressure	Air	At weir	01.06.2013 to 17.08.2014	–
Throughfall	Water	4 locations	26.05.2013 to 01.09.2013	12.06.2014 to 11.08.2014
Precipitation	Water	1 location 850 m from the site, open space	26.05.2013 to 01.09.2013	12.06.2014 to 11.08.2014
Water table level (head pressure)	Water	12 locations, different depths	01.06.2013 to 01.09.2013	09.06.2014 to 17.08.2014
Volumetric water content	Soil	4 locations, 3 depths per location	15.05.2013 to 01.09.2013	09.06.2014 to 13.08.2014
Temperature	Soil	4 locations, 3 depths per location	15.05.2013 to 01.09.2013	09.06.2014 to 13.08.2014
Depth	Soil	50 locations	Discrete	–
Infiltration rate	Soil surface	18 locations	Discrete	–
Tree height	Vegetation	9 locations	Discrete	–
Diameter of tree at breast height (DBH)	Vegetation	9 locations	Discrete	–
Tree age	Vegetation	9 locations	Discrete	–
Tree species	Vegetation	9 locations	Discrete	–

Appendix – Metadata of Measurements, Sampling and Analyses

Measurements (continued)

Measurement	Frequency	Unit	Instrument or Method
Stage	5 minutes	cm	Levellogger Gold M10, Solinst Canada Ltd., Georgetown, Canada
Temperature	5 minutes	degree Celsius	Levellogger Gold M10, Solinst Canada Ltd., Georgetown, Canada
Electrical conductivity	5 minutes	microsiemens per centimeter	Cond 340i, WTW GmbH, Weilheim, Germany
Discharge	–	liter per second	Timed volumetric method
Temperature	5 minutes	degree Celsius	HOBO Pendant UA-002-08, Onset Computer Corp., Bourne, US
Throughfall	5 minutes	mm	WS-GP1, Delta-T Devices Ltd., Cambridge, UK
Temperature	5 minutes	degree Celsius	WS-GP1, Delta-T Devices Ltd., Cambridge, UK
Relative humidity	5 minutes	percentage	WS-GP1, Delta-T Devices Ltd., Cambridge, UK
Radiation (downwelling)	5 minutes	Watt per meter square	WS-GP1, Delta-T Devices Ltd., Cambridge, UK
Barometric pressure	5 minutes	cm	Barologger Gold M1.5, Solinst Canada Ltd., Georgetown, Canada
Throughfall	during or following every rainfall event	mm	Passive collectors
Precipitation	during or following every rainfall event	mm	Passive collector
Water table level (head pressure)	5 minutes	cm	Levellogger Junior Model 3001, Solinst Canada Ltd., Georgetown, Canada (installed in piezometer)
Volumetric water content	5 minutes	meter cube of water per meter cube of soil	5TE, Decagon Devices Inc., Pullman, USA
Temperature	5 minutes	degree Celsius	5TE, Decagon Devices Inc., Pullman, USA
Depth	–	cm	Rod or auger (Edelmann-Bohrer)
Infiltration rate	–	millimeter per second	Single-ring infiltrometer
Tree height	–	m	Forest inventory
Diameter of tree at breast height (DBH)	–	cm	Forest inventory
Tree age	–	year	Forest inventory
Tree species	–	Latin name	Forest inventory

Appendix – Metadata of Measurements, Sampling and Analyses

Sampling

Sampling Source	Location	1st Period	2nd Period
Throughfall	4 locations, randomly distributed within the site	26.05.2013 to 01.09.2013	12.06.2014 to 11.08.2014
Precipitation	1 location 700 m from the site, in an open space	26.05.2013 to 01.09.2013	12.06.2014 to 11.08.2014
Soil water	30 locations in 2013; 20 locations in 2014	25.05.2013 to 12.08.2013	12.06.2014 to 11.08.2014
Stream water	At weir and 2 other upstream locations	28.05.2013 to 01.09.2013	11.06.2014 to 17.08.2014
Spring water	2 locations along the stream	28.05.2013 to 01.09.2013	11.06.2014 to 17.08.2014

Sampling Source	Sample Amount	Frequency	Instrument or Method
Throughfall	150	during or following every rainfall event	Grab from passive collectors
Precipitation	33	during or following every rainfall event	Grab from passive collector
Soil water	1212	at least once per two days over the entire study period; almost every day during the most intensive period of the summer monsoon in terms of rainfall events	Suction cup lysimeters
Stream water	837	at least once per two days over the entire study period; at least every two hours during and following major rainfall events	Grab or ISCO autosampler (6712 Portable Sampler, Teledyne Isco Inc., Lincoln, USA)
Spring water	69	following the activation of springs	Grab

Analyses

Measurement	Medium	Realized by
Chloride (Cl ⁻)	Throughfall, precipitation, soil water, stream water, spring water	Limnological Research Station at Universität Bayreuth
Nitrate (NO ₃ ⁻)	Throughfall, precipitation, soil water, stream water, spring water	Limnological Research Station at Universität Bayreuth
Sulphate (SO ₄ ²⁻)	Throughfall, precipitation, soil water, stream water, spring water	Limnological Research Station at Universität Bayreuth
Calcium (Ca ²⁺)	Throughfall, precipitation, soil water, stream water, spring water	Department of Hydrology at Universität Bayreuth
Magnesium (Mg ²⁺)	Throughfall, precipitation, soil water, stream water, spring water	Department of Hydrology at Universität Bayreuth
Potassium (K ⁺)	Throughfall, precipitation, soil water, stream water, spring water	Department of Hydrology at Universität Bayreuth

Appendix – Metadata of Measurements, Sampling and Analyses

Analyses (continued)

Measurement	Medium	Realized by
Sodium (Na ⁺)	Throughfall, precipitation, soil water, stream water, spring water	Department of Hydrology at Universität Bayreuth
Silica (SiO ₂)	Throughfall, precipitation, soil water, stream water, spring water	Department of Hydrology at Universität Bayreuth
Electrical conductivity	Throughfall, precipitation, soil water, stream water, spring water	Observer, at time of sampling
Deuterium (² H)	Throughfall, precipitation, stream water – 2013	Laboratory of Isotope Biogeochemistry at Universität Bayreuth
Deuterium (² H)	Soil water – 2013	Laboratory of the Institute of Landscape Ecology at Universität Münster
¹⁸ O	Throughfall, precipitation, soil water, stream water – 2014	Laboratory of the Institute of Landscape Ecology at Universität Münster
¹⁷ O	Throughfall, precipitation, soil water, stream water – 2014	Laboratory of the Institute of Landscape Ecology at Universität Münster
Dissolved organic carbon (DOC)	Stream water – 2014 (subset of samples)	Department of Hydrology at Universität Bayreuth
Total dissolved nitrogen (TDN)	Stream water – 2014 (subset of samples)	Department of Hydrology at Universität Bayreuth

Measurement	Unit	Instrument or Method
Chloride (Cl ⁻)	milligram per liter	Ion chromatography (Metrohm IC Separation Center with Suppressor Module, Metrohm AG, Herisau, Switzerland)
Nitrate (NO ₃ ⁻)	milligram per liter	Ion chromatography (Metrohm IC Separation Center with Suppressor Module, Metrohm AG, Herisau, Switzerland)
Sulphate (SO ₄ ²⁻)	milligram per liter	Ion chromatography (Metrohm IC Separation Center with Suppressor Module, Metrohm AG, Herisau, Switzerland)
Calcium (Ca ²⁺)	milligram per liter	Inductively coupled plasma optical emission spectrometry (Optima 3200 XL, PerkinElmer LAS GmbH, Rodgau, Germany)
Magnesium (Mg ²⁺)	milligram per liter	Inductively coupled plasma optical emission spectrometry (Optima 3200 XL, PerkinElmer LAS GmbH, Rodgau, Germany)
Potassium (K ⁺)	milligram per liter	Inductively coupled plasma optical emission spectrometry (Optima 3200 XL, PerkinElmer LAS GmbH, Rodgau, Germany)
Sodium (Na ⁺)	milligram per liter	Inductively coupled plasma optical emission spectrometry (Optima 3200 XL, PerkinElmer LAS GmbH, Rodgau, Germany)

Appendix – Metadata of Measurements, Sampling and Analyses

Analyses (continued)

Measurement	Unit	Instrument or Method
Silica (SiO ₂)	milligram per liter	Inductively coupled plasma optical emission spectrometry (Optima 3200 XL, PerkinElmer LAS GmbH, Rodgau, Germany)
Electrical conductivity	microsiemens per centimeter	Cond 340i, WTW GmbH, Weilheim, Germany
Deuterium (² H)	relative abundance in relation to VSMOW (‰)	Mass spectrometer (DELTA V Advantage, Thermo Fisher Scientific GmbH, Bremen, Germany) coupled to a high-temperature pyrolysis reactor (HTO, HEKAtech GmbH, Wegberg, Germany) and a continuous flow interface (ConFlo IV, Thermo Fisher Scientific GmbH)
Deuterium (² H)	relative abundance in relation to VSMOW (‰)	Off-axis integrated cavity output spectroscopy (TIWA-45EP, Los Gatos Research Inc., Mountain View, US)
¹⁸ O	relative abundance in relation to VSMOW (‰)	Off-axis integrated cavity output spectroscopy (TIWA-45EP, Los Gatos Research Inc., Mountain View, US)
¹⁷ O	relative abundance in relation to VSMOW (‰)	Off-axis integrated cavity output spectroscopy (TIWA-45EP, Los Gatos Research Inc., Mountain View, US)
Dissolved organic carbon (DOC)	milligram of carbon per liter	Total organic carbon analyzer (TOC-V, Shimadzu Corporation, Kyoto, Japan)
Total dissolved nitrogen (TDN)	milligram of nitrogen per liter	Total organic carbon analyzer (TOC-V, Shimadzu Corporation, Kyoto, Japan)

Eidesstattliche Versicherungen und Erklärungen

Eidesstattliche Versicherungen und Erklärungen zur Promotionsarbeit “Hydrological Dynamics of Forested Catchments as Influenced by the East Asian Summer Monsoon”, eingereicht von Herrn Jean-Lionel Payeur-Poirier, geb. am 17.03.1982 in Beauceville, Kanada.

Hiermit erkläre ich mich damit einverstanden, dass die elektronische Fassung meiner Dissertation unter Wahrung meiner Urheberrechte und des Datenschutzes einer gesonderten Überprüfung hinsichtlich der eigenständigen Anfertigung der Dissertation unterzogen werden kann.

Hiermit erkläre ich eidesstattlich, dass ich die Dissertation selbständig verfasst und keine anderen als die von mir angegebenen Quellen und Hilfsmittel benutzt habe.

Hiermit erkläre ich, dass ich habe die Dissertation nicht bereits zur Erlangung eines akademischen Grades anderweitig eingereicht und habe auch nicht bereits diese oder eine gleichartige Doktorprüfung endgültig nicht bestanden.

Hiermit erkläre ich, dass ich keine Hilfe von gewerblichen Promotionsberatern bzw. -vermittlern in Anspruch genommen habe und auch künftig nicht nehmen werde.

Bayreuth, 25.11.2016

Jean-Lionel Payeur-Poirier